

THE DESIGN AND SYNTHESIS OF ANTI-ICTOGENIC AND  
ANTIEPILEPTOGENIC DRUGS BASED ON ENDOGENOUS MOLECULES

by

Kathryn Ellen Tiedje

Submitted in partial fulfillment of the requirements  
for the degree of Doctor of Philosophy

at

Dalhousie University  
Halifax, Nova Scotia  
November 2006

© Copyright by Kathryn Ellen Tiedje, 2006



Library and  
Archives Canada

Bibliothèque et  
Archives Canada

Published Heritage  
Branch

Direction du  
Patrimoine de l'édition

395 Wellington Street  
Ottawa ON K1A 0N4  
Canada

395, rue Wellington  
Ottawa ON K1A 0N4  
Canada

*Your file    Votre référence*

*ISBN: 978-0-494-27202-2*

*Our file    Notre référence*

*ISBN: 978-0-494-27202-2*

#### NOTICE:

The author has granted a non-exclusive license allowing Library and Archives Canada to reproduce, publish, archive, preserve, conserve, communicate to the public by telecommunication or on the Internet, loan, distribute and sell theses worldwide, for commercial or non-commercial purposes, in microform, paper, electronic and/or any other formats.

The author retains copyright ownership and moral rights in this thesis. Neither the thesis nor substantial extracts from it may be printed or otherwise reproduced without the author's permission.

#### AVIS:

L'auteur a accordé une licence non exclusive permettant à la Bibliothèque et Archives Canada de reproduire, publier, archiver, sauvegarder, conserver, transmettre au public par télécommunication ou par l'Internet, prêter, distribuer et vendre des thèses partout dans le monde, à des fins commerciales ou autres, sur support microforme, papier, électronique et/ou autres formats.

L'auteur conserve la propriété du droit d'auteur et des droits moraux qui protègent cette thèse. Ni la thèse ni des extraits substantiels de celle-ci ne doivent être imprimés ou autrement reproduits sans son autorisation.

---

In compliance with the Canadian Privacy Act some supporting forms may have been removed from this thesis.

Conformément à la loi canadienne sur la protection de la vie privée, quelques formulaires secondaires ont été enlevés de cette thèse.

While these forms may be included in the document page count, their removal does not represent any loss of content from the thesis.

Bien que ces formulaires aient inclus dans la pagination, il n'y aura aucun contenu manquant.

  
**Canada**

DALHOUSIE UNIVERSITY

To comply with the Canadian Privacy Act the National Library of Canada has requested that the following pages be removed from this copy of the thesis:

Preliminary Pages

Examiners Signature Page (pii)

Dalhousie Library Copyright Agreement (piii)

Appendices

Copyright Releases (if applicable)

## TABLE OF CONTENTS

LIST OF FIGURES .....	xiii
LIST OF TABLES.....	xvii
LIST OF SCHEMES.....	xix
ABSTRACT.....	xxi
LIST OF ABBREVIATIONS AND SYMBOLS USED.....	xxii
ACKNOWLEDGEMENTS.....	xxiv

### PART A: THE PROBLEM AND THE APPROACH

<b>CHAPTER 1: INTRODUCTION.....</b>	<b>1</b>
1.1 What Is Epilepsy?.....	2
1.2 Neurons: Activation And Inhibition.....	2
1.3 Targets For Anticonvulsant Drug Development.....	5
1.3.1 Voltage-Gated Ion Channels.....	5
1.3.2 GABAergic Enhancement And Receptors.....	7
1.3.3 Glutamergic Inhibition And NMDA/Glycine Receptors.....	10
1.4 The Blood-Brain Barrier.....	12
1.5 Classification Of Epilepsy.....	13
1.5.1 Partial Seizures.....	13
1.5.2 Simple Partial Seizures.....	13
1.5.3 Complex Partial Seizures.....	14
1.5.4 Generalized Seizures.....	14
1.5.5 Tonic-Clonic Seizures.....	14



1.5.6	Absence Seizures.....	15
1.6	Epileptogenesis And Ictogenesis.....	15
1.7	Current Drug Treatments.....	17
1.7.1	Phenobarbital.....	20
1.7.2	Carbamazepine.....	21
1.7.3	Phenytoin.....	21
1.7.4	Valproate.....	22
1.7.5	Benzodiazepines.....	22
1.7.6	Vigabatrin.....	24
1.7.7	Lamotrigine.....	24
1.7.8	Oxcarbazepine.....	24
1.7.9	Felbamate.....	25
1.7.10	Leviteracetam.....	25
1.8	Need for New Treatment Options.....	26
1.9	Epilepsy Treatment: Present And Future.....	27
1.9.1	Endogenous Molecules.....	28
1.9.2	Goal Of Thesis.....	30
<b>CHAPTER 2: DRUG DISCOVERY AND DEVELOPMENT.....</b>		<b>31</b>
2.1	Medicinal Chemistry: A Definition.....	32
2.2	The Receptor.....	33
2.2.1	Pharmacophore And Toxicophore.....	34
2.3	Drug Development.....	35

2.3.1	Pharmaceutical Phase.....	36
2.3.2	Pharmacokinetic Phase.....	36
2.3.3	Pharmacodynamic Phase And Receptor Interactions.....	37
2.3.4	Drug Absorption And Lipinski's Rules.....	38
2.3.5	ADMET.....	40

## **PART B: DEVELOPING ANTI-ICTOGENICS BASED ON ENDOGENOUS SCAFFOLDS**

<b>CHAPTER 3: DEDUCING THE BIOACTIVE FACE OF HYDANTOIN ANTICONVULSANTS.....</b>		<b>42</b>
3.1	Introduction.....	43
3.2	Methods and Materials.....	44
3.2.1	Compound Selection And Preparation.....	44
3.2.2	Biological Testing.....	48
3.2.3	NMR Conformational Analysis.....	48
3.2.4	Molecular Modelling Calculations.....	49
3.3	Results.....	49
3.4	Discussion.....	51
<b>CHAPTER 4: NICOTINAMIDE.....</b>		<b>53</b>
4.1	Nicotinamide Derivatives: Potential Anti-Ictogenic Treatment.....	54
4.2	Targeting The Fast-Inactivated State Of The Neuronal Sodium Channel.....	57
4.2.1	Nicotinamide Analogues.....	60
4.3	Nicotinamide Derivatives: Synthetic Considerations.....	62

4.3.1	Nicotinamide Derivatives: Using DCC (Route A).....	63
4.3.2	Nicotinamide Derivatives: Using EEDQ (Route B).....	65
4.3.3	Nicotinamide Derivatives: Synthesis Of Nicotiny Chloride (Route C).....	67
4.3.4	Nicotinamide Derivatives: Using DPPA (Route D).....	69
4.3.5	Nicotinate Derivatives: Synthetic Route 1.....	72
4.3.6	Nicotinate Derivatives: Synthetic Route 2.....	73
4.4	5'- Substituted Nicotinamide Analogues.....	74
4.4.1	5-Bromonicotinamides.....	75
4.4.1.1	5-Bromonicotinamides: Synthetic Considerations.....	78
4.4.2	5-Bromonicotinamides And Heck Coupling.....	80
4.4.3	5-Bromonicotinamides And Suzuki Coupling.....	87
4.4.3.1	Suzuki Synthetic Details.....	91
4.5	Targeting The GABA <sub>A</sub> -Benzodiazepine Receptor.....	94
4.5.1	Synthetic Considerations.....	98
4.6	Experimental.....	102
4.6.1	Nicotinamide Derivatives: Route A (DCC coupling) – General Procedure.....	112
4.6.2	Nicotinamide Derivatives: Route B (EEDQ coupling) – General Procedure .....	113
4.6.3	Nicotinamide Derivatives: Route C (Nicotiny Chloride) – General Procedure.....	113
4.6.4	Nicotinamide Derivatives: Route D (DPPA coupling) – General Procedure.....	114
4.6.5	General Procedure for the Synthesis of Nicotimates, Route 1.....	118

4.6.7	General Procedure for the Synthesis of Nicotines, Route 2.....	119
4.6.8	5-Bromonicotinamide Analogues.....	120
4.6.9	Heck Coupling Procedure Development.....	124
4.6.10	Suzuki Coupling Procedure Development.....	130
4.6.11	Synthesis Of 2-(Benzylthio)pyridine-3-carboxylic Acid.....	136
4.6.12	Synthesis Of 2-(Benzylthio)nicotinamides.....	137
4.6.13	Synthesis Of 2-(Benzylsulfinyl)nicotinamides.....	141
<b>CHAPTER 5: QUANTITATIVE STRUCTURE ACTIVITY RELATIONSHIP OF THE NICOTINAMIDE ANALOGUES.....</b>		<b>143</b>
5.1	QSAR Introduction.....	144
5.2	Computational Methods.....	147
5.2.1	QSAR Equation Overview.....	147
5.2.2	Computational Application.....	148
5.3	QSAR.....	151
5.3.1	Data Analysis.....	151
5.3.2	Descriptor Reduction.....	152
5.4	Biological Testing.....	156
5.5	Biological Results.....	162
5.5.1	Voltage Gated Sodium Channel: Maximal Electroshock Seizure Model (MES).....	163
5.5.2	GABA <sub>A</sub> -Benzodiazepine Receptors: Pentylenetetrazole Seizure Model (PTZ).....	168
5.5.3	Neurotoxicity.....	170

5.6	Conclusions.....	171
-----	------------------	-----

## **PART C: DEVELOPING ANTI-ICTOGENIC/ANTIEPILEPTOGENIC HYBRID BASED ON ENDOGENOUS SCAFFOLDS**

<b>CHAPTER 6: DIHYDROURACILS.....</b>	<b>172</b>
6.1	Introduction.....173
6.2	Part A – Overview Of $\beta$ -Alanine Neurochemistry..... 175
6.2.1	$\beta$ -Alanine Synthesis.....175
6.2.1.1	$\beta$ -Alanine Synthesis From Uracil.....177
6.2.2	$\beta$ -Alanine Transport.....179
6.2.3	$\beta$ -Alanine Transport In The CNS..... 182
6.2.4	$\beta$ -Alanine Receptors..... 183
6.2.5	$\beta$ -Alanine: Chemical Neuroanatomy.....185
6.2.6	$\beta$ -Alanine In Carnosine..... 188
6.2.7	$\beta$ -Alanine In Pantothenic Acid..... 190
6.2.8	$\beta$ -Alanine Inactivation And Breakdown..... 190
6.3	Is $\beta$ -Alanine A Neurotransmitter?..... 192
6.3.1	Presence And Storage Of The Transmitter Molecule In Neural Tissue..... 192
6.3.2	Specific Release Mechanism And Specific Receptor (Site Of Action).....194
6.3.3	Presence of Precursors, Synthesizing Enzymes, And Inactivating Enzymes.....195
6.3.4	Identical Action, Pharmacological Identity.....196
6.3.5	$\beta$ -Alanine Is A Neurotransmitter..... 196

6.4	Implications of $\beta$ -Alanine As A Neurotransmitter.....	197
6.4.1	Exposure To $\beta$ -Alanine Or $\beta$ -Alanine Derivatives.....	197
6.4.1.1	Non-Pharmacologic Exposure To $\beta$ -Alanine Or $\beta$ -Alanine Derivatives.....	197
6.4.1.2	Pharmacologic Exposure To $\beta$ -Alanine Or $\beta$ -Alanine Derivatives.....	199
6.4.2	$\beta$ -Alanine Is Widely Distributed In Our Environment.....	202
6.5	$\beta$ -Alanine As A Neurotransmitter Conclusions.....	203
6.6	Dihydrouracils And $\beta$ -Alanine: Potential Anti-Epileptogenic Treatments..	204
6.6.1	The BBB and Metabolites Of The Pyrimidine Pathway.....	204
6.6.2	CNS Receptors And Dihydrouracils.....	205
6.7	Dihydrouracil Analogues.....	208
6.7.1	6-Aryl Substituted Dihydrouracil Analogues: Route A.....	210
6.7.2	6-Aryl Substituted Dihydrouracil Analogues: Route B.....	212
6.8	Dihydrouracils: Biological Results.....	217
6.8.2	Biological Discussion.....	219
6.9	Experimental: Dihydrouracil Derivatives.....	220
6.9.1	Synthesis Of 6-Aryl Substituted Dihydrouracils: Route A.....	221
6.9.2	6-Aryl Substituted Dihydrouracil Analogues: Route B.....	222
<b>CHAPTER 7: ENZYMES IN THE PYRIMIDINE METABOLIC PATHWAY.....</b>		<b>228</b>
7.1	Introduction.....	229
7.2	Project Goals.....	231
7.3	Background Information: FlexX Program.....	232

7.3.1	Input Data.....	233
7.3.2	Molecular Interactions.....	234
7.3.3	Docking Algorithm.....	237
7.4	Computational Methods.....	240
7.4.1	Dihydrouracil Dehydrogenase (DHD).....	242
7.4.2	Dihydropyrimidinase (DHP).....	245
7.4.3	3-Ureidopropionase/ $\beta$ -Alanine Synthase ( $\beta$ -AS).....	247
7.5	Results And Discussion.....	249
7.6	Conclusions.....	255

## **CHAPTER 8: MOLECULAR MODELLING OF PHENYTOIN AND DIHYDROURACILS.....257**

8.1	Introduction.....	258
8.2	Computational Methods.....	260
8.3	Calculated Results: Phenytoin And Dihydrouracil.....	260
8.4	Pharmacophore Discussion.....	263
8.4.1	Minimization Techniques.....	264
8.4.2	Pharmacophore.....	266
8.4.3	Toxicophore.....	269
8.5	Conclusions.....	271

## **PART D: SUMMARY**

<b>Chapter 9: CONCLUSIONS...</b>	<b>273</b>
9.1 Summary .....	274

9.2	Endogenous Anti-Ictogenics .....	274
9.3	Anti-Ictogenics/Antiepileptogenics: A Novel “Bioactive” Pro-drug .....	275
9.4	Future Directions.....	275
<b>APPENDIX: Methods Used To Produce Figure 26.....</b>		<b>277</b>
<b>REFERENCES.....</b>		<b>278</b>



## LIST OF FIGURES

Figure 1. The representation of a neuron, showing the various components and direction in which a nerve impulse travels when initiated .....	3
Figure 2. The excitatory and inhibitory neurotransmitters in the CNS.....	4
Figure 3. The sodium channel as it moves through its various stages; from its resting state to the active open channel to the inactivated blocked channel ( <a href="http://www.clabs.de/na_ch.jpg">http://www.clabs.de/na_ch.jpg</a> ) .....	6
Figure 4. Biochemical route for the formation of GABA.....	7
Figure 5. The representation of the GABA <sub>A</sub> receptor.....	9
Figure 6. The representation of the NMDA receptor.....	11
Figure 7. Current drug therapies available target the process of ictogenesis. Presently there are no drugs available to prevent the process of epileptogenesis, creating a new target for the treatment of epilepsy .....	16
Figure 8. Structures of current anticonvulsant drugs.....	20
Figure 9. Current anticonvulsant structures.....	23
Figure 10. Optimization of the bioavailability of a peptide sequence that has shown the ability to act as a fibrinogen receptor antagonist, using the rule of five.....	39
Figure 11. Tumor cell prodrug, cyclophosphamide, which is metabolized to the active drug phosphoramidate mustard.....	41
Figure 12. General structure of the hydantoin derivatives synthesized, where the R group are represented in the table below (Bn = benzyl(-CH <sub>2</sub> C <sub>6</sub> H <sub>5</sub> ), Ph = phenyl (-C <sub>6</sub> H <sub>5</sub> ), H=hydrogen.....	44
Figure 13. Relevant nOes observed for the (S)-5-benzylhydantoin and (S)-5-phenylhydantoin. Solid and dotted lines represent strong and weak nOes respectively.....	50
Figure 14. The chemical structure of nicotinamide and nicotinic acid.....	54
Figure 15. The pharmacophore regions of anticonvulsants and nicotinamide derivatives: HBD- hydrogen bonding domain, D- electron-donor, R- hydrophobic unit.....	58

Figure 16. The thyroid hormone tetraiodothyroxine is an endogenous iodinated molecule.....	76
Figure 17. The conformation of the Pd intermediate for the Heck coupling using styrene to generate the trans product.....	82
Figure 18. The conformation of the Pd intermediate for the Heck coupling using methyl acrylate, to generate the trans product.....	83
Figure 19. Compounds that target the benzodiazepine GABA <sub>A</sub> receptor (1) Diazepam and (2) Quazepam.....	95
Figure 20. The pseudo 7-membered ring of the nicotinamide analogue showing the hydrogen bond.....	98
Figure 21. The nicotinamide framework used to align the nicotinamide training-set.....	149
Figure 22. $\beta$ -Alanine is a structural hybrid between the neurotransmitters glycine and GABA.....	174
Figure 23. Decarboxylation of L-aspartate to $\beta$ -alanine by gastrointestinal microbes.....	176
Figure 24. $\beta$ -Alanine is a metabolic by-product of the interchangeable reaction of L-alanine and pyruvate.....	176
Figure 25. Pyrimidine metabolic pathway used for the metabolism of uracil to $\beta$ -alanine.....	177
Figure 26. Immunohistochemical analysis of $\beta$ -alanine localization in mouse retina.....	187
Figure 27. Carnosine and pantothenic acid chemical structure.....	189
Figure 28. The receptors, proteins, and distribution of $\beta$ -alanine in the CNS.....	193
Figure 29. Current drugs that contain the $\beta$ -alanine scaffold in their chemical structure. $\beta$ -Alanine scaffold is the bolded portion of each molecule.....	200
Figure 30. The uracil, dihydrouracil, and $\beta$ -amino acid derivatives.....	207
Figure 31. Model showing how a carbonyl is represented in the FlexX suite, with its calculated interaction centre (IC) and interaction surface (IS).....	234

Figure 32. A hydrogen bond interaction between Group A (carbonyl) and Group B (amine) where each of the IC is contained on the required IS.....	235
Figure 33. Description of the receptor pocket where the active site residues are represented as black interaction surfaces and the ligand base fragment is represented as grey interaction surfaces. In order for the ligand base fragment to dock with the receptor active site residues there must be three reciprocal interactions between the two.....	238
Figure 34. The active residues and cofactors of dihydrouracil dehydrogenase (DHD) involved in metabolizing uracil to dihydrouacil.....	243
Figure 35. The active residues and zinc cofactors of dihydropyrimidinase (DHP) involved in metabolizing dihydrouacil to 3-ureidopropionate.....	246
Figure 36. The active residues and zinc cofactors of 3-ureidopropionase/ $\beta$ -alanine synthase ( $\beta$ -AS) involved in metabolizing 3-ureidopropionate to $\beta$ -alanine.....	248
Figure 37. The structure of the uracil derivatives that were docked with the DHD enzyme active site using FlexX program.....	250
Figure 38. The structure of the dihydrouracil derivatives that were docked with the DHP enzyme active site using FlexX program. The black dots over the specific molecular location indicate those chemical centres that can have either an R or S configuration.....	251
Figure 39. Phenytoin (5,5-diphenylhydantoin) and its respective pharmacophore and toxicophore units.....	259
Figure 40. Dihydrouacil analogue where the R groups can be a variety of substituents.....	260
Figure 41. Phenytoin with the phenyl rings, angles (A1, A2, A3, A4, A5) and atoms labelled for comparison to the calculated results.....	262
Figure 42. 5-Phenyl dihydrouracil with the angles (A1, A2, A3, A4, A5, A6) and atoms labelled for comparison to the calculated results.....	262
Figure 43. 6-Phenyl dihydrouracil with the angles (A1, A2, A3, A4, A5, A6) and atoms labelled for comparison to the calculated results.....	263
Figure 44. Phenytoin with the calculated distance between the atoms and the centroid of the aromatic ring (phenyl 1) determined using AMBER.....	267

Figure 45. 5-Phenyl dihydrouracil and 6-phenyl dihydrouracil with the calculated distance between the atoms and the centroid of the aromatic ring determined using AMBER.....	268
Figure 46. The AMBER calculated bond angles of the phenytoin ring, when A3 and A4 are the angles of interest for the toxicophore face.....	270
Figure 47. The AMBER calculated bond angles of the 5-phenyl dihydrouracil ring, when A3 and A4 are the angles of interest for the toxicophore face.....	270
Figure 48. The scaffold of the next compounds to be developed in the nicotinamide series.....	276

## LIST OF TABLES

Table 1: Summary of current anti-ictogenic therapies including their molecular targets and the seizure classifications they effect.....	17
Table 2. Side effects associated with some of the new common anticonvulsant drugs.....	26
Table 3. Drug receptor interactions and their associated binding energies.....	38
Table 4. The calculated mean distances and standard deviations between the center of the amide bond and the centroid of the aromatic ring and the anticonvulsant activities, where the values indicate the number of animals tested compared to the number of animals that exhibited seizure protection.....	50
Table 5. Nicotinamide derivatives to be developed as anticonvulsants based on the corresponding 4-amino-N-substituted-benzamides. The number of +’s indicates anticonvulsant activity in MES testing .....	62
Table 6. Percent yields obtained for the synthesis of specific nicotinamides using a variety of different synthetic routes. (Route A: DCC coupling, Route B: EEDQ coupling, Route C: Thionyl chloride, Route D: DPPA coupling).....	71
Table 7. The reagents used for the development of the Heck coupling for 5-bromonicotinic acids.....	85
Table 8. The reagents used for the development of the Heck coupling for 5-bromonicotinamides.....	86
Table 9. The reagents used for the development of the Suzuki coupling for 5-bromonicotinamides.....	93
Table 10. The calculated hydrogen bonds for the nicotinamide analogues targeting the GABA <sub>A</sub> -benzodiazepine receptor.....	98
Table 11. The nicotinamide analogues synthesized with their corresponding identification numbers (ID) and their IUPAC names.....	104
Table 12. List of descriptors used for 2D QSAR calculation.....	150
Table 13. The chemical structure and identification numbers (ID#) for the synthesized nicotinamides analogues.....	160
Table 14. Activity codes and the corresponding animal protection ratios and dosages.....	162

Table 15. Biological testing results and activity codes for nicotinamide analogues in the QSAR training-set. The ratios indicated the number of animals protected over the number of animals tested.....	164
Table 16. The ED <sub>50</sub> value results for N-benzylnicotinamide ( <b>5</b> ) in the both the MES and PTZ tests.....	166
Table 17. The results for the 6 Hz psychomotor test at varying time intervals. The ratios indicated the number of animals protected over the number of animal tested.....	169
Table 18. Representative dihydrouracil derivatives to be developed as anticonvulsants and anti-ictogenics.....	209
Table 19. The 6-aryl substituted dihydrouracil analogues synthesized using Route A and/or Route B, with their respective identification numbers (ID).....	215
Table 20: The yields obtained for the synthesis of 6-aryl substituted dihydrouracil analogues using Route A and Route B.....	217
Table 21. Biological testing results and activity codes for 6-aryl substituted dihydrouracil analogues. The ratios indicated the number of animals protected over the number of animals tested.....	218
Table 22. Activity codes and the corresponding animal protection ratios and dosages.....	218
Table 23. The amount of each brominated compound that was used in Route B for the organolithium preparation.....	224
Table 24. Relative docking energies for uracil derivatives in the DHD enzyme.....	252
Table 25. Relative docking energies for dihydrouracil derivatives in the DHP enzyme.....	254
Table 26. The calculated results for phenytoin, 5-phenyldihydrouracil and 6-phenyl dihydrouracil. Angles are all expressed in degrees and the distances in angstroms.....	261

## LIST OF SCHEMES

Scheme 1. DCC coupling technique used for the synthesis of nicotinamide derivatives.....	64
Scheme 2. DCC/ DMAP coupling technique used for the synthesis of nicotinamide derivatives.....	65
Scheme 3. EEDQ coupling technique used for the synthesis of nicotinamide derivatives.....	66
Scheme 4. Synthesis of benzamide derivatives used to evaluate the use DCC and EEDQ to synthesize amide bonds.....	67
Scheme 5. The synthesis of nicotinamide derivatives using nicotinyl chloride.....	68
Scheme 6. Synthesis of nicotinyl chloride and nicotinamide.....	69
Scheme 7. DPPA coupling technique used for the synthesis of nicotinamide derivatives.....	71
Scheme 8. The synthetic route used for the synthesis of the nicotinate derivatives using synthetic Route 1.....	72
Scheme 9. The synthetic route used for the synthesis of the nicotinate derivatives using synthetic Route 2.....	74
Scheme 10. The synthesis of 5-bromonicotinic acid.....	79
Scheme 11. DPPA coupling used to synthesize the amide bond of the 5-bromonicotinamides.....	79
Scheme 12. Heck coupling reaction details and yields observed for styrene.....	87
Scheme 13. Heck coupling reaction details and yields observed for methyl acrylate.....	87
Scheme 14. Compounds synthesized using Suzuki procedure D.....	93
Scheme 15. Synthetic route used for the development of 2-(benzylthio)pyridine-3-carboxylic acid.....	99
Scheme 16. Synthetic route used for the development of 2-(benzylthio)pyridine-3-nicotinamides.....	100

Scheme 17. Synthetic route used for the development of 2-(benzylsulfinyl) pyridine-3-nicotinamides.....	101
Scheme 18. Synthetic scheme for the synthesis of 6-aryl-substituted dihydrouracil analogues using Route 1.....	210
Scheme 19: The first two steps of synthetic Route 2 used for the synthesis of the 2,4-dimethoxypyrimidine intermediate.....	212
Scheme 20: Synthetic route used for the synthesis of the lithioarene intermediates.....	213
Scheme 21. The synthetic route used to synthesize the 6-aryl substituted dihydrouracil analogues.....	214



## ABSTRACT

Epilepsy is a chronic neurological disorder whose main feature is the occurrence of recurrent seizures. In spite of the variability in epileptic symptoms, all have a common mechanistic basis, which results from excessive abnormal firing of a group of neurons known as the “seizure focus”. Although new drug therapies are emerging, few offer any significant improvements over the drugs that have been conventionally used.

Drug therapies (anticonvulsants) that are presently available target the process of ictogenesis, “anti-ictogenic drugs” therefore act only to suppress the symptoms of epilepsy. Currently there are no drugs on the market that prevent the process of epileptogenesis, which is the development of a seizure focus after a traumatic brain injury. It is apparent that there is a great need for further research into new drug therapies that cannot only improve upon the anticonvulsants currently available, but also halt the pathological process of epileptogenesis. The primary goal of this research project is to discover a series of new pioneering “antiepileptogenic drugs” designed to prevent the onset of epilepsy after head injury, while also improving upon current “anti-ictogenic drugs”.

The first research goal will be to design and synthesize novel anticonvulsant (antiseizure, anti-ictogenic) drugs based on nicotinamide. Surprisingly, nicotinamide derivatives have not been studied in medicinal chemistry, and their therapeutic potential remains unexploited. Nicotinamide derivatives will be developed as potential anticonvulsants.

The second goal will be to design and synthesize novel anti-ictogenic / antiepileptogenic drugs based on a dihydrouracil structure. Through previous research that revealed the anti-epileptogenic properties of both  $\beta$ -alanine and uracil derivatives, it was concluded that research into the potential of dihydrouracils as putative drugs was an area that was in need of further development. Dihydrouracils derivatives will be developed as potential anti-ictogenic/antiepileptogenic “bioactive” prodrugs.

## LIST OF ABBREVIATIONS AND SYMBOLS USED

Ac:	Acetyl
AcOH:	Acetic acid
ADD:	Anticonvulsant Drug Development Program
ADP:	Adenosine diphosphate
AMBER:	Assisted model building with energy refinement
BBB:	Blood-brain barrier
$\beta$ -Ala:	$\beta$ -Alanine
$\beta$ -AA:	$\beta$ -Amino acid
$^{13}\text{C}$ NMR:	Carbon nuclear magnetic resonance
CoMFA:	Comparative molecular field analysis
CoMSIA:	Comparative molecular similarity indices analysis
CNS:	Central nervous system
D:	Electron donor region
DCC:	1,3-Dicyclohexylcarbodiimide
DCM:	Dichloromethane
DCU:	1,3-Dicyclohexylurea
DMAP:	4-(Dimethylamino)pyridine
DMF:	<i>N,N</i> -Dimethylformamide
DMSO:	Dimethyl sulfoxide
DPPA:	Diphenylphosphoryl azide
EC <sub>50</sub> :	Median effective concentration
EDG:	Electron donating group
EEDQ:	N-Ethoxycarbonyl-2-ethoxy-1,2-dihydroquinoline
EI:	Electron impact
eq.:	Equivalent
ESI:	Electrospray ionization
EtOAc:	Ethyl acetate
EtOH:	Ethanol
GABA:	$\gamma$ -Aminobutyric acid

h:	Hour
HBD:	Hydrogen bonding domain
<sup>1</sup> H NMR:	Proton nuclear magnetic resonance
HRMS:	High resolution mass spectrometry
IC <sub>50</sub> :	Median inhibitory concentration
MeOH:	Methanol
MES:	Maximal electroshock
<i>m</i> CPBA:	3-Chloroperoxybenzoic acid
min:	Minute
MM2:	Molecular mechanics
mp:	Melting point
NAD:	Nicotinamide adenine dinucleotide
NADP:	Nicotinamide adenine dinucleotide phosphate
NAADP:	Nicotinic acid dinucleotide phosphate
NMDA:	<i>N</i> -Methyl-D-aspartate
NMN:	Nicotinamide 5'-mononucleotide
NIH:	National Institute of Health
nOe:	Nuclear Overhauser enhancement
PDB:	Protein Data Bank
PLS:	Partial least squares
PTZ:	Pentylentetrazol
QSAR:	Quantitative structure-activity relationship
rdf:	Receptor description file
s:	Second
TLC:	Thin layer chromatography
TMS:	Tetramethylsilane
THF:	Tetrahydrofuran

## ACKNOWLEDGEMENTS

I wish to extend my thanks to Dr. Donald Weaver, my supervisor for providing me with this opportunity to pursue research that combines chemistry, drug discovery and medicine. I am also very grateful for his guidance, support and knowledge that he has shared with me during all aspects of this project.

I would also like to extend my appreciation to Fan Wu for his unbelievable synthetic help and expertise over the last 5 years, as well as Mike Carter, Musole Buhendwa and Felix Meier-Stephenson for their day-to-day help and support in the lab. I am also very appreciative of Chris, Valerie and Shenna, for all their help, and for making computational chemistry so entertaining.

My thanks is extended to Mike Lumsden and Bob Berno for their assistance with NMR spectroscopy, Xiao Feng for performing the mass spectrometry analysis and Kelly Stevens and Steven Barnes for completing the  $\beta$ -alanine retina staining experiment. I am also very grateful to Cheryl Weaver for all the work she does to keep our lab running smoothly.

I gratefully acknowledge the financial support of scholarships and stipends from the Nova Scotia Health Research Foundation (NSHRF), Epilepsy Canada and Dalhousie University.

Finally I wish to thank my family, and all the special friends in my life for their incredible support, encouragement and love.

## **CHAPTER 1**

### **INTRODUCTION**

---

## **1.1 What Is Epilepsy?**

The word epilepsy is derived from the Greek verb *epilamvanein*, which means “to be seized” or “to be attacked”. The concept of epilepsy has evolved over the centuries; however, the disorder has always been characterized by the manifestation of seizures. Throughout ancient times these seizures were thought to be punishment inflicted by gods or evil spirits on individuals. Epilepsy is characterized as a group of chronic neurological disorders whose common characteristic is the display of recurrent seizures [1]. The clinical symptoms presented by people with epilepsy are quite variable and range in severity from lapses in awareness through to convulsions [2]. In spite of this variability in symptoms, all epileptic seizures result from a central cause: excessive abnormal firing of a group of neurons [3]. This group of neurons, known as the “seizure focus” is always located in a specific region of the brain, most prevalently in the cerebral cortex. This cortical region of the brain is composed of the occipital, parietal, frontal and temporal lobes. The location of the focus in the brain influences the symptoms observed by the seizure. For example, if the focus is located in the motor cortex region, the seizure may begin with shaking of various parts of the body.

## **1.2 Neurons: Activation And Inhibition**

The human brain is composed of nerve cells, known as neurons, that have the ability to generate and transmit electrical signals, known as nerve impulses. These pulses are created when the electrochemical gradient that exists across each neuronal cell membrane is altered. The neuron is composed of the soma, the axon, dendrites and terminal buttons (Figure 1).

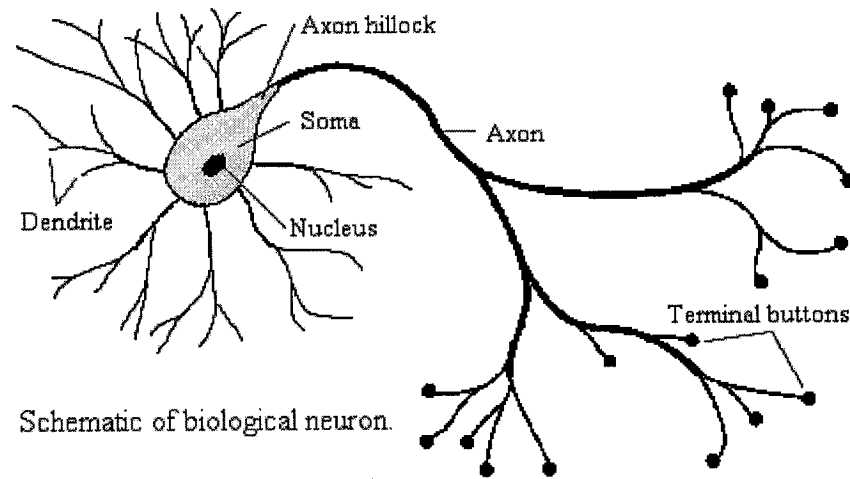


**Figure 1.** The representation of a neuron, showing the various components and direction in which a nerve impulse travels when initiated.

The dendrite is involved in receiving the electrical information from adjacent nerve cells. When excitation occurs, sodium ion channels composed of submicroscopic proteins open in the soma. Since the normal resting potential of the neuron is between -60 to -90 millivolts (with the intracellular compartment being negative relative the extracellular compartment), sodium ions move into the neuron [1, 2]. This produces a localized depolarization (action potential) that induces conformational change in adjacent sodium channels. This generated action potential then travels down the axon until it reaches the terminal buttons, where it stimulates the opening of the voltage-gated calcium channels. The opening of these channels causes an influx of calcium into the neuron, which mediates the release of a chemical messenger known as a neurotransmitter. The

neurotransmitter then diffuses across the synapse (the space between the pre-synaptic and post-synaptic neuron) and binds to an adjacent dendrite receptor where it reinitiates the electrical signal in the neuron.

Neurotransmitters are either excitatory or inhibitory. Excitatory neurotransmitters are those that cause the spread of electrical excitation to adjacent neurons, whereas inhibitory neurotransmitters act to decrease electrical excitation. Examples of excitatory neurotransmitters are the amino acids L-glutamic acid and L-aspartic acid, which are involved in the depolarization of the neuron. Inhibitory neurotransmitters include glycine and  $\gamma$ -aminobutyric acid (GABA) (Figure 2). In the case of epilepsy, a prolonged depolarization results. This is due to an increase in excitation or lack of inhibition in the seizure focus area where the abnormal discharge originated [4].

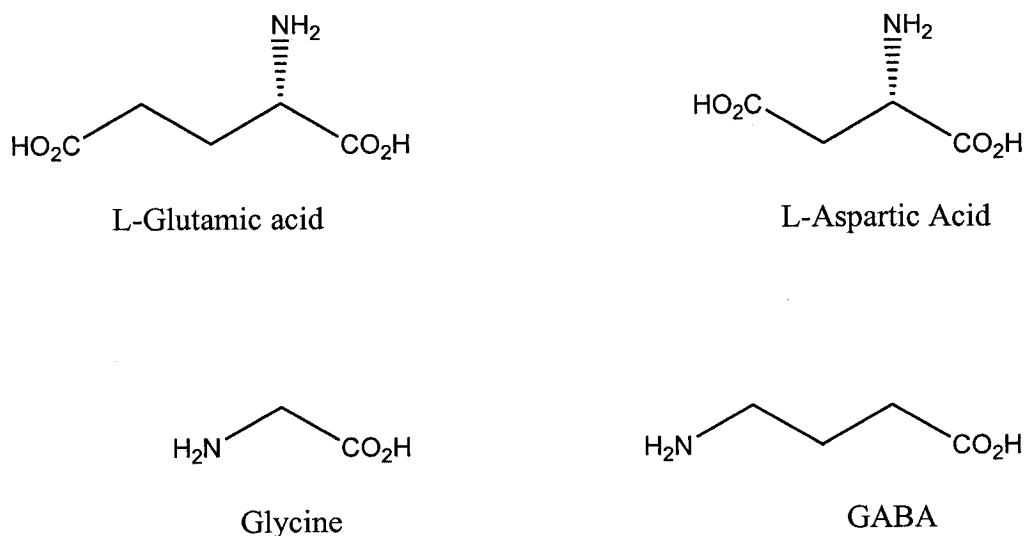


**Figure 2.** The excitatory and inhibitory neurotransmitters in the CNS.



### **1.3 Targets For Anticonvulsant Drug Development**

Three main, recognized targets for the development of anticonvulsant drugs are: voltage-gated ion channels, GABAergic enhancement, and glutamergic inhibition.

#### **1.3.1 Voltage-Gated Ion Channels**

For controlling epilepsy, one of the first target areas that is exploited is the voltage-gated ion channel, such as the  $\text{Na}^+$ ,  $\text{Ca}^{2+}$ , or  $\text{K}^+$  channel. The ion channels are important in controlling the directional influx of specific ions both into and out of the neuronal cell.

Of the channels available, the  $\text{Na}^+$  channel is of primary importance for correct functioning of the CNS and is particularly involved in controlling the excitability and action potential of the neuron. The  $\text{Na}^+$  channels are responsible for the initiation and propagation of an action potential in the neuron. These channels are located at the nodes of Ranvier, the dendrites and synapses [5]. When neurons are in their resting position the sodium channels are closed; however when depolarization occurs the channels open, allowing for an influx of  $\text{Na}^+$  into the neuron. Once the appropriate number of ions has crossed through the channel, the  $\text{Na}^+$  channels are inactivated, making it difficult to remove the excess  $\text{Na}^+$  from the internal portion of the neuron [3, 6]. This process of inactivation is an important mechanism preventing excessive firing of a group of neurons [7]. In epilepsy the sodium channels remain in the open position, and this allows a continuous influx of  $\text{Na}^+$  in the neuron, leading to excessive firing and stimulation of the neuron (Figure 3).

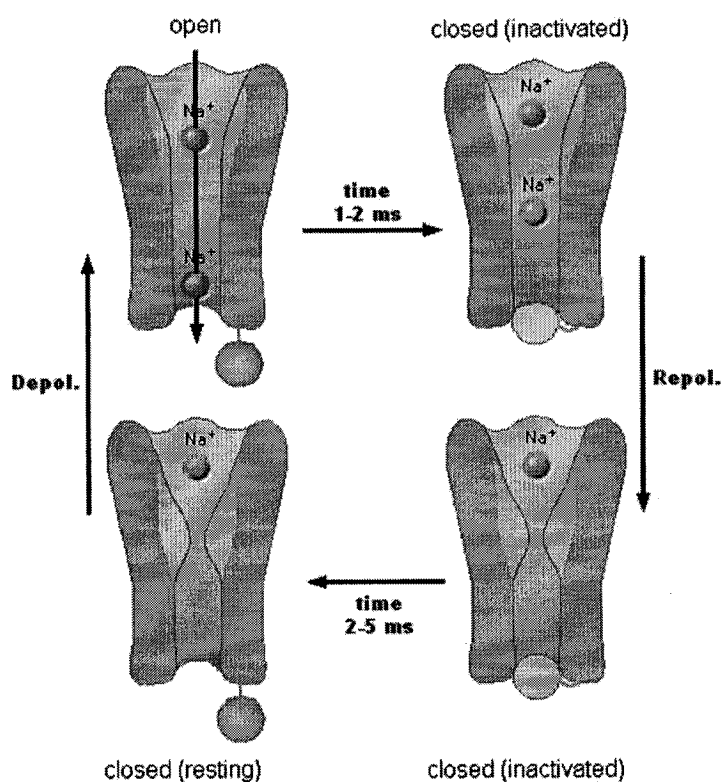


**Figure 3.** The sodium channel as it moves through its various stages; from its resting state to the active open channel to the inactive blocked channel ([http://www.clabs.de/na\\_ch.jpg](http://www.clabs.de/na_ch.jpg)).

Despite this inactivation, the neuronal cells return to their resting potential through another group of channels known as the  $\text{K}^+$  channels. When these channels open,  $\text{K}^+$  moves into the neuron allowing for  $\text{Na}^+$  to be pumped back out into the extracellular space, eventually resulting in a return to the correct charge balance between the inside and the outside of the neuron.  $\text{K}^+$  channels play a fundamental role in the repolarization of the neuron and are another key drug design location for epilepsy. By activating the  $\text{K}^+$  channel, the action potential firing of the neuron will be limited and controlled. Drug candidates that can act as  $\text{K}^+$  channel agonists will exhibit anticonvulsant effects, while  $\text{K}^+$  channel antagonists will induce seizure activity by preventing hyperpolarization of the neuron.

The final ion channel that is an important target in the design of new epilepsy treatments is the  $\text{Ca}^{2+}$  channel. The  $\text{Ca}^{2+}$  channels are located throughout the CNS on cell bodies, dendrites and nerve terminals and are involved in controlling the release of neurotransmitters at the synapse. By acting at these receptors, specific neurotransmitters that are released in a calcium dependent manner could be controlled. By developing drugs that act as either agonists or antagonists of the  $\text{Ca}^{2+}$  channel, new epilepsy treatments could result.

While the targeting of various ion channels in the CNS is a widely accepted route for the development of new epilepsy treatment drugs, there are other more influential targets in the CNS.

### 1.3.2 GABAergic Enhancement And Receptors

GABA is recognized as the principal inhibitory neurotransmitter in the cerebral cortex and acts to counterbalance neuronal excitation [8]. GABA is formed in the terminal buttons by transamination of  $\alpha$ -ketoglutarate to glutamic acid, followed by decarboxylation to form GABA (Figure 4).

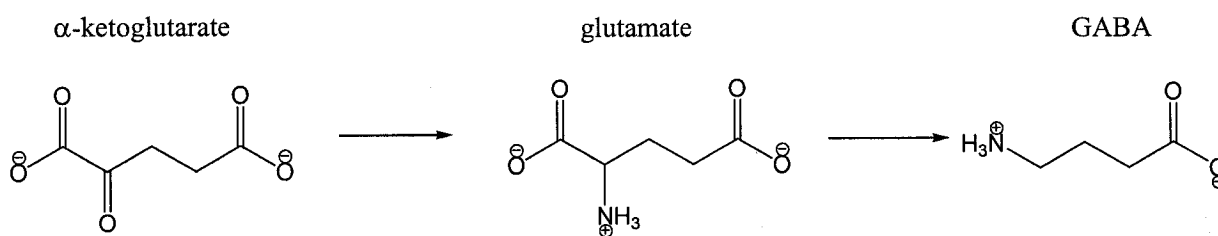


**Figure 4.** Biochemical route for the formation of GABA

Once this inhibitory neurotransmitter is released into the synapse it can act on one of three available receptors, GABA<sub>A</sub>, GABA<sub>B</sub>, and GABA<sub>C</sub>. The GABA<sub>A</sub> receptors have the ability to hyperpolarize the neuron by increasing the inward flow of chloride (Cl<sup>-</sup>) into the neuron, thus helping to restore the neuronal resting potential (Figure 5). These receptors are fast acting and are the most important in controlling neuron hyperexcitability. The GABA<sub>B</sub> receptors are responsible for decreasing the calcium entry and increasing potassium conductance into the neuron, therefore producing a slow inhibitory effect [8]. The GABA<sub>C</sub> receptors are located primarily in the retina and are not involved in controlling CNS functions [8]. GABA is taken up from the synaptic cleft by transporters on either the presynaptic neuron or by the glial cells. Glial cells are contained within the CNS and provide support for neurons by supplying them with essential chemicals and breaking down neurotransmitters in the synaptic cleft [1, 2]. Neurotransporters are involved in removing neurotransmitters from the synapse therefore terminating excitation/inhibition as well as playing an important role in neuroregulation [9].

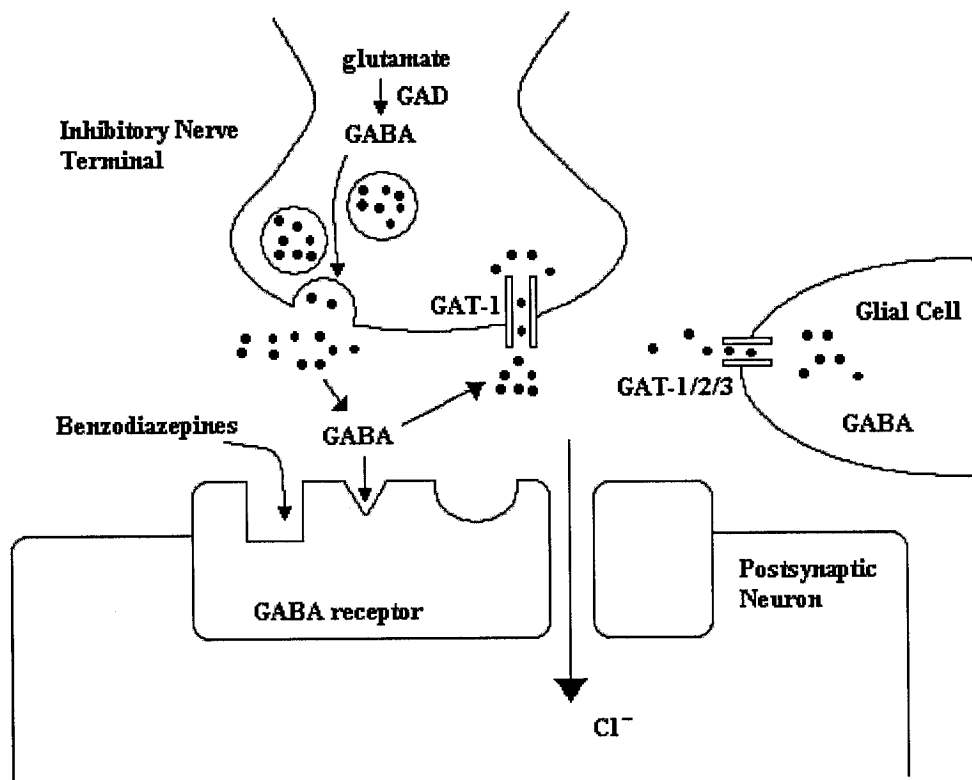


**Figure 5.** The representation of the GABA<sub>A</sub> receptor, which is located on the post-synaptic cleft and is associated with ion channel permeability to  $\text{Cl}^-$  ions. When GABA binds to its appropriate site it increases the inward flow of  $\text{Cl}^-$  thus helping to restore the neuronal resting potential. It can also be noted that barbiturates also have the ability to bind to the GABA<sub>A</sub> receptor and exhibit similar abilities to reduce neuronal excitation.

Four GABA transporters (GAT) have been identified, each having a unique localization in the brain. GAT-1 has been found on both neurons and glial cells and transports GABA exclusively [10]. GAT-2 and GAT-3 are glial cell localized and transport both GABA and  $\beta$ -alanine. It has also been found that GABA uptake in these transporters is inhibited by  $\beta$ -alanine [9, 11, 12]. Both these transporters are also involved in regulating the concentration of GABA in the CNS. GAT-4 is thought not to be concentrated in the CNS for the uptake of GABA.

### 1.3.3 Glutamergic Inhibition And NMDA/Glycine Receptors

Another important neurotransmitter is glycine, which shows inhibitory and excitatory effects. The glycine receptors in the CNS are the strychnine-sensitive site, primarily located in the brain stem and spinal cord, and the strychnine-insensitive site, found on the *N*-methyl-D-aspartate (NMDA) receptors located throughout the brain [8]. Glycine shows inhibitory effects at the strychnine-sensitive site and excitatory effects at the strychnine-insensitive site. The NMDA receptor is widely distributed in the brain and spinal cord on the dendrites of postsynaptic neurons and when NMDA is activated it controls the opening of ion channels that are permeable to  $\text{Na}^+$ ,  $\text{K}^+$  and  $\text{Ca}^{2+}$ . For proper activation of the receptor, occupation by both glutamate and glycine subunits is required. Therefore, the NMDA receptor can be blocked by antagonists that act at either the glutamate or glycine site. Since the NMDA receptor allows for the influx of cations into the neuron, it is considered to exhibit properties that are implicated in neuronal hyperpolarization [10] (Figure 6).

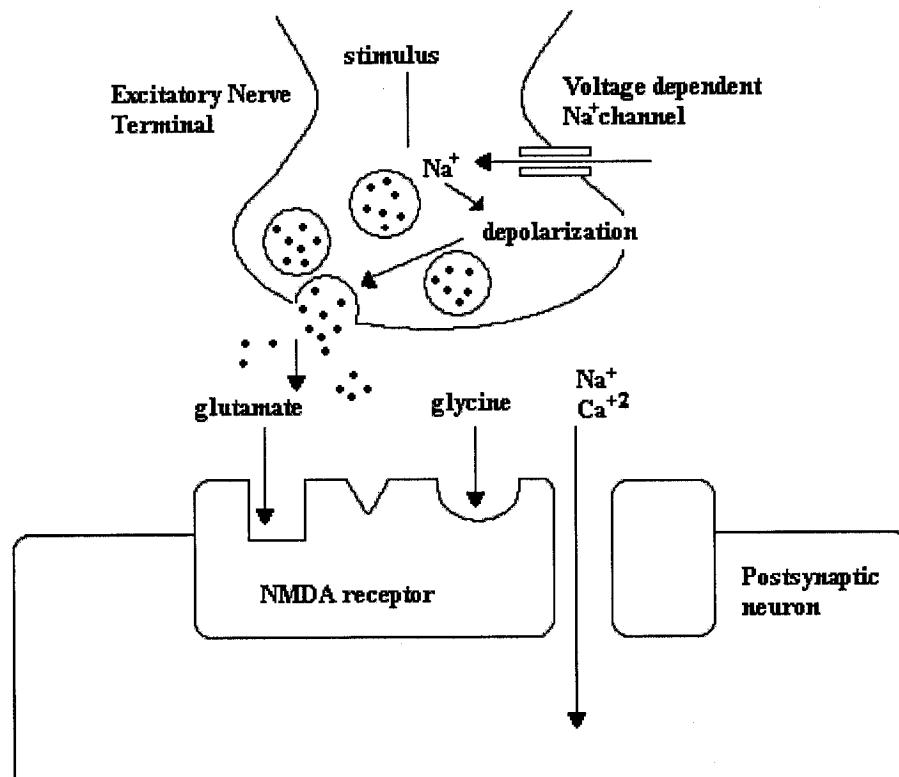


**Figure 6.** The representation of the NMDA receptor, which is located on the post-synaptic neuron and is associated with ion channel permeability to Na<sup>+</sup>, and Ca<sup>+2</sup> ions. This receptor is involved with excitation of neural activity, which requires both glutamate and glycine binding to their associated receptor sites in order to be initiated.

Through this background information it can be seen that a lack of GABA-mediated inhibition and an increase in NMDA receptor functioning can lead to a prolonged depolarizing potential which is seen in an epileptic seizure focus. Therefore epilepsy could be potentially controlled by increasing the amount of available GABA in the brain, decreasing excessive NMDA activation, and controlling ion channels.

## 1.4 The Blood-Brain Barrier

When developing new drugs for the CNS, there are some important physiological differences between the brain and the rest of the body that need to be accounted for. The most influential of these is the blood-brain barrier (BBB). The BBB is important in segregating the circulating blood of the body from the interstitial fluid in the brain and spinal cord [1, 3], providing a protective barrier from harmful toxins and pathogens. There are two important anatomical features that make brain capillaries unique. The first is the presence of high-resistance, epithelial-like tight junctions. These tight junctions prevent free diffusion across the capillary wall via para-cellular routes. Second is the minimal endothelial pinocytosis, which removes the trans-cellular route for the free movement of solutes into the brain.

The BBB allows for the passage of lipid-soluble or water-soluble substances (e.g. oxygen and CO<sub>2</sub>), nutritional molecules with a molar mass less than 600 g/mol, and molecules with a distribution coefficient (logP) between 1.5 and 3, thus preventing the movement of highly charged molecules into the brain [13]. Potential candidate drugs must have the capability to cross the BBB, which is one of the most important limiting agents for delivering drugs to the CNS [14]. When new therapeutic agents are being developed to target neurological disease, their molecular weight and logP values are important considerations that must be evaluated and accounted for early in the drug development process.



## **1.5 Classification Of Epilepsy**

The classification of epilepsy is important in daily clinical practice and is based on the aetiology of the disorder and its location in the brain. Aetiology assumes that epilepsy is the result of either an acquired lesion in the brain, known as symptomatic, or due to an inborn error in metabolism known as idiopathic. The classification of the seizure is based on clinical symptoms and the characteristics of the electrocephalogram (EEG). These classifications are important for prognosis and for the choice of the therapeutic medication. Although the functionings of the brain are not always well predicted, the classification of seizures is a useful tool for the proper treatment of epilepsy patients. Provided below in detail are the various groupings of epilepsy disorders.

### **1.5.1 Partial Seizures**

Partial seizures are those where the EEG changes in a characteristic fashion in only one hemisphere of the brain. They are categorized into two main types: simple partial seizures and complex partial seizures [15].

### **1.5.2 Simple Partial Seizures**

In simple seizures consciousness is not impaired, however the individual loses some muscle control, leading to involuntary twitching of the muscles on one side of the body. Since these seizures typically involve only one hemisphere of the brain, there is often altered sensations in specific parts of the body as well as turning of the head and

eyes. These seizures have the capability of proceeding to complex partial or generalized seizures over time [1, 15].

### **1.5.3 Complex Partial Seizures**

In complex seizures there is a definite change in consciousness leading to the impairment of awareness and/or responsiveness. They often begin as simple partial seizures and then eventually begin to involve both hemispheres of the brain leading to generalized seizures. They have similar physical impairments as those recognized with simple partial seizures [1, 15].

### **1.5.4 Generalized Seizures**

With generalized seizures the activity of the seizure involves both hemispheres of the brain and results in major motor movement throughout the entire brain. They are categorized into two main areas: tonic-clonic seizures and absence seizures [1, 15].

### **1.5.5 Tonic-Clonic Seizures**

These seizures were formally known as grand-mal seizures and last between one and seven minutes. These seizures are tonic since there is a loss of consciousness, stiffening of the body and falling; and clonic since the limbs of the patient during the seizure often appear to jerk and twitch [1, 15].

### **1.5.6 Absence Seizures**

These seizures were originally categorized as a petit-mal seizures and last between one and five seconds. In these seizures there is a brief loss in awareness which often appears as daydreaming but with no memory of the event. In some cases there may be mild clonic movements associated with the body [1, 15].

## **1.6 Epileptogenesis And Ictogenesis**

Epileptogenesis is a gradual process whereby a normal brain is transformed into a state susceptible to spontaneous recurrent seizures, through the initiation and maturation of a seizure focus. This process of developing a seizure focus occurs over months to years following a traumatic brain injury and is a slow process that alters the brain both biochemically and histologically, resulting in the appearance of seizures [16].

Through research it has been found that epileptogenesis is a two-phase process. Phase 1 is characterized as the initiation of the epileptogenic process as a result of a stroke, CNS infection, or brain trauma (from a blow to the head due to a car accident, or sports injury). Phase 2 refers to the process during which an individual who is already susceptible to seizures shows an increase in the frequency and severity of the seizures. It is hypothesized that epileptogenesis may arise due to the “up-regulation” of excitatory routes, mainly at the NMDA receptor [17]. Other researchers implicate the “down-regulation” of inhibitory coupling between neurons which are controlled by the GABA receptors [17]. This change in neuronal regulation may result in the development of an epileptic focus after head trauma [17]. It has been found that activation of the NMDA

receptors in epileptic patients occurs under conditions that do not appear to result in neuronal activation in an unaffected individual [11].

Ictogenesis is a rapid event that occurs over a few seconds and leads to the initiation of a seizure through a series of chemical and electrical events. Presently all drugs on the market are anticonvulsants and target this process of ictogenesis (Figure 7). The drugs currently on the market for the treatment of epilepsy only suppress the symptoms and do not have the capability of influencing the process of epileptogenesis.

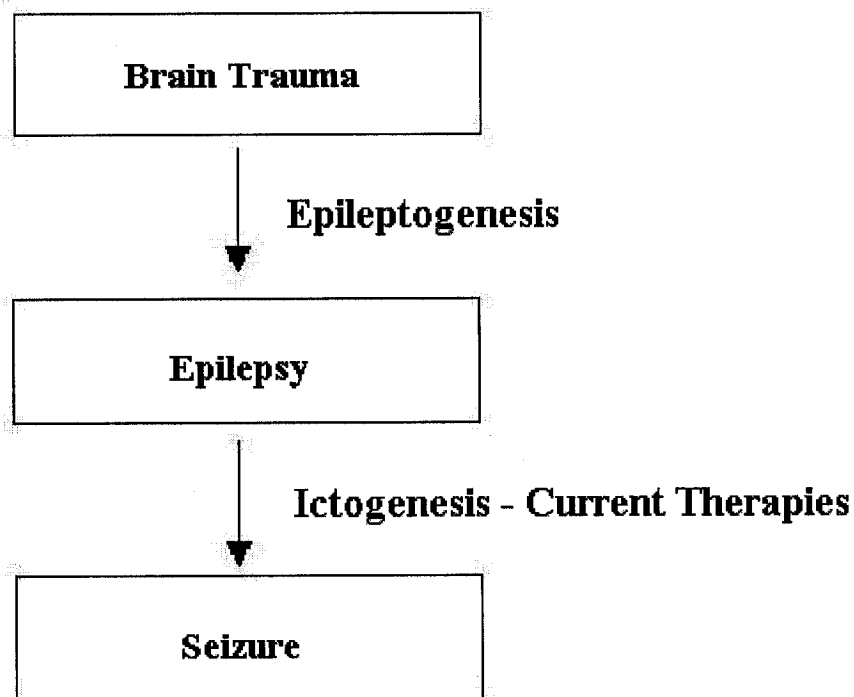


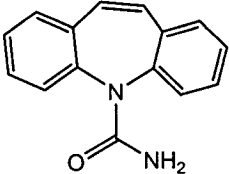
**Figure 7.** Current drug therapies available target the process of ictogenesis. Presently there are no drugs available to prevent the process of epileptogenesis, creating a new target for the treatment of epilepsy.

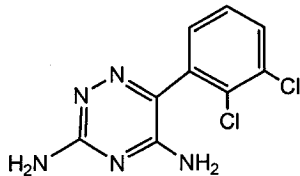
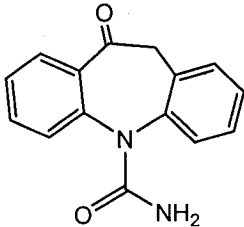
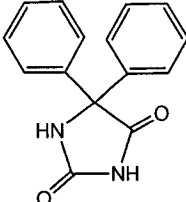
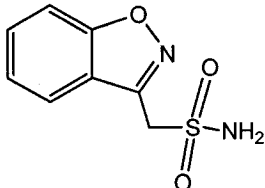
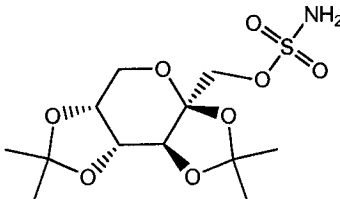
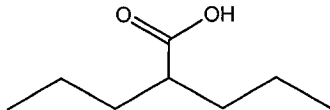
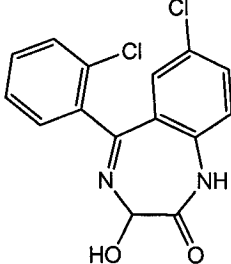
Although many new drug therapies are emerging, few offer any significant improvement over the drugs that have been conventionally used. Many anticonvulsant drugs, which do help to suppress seizures, also have adverse side effects, which range from uncomfortable and inconvenient to life-threatening. Indeed for up to one-third of epilepsy patients [18, 19], current drugs fail to adequately control their symptoms; therefore, new therapeutic agents are desired [20].

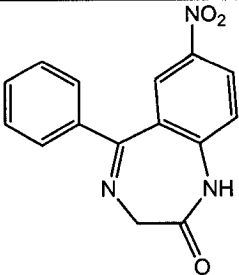
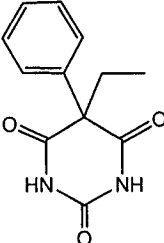
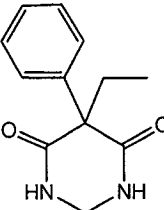
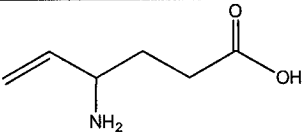
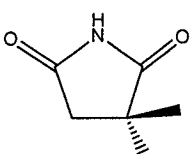
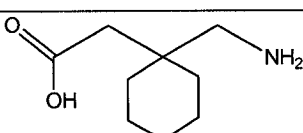
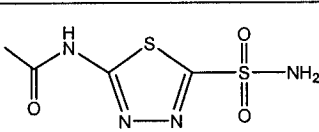
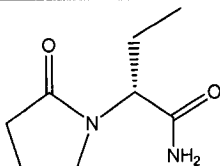
### 1.7 Current Drug Treatments

A variety of drugs are available for the management of epileptic seizures. Epileptic seizures are rarely fatal; however, for a large number of patients, medication is required to alleviate the symptoms associated with epilepsy and to avoid the disruptive and potentially dangerous consequences. For many patients who suffer from epilepsy, prescription medication is required for an extended period of time or is taken for life [1, 21]. All the current drugs for epilepsy are anticonvulsant agents also known as anti-seizure, or anti-ictogenic drugs, which suppress seizures by preventing the process of ictogenesis. Drugs that are currently on the market are categorized based on the CNS receptors that they target (Table 1).

**Table 1.** Summary of current anti-ictogenic therapies including their molecular targets and the seizure classifications they effect.

Drug Generic Name	Chemical Structure	Molecular Target	Seizure Classification
Carbamazepine		Na <sup>+</sup> -channel antagonist	Generalized tonic-clonic, simple partial, complex partial

Lamotrigine		Na <sup>+</sup> -channel antagonist	Simple partial, complex partial, generalized tonic-clonic, generalized absence
Oxcarbazepine		Na <sup>+</sup> -channel antagonist	Generalized tonic-clonic, simple partial, complex partial
Phenytoin		Na <sup>+</sup> -channel antagonist	Generalized tonic-clonic, simple partial, complex partial
Zonisamide		Na <sup>+</sup> -channel antagonist	Simple partial, complex partial, somewhat effective against generalized tonic-clonic, generalized absence
Topiramate		Na <sup>+</sup> -channel antagonist; GABA <sub>A</sub> agonist; AMPA-antagonist; Carbonic anhydrase inhibitor	Adjunctive therapy for generalized seizures, effective against absence, tonic-clonic and Lennox-Gastaut syndrome
Valproic acid		Na <sup>+</sup> -channel antagonist	Atonic, myoclonic, infantile spasms, generalized tonic-clonic, generalized absence, simple partial, complex partial
Lorazepam		GABA <sub>A</sub> receptor agonist	Status epilepticus.

Nitrazepam		GABA <sub>A</sub> receptor agonist	Myoclonic and infantile spasms such as West's syndrome
Phenobarbital, Barbiturate		GABA <sub>A</sub> receptor agonist	Myoclonic, simple partial, generalized tonic-clonic
Primidone		GABA <sub>A</sub> receptor agonist; Na <sup>+</sup> -channel antagonist	Generalized tonic-clonic, simple partial, complex partial
Vigabatrin		Inhibits GABA transaminase	Simple partial, complex partial
Ethosuximide, Succinimide		T-type Ca <sup>2+</sup> -channel blocker in the thalamus	Generalized absence seizures
Gabapentin		Ca <sup>2+</sup> -channel antagonist	Simple partial, complex partial, generalized tonic-clonic
Acetazolamide		Carbonic anhydrase inhibitor	Generalized absence seizures
Levetiracetam		Not well understood	Simple partial, complex partial, somewhat effective against generalized tonic-clonic

The traditional drugs that have been used for the treatment of epileptic symptoms include phenobarbital, carbamazepine, phenytoin, valproate, primidone, and benzodiazepines (diazepam, lorazepam and clonazepam) (Figure 8).

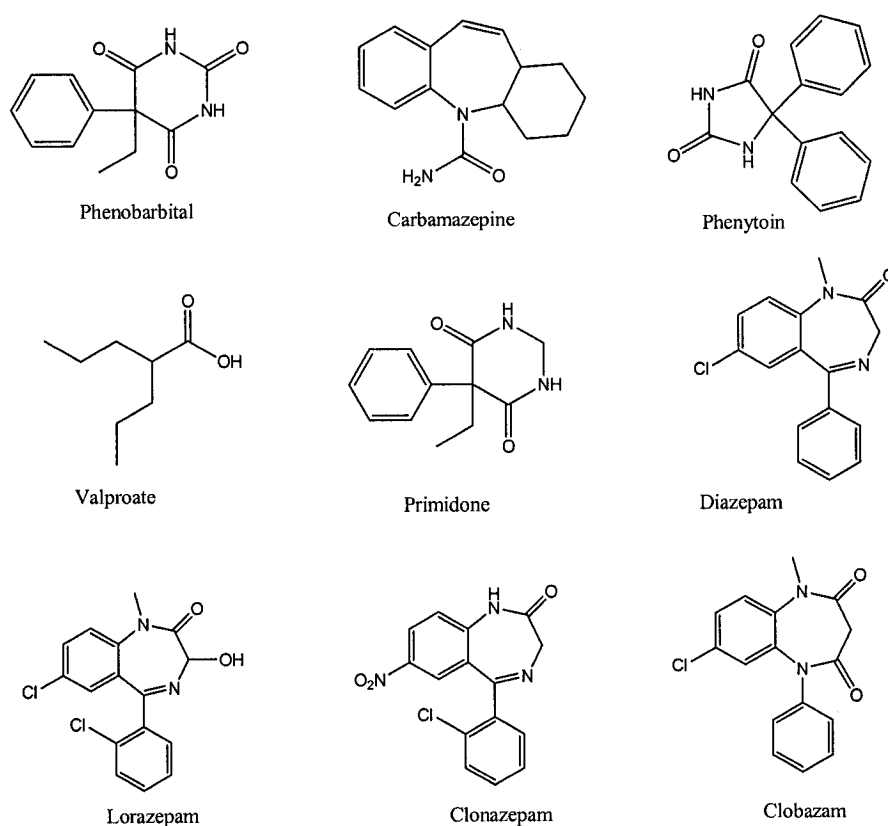


**Figure 8.** Structures of current anticonvulsant drugs.

### 1.7.1 Phenobarbital

Phenobarbital is a member of the barbiturate family and has been used since the early 1900's as a sedative, anaesthetic and anticonvulsant [1, 21]. Barbiturates are a nonselective CNS depressant, the extent of the activity varies depending on the route of administration and dosage. Their main pharmacological effects are exerted through allosteric activation of the GABA<sub>A</sub> receptor, therefore increasing the duration of the Cl<sup>-</sup>



channel opening without affecting the frequency of the channel opening or conductance [1, 21]. They act by enhancing the synaptic action of GABA and still show sedative effects even in the absence of GABA. Another mechanism of action involves the blockage of the  $\text{Ca}^{2+}$  channels and direct inhibition of the AMPA/kinate subtypes of the glutamate receptor. Despite its ability to control generalized tonic-clonic and complex partial seizures, side effects associated with phenobarbital include behavioural and cognitive changes.

### **1.7.2 Carbamazepine**

This drug was introduced in 1963 and is similar in structure to the tricyclic antidepressants. It has the ability to control seizure activity by stabilizing the inactive form of the  $\text{Na}^+$  channel in a frequency, voltage, and time-dependent manner [1, 21]. By maintaining the  $\text{Na}^+$  channel in an inactive conformation the repetitive firing of a neuron is prevented thus reducing seizure activity. These drugs are also known to inhibit the glutamergic system by blocking the release of endogenous glutamate, leading to inhibition of the NMDA receptor and preventing a rise in intracellular  $\text{Ca}^{2+}$  [1, 21]. Carbamazepine is usually used for the treatment of partial and generalized tonic-clonic seizures.

### **1.7.3 Phenytoin**

Phenytoin (Dilantin) was discovered in 1938 during a screening program using a newly developed cat model of epilepsy. Its main mechanism of action is through binding to the fast-inactivated state of the  $\text{Na}^+$  channel, helping to reduce repetitive firing of the

action potential in a neuron. This inhibition is dependent on the voltage and increases after depolarization has occurred in a neuron. Although it exhibits similar activity to carbamazepine, it has a lower binding rate constant and a higher affinity for the inactive  $\text{Na}^+$  channel, therefore reducing possible dose-associated side effects. Phenytoin is used in the treatment of partial and generalized seizures.

#### **1.7.4 Valproate**

Valproate as a drug was discovered in a serendipitous manner, since it was used as a solvent for other drugs being studied for anticonvulsant properties. Although its precise mechanism of action is unknown, it is believed to be involved in again blocking the  $\text{Na}^+$  channel in a voltage-dependent manner. Another possible action is that valproate enhances GABA production while inhibiting its metabolism, therefore elevating brain GABA levels. Its final proposed mechanism of action is that it decreases the CNS level of aspartate an excitatory neurotransmitter, without affecting the concentration of GABA in the brain. Its main treatment is for simple and complex absence seizures, including petit mal, and primary generalized tonic-clonic seizures.

#### **1.7.5 Benzodiazepines**

The benzodiazepines encompass a significant number of currently available anticonvulsant drugs including diazepam, lorazepam, clonazepam and clobazam. Their main mechanism of action is allosteric activation of the  $\text{GABA}_A$  receptor allowing for an increase in the frequency of  $\text{Cl}^-$  channel opening, helping to restore the resting potential of the neuron. However, unlike barbiturates, benzodiazepines are unable to activate

directly the GABA<sub>A</sub> receptor since GABA needs to be present as well [22]. These compounds have been used for the treatment of partial and idiopathic generalized epilepsies as well as *status epilepticus*. The tendency to develop tolerance to these drugs has restricted their use as a general treatment [23].

Some of the anti-ictogenic drugs that have appeared on the market in the past 20 years attempt to improve upon those available while reducing the associated side effects. Some of these new drugs include vigabatrin, lamotrigine, oxcarbazepine, felbamate, and leviteracetam (Figure 9). They all exhibit better pharmacokinetics and better tolerability.

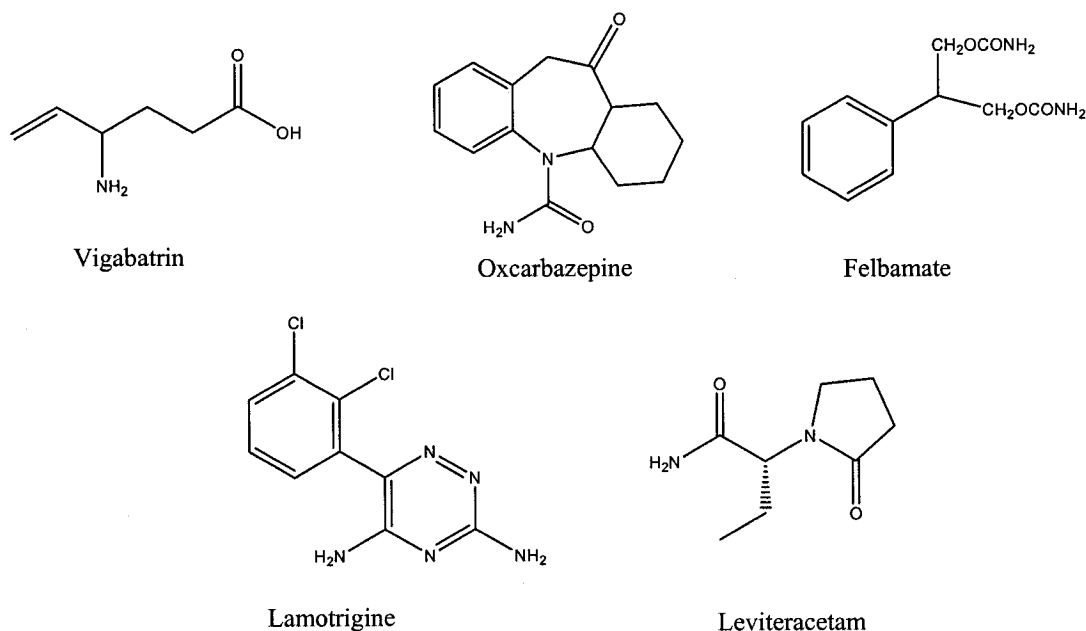


**Figure 9.** Current anticonvulsant structures.

### **1.7.6 Vigabatrin**

Originally released in 1989, vigabatrin was in the first wave of new anticonvulsant therapies. Its main mechanism of action is inhibition of the GABA transaminase (GABA-T) enzyme, which is responsible for the catabolism of CNS GABA. By inhibiting this enzyme, GABA levels in the CNS are elevated therefore increasing inhibitory transmission in the brain. Since vigabatrin is a vinyl analogue of GABA it is postulated to also block glial uptake of GABA. It is mainly used for the treatment of partial seizures [21].

### **1.7.7 Lamotrigine**

Lamotrigine mechanism of action is through inhibition of the  $\text{Na}^+$  channel by inhibiting sustained action potential firing, blocking the  $\text{Na}^+$  channel in a voltage dependent manner. This drug acts mainly on the slow inactivated state of the  $\text{Na}^+$  channel and selectively targets neurons that synthesize the excitatory neurotransmitters glutamate and aspartate [19, 21].

### **1.7.8 Oxcarbazepine**

The chemical structure of oxcarbazepine is similar to carbamazepine, and its structural differences lead to a better metabolism and tolerance, while maintaining an equivalent therapeutic profile. This drug is a pro-drug approach, as its ketone functional group is rapidly reduced by the liver. Its mechanism of action involves blockage of the  $\text{Na}^+$  channel and a reduction in the release of presynaptic glutamate, increasing  $\text{K}^+$  channel conductance [19, 21].

### **1.7.9 Felbamate**

Felbamate is known to have multiple mechanisms of action. These include reduction of voltage-dependent  $\text{Na}^+$  currents, direct inhibition of the NMDA subtype of the glutamate receptor, and inhibition of the high voltage-activated  $\text{Ca}^{2+}$  channel [19]. It is the first anticonvulsant of its kind to inhibit the NMDA/glycine stimulated increase in intracellular  $\text{Ca}^{2+}$ , therefore reducing inward currents caused by the NMDA receptor and blocking NMDA-receptor-mediated excitatory post-synaptic potentials [19].

### **1.7.10 Leviteracetam**

This drug is the most recently FDA approved anticonvulsant drug on the market, however its mechanism of action is still not well understood. Studies that have been conducted have eliminated the interaction of this drug with any of the traditional sites of action including  $\text{Na}^+$ ,  $\text{Ca}^{2+}$ , and the  $\text{K}^+$  ion channels as well as the GABA and glutamate neurotransmitter systems. Its activity and pharmacodynamics are believed to be specific but are still not known [19].

## 1.8 Need For New Treatment Options

Despite the new drugs for the treatment of epilepsy that have appeared on the market over the past decade, proper seizure control is still a major concern. The drugs that are used also have negative side effects associated with their drug scaffold and toxicophore faces. Although new anticonvulsants are more selective in their mechanism of action, harmful side effects are still a major concern that needs to be dealt with. By understanding the mechanism of action associated with the drug's pharmacophore and determining the toxicophore face, development of new drugs that can maintain seizure control while alleviating side effects would be beneficial. Some of the common and adverse side effects associated with the drugs discussed above are available below in Table 2 [21, 24, 25] .

**Table 2.** Side effects associated with some of the new common anticonvulsant drugs.

<b>Drug</b>	<b>Common Side Effects</b>	<b>Adverse Side Effects</b>
Felbamate	Nausea/vomiting, headache, insomnia, behavioral disturbances	Aplastic anemia, hepatotoxicity
Vigabatrin	Weight gain, sedation, fatigue, dizziness, behavior disturbances	Depression, psychosis, blindness
Lamotrigine	Blurred vision, dizziness, headache, fatigue	Depression, fatal skin rash
Oxcarbazepine	Fatigue, headache, dizziness, ataxia	Skin rashes
Leviteracetam	Dizziness, fever, loss of strength, pain, drowsiness	Depression, painful urination, trouble breathing, pain, psychosis

## **1.9 Epilepsy Treatment: Present And Future**

Several important mechanisms at the cellular level have been identified for the treatment of epilepsy. These mechanisms include the modulation of voltage-dependent ion channels, attenuation of excitatory neurotransmitters and enhancement of inhibitory neurotransmitters [11, 26]. Therefore when developing new drugs, it is highly preferable that they have the ability to interact simultaneously at several different target sites that show the possibility to control neural activity [6]. This reduction in activity that would be produced at each of the different target sites could potentially act synergistically to create a neuroprotective effect [6]. Maximizing drug activity at several specific target locations in the brain could potentially reduce the drug's interference at other non-targeted locations, therefore optimizing therapeutic treatment for epilepsy and minimizing side effects [18].

The NMDA receptor and GABA are involved in the processes of both ictogenesis and epileptogenesis [27-29]. When GABA concentrations in the human brain are increased, it has been found that anticonvulsant properties are observed [30]. Through research, it has been proposed that drugs that could be converted to GABA endogenously or are able to structurally mimic GABA, show great potential of enhancing inhibition, thereby preventing seizures. By presenting the brain with a structure similar to GABA, it is thought that the GAT-1, -2, and -3, transporters may take up this GABA mimic, therefore increasing the amount of available true GABA in the synaptic cleft for inhibitory effects. Alternatively, or perhaps simultaneously, the NMDA receptor could be inactivated by binding an antagonist at its glycine site. Binding at this site would block the conformational change in the receptor protein required for the binding of glutamate,

thereby preventing the influx of ions into the neuron. Since epilepsy is a result of improper functioning of a group of neurons by both excessive excitation and a deficiency in inhibition, drugs that target these imbalances could have the potential to be novel treatment drugs. A drug that has the capability of increasing the amount of available GABA by being structurally similar to GABA, acting as an NMDA glycine receptor site antagonist as well as influencing ion channels, could protect against the development and symptoms of epilepsy [20].

### **1.9.1 Endogenous Molecules**

The CNS produces numerous chemicals that exhibit powerful controlling effects on the body. These substances are known as “endogenous” molecules, from the Greek word meaning “made within”. These natural compounds have known biological activity and control many biochemical processes in the body. Endogenous compounds are also useful starting points in the development of new drugs since they are biologically active, have low toxicity, and are ligands for specific receptors. By understanding their mode of action and receptor targets, endogenous CNS compounds could provide a useful platform from which new drug candidates could be developed to treat specific diseases like epilepsy, which has a well understood etiology.

Important evidence exists for the presence of an endogenous anticonvulsant substance. Epileptic seizures are normally arrested spontaneously followed by a protective refractory stage for the brain. During this post-ictal period the likely onset of another seizure is greatly reduced. It is now believed that this refractory period is controlled by the release of seizure-induced endogenous molecules that exhibit



anticonvulsant properties, rather than the previous hypotheses of neuronal fatigue [31]. Neuropeptides, which are small peptidergic compounds that are available in the CNS, have been proposed as endogenous mediators of epilepsy. Many of these neuropeptides, like the adrenocorticotrophic hormone, opioid peptides, vasopressin, somatostatin, and some hypothalamic releasing factors, have demonstrated endogenous roles in the post-ictal phase in some forms of epilepsy. After a seizure these endogenous compounds are important in mediating the post-ictal seizure refractory period by limiting the spread of seizure activity and modulating susceptibility of the brain to further seizures [32, 33]. Although this protective effect has been documented, no endogenous anticonvulsant molecule has yet been recognized and researched extensively.

In the search for an endogenous compound for the treatment and prevention of epilepsy, receptor targeting is crucial. The voltage-gated sodium channel is central to the process of ictogenesis, while the GABA and NMDA receptors are central to epileptogenesis [20].

After extensive literature review, several endogenous molecules were chosen on the basis of their receptor properties as suitable molecular platforms for the development of new epilepsy treatments. They can be categorized into two main types: anti-ictogenic (anticonvulsant) and anti-epileptogenic endogenous agents. The present research involves the development of two new classes of therapeutic molecules: (1) nicotinamide derivatives which act as anti-ictogenic agents and (2) dihydrouracil derivatives which act as anti-epileptogenic agents. By using these two endogenous molecular platforms, a comprehensive treatment of epilepsy can be obtained.

### 1.9.2 Goal Of Thesis

The overall goal of this thesis was to devise new therapeutic approaches to epilepsy based on endogenous molecules. This was a novel approach since most conventional drugs for epilepsy were purely synthetic molecules. To achieve this goal, the thesis was divided into four parts.

Part A (Chapters 1, 2) discusses the basic background principles of epilepsy and drug design. Part B (Chapters 3, 4, 5) discusses the design and discovery of novel nicotinamide anticonvulsants developed as analogues of endogenous compounds. Chapter 3 discusses the identification of N(H)-C(=O)-X-aromatic as an anticonvulsant molecular fragment. Chapter 4 designs nicotinamides containing this fragment and discusses nicotinamides as an endogenous platform for drug design. Chapter 5 presents an optimization of nicotinamides using quantitative structure-activity relationship calculations.

Part C (Chapter 6, 7, 8) discusses the design and discovery of novel dihydrouracil antiepileptogenics developed as analogues of endogenous compounds. Chapter 6 presents the design and synthesis of dihydrouracil analogues as antiepileptogenic agents that are  $\beta$ -amino acid pro-drugs. Chapter 7 uses molecular modeling of enzyme active sites to demonstrate the metabolic activation of dihydrouracils. Chapter 8 uses additional molecular modeling calculations to demonstrate that these compounds are anti-ictogenic/antiepileptogenic hybrids. Part D presents conclusions and future directions.

## **CHAPTER 2**

### **DRUG DISCOVERY AND DEVELOPMENT**

---

## **2.1 Medicinal Chemistry: A Definition**

Medicinal chemistry is the design, synthesis and evaluation of molecules for the treatment of a specific disease. In order to develop new drugs, the biochemical mechanisms of the disease process must be well understood so that receptor targeting can be achieved. Drugs can be categorized into two main treatment areas: symptomatic or curative [34]. Symptomatic drugs help to alleviate the symptoms that are often associated with a disease in order to increase the quality of life for the patient. Curative agents are used to prevent or halt the progress of a disease.

Drug discovery as a science is still considered to be a new area of research and is less than a century old [34-36]. Once the fundamentals of chemistry were well understood they could easily be applied to the area of drug discovery and allow for its development as an independent research area. Drug discovery based on chemistry has contributed more to the progress of medicine than any of the other sciences over the last 50 years [36].

Every year, new medical concerns arise and with these comes the need for new treatment capabilities. The impact that new drugs can exert on the general population is immense. In many clinical situations there is a need for new symptomatic and curative drug therapies, and this is only accomplished through a great amount of research into the disease of interest.

## 2.2 The Receptor

Before one can begin to design and develop drugs, the disease in question needs to be well understood from a biochemical perspective. The use of receptor targeting has become an important aspect of drug discovery over the last 20 years, since it enables researchers to target specific disease mechanisms. A receptor is a biological macromolecule that is central to a specific disease and has an accessible face that is capable of binding to a molecule that elicits a biological response [36]. In drug design the goal is to exploit the receptor involved in controlling the disease. New drugs that interact at a receptor can either be agonists or antagonists. An agonist is a molecule that binds to the receptor of interest and elicits a desired biological response. An antagonist is a molecule that still binds to the desired receptor but prevents the biological response and blocks the agonist from binding.

The receptor is influenced by both exogenous and endogenous molecules. Exogenous substances are those that originate outside the human body; some examples include those chemical substances produced by plants, viruses, bacteria, fungi, and parasites. Endogenous substances, on the other hand, are those that originated, or are synthesized, in the human body and can either be chemical messengers, like neurotransmitters or non-messengers, or proteins, like enzymes, DNA or amino acids. In many cases there are numerous receptors distributed in the body that are available to be influenced by endogenous compounds. An example is the neurotransmitter  $\gamma$ -amino-butyric acid (GABA), which has three main receptors available in the body: GABA<sub>A</sub>, GABA<sub>B</sub>, and GABA<sub>C</sub>. The main way that a single molecule framework can act at

numerous receptors is by presenting a different active face to each of the available receptors.

### **2.2.1 Pharmacophore And Toxicophore**

Drug molecules are composed of several main elements that are important for receptor binding and biological activity. The drug scaffold is the chemical backbone that maintains the three dimensional (3D) conformation of the drug and holds the pharmacophore in the desired orientation. The pharmacophore is known as the bioactive face of a drug molecule, producing positive effects on a disease by binding to the required receptor. The pharmacophore is a set of regional features that elicit bioactivity. These features include hydrogen bond donors and acceptors, hydrophobic and hydrophilic regions, and positively and negatively charged groups just to name a few of the important contributors [37, 38]. For molecules, a 3D pharmacophore is used since it indicates the spatial arrangement between the above-mentioned groups [37, 39]. In order to develop drugs that can improve upon those available, an understanding of the mechanism of action is crucial, as well as determination of the pharmacophore. Another component of a drug that needs to be considered is the toxicophore face of the drug molecule. This is the portion of a drug molecule that binds to a receptor in the body producing unwanted side effects. Numerous drugs have associated side effects that are caused by the toxicophore regions of the drug scaffold.

The pharmacophore and toxicophore regions both represent sites of activity in a molecule, one with positive effects on a disease and the other promoting unwanted side effects by interacting undesirably with an active site, DNA or other regions in the body.

When attempting to develop new drug treatments, the main goal is to maintain the active component of the drug while eliminating associated toxic side effects. This can only be accomplished by determining the key features of the molecule's active face as well as those of the toxic effects.

### **2.3 Drug Development**

Several methods have been conventionally used for the development of new drugs over that last century. Of those available, serendipity has had the greatest impact over time. A significant number of drugs that are prescribed today were in fact originally discovered by complete accident. The classic example is the discovery of penicillin by Alexander Fleming in 1929 [34]. Through accidental contamination, he found that the penicillium mold had the ability to lyse staphylococci [34].

In today's world, with an increase in the biological understanding of the mechanisms associated with disease, drug discovery has taken new research directions, one of these being rational drug design. In random drug design approaches, many analogues are produced with no inherent understanding of their possible binding sites in the body. Rational drug development, however, builds on the concept that new drugs are a result of understanding the biochemical mechanisms of a disease. By pharmacologically characterizing the receptors and proteins that are central to a disease, a diverse number of drugs can be generated in a logical stepwise manner. For example, by understanding the amino acid residues that are important in an enzyme binding pocket or allosteric site, new drug scaffolds can be developed so that they can bind to a specific location. By rationally synthesizing functional groups in specific drug scaffolds,

pharmacophore units could be discovered while reducing the number of unwanted toxicophore interactions. In rational drug design, one must consider the three phases of drug action: pharmaceutical, pharmacokinetic, and pharmacodynamic.

### **2.3.1 Pharmaceutical Phase**

The absorption of a drug is dependent on several important aspects. The first of these is known as the pharmaceutical phase, during which the drug dissolves in the aqueous medium of the gastro-intestinal (GI) tract and moves across the membrane barrier of the GI to reach the blood stream. There are several properties that affect a drug's absorption. These include water solubility, lipid solubility,  $pK_a$  and pill formation or bioavailability. If a drug is extremely polar, it will remain in the aqueous environment of the GI tract and be excreted instead of being absorbed. If a drug is too non-polar, it will be absorbed but deposited in lipid layers in the body, decreasing its bioavailability. A delicate balance in polarity is required for the correct partition between the water and lipid environments of the body.

### **2.3.2 Pharmacokinetic Phase**

The second phase for drugs in the body is known as the pharmacokinetic stage, which is the movement of the drug once it has been absorbed from the GI tract into the microenvironment of the receptor. This stage is dependent on blood transport of the drug, metabolism of the drug by the liver and elimination of the drug via the kidneys. The liver is responsible for the metabolism of the drugs affecting their half-life in the body. Side chains that are susceptible to hydrolysis, oxidation and reduction include



esters, amides, alcohols, and aldehydes. Alkanes, alkenes and cycloalkanes are metabolically inert and remain unaltered by the liver. When designing drugs, metabolism is an important characteristic that should be accounted for. If the drug is chemically inert, it may remain in circulation longer than required. If the drug is easily metabolized it may be broken down before it can exert its effects. Drugs that have a “first pass effect” are broken down by the liver before they are able to reach their receptor, causing them to have a short half-life. The goal in designing drugs is for them to have between a 3<sup>rd</sup> and 4<sup>th</sup> pass effect in the liver giving them time to influence the disease receptor but still be broken down and excreted from the body to reduce toxic side effects.

### **2.3.3 Pharmacodynamic Phase And Receptor Interactions**

The final stage for a drug is known as the pharmacodynamic phase and is the interaction of a drug at the microenvironment of the desired receptor. There are several ways that a drug can interact with its receptor, some being more energetically favourable than others. When developing drugs, researchers want as many points of contact to allow for drug-receptor interaction uniqueness, but not so many that the polarity of the drug is compromised. Usually a 4-point pharmacophore is used for drugs targeting general regions in the body and a 2-point pharmacophore is used when designing drugs to target the brain. Some of the important interactions are listed in Table 3, along with the binding energies associated with them.

**Table 3.** Drug receptor interactions and their associated binding energies.

Interaction	Binding Energy (kcal/mol)
Covalent	100
Ionic	15
Ion-Dipole	5-10
Dipole-Dipole	2-5
Hydrogen Bonding	2-7
Charge Transfer ( $\pi$ - $\pi$ stacking)	1-5
Hydrophobic	1

The bulk of the interactions utilized in binding drugs to their receptor pockets are the ion-dipole, dipole-dipole, and hydrogen bonding. They are all of medium binding strength, allowing for reversible binding, while maintaining polarity of the drug molecule. Charge transfer and hydrophobic interactions are particularly useful for designing drugs that have brain-penetrating capabilities, since they have low binding energies and will not influence drug polarity, which is a major concern when designing drug for the CNS.

#### **2.3.4 Drug Absorption And Lipinski's Rules**

Drug delivery and absorption is a difficult aspect of drug design and thus important tools have been developed. The “rule of five” was developed by Lipinski in 1997 and hypothesized some of the important parameters that influence the absorption of active substances [40]. By combining both experimental drug research and computer aided screening, Lipinski developed a new set of rules [40, 41]. Based on these rules, which are multiples of five, poor absorption is likely if the active compound has more than five hydrogen bond donors, its molecular weight is greater than 500, the distribution coefficient (logP) is more than five and if there are more than 10 hydrogen bond

acceptors [35, 40]. Lipinski's rules are only considered drug expectations, but have been developed as a convenient way of estimating the absorption of active substances in the body [35, 41]. Provided below is an illustrative example of how the rule of five (Figure 10) can be applied to develop a drug candidate or viable starting point.

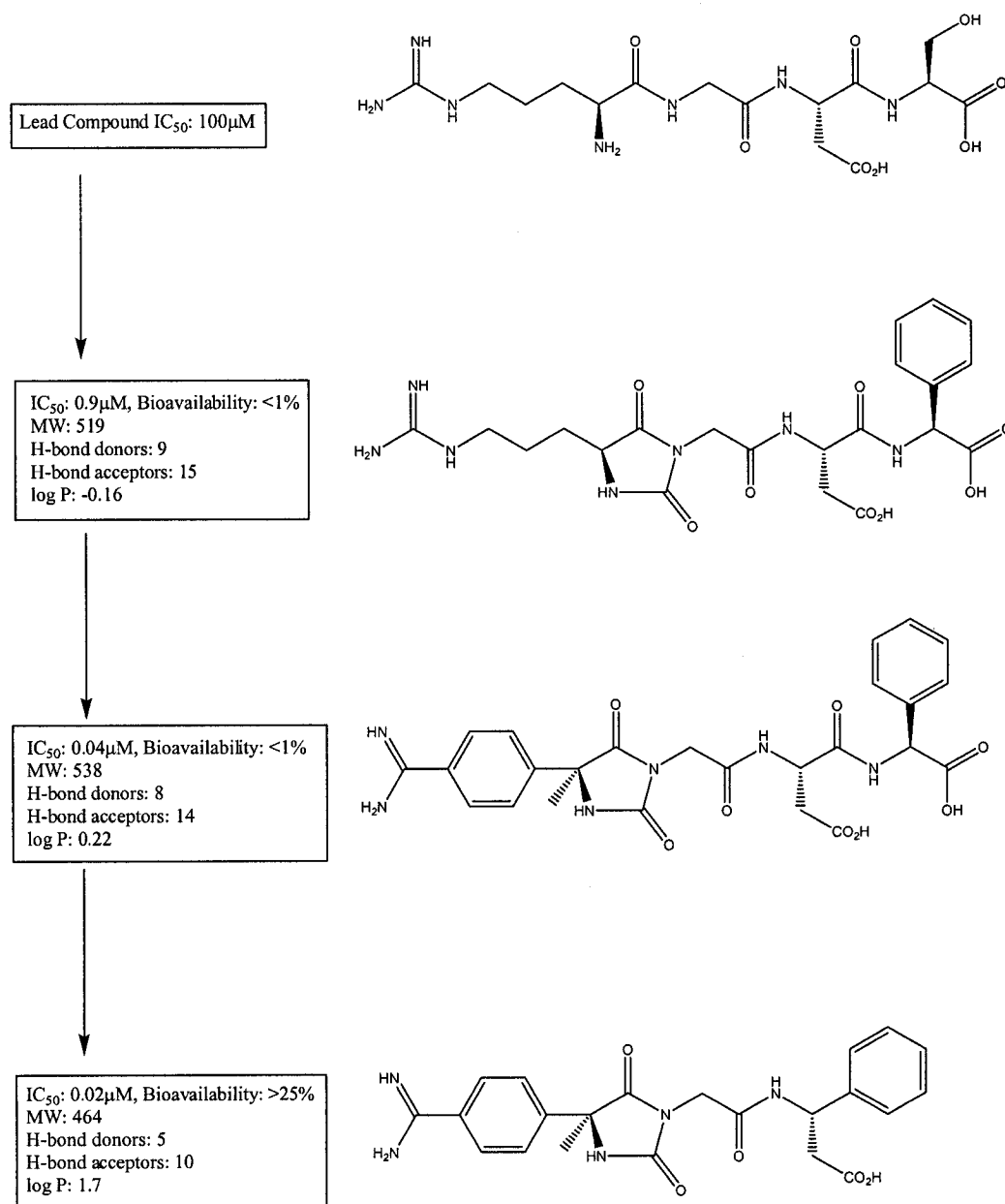


**Figure 10.** Optimization of the bioavailability of a peptide sequence that has shown the ability to act as a fibrinogen receptor antagonist, using the rule of five.

### 2.3.5 ADMET

The final area that is crucial in the development of new therapeutic agents is known as the absorption, distribution, metabolism, excretion and toxicity (ADMET) parameters. Originally these aspects of drug design were not taken into consideration until later phases of the drug development process [35]. In today's expanding pharmaceutical market, these parameters have become increasingly important in rational drug design strategies. The more of these parameters that need to be optimized the more complex the task of designing drugs becomes, so by optimizing several parameters simultaneously instead of considering them independently, the process is simplified [42]. Although these parameters are hurdles in drug design, fine-tuning techniques like pro-drug or soft-drug approaches can be used [36].

A pro-drug is an inactive molecule that requires metabolism, usually by the liver, to achieve bioactivity [36, 43]. There are several important purposes for utilizing a pro-drug approach. Pro-drugs are useful for increasing or decreasing the metabolic stability of the active drug while masking possible side effects or toxicity. A pro-drug can increase the active drugs *in vivo* stability and prolong its actions, or it can be used to limit a drug's duration in the body preventing toxicity. An example where this has been used is among tumor cell treatments. Cyclophosphamide was developed in the hope of exploiting the increased level of phosphoramidase enzymes in specific tumor cells. Cyclophosphamide is inactive but is metabolized in the liver to form the active drug phosphoramidate mustard (Figure 11) [36, 43].

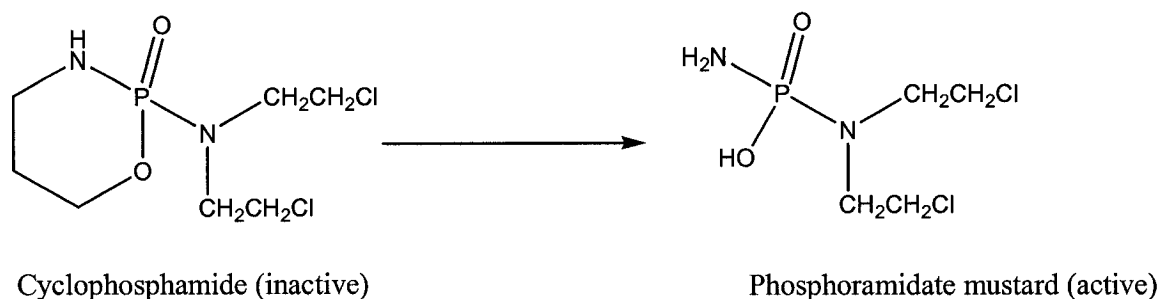


**Figure 11.** Tumor cell pro-drug, cyclophosphamide, which is metabolized to the active drug phosphoramidate mustard.

Pro-drugs can also interfere with transport mechanisms. Using this action of interference, drugs can be designed so that they are restricted to a specific location in the body or that the active drug is released slowly over time. By introducing hydrophilic or polar moieties, a drug can be restricted to the GI tract, preventing absorption into the blood stream and thus targeting GI tract infections. By using lipophilic or non-polar groups, which are not hydrolyzed easily, a drug can enter the blood stream, and the active compound will be liberated slowly and metabolized [44, 45].

A soft-drug is the opposite of a pro-drug approach: it is an active drug that is readily deactivated enzymatically in a known fashion [36, 46]. The main use of these drugs is to assure metabolism occurs in a controllable and predictable fashion. Drugs that are designed around endogenous scaffolds, such as neurotransmitters and hormones, are natural soft drugs. These compounds have rapid and efficient routes for their breakdown and do not produce any reactive intermediates [47]. By using a simple breakdown cascade, intermediates that may have the ability to interact with DNA and produce toxic and mutagenic effects are prevented, since the body has evolved these enzymatic steps over thousands of years [36].

## **CHAPTER 3**

### **DEDUCING THE BIOACTIVE FACE OF HYDANTOIN ANTICONVULSANTS**

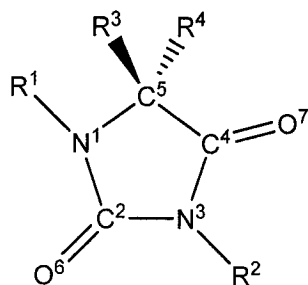
---

### 3.1 Introduction

Anticonvulsant drugs are molecules whose three-dimensional shape dictates their ability to interact with a receptor and elicit a desired antiseizure response; the portion of the molecule that actually interfaces with the receptor is termed the “bioactive face” or pharmacophore. In modern drug design, an understanding of the geometry of the bioactive face is crucial for rational drug design or for permitting the high throughput screening of an *in silico* library of putative drug molecules. Although heterocyclic molecules such as hydantoins (*e.g.* phenytoin) have long been the mainstay of anticonvulsant therapy, the bioactive face of hydantoin remains incompletely elucidated [48]. This is a stumbling block to the continued rational development of Na<sup>+</sup> channel-active agents for seizure suppression [49].

Previous work from our laboratory and others has clearly shown that the bioactive face of hydantoin consists of an amide group (-N(H)-C(=O)-) bonded through a tetrahedral carbon atom to a bulky and preferably aromatic (*e.g.* phenyl) group (N<sup>3</sup>-C<sup>4</sup>(=O<sup>7</sup>)-C<sup>5</sup>-R<sup>4</sup> ; Figure 12) [50, 51]. Although this work has identified the molecular building blocks of the bioactive face, it has not deduced the precise geometric relationship between the phenyl group and the amide group.

The focussed purpose of this study is to synthesize selective hydantoin analogues as structural probes and then to use nuclear magnetic resonance (NMR) spectroscopy and molecular modelling calculations to determine the geometric relationship between the aromatic group and the amide group (Figure 1); this will then be correlated with bioactivity. This study will afford an improved understanding of the geometry of the bioactive face of hydantoin.



	Compound name	R <sub>1</sub>	R <sub>2</sub>	R <sub>3</sub>	R <sub>4</sub>
<b>1</b>	(S)-5-benzylhydantoin	H	H	Bn	H
<b>2</b>	(S)-5-phenylhydantoin	H	H	Ph	H
<b>3</b>	5,5-diphenylhydantoin	H	H	Ph	Ph
<b>4</b>	3-benzylhydantoin	H	Bn	H	H
<b>5</b>	3-phenylhydantoin	H	Ph	H	H
<b>6</b>	(R)-3,5-diphenylhydantoin	H	Ph	Ph	H

**Figure 12.** General structure of the hydantoin derivatives synthesized, where the R group are represented in the table below (Bn = benzyl(-CH<sub>2</sub>C<sub>6</sub>H<sub>5</sub>), Ph = phenyl (-C<sub>6</sub>H<sub>5</sub>), H = hydrogen).

## 3.2 Methods And Materials

### 3.2.1 Compound Selection And Preparation

Specific hydantoin derivatives were chosen to probe the influence of aromatic/amide geometry on bioactivity. These compounds all contain an aromatic group at either the N<sup>3</sup> or C<sup>5</sup> position, which have been shown to be an important component of the bioactive face of the commercial drug Phenytoin or 5,5-diphenylhydantoin.

Provided below is the synthesis of compounds **1**, **2**, **3**, **4**, **5** and **6**, which were synthesized according to similar literature preparations [52-58]. <sup>1</sup>H and <sup>13</sup>C nuclear magnetic resonance (NMR) spectra were recorded using a Bruker AVANCE 500MHz spectrometer. Chemical shifts (δ) are reported as parts per million downfield from the tetramethylsilane (TMS) and are calibrated using the solvent peaks or when possible, the



TMS peak present some of the deuterated solvents. Coupling constants (*J*) are reported in Hz.

***(S)*-5-Benzylhydantoin (1)**

A solution of L-phenylalanine (8.3 g, 0.05 mol) and potassium cyanate (4.0 g, 0.05 mol) in water (20 mL) were combined and heated at reflux for 1h. After one hour, conc. HCl (7.5 mL) was added, and the reaction mixture was heated at reflux for an additional 10 minutes. The solution was then cooled in an ice bath, which promoted crystal formation. The product was collected by suction filtration and recrystallized using an ethanol and water (95:5) mixture.

Crystalline solid (8.21 g, 85%); mp 189-191 °C (lit. mp: 189-190 °C [55]); <sup>1</sup>H NMR (DMSO-*d*<sub>6</sub>): 2.91 (dd, 1H, *J* = 5.6, 14.2), 2.99 (dd, 1H, *J* = 4.9, 14.2), 4.33 (m, 1H), 7.18-7.29 (m, 5H), 7.92 (d, 1H, *J* = 9.8), 10.4 (s, 1H); <sup>13</sup>C NMR (DMSO-*d*<sub>6</sub>): 36.8, 59.6, 126.8, 128.2, 129.6, 135.4, 158.5, 176.1; HRMS: C<sub>10</sub>H<sub>10</sub>N<sub>2</sub>O<sub>2</sub> calculated 190.0742 amu, found 190.0739 amu.

***(S)*-5-Phenylhydantoin (2)**

The synthesis was conducted in a similar manner to *(S)*-5-benzylhydantoin (1), however, L-phenylglycine (7.5 g, 0.05 mol) was used instead of L-phenylalanine. The product was recrystallized using an ethanol and water (95:5) mixture.

Crystalline solid (7.25 g, 92%); mp 176-177 °C (lit. mp: 177-178 °C [55]); <sup>1</sup>H NMR (DMSO-*d*<sub>6</sub>): 5.18 (d, 1H, *J* = 10.1), 6.80 (d, 1H, *J* = 10.1), 7.32-7.39 (m, 5H), 12.82 (s,

1H);  $^{13}\text{C}$  NMR (DMSO- $d_6$ ): 57.2, 127.1, 127.9, 128.5, 137.9, 159.9, 173.3; HRMS:  $\text{C}_9\text{H}_{18}\text{N}_2\text{O}_2$  calculated 176.0586 amu, found 176.0588 amu.

### ***5,5-Diphenylhydantoin (3)***

A solution of benzil (5.8 mL, 0.05 mol) and urea (0.1 mol) in 95% ethanol (20 mL) was stirred. To this solution 6M NaOH (1.2 mL) was added and the mixture was heated at reflux for 90 min. The solution was then cooled to room temperature and the unreacted solid was filtered off. The remaining solution was acidified with 2M HCl until a precipitate was formed. The solid was collected by filtration and was crystallized using an ethanol and water (95:5) mixture.

Crystalline product (11.4 g, 92%); mp 296-298 °C (lit. mp: 295-298 °C [58]);  $^1\text{H}$  NMR ( $\text{CD}_3\text{OD}$ ): 7.33-7.39 (m, 10H);  $^{13}\text{C}$  NMR ( $\text{CD}_3\text{OD}$ ): 70.6, 126.5, 127.5, 128.6, 140.0, 156.9, 175.6; HRMS:  $\text{C}_{15}\text{H}_{12}\text{N}_2\text{O}_2$  calculated 252.0899 amu, found 252.0891 amu

### ***3-Benzylhydantoin (4)***

A solution of sodium hydroxide (2.0 g, 0.05 mol) was dissolved in water (20 mL) and hydantoin (5.0 g, 0.05 mol) was added, and the solution was brought to reflux for 15 min. To this solution benzyl chloride (5.8 mL, 0.05 mol), was added and the mixture was stirred and heated for an additional 20 h. The reaction mixture was then poured over 40 g of crushed ice. The product quickly precipitated and was then filtered off and crystallized using an ethanol and water (95:5) mixture.

Crystalline product (7.6 g, 80%); mp=140-141 °C (lit. mp=141 °C [55]);  $^1\text{H}$  NMR ( $\text{CD}_3\text{OD}$ ): 3.08 (s, 2H), 4.32 (s, 2H), 7.33-7.39 (m, 5H);  $^{13}\text{C}$  NMR ( $\text{CD}_3\text{OD}$ ): 35.9, 57.4,

126.8, 127.9, 129.4, 132.3, 156.4, 174.5; HRMS:  $C_{10}H_{10}N_2O_2$  calculated 190.0742 amu, found 190.0744 amu.

### ***3-Phenylhydantoin (5)***

A solution of glycine (3.8 g, 0.05 mol) was dissolved in water (20 mL) containing potassium hydroxide (3.0 g, 0.05 mol). After the solution was stirred for 10 min, phenylisocyanate (6.0 g, 0.05 mol) was added and the mixture was warmed to 65 °C for 5 h. The solution was then cooled and left to sit for 2 h. The solid diphenylurea which formed, was filtered off and the filtrate was acidified with concentrated HCl to precipitate the hydantoic acid. The hydantoic acid was cyclized by refluxing for 1 h in 50mL of water and 50mL of concentrated HCl (5 mL). When the solution had cooled the product crystallized. It was then collected by filtration and then recrystallized using an ethanol and water (95:5) mixture.

Crystalline product (7.4 g, 84%); mp=155-157 °C (lit. mp = 154-155 °C [55]);  $^1H$  NMR ( $CD_3OD$ ): 4.21 (s, 2H), 7.31-7.45 (m, 5H);  $^{13}C$  NMR ( $CD_3OD$ ): 58.8, 126.8, 127.4, 128.2, 129.3, 158.7, 174.4; HRMS:  $C_9H_{18}N_2O_2$  calculated 176.0586 amu, found 176.0583 amu.

### ***(S)-3,5-Diphenylhydantoin (6)***

A solution of L-phenylglycine (7.5 g, 0.05 mol) was dissolved in water (20 mL) containing potassium hydroxide (3.0 g, 0.05 mol), after the solution was stirred for 10 min, phenylisocyanate (6.0 g, 0.05 mol) was added and the mixture was warmed to 65 °C for 5 h. The solution was then cooled and left to sit for 2 h at which time the precipitated

diphenylurea was filtered off and the filtrate was acidified with concentrated HCl (5 mL) to precipitate the hydantoic acid. The hydantoic acid obtained was then cyclized by heating it at reflux for 1 h in 50 mL of water and 50 mL of concentrated HCl. When the solution was cooled the product crystallized and was collected by filtration. It was then recrystallized using an ethanol and water (95:5) mixture.

Crystalline product (9.84 g, 78%); mp=157-159 °C (lit. mp=158-160 °C [55]);  $^1\text{H}$  NMR ( $\text{CD}_3\text{OD}$ ): 4.14 (s, 1H), 7.39-7.48 (m, 10H);  $^{13}\text{C}$  NMR ( $\text{CD}_3\text{OD}$ ): 57.4, 126.6, 127.4, 127.6, 127.9, 128.3, 128.4, 129.1, 129.7, 159.3, 173.2; HRMS:  $\text{C}_{15}\text{H}_{12}\text{N}_2\text{O}_2$  calculated 252.0899 amu, found 252.0889 amu.

### 3.2.2 Biological Testing

The relative biological activities of the compounds were taken from literature sources as determined in a maximal electroshock assay [59]. To confirm these results (which were obtained in different laboratories) all six compounds were re-evaluated. The hydantoin analogue was administered to five adult male Sprague Dawley rats at 20 mg/kg intraperitoneally; 15 minutes later pilocarpine (300 mg/kg) was administered intraperitoneally [60-62]. The number of rats showing generalized convulsions was determined.

### 3.2.3 NMR Conformational Analysis

Chemical conformation was determined through one dimensional nuclear-Overhauser effect spectroscopy (1D-NOESY and nOe) experiments. All NMR experiments were performed on a Bruker AVANCE 500 MHz spectrometer, in

deuterated DMSO- $d_6$  at 25 °C. The  $N^1$  and  $N^3$  protons at 7.92 ppm and 10.43 ppm for compound **1** and the  $N^1$  and  $N^3$  protons at 6.80 ppm and 12.82 ppm for compound **2** were chosen and excited to study the nOe effects for each molecule.

#### 3.2.4 Molecular Modelling Calculations

Energy minimization calculations were performed using the MM2 force field implemented in Chem 3D Ultra 8.0 [63].

### 3.3 Results

Compounds **1** and **2** are both substituted at the  $C^5$  position but show varying ability to prevent seizure activity with only a one carbon chain length difference at the  $C^5$  position (benzyl vs. phenyl); compounds **4** and **5** are both substituted at the  $C^3$  position but show varying ability to prevent seizure activity with only a one carbon chain length difference at the  $C^3$  position (benzyl vs. phenyl).

The computationally optimized geometries of (S)-5-benzylhydantoin and (S)-5-phenylhydantoin show clear differences in the calculated distance between the  $N^3$  amide bond and the aromatic ring (Table 4). The  $^1H$  NMR nOe studies of (S)-5-benzylhydantoin (**1**) showed an nOe effect between the protons of the  $N^1$  amide bond and the protons of the aromatic ring (Figure 13); the nOe effects observed in (S)-5-phenylhydantoin (**2**) between the  $N^1$  amide bond protons and the aromatic protons was weaker in comparison.

**Table 4.** The calculated mean distances and standard deviations between the center of the amide bond and the centroid of the aromatic ring and the anticonvulsant activities, where the values indicate the number of animals tested compared to the number of animals that exhibited seizure protection.

#	Compound Name	Calculated Distance (Å)	Biological Testing	
			Animals Tested	Animals Protected
1	(S)-5-benzylhydantoin	N <sup>1</sup> 3.8 ± 0.1 N <sup>3</sup> 4.0 ± 0.1	5	0
2	(S)-5-phenylhydantoin	N <sup>1</sup> 4.2 ± 0.1 N <sup>3</sup> 4.3 ± 0.1	5	3
3	5,5-diphenylhydantoin	N <sup>1</sup> 4.2 ± 0.1/ 4.1 ± 0.1 N <sup>3</sup> 4.3 ± 0.1/ 4.3 ± 0.1	5	5
4	3-benzylhydantoin	N <sup>1</sup> 5.5 ± 0.1 N <sup>3</sup> 3.9 ± 0.1	5	0
5	3-phenylhydantoin	N <sup>1</sup> 4.4 ± 0.1 N <sup>3</sup> 3.5 ± 0.1	5	3
6	(S)-3,5-diphenylhydantoin	N <sup>1</sup> 4.7 ± 0.1/ 4.2 ± 0.1 N <sup>3</sup> 3.5 ± 0.1/ 4.2 ± 0.1	5	0

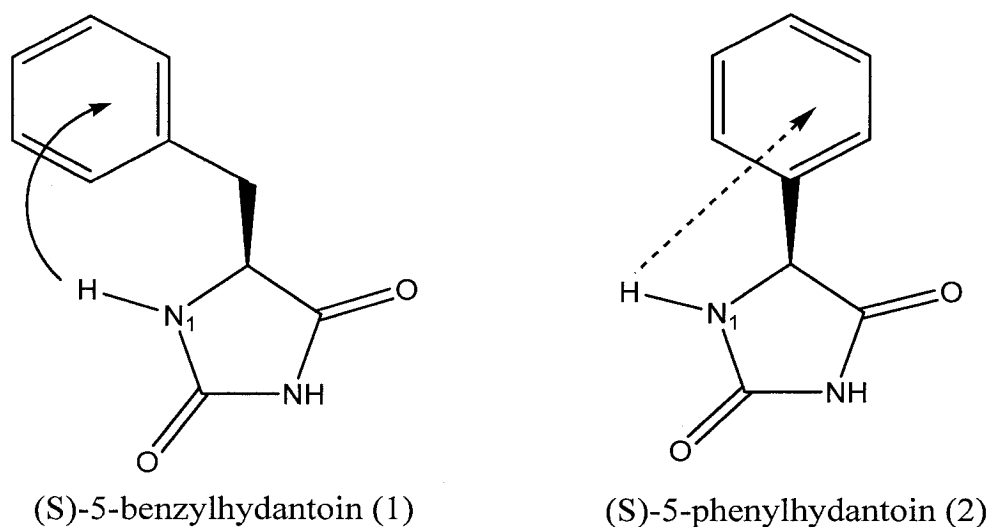


**Figure 13.** Relevant nOes observed for the (S)-5-benzylhydantoin and (S)-5-phenylhydantoin. Solid and dotted lines represent strong and weak nOes respectively.

### 3.4 Discussion

The connection between structure and anticonvulsant activity is apparent from the biological results in Table 4. The  $^1\text{H}$  NMR data that were obtained provide important conformational information that supports the molecular modelling results. The  $^1\text{H}$  NMR nOe study for (S)-5-benzylhydantoin shows a through space interaction between the  $\text{N}^1$  proton and the protons of the aromatic ring. The nOe data help to support the hypothesis of a folded conformation for the (S)-5-benzylhydantoin, with the benzene ring being flopped over the hydantoin ring. This confirms a spatial relationship between the  $\text{N}^1$  amide and the aromatic moiety of the benzyl group. The nOe for (S)-5-phenylhydantoin support the hypothesis that the aromatic ring is in an extended position relative to the hydantoin ring, and is not in a folded conformation as in the 5-benzyl analogue.

Computational studies support the experimental results. For (S)-5-benzylhydantoin, an intramolecular interaction between the aromatic ring and the hydrogen of the  $\text{N}^1$  amide bond creates a folded geometry which is controlled by a non-bonded interaction between the  $\pi$ -electrons of the aromatic ring and the dipole of the amide bond [64-66]. The (S)-5-phenylhydantoin is an active compound and assumes a conformation with the aromatic ring extended away from the hydantoin ring and the  $\text{N}^3$  amide bond. For the  $\text{C}^5$  substituted bioactive hydantoin analogues, the  $\text{N}^3\text{-C}^4(=\text{O}^7)$  amide-to-phenyl distance is  $4.3 \pm 0.1 \text{ \AA}$ .

3-Phenylhydantoin is a biologically active compound with a calculated amide bond-to-phenyl ring distance of  $4.4 \pm 0.1 \text{ \AA}$ . This distance is similar to the bioactive  $\text{C}^5$  substituted compounds. The inactivity of 3,5-diphenylhydantoin probably arises from the steric bulk of having a phenyl ring attached to the amide moiety.

In conclusion, the bioactive face for hydantoins consists of a  $\text{N(H)-C(=O)-X-phenyl}$  molecular fragment, where X is a carbon or nitrogen atom and where the distance between the center of the amide bond and the centroid of the phenyl ring is 4.3 Å. For compounds **2** and **3**, the bioactive face is the  $\text{N}^3\text{-C}^4(\text{=O}^7)\text{-C}^5\text{-R}^4$ ; for compound **5** an equivalent bioactive face is  $\text{N}^1\text{-C}^2(\text{=O}^6)\text{-N}^3\text{-R}^2$ . This extended geometry of the amide bond/aromatic ring pharmacophore aids in binding to the fast-inactivated state of the neuronal sodium channel, thereby inhibiting seizure activity. Using this knowledge of bioactivity in relation to the spatial configuration of specific chemical groups, it will be utilized to develop nicotinamide analogues as new anti-ictogenic agents.



## **CHAPTER 4**

### **NICOTINAMIDE**

---

#### 4.1 Nicotinamide Derivatives: Potential Anti-Ictogenic Treatment

Nicotinamide (3-pyridinecarboxamide) is present in the body and is in one of the two principal forms of the B-complex vitamin niacin. Niacin is used collectively to refer to both nicotinamide and nicotinic acid, which have identical vitamin activities but different pharmacological effects (Figure 1). Nicotinamide's major metabolite is nicotinamide adenine dinucleotide ( $\text{NAD}^{++}$ ), which is involved in the production of energy, signal transduction, and synthesis of cholesterol, fatty acids and other steroids [67].

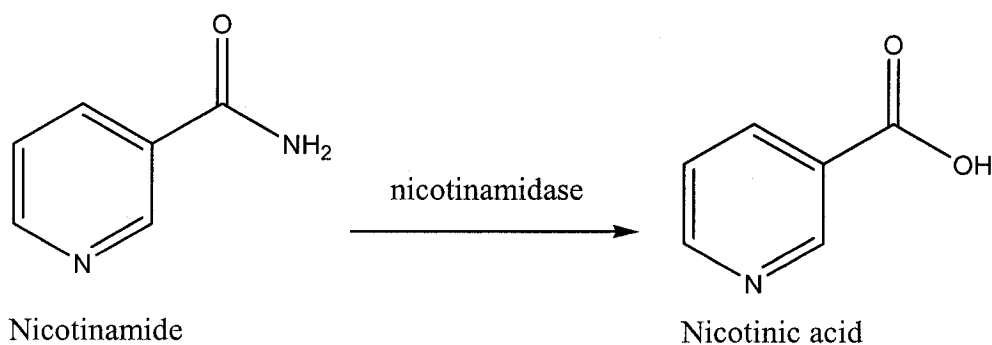


**Figure 14.** The chemical structure of nicotinamide and nicotinic acid.

Nicotinamide is absorbed from the GI tract at both low and high doses. At low doses the main mechanism of absorption is through sodium-dependent facilitated diffusion, but at higher doses absorption occurs through passive diffusion. After absorption, nicotinamide is transported via portal circulation to the liver and then through the systemic circulation to the rest of the body where it enters the cells through passive diffusion. Nicotinamide is metabolized in the body to  $\text{NAD}^{++}$  and then has the ability to be further metabolized to  $\text{NADP}^{++}$  (nicotinamide adenine dinucleotide phosphate), NAADP (nicotinic acid dinucleotide phosphate), NMN (nicotinamide 5'-

mononucleotide) and cyclic-ADP-ribose [68]. Nicotinamide may in fact be converted to nicotinic acid by the enzyme nicotinamidase. In the liver, nicotinamide's principal catabolic products include N'-methylnicotinamide, N'-methyl-5-carboxamide-2-pyridone, N'-methyl-5-carboxamide-4-pyridone and nicotinamide-N-oxide, which are excreted in the urine under high dosages of nicotinamide [68].

Based on previous research it has been found that nicotinamide shows favourable therapeutic effects in the treatment of CNS diseases like epilepsy and schizophrenia [69]. Experimentation with nicotinamide has found that it is able to reduce seizure occurrence in picrotoxin-induced seizures and completely protect some animals from biculline-induced seizures. Through the observation of this anti-ictogenic action of nicotinamide, it was concluded that nicotinamide was potentially involved in mediating the GABA-benzodiazepine receptor located on the post-synaptic neuron [70]. Nicotinamide has also been shown to be an endogenous ligand for the voltage-gated sodium channel and for the benzodiazepine receptor producing anti-ictogenic capabilities in isoniazid-induced seizures in mice [71]. Experiments conducted by Bourgeois in the 1980's concluded that nicotinamide has anticonvulsant activity against pentylenetetrazol (PTZ) induced seizures and increases the therapeutic index of phenobarbital when co-administered. Based on the results found in this study, nicotinamide was concluded to be both a therapeutic agent and adjunct treatment for epilepsy [71]. A similar study conducted with diazepam, found that diazepam produced a dose-dependent anticonvulsant effect, but when diazepam was co-administered with nicotinamide the anticonvulsant effect was potentiated, toxicity was reduced and lower dosages were possible [70, 72]. Upon

treatment with nicotinamide, the occurrence and severity of experimental seizures have been observed to be greatly reduced [73].

Nicotinamide has been shown to influence a range of different seizure types including complex partial and primary-generalized [74]. Preliminary injection studies of nicotinamide in bemegride-induced seizures found that the latency in the emergence of the first epileptic seizure was substantially increased [75]. Nicotinamide is a dietary supplement, and a deficiency of it in the diet is involved in pellagra, a nutritional disease [76]. Pellagra is often diagnosed in patients that have dietary inadequacies in the essential nutrients, especially nicotinamide [77, 78]. Some of the neurologic symptoms associated with pellagra include cognitive dysfunction, insomnia, depression seizures and acute psychosis [77]. Although convulsions are one of the many symptoms associated with the disease, they are readily dissipated upon treatment with dietary supplements containing nicotinamide, potentially indicating nicotinamide's endogenous involvement in the CNS.

Based on these studies, it can be concluded that nicotinamide not only increases anticonvulsant activity but also shows the ability to control seizures when administered alone, making it and its derivatives a new therapeutic niche that has not been exploited in medicinal chemistry.

Developing nicotinamides as new anticonvulsant agents can be broken down into two main areas. The first important direction is to determine and examine the pharmacophore face of nicotinamides and to develop the analogues of nicotinamide that should potentiate its ability to suppress seizure activity. Various nicotinamide derivatives were synthesized in attempts to evaluate their capability to act as endogenous anti-ictogenic agents. Through previous research, nicotinamide and its derivatives had

presented the capability of binding to the fast-inactivated state of the neuronal sodium channel. A variety of nicotinamide analogs were synthesized in an attempt to try and block the sodium channel and the GABA<sub>A</sub>-benzodiazepine receptor, thus preventing seizure activity.

#### **4.2 Targeting The Fast-Inactivated State Of The Neuronal Sodium Channel**

When developing new medicinal analogues, the pharmacophore and molecular binding sites are important locations that need to be considered. Although analogues of nicotinamide are an unexploited area for the treatment of epilepsy, they have important structural similarities to some of the current anticonvulsants making them useful new drug candidates. Research conducted by Dimmock *et al.* [79, 80] on the anticonvulsant properties of semicarbazone derivatives has helped to determine the important binding pocket interactions that enable certain classes of drugs to interact with the fast-inactivated state of the neuronal sodium channel and prevent the spread of neuronal excitation. Through biological testing in various chemically induced seizure assays it was found that the semicarbazone derivatives offered anticonvulsant protection. These results then led to the development of a pharmacophore model with the important binding areas for anticonvulsant activity identified. This research was not only based on the new anticonvulsant derivatives but also on the current anticonvulsants like phenytoin, carbamazepine and felbamate. These compounds all interact at three distinct locations in the receptor pocket of the sodium channel, a hydrogen bonding domain, an aryl binding site or hydrophobic pocket and an electron donor region [79, 81, 82]. It was found that peptide mimics, like amide bonds, have the required hydrogen bonding interactions and

that aromatic rings will additionally strengthen the interaction at the hydrophobic binding site [83]. Alkyl groups could also interact at the hydrophobic pocket through van der Waals interactions, assisting with proper alignment leading to increased anticonvulsant activity [80]. This concept was further explored and it was determined that the alkyl group's size and chain length was crucial to activity, and that when steric interactions between the alkyl group and the binding site occurred there was a lowering in binding capability (Figure 15) [80].

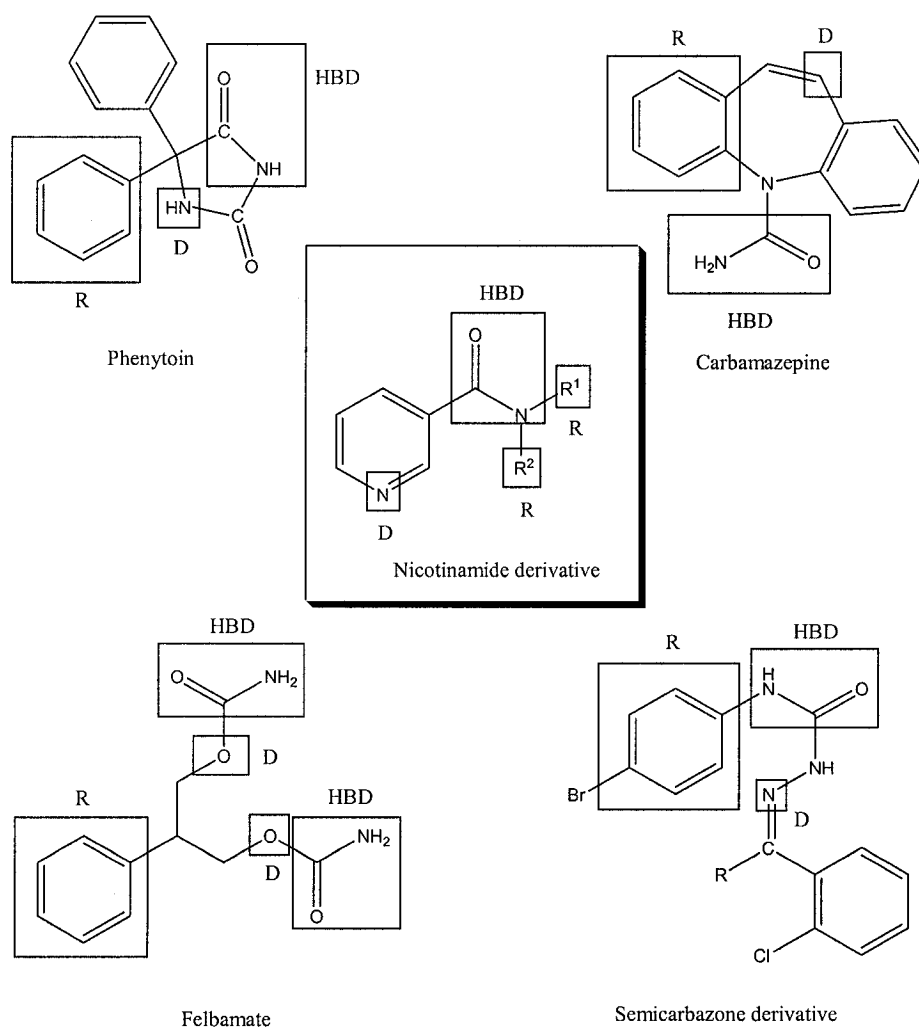


**Figure 15.** The pharmacophore regions of anticonvulsants and nicotinamide derivatives: HBD- hydrogen bonding domain, D- electron-donor, R- hydrophobic unit.

An important balancing act needs to be achieved when determining the substituents to attach to the amide bond moiety. With semicarbazones it was found that the dicarboimide function was contributing to the toxic side effects that were apparent when the drugs were tested in animal models [79]. In developing new drug candidates, removal of the toxicophore units while retaining the pharmacophore face would be required. Given the above discussion, nicotinamide has shown the potential to act as a new anticonvulsant since it contains the recognized pharmacophore units of the semicarbazones while not having the associated toxicophore face. Nicotinamide analogues contain an amide bond that would allow for the hydrogen bonding interactions; as well, the amide can be derivatized, either once or twice to allow for a variety of analogues to be produced. The R1 and R2 groups would allow for introduction of specific alkyl chains and aromatic groups promoting interaction within the hydrophobic pocket. The final interaction that would need to be considered is the electron donor region. Nicotinamide's structure contains a pyridine ring that could interact with the hydrophobic pocket or could donate a lone pair of electrons from the nitrogen to interact with the donor region of the receptor pocket.

Fortunately, nicotinamide has similar pharmacophore regions to the semicarbazone derivatives and space filling capacities to act at similar receptors. Although the exact location for the interaction of nicotinamide is unknown, the fast-inactivated state of the neuronal sodium channel is a key possibility. Nicotinamide derivatives contain a two point pharmacophore with the possibility of a third point of contact; this is important when designing drugs for the CNS. The proposed interactions (hydrogen bonding and hydrophobic) of nicotinamide with the receptor are all of a weak

nature ranging in binding energies from 1-7 kcal/mol. With most epilepsy drugs the goal is to reduce neuronal activity, but if the drug has a strong binding constant it will sit on the receptor for an extended period of time leading to unwanted side effects like fatigue, cognitive dysfunction, sedation, dizziness, and many others (which were presented in Chapter 1).

#### 4.2.1 Nicotinamide Analogues

Once nicotinamide's endogenous capabilities and pharmacophore region had been determined the second step was to develop analogues with anticonvulsant activity. The analogues that were proposed were based on research conducted by several groups into the anticonvulsant properties of carboxylic acids and their amides, and more specifically the amides of substituted benzoic acids that have proven to be effective in preventing seizures induced in mice and rats [84-87]. The research that was initially investigated was that conducted by Clark *et al.* [88], which examined the anticonvulsant activity of 4-amino-benzamides.

The Clark group produced a wide variety of amide substitutions including short and long alkyl chains, branched and unbranched chains, aromatic and non-aromatic groups as well as mono and di-substitutions [88]. The compounds were then tested for their anticonvulsant capabilities using maximal electroshock (MES) screening, which examines the ability of drug candidates to influence and target the fast-inactivated state of the neuronal sodium channel. Upon examination of the results, it was found that when the chain length was increased anticonvulsant activity also increased; however, this was also associated with the toxic side effects [85-87]. By increasing the chain length the

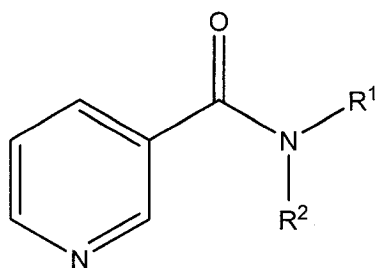


flexibility of the molecule also increases, giving it the ability to present a variety of different active faces to different receptors in the body, some producing the desired pharmacophore effects and others the toxicophore. The next set of compounds that showed increased anticonvulsant activity were those that contained an aromatic ring bound to the amide nitrogen. These results indicated that one aromatic ring produced optimal activity and greater potency than that found with the N-alkyl amides [88]. However, when an additional phenyl group was added anticonvulsant effects decreased, possibly due to space-filling considerations in the receptor pocket. The aromatic compounds also showed lower toxicity than the alkyl groups, most likely because the structures were more geometrically constrained preventing the molecules from interacting with other unwanted receptors in the body.

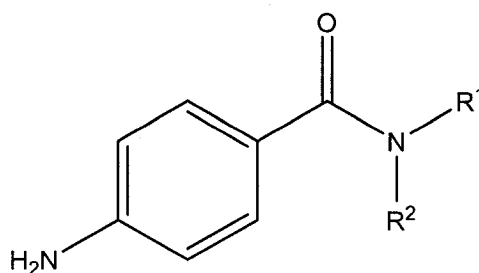
From all the compounds that were synthesized and tested by Clark, the N- $\alpha$ -methylbenzyl analogue produced the greatest activity in the anticonvulsant testing while having low toxicity. This compound's activity compared favourably with current anticonvulsant drugs on the market, affecting both seizure spread and threshold [88]. The N- $\alpha$ -methylbenzyl moiety resembles endogenous GABA on a superficial level but lacks the zwitterionic characteristics, indicating that it could potentially be binding to the sodium channel to reduce seizure activity [88]. The anticonvulsant profile and possible receptors for the N- $\alpha$ -methylbenzyl analogue were examined using chemically-induced seizures. When tested against bicuculline, which is a GABA antagonist, N- $\alpha$ -methylbenzyl analogue showed the ability to compete and prevent seizure activity indicating that some of its anticonvulsant effects were mediated through a GABA-agonist effect. Based on the anticonvulsant activity results found by Clark *et al.*, [88] specific

nicotinamide analogues were chosen to be synthesized that would correspond to Clark's best lead compounds: these are listed in Table 5.

**Table 5.** Nicotinamide derivatives developed as anticonvulsants based on the corresponding active 4-amino-N-substituted-benzamides. The number of +'s indicate anticonvulsant activity in MES testing.



Nicotinamide derivative



4-Amino-N-substituted-benzamides

R <sup>1</sup>	R <sup>2</sup>	Anticonvulsant activity of the corresponding 4-amino-N-substituted benzamides
CH <sub>2</sub> CH <sub>2</sub> CH <sub>3</sub>	H	+++
Cyclohexyl	H	+++
C <sub>6</sub> H <sub>5</sub>	H	++++
CH <sub>2</sub> - C <sub>6</sub> H <sub>5</sub>	H	+++++
CH <sub>2</sub> (CH <sub>3</sub> )- C <sub>6</sub> H <sub>5</sub>	H	+++++
CH <sub>2</sub> - C <sub>6</sub> H <sub>5</sub>	CH <sub>3</sub>	+++

#### 4.3 Nicotinamide Derivatives: Synthetic Considerations

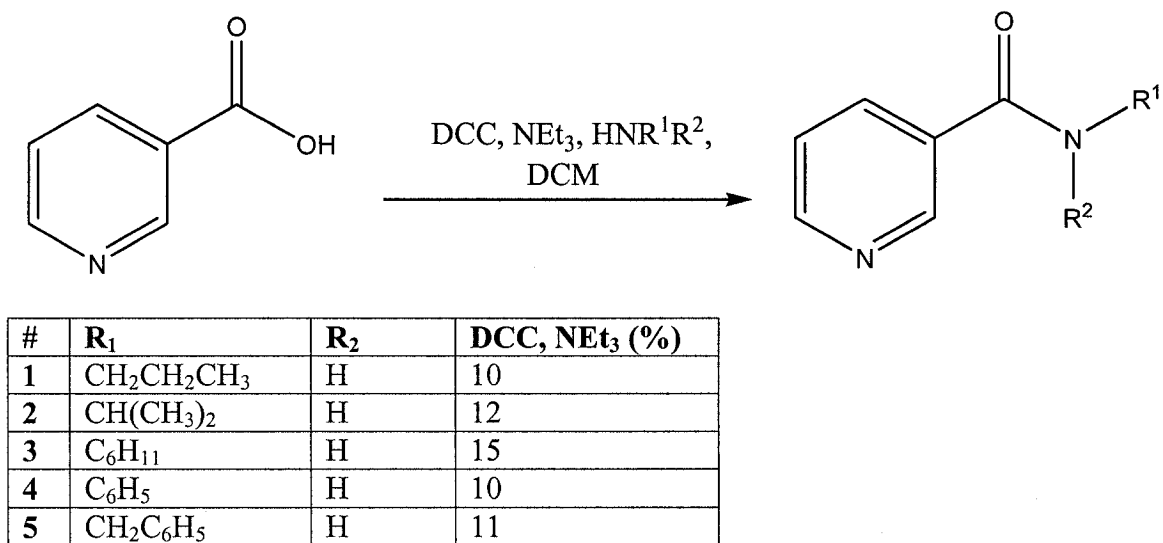
For the synthesis of the amide bond of the nicotinamide structure, a comprehensive literature review was conducted to evaluate the available synthetic routes. Several routes were recognized as having the potential to synthesize the amide bond and were experimented with synthetically to determine if they could be applied to the drug development process. When synthesizing possible new drug candidates there are several

important goals that are considered when evaluating synthetic routes. The first of these is to develop routes that are either a one-pot synthesis or a short synthetic scheme, for the longer the synthetic route becomes, the more vital the yield, cost and time considerations. The main goal was to develop a route that was balanced in time, yield and cost. If a drug is extremely expensive to produce and requires numerous synthetic steps it will not lead to the development of a new drug therapy. Drug companies not only want to invest in drugs that have a market, but in drugs that can be produced quickly and cheaply. The more expensive the drug becomes to produce the less likely the drug company will invest in it, therefore the general public will not reap its rewards as a therapeutic agent. This important knowledge was taken into consideration when developing the synthetic routes for the nicotinamide derivatives.

#### **4.3.1 Nicotinamide Derivatives: Using DCC (Route A)**

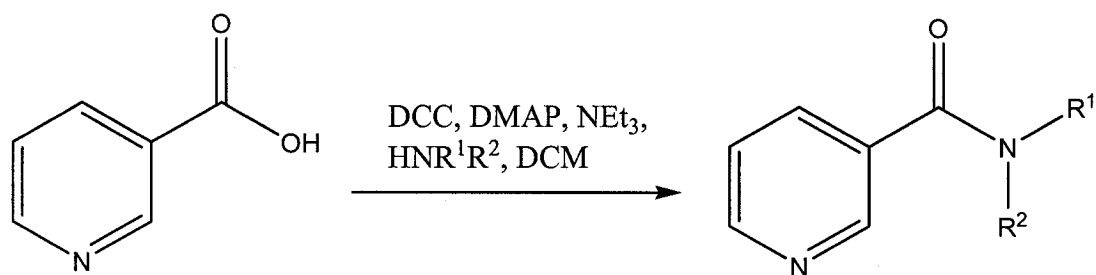
A variety of different methods were used for the activation of the carboxylic acid and its subsequent conversion to an amide bond. The first synthetic route attempted involved using the coupling reagent DCC (1,3-dicyclohexylcarbodiimide) (Scheme 1). DCC coupling of carboxylic acid with amines is a well described method that has been used for the synthesis of amide bonds [89-93]. A variety of amides were synthesized, and it was found that yields were lower than expected based on comparable literature data. These lower yields were due to several issues including product separation and unwanted side products. The DCU (1, 3-dicyclohexylurea) was difficult to separate from the nicotinamide derivatives. Several different solvents were utilized for both column chromatography and crystallization, however, it appeared that the DCU was similar in

polarity to the product and tended to elute and co-crystallize with the nicotinamide derivatives.



**Scheme 1.** DCC coupling technique used for the synthesis of nicotinamide derivatives.

After several amides had been synthesized the reaction conditions were changed to ascertain if yields could be improved. This involved replacing NEt<sub>3</sub> with DMAP in attempts to solve the issue of side product formation. DMAP (4-(dimethylamino)pyridine) was added to the reaction in the hopes of reducing side-product formation by accelerating the DCC-activated amide formation of the carboxylic acid (Scheme 2). Through previous research using DCC/ DMAP for the formation of esters and thioesters, it was found that the yields were higher by approximately 10% for the DMAP-catalyzed reactions compared to those that were not catalyzed [91]. Although these changes did improve the yields, they were not substantial enough to make to make this DCC-coupling route to amide-bond formation as useful as described in the literature.

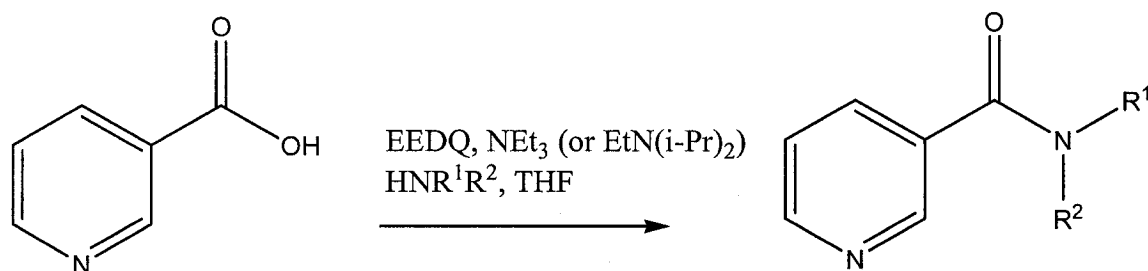


**Scheme 2.** DCC/ DMAP coupling technique used for the synthesis of nicotinamide derivatives.

#### 4.3.2 Nicotinamide Derivatives: Using EEDQ (Route B)

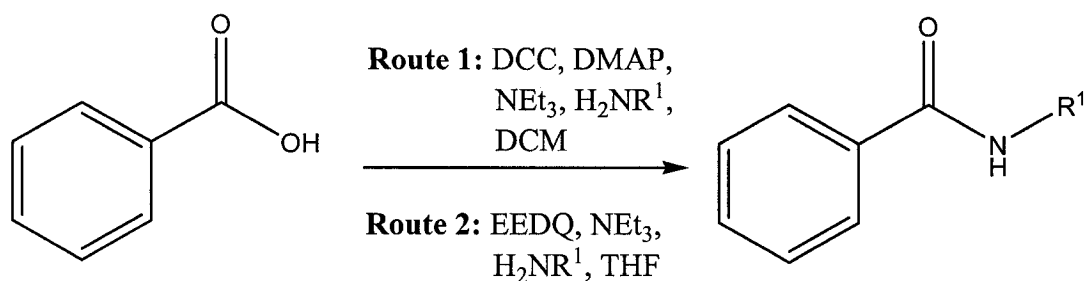
The second coupling route that was utilized involved the use of EEDQ (N-ethoxycarbonyl-2-ethoxy-1,2-dihydroquinoline) (Scheme 3). EEDQ is a reagent that has been used for the formation of peptide bonds because it allows for the coupling of acylamino acids and amino acid esters in a single step without any racemization [94]. EEDQ is a stable reagent that offers a variety of advantages over other coupling reagents and procedures. For example, it is a suitable reagent for use on a variety of amines, does not require completely anhydrous conditions or inert atmosphere, purification is relatively simple, and is handled more easily than carbodiimides (like DCC), which can cause contact dermatitis [95]. The side product generated from DCC is urea and is more difficult to remove than the quinoline produced from EEDQ. One of the advantages of EEDQ is that it cannot react with the amine starting materials under the conditions used to generate the amide bond. This allows for the reaction to be set up as a one-pot synthesis [95, 96]. This selective activation of carboxyl functional groups by EEDQ in the presence of other nucleophiles, like amines, offers advantages over the previously used DCC. The mechanism of the reaction involves activation by EEDQ to generate a

transient mixed carbonic anhydride [96], which then further reacts with the amine nucleophile to produce the desired nicotinamide product.



**Scheme 3:** EEDQ coupling technique used for the synthesis of nicotinamide derivatives.

In both the DCC and EEDQ reaction the product yields were quite low; this was a result of an unwanted side product being formed during the reaction. In attempts to determine why the yields were lower than expected for amide bond formation, the DCC and EEDQ methods were tested using benzoic acid instead of nicotinic acid as the starting material (Scheme 4). The reactions were run using the same conditions, as those of the nicotinic acid, and the two amines chosen were benzylamine and propylamine. Upon work up and <sup>1</sup>H NMR characterization, it was determined that the expected products had been formed with yields above 75%.



$\text{R}^1$	Route 1: Yield (%)	Route 2: Yield (%)
$\text{CH}_2\text{-C}_6\text{H}_5$	82	84
$\text{CH}_2\text{CH}_2\text{CH}_3$	78	81

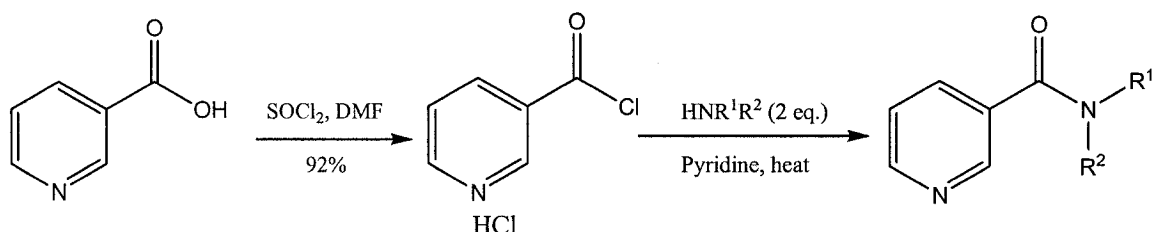
**Scheme 4:** Synthesis of benzamide derivatives used to evaluate the use of DCC and EEDQ to synthesize amide bonds.

The only difference between the two starting materials is the presence of a pyridine ring which could have an impact on the reaction mechanism and overall yield of the reaction. The pyridine ring contains nitrogen, which is considered a deactivating substituent or electron withdrawing group (EWG). Nitrogen is an EWG in this situation because it cannot donate its unshared electrons with the pi-system of the aromatic ring, since they reside in a  $\text{sp}^2$  hybridized orbital therefore these electrons are available and could act as a nucleophile or Lewis base.

#### 4.3.3 Nicotinamide Derivatives: Synthesis Of Nicotinyl Chloride (Route C)

The third method that was explored for the synthesis of the amide bond involved first producing an acyl chloride intermediate from nicotinic acid and then reacting this nicotinyl chloride with the desired amine, in a nucleophilic addition step to generate the nicotinamide derivative.

The HCl salt associated with the pyridine ring of the nicotinyl chloride, which offers stability and protection from oxidation, also makes the compound difficult to dissolve. In attempts to dissolve the nicotinyl chloride HCl salt for amide synthesis a variety of solvents were attempted including THF, DMF, DCM, and chloroform, although none of them was effective. Upon further examination of the literature, a synthetic route was found which involved first treating the nicotinyl chloride HCl salt with pyridine for neutralization and then proceeding with the amide substitution reaction [97, 98] (Scheme 5).



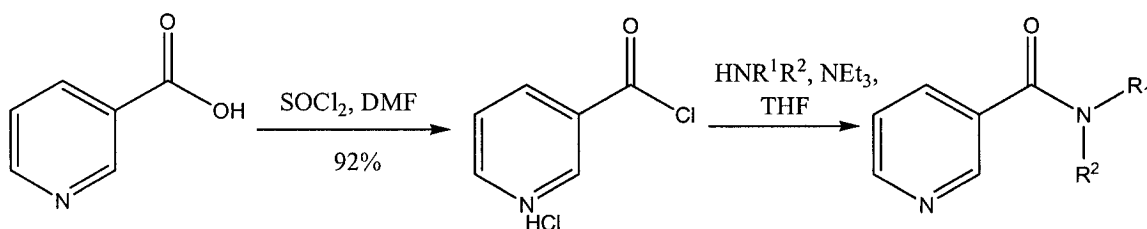
Compound #	R <sup>1</sup>	R <sup>2</sup>	Yield (%)
1	CH <sub>2</sub> CH <sub>2</sub> CH <sub>3</sub>	H	25
2	CH(CH <sub>3</sub> ) <sub>2</sub>	H	20
3	C <sub>6</sub> H <sub>11</sub>	H	18
4	C <sub>6</sub> H <sub>5</sub>	H	22
5	CH <sub>2</sub> -C <sub>6</sub> H <sub>5</sub>	H	11
6	C <sub>6</sub> H <sub>5</sub>	C <sub>6</sub> H <sub>5</sub>	15

**Scheme 5.** The synthesis of nicotinamide derivatives using nicotinyl chloride.

Although this dealt with the solubility issue, the yields were lower than expected and the initial heating of the solution led to rapid decomposition of the starting material, which later led to separation complications. Both the solubility of the starting material and the separation concerns were addressed by using the required amine for the reaction in excess [88, 99, 100] (Scheme 6). By using this amine in excess it not only acted as the



attacking nucleophilic group, but also as the base to neutralize the salt of nicotinyl chloride. The yields over these two steps ranged from 79% to 91% and were significantly better than those obtained for both the DCC and EEDQ coupling methods.



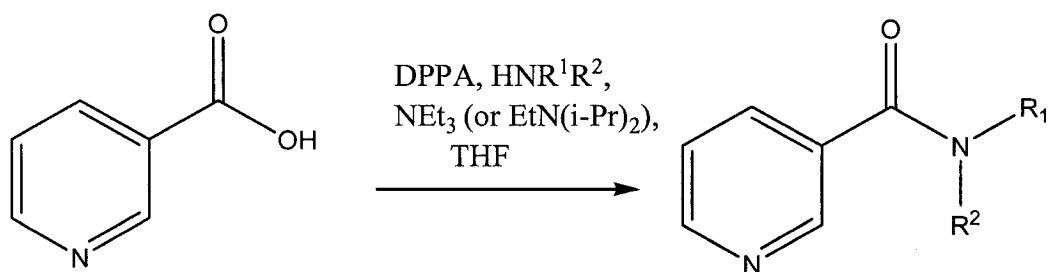
**Scheme 6:** Synthesis of nicotinyl chloride and nicotinamide.

#### 4.3.4 Nicotinamide Derivatives: Using DPPA (Route D)

The final method that was explored for the synthesis of the amide bond involved using the coupling reagent DPPA (diphenylphosphoryl azide). DPPA is a stable, non-explosive liquid that is prepared industrially by allowing diphenylphosphorochloridate to react with an excess of sodium azide at room temperature in acetone. The DPPA reagent can be used for a variety of different reactions depending on the conditions used. DPPA can be used to convert carboxylic acids to amines through a simplified Curtius reaction. This is accomplished by combining DPPA and water and heating to reflux. This reaction occurs under nonoxidizing and neutral conditions making it less involved than both the Hofmann and Schmidt reactions [101]. When an amine derivative and  $\text{NEt}_3$  are added to the reaction mixture in place of water, and heated at reflux for 5 to 25 hours, the final result is the exclusive synthesis of an amide bond. It has been shown that both aliphatic and aromatic carboxylic acids react to produce amide bonds in acceptable yields. This

DPPA synthesis of amide bonds had also been applied to the synthesis of a variety of peptides containing different amino acids including glutamine, valine, threonine, tryptophan, histidine, asparagine and methionine [101]. Through research conducted by Qian *et al.* [102] it was found that DPPA had improved yields of synthesizing amide bonds in macrolytic lactams when compared to those obtained from starting with the acyl chloride or using DCC [103]. It was, however, noticed that maintaining a stable temperature was important because at higher temperatures a Curtius rearrangement could occur and produce unwanted side products [101, 102].

Upon application of DPPA to the synthesis of nicotinamide it was determined that a variety of amides could be readily synthesized with yields ranging from 87% to 96%, with no side products being formed in appreciable amounts (Scheme 7). Given this success the DPPA reaction was scaled up from 1 g to 10 g for five of the amides under consideration (N-cylcohexylnicotinamide (**3**), N-phenylnicotinamide (**4**), N-benzyl nicotinamide (**5**), N-benzyl-N-methylnicotinamide HCl (**7**), N-(1-phenylethyl) nicotinamide (**8**)). These reactions were run using similar conditions and provided yields that were again all above 80% (Table 6). The use of the coupling reagent DPPA was chosen over the nicotinyl chloride route for the future development of nicotinamide derivatives since it was a one step reaction and could be easily scaled up to produce large quantities for testing.



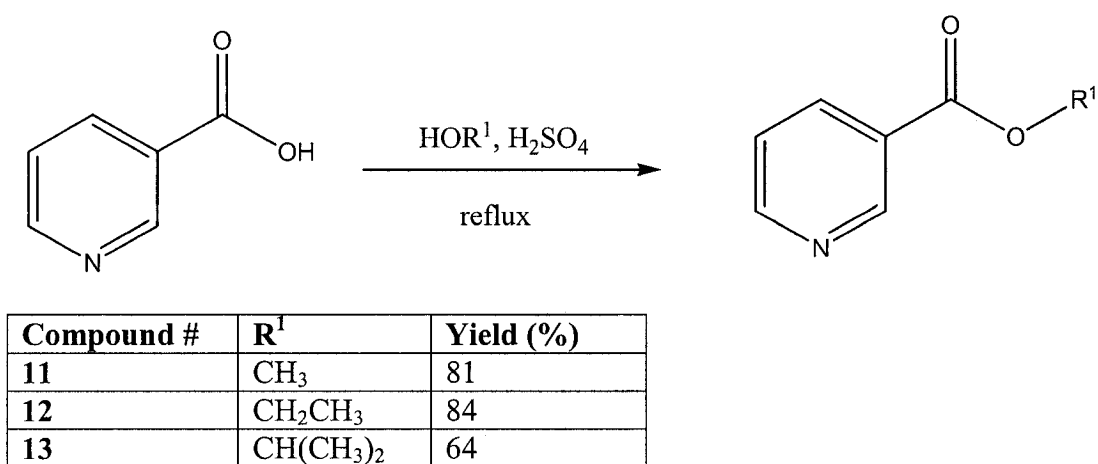
**Scheme 7.** DPPA coupling technique used for the synthesis of nicotinamide derivatives.

**Table 6.** Percent yields obtained for the synthesis of specific nicotinamides using a variety of different synthetic routes. (Route A: DCC coupling, Route B: EEDQ coupling, Route C: Thionyl chloride, Route D: DPPA coupling).

#	R <sub>1</sub>	R <sub>2</sub>	Route A	Route B	Route C	Route D
1	CH <sub>2</sub> CH <sub>2</sub> CH <sub>3</sub>	H	18	24	85	95
2	CH(CH <sub>3</sub> ) <sub>2</sub>	H	15	28	89	89
3	C <sub>6</sub> H <sub>11</sub>	H	21	25	82	91
4	C <sub>6</sub> H <sub>5</sub>	H	15	28	91	89
5	CH <sub>2</sub> C <sub>6</sub> H <sub>5</sub>	H	19	21	82	91
6	C <sub>6</sub> H <sub>5</sub>	C <sub>6</sub> H <sub>5</sub>	14	24	78	88
7	CH <sub>2</sub> C <sub>6</sub> H <sub>5</sub>	CH <sub>3</sub>	13	28	85	96
8	CH(CH <sub>3</sub> )C <sub>6</sub> H <sub>5</sub>	H	14	26	85	92
9	CH <sub>2</sub> (CH <sub>2</sub> ) <sub>3</sub> CH <sub>3</sub>	H	16	26	82	87
10	C <sub>6</sub> H <sub>5</sub> ( <i>o</i> -CH <sub>3</sub> ) <sub>2</sub>	H	22	24	86	91

#### 4.3.5 Nicotinate Derivatives: Synthetic Route 1

Several known literature routes were attempted to produce the desired nicotinate derivatives. These compounds were synthesized to confirm biological activity of nicotinic acid, since the esters would initially be cleaved in the stomach through acid catalyzed hydrolysis. Ester groups are synthesized onto drug templates in attempts to make drug administration easier or are used as a pro-drug approach. The first of these synthetic attempts involved using a Fisher esterification technique, where nicotinic acid was reacted with the desired alcohol under acidic conditions ( $\text{H}_2\text{SO}_4$ ) (Scheme 8) [104]. This proved to be highly successful and the methyl, ethyl and iso-propyl nicotinate derivatives were synthesized.



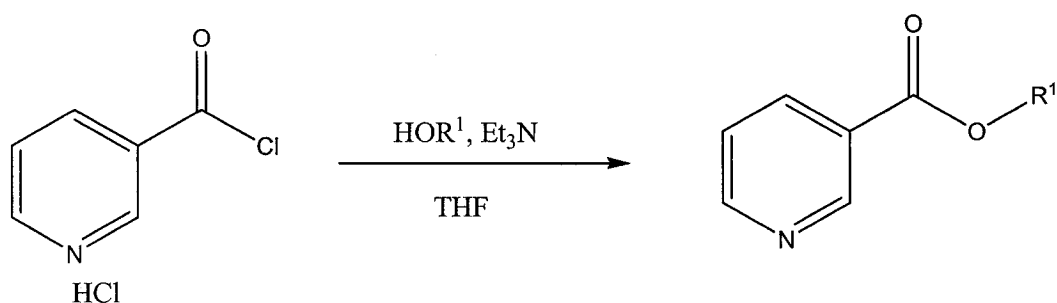
**Scheme 8.** The synthetic route used for the synthesis of the nicotinate derivatives using synthetic Route 1.

This same synthetic route was attempted to produce the benzyl nicotinate analogue, but it was unsuccessful. In theory this analogue should have proceeded with the greatest amount of ease, due to the stabilized intermediate step in which the aromatic

group can act as an electron-donating group stabilizing the positive build up on the ester oxygen. Some product was obtained, appearing in the TLC analysis, but work-up difficulties led to a reaction mixture. In the initial work-up procedures the reaction mixture was neutralized with potassium carbonate and so when the solution was extracted with ether both the product and the benzyl alcohol were in the organic phase since they were both hydrophobic. Since benzyl alcohol has a high boiling point it could not be easily removed by evaporation, leading to the separation problems. Not neutralizing the reaction mixture and extracting with a non-polar solvent like an ether/hexane mixture would allow for the acid salt of the benzyl nicotinate to precipitate out, alleviating separation issues. The benzyl alcohol would remain in the non-polar organic solvents.

#### **4.3.6 Nicotinate Derivatives: Synthetic Route 2**

The second synthetic route involved the use of nicotiny chloride as the starting material and upon treatment with the desired alcohol in THF and triethylamine, esterification occurred (Scheme 9). This route was used for the synthesis of phenyl nicotinate and was comparable in yield to the Fisher esterification method. This method and the Fisher esterification were used for the synthesis of sec-butyl nicotinate, however no product was obtained. The main reason was probably that the sec-butanol was wet and this excess of water competed with the alcohol for attack on the nicotiny chloride and nicotinic acid. In the end only nicotinic acid was recovered from both synthetic routes, and no product.



Compound #	R <sup>1</sup>	Yield (%)
14	C <sub>6</sub> H <sub>5</sub>	50

**Scheme 9.** The synthetic route used for the synthesis of the nicotinate derivatives using synthetic Route 2.

#### 4.4 5'- Substituted Nicotinamide Analogues

After the initial amides had been synthesized and biologically tested (see Chapter 5) the next direction was to examine substituted pyridine rings, specifically those at the 5' position. The 5' position was chosen as the next synthetic direction for several important reasons. Based on the activity profiles of the nitrogen-substituted analogues it was determined that those molecules that maintained a low energy extended conformation had a greater ability to prevent the development of a seizure in the rat and mouse models utilized (the low energy conformations for each of the nicotinamide analogues were calculated using the Sybyl 7.1 package). This extended conformation may allow these molecules to fit more selectively into the required binding pocket of the fast-inactivated state of the voltage gated sodium channel. By targeting the 5' position of the pyridine ring the goal was to develop new nicotinamide analogues that could maintain an extended conformation and thus create another location on the molecule that confers activity.

This position was also chosen since it was a synthetically accessible location on the pyridine ring for electrophilic aromatic substitution. For a pyridine ring with no substitution, the nitrogen in the ring acts as a pseudo-deactivating substituent or electron-withdrawing group. Nitrogen cannot donate its unshared electrons with the pi-system since they reside on a  $sp^2$  hybridized orbital, thus making the electron pair vinylic and unable to overlap with the aromatic pi-electrons. Electrophilic aromatic substitution reactions are performed under acidic conditions, thus the nitrogen of pyridine becomes protonated or complexes with a Lewis acid, therefore making the nitrogen an electron-withdrawing/ deactivating group. Being an electron-withdrawing group, nitrogen destabilizes the intermediate cation by withdrawing electron density from the aromatic ring specifically in the ortho (2') and para (4') positions. This means that the most reactive positions are the 3' and 5' (meta) since they have a greater electron density enabling them to attack electrophiles. Both the 2' and 4' positions are also electronically unfavorable compared to the 3' and 5' positions, since they result in a positive charge that can be positioned on the nitrogen atom. In addition, when the pyridine ring is substituted with an amide at the 3' position, it also acts as an electron withdrawing group producing substitution at the 5' position. Based on the above information the 5'/meta position was chosen as the next biological and synthetic target.

#### **4.4.1 5-Bromonicotinamides**

The first goal was to introduce a halogen at the 5' position. Halogens are useful additions to drug molecules for several important reasons. Halogens have important chemical properties both in therapeutics and in natural systems. For example, thyroid

hormones like tetraiodothyroxine are endogenous iodinated molecules where the halogen plays a crucial role in the hormones recognition, transport and activity [105, 106] (Figure 16). There are approximately 3500 known halogen-containing metabolites and drugs [107].

When developing new therapeutics, metabolic stability is an important challenge that needs to be considered. Molecules that are lipophilic can be easily oxidized in the liver by cytochrome P450 enzymes. Halogens increase metabolic stability by reversibly blocking the reactive center of cytochrome P450 [108, 109]. By blocking this enzyme's active site, metabolism of the drug is reduced, resulting in increased bioavailability. It has been shown that the introduction of a fluorine atom at metabolically labile locations on a phenyl ring prevents the oxidation of phenyl to phenol, thus increasing a drug's half life [109].

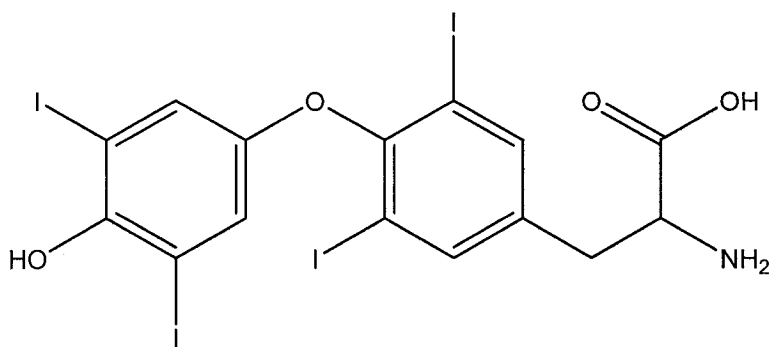


**Figure 16.** The thyroid hormone tetraiodothyroxine is an endogenous iodinated molecule.

Halogens are also instrumental in enhancing membrane binding and permeation [108]. How easily a drug permeates the membrane is dependent both on the properties of the membrane and those of the drug molecule. Most drugs are transported by passive diffusion across membranes, and halogens like chlorine or bromine are used as a strategy



to enhance this capability. Both the lipid-water partition coefficient and the permeability coefficient have been shown to increase in order from  $H < Cl < Br < CF_3$  due to an increase in hydrophobicity [108].

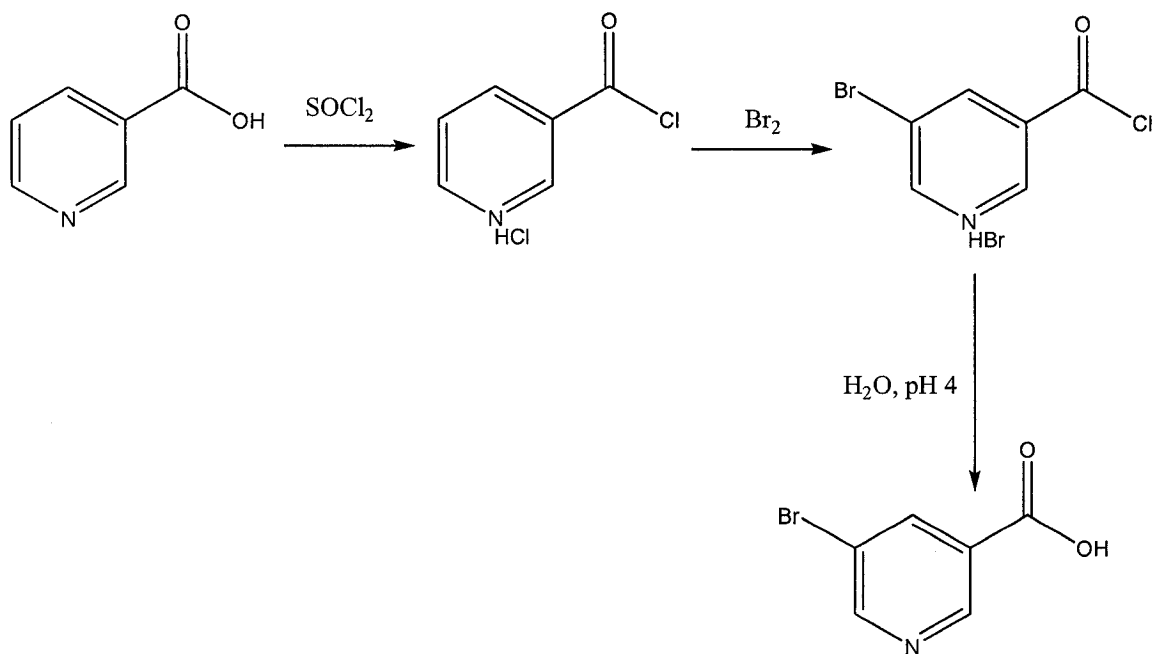
The lipophilicity of a drug candidate molecule is a critical parameter that needs to be considered since it is important for determining membrane diffusion and binding affinity. When developing a drug there needs to be a balance between lipophilicity and the overall polarity of a molecule [109]. Charged or highly basic residues decrease the bioavailability of a drug by preventing diffusion across the lipid bilayer. Halogens have the ability to influence these residues by increasing hydrophobicity and membrane permeability [109, 110]. Halogens can also increase the binding constant between the drug molecule and its receptor site, either through direct interaction of the halogen with the amino acid residues or by modulating the polarity of other residues on the drug scaffold [109, 111]. Halogens increase binding affinity by lipophilic interactions with a gradual increase from  $F < Cl < Br$  [112].

For the further development of nicotinamides as voltage-gated sodium channel blockers, 5'-bromonicotinic acid was synthesized following literature procedures [113-115]. Once this was completed, seven specific amines were chosen and coupled to 5-bromonicotinic acid using the DPPA method that was previously optimized. These amines were chosen based on their biological results obtained from NIH using the MES and PTZ testing models (biological data available in Chapter 5). Through this biological testing compounds that contained an aromatic substituent in the R1 position were found to have the most significant biological activity in the MES model of epilepsy. The aromatic amide substituents that were chosen included the amines:  $\alpha$ -methylbenzylamine,

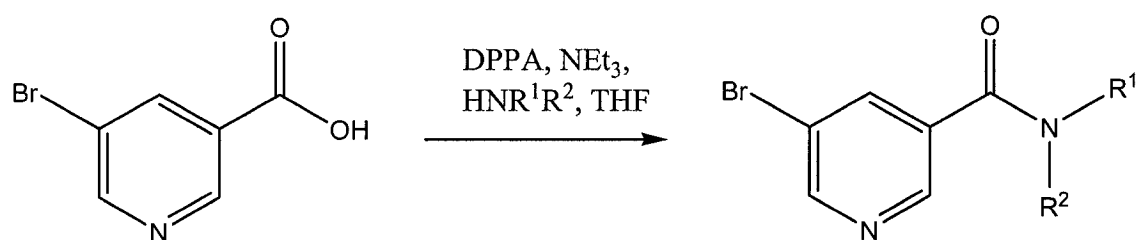
benzylamine, phenylamine and *N*-benzyl-*N*-methylamine; these amines all had significant activity. The other amines chosen had no aromaticity and were used to examine how alkyl groups could influence the activity of brominated compounds.

#### 4.4.1.1 5-Bromonicotinamides: Synthetic Considerations

Several literature preparations were available for electrophilic aromatic substitution of pyridine rings with bromine [113-115]. These procedures all involved initially converting the carboxylic acid to an acid chloride followed by the addition of bromine (Scheme 10). This led exclusively to the regioselective product of 5-bromo nicotinic acid. Using the literature preparations the reactions were run on 100 mg and 500 mg scales. Making some minor adjustments to the conditions, the reaction was scaled up to 10 g. Some of these changes included using 2.0 equivalents of thionyl chloride, adding DMF in a catalytic amount (1 mL) and eliminating the use of all other solvents. The reaction was originally run using the same synthetic conditions as the small scale, but it was found that during the work-up the excess thionyl chloride and DMF were difficult and time-consuming to remove. By reducing the amount of thionyl chloride and eliminating the solvent the reaction proceeded more quickly (12 hours vs. 20 hours) and the work-up was cleaner with less waste. The amount of thionyl chloride was originally reduced to 1.5 equivalents, but this led to a reduction in yield from 83% to 55%. When 2.0 equivalents of the thionyl chloride were used, it produced an overall yield of 80%, which was similar to what had been previously obtained. This bromination reaction was scaled up so that it could be effectively used to synthesize a large quantity of starting material to be utilized in the DPPA amide coupling reactions (Scheme 11).



**Scheme 10.** The synthesis of 5-bromonicotinic acid.



#	R <sup>1</sup>	R <sup>2</sup>	Yield (%)
15	CH(CH <sub>3</sub> )C <sub>6</sub> H <sub>5</sub>	H	74
16	CH <sub>2</sub> CH <sub>2</sub> CH <sub>3</sub>	H	92
17	CH <sub>2</sub> C <sub>6</sub> H <sub>5</sub>	CH <sub>3</sub>	85
18	C <sub>6</sub> H <sub>11</sub>	H	70
19	CH <sub>2</sub> C <sub>6</sub> H <sub>5</sub>	H	83
20	C <sub>6</sub> H <sub>5</sub>	H	87
21	CH <sub>2</sub> (CH <sub>2</sub> ) <sub>3</sub> CH <sub>3</sub>	H	82

**Scheme 11.** DPPA coupling used to synthesize the amide bond of the 5-bromonicotinamides.

#### 4.4.2 5-Bromonicotinamides And Heck Coupling

The Heck reaction is one of the most synthetically versatile C-C bond forming reactions that enables the addition of aryl or substituted vinyl groups to organic halides. The reaction is considered to be an efficient method for the synthesis of carbon bonds (only  $sp^2$  hybridized carbons), which are usually more difficult to produce using traditional techniques [116, 117]. The Heck reaction is tolerant of numerous unprotected functional groups like hydroxyls, ketones, aldehydes, carboxyls, esters, and amino acids and is often employed since it is a stereoselective coupling reaction with a predisposition towards forming a trans double bond [116, 117]. In the 5' position of the nicotinamide molecules two groups, styrene and methyl acrylate were chosen and introduced using the Heck coupling reaction. Styrene and methyl acrylate were chosen because they contain a double bond, which limited conformational flexibility of the nicotinamide molecules. This was useful for synthesizing molecules in an extended geometry, possibly preventing unwanted side effects but reducing interactions with other receptors. Alkenes are generally considered to be metabolically stable and are often used in drug scaffolds to increase half-life. Another goal of these Heck coupling reactions was to observe how styrene, which is an electron-donating group and methyl acrylate, which is an electron-withdrawing group might influence activity of the nicotinamide analogues. By changing the electron density of the pyridine ring, the nitrogen, which is an electron donor, may be affected and this could either limit or increase activity.

Based on the preliminary results some of the nicotinamide analogues had unwanted side effects which could be a result of either prolonged half lives or unanticipated receptor interactions. Both the aromatic and ester groups were chosen as a means of controlling the half-life of these nicotinamide analogues. Generally aromatic

hydrocarbons are oxidized in the para position to a phenol, thus increasing the compounds hydrophilicity and decreasing its half-life. The same is true for esters, which are metabolically unstable. This functional group is readily hydrolyzed to a carboxylic acid and alcohol through a nonspecific esterase enzyme. In both situations these functional groups (carboxyl and hydroxyl) are susceptible to conjugation, which involves the attachment of small polar molecules to the drug by enzyme catalysis [36]. These polar groups make a drug more water soluble, increasing excretion and reducing half-life. By introducing these functional groups at the 5' position they may make an important contribution at influencing and controlling the half-life of nicotinamides.

The proposed Heck mechanism involves an olefin insertion across the double bond of styrene or methyl acrylate by the palladium halide and nicotinamide [118, 119]. The trans product is formed through an internal rotation where the palladium halide and the organic residue move away from one another, followed by syn  $\beta$ -hydride elimination. The internal rotation step favors one direction over the other due to steric interactions between the phenyl/ acetate groups and the nicotinamide. These mechanistic details, shown in Figures 17 and 18, visually explain why the trans product is favored in both the styrene and methyl acrylate situations. The trans stereoisomer can be confirmed by observing the experimental coupling constants between the hydrogens across the double bond. For a trans stereoisomer the coupling constant range is  $J = 16 - 18$  Hz and for a cis stereoisomer the coupling constant range is  $J = 10-12$  Hz. By observing the proton NMR's for the compounds synthesized using the Heck coupling method, the trans stereoisomer was confirmed to be the final result.

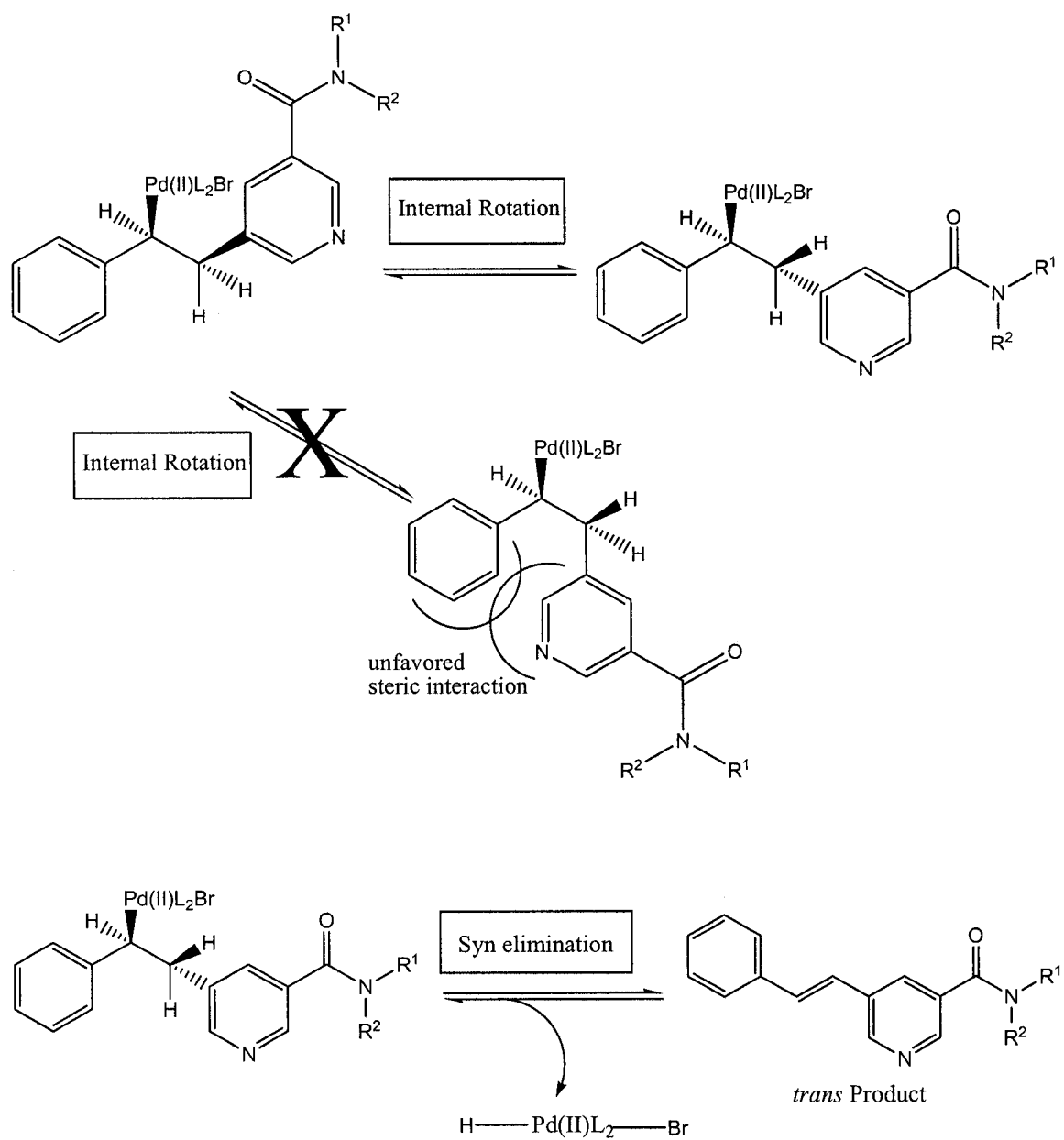


**Figure 17.** The conformation of the Pd intermediate for the Heck coupling using styrene to generate the *trans* product.

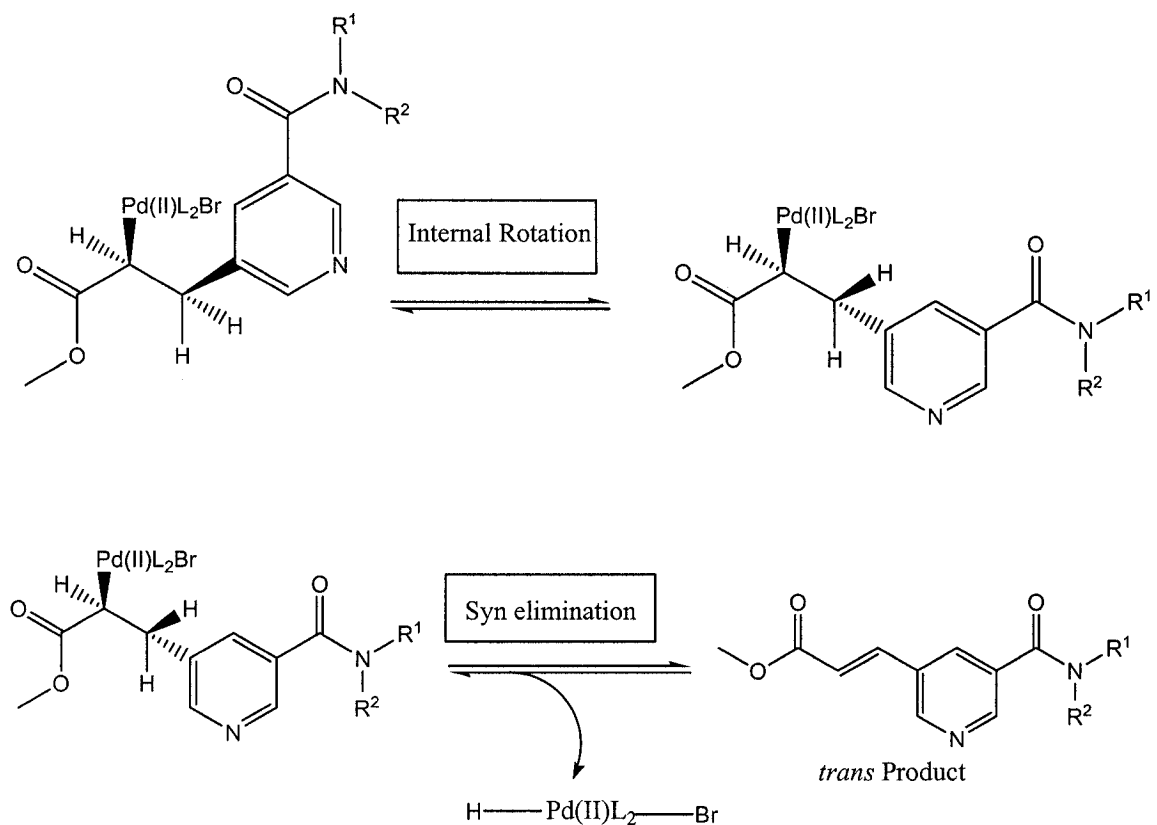


**Figure 18.** The conformation of the Pd intermediate for the Heck coupling using methyl acrylate, to generate the *trans* product.

For the Heck coupling reactions different conditions were utilized in attempts to find a procedure that produced the highest reaction yields. The palladium catalyst used was Pd(OAc)<sub>2</sub> which was chosen based on literature examples [116, 118]. Two solvents were chosen, THF and DMF, since they were both aprotic and had varying degrees of polarity, and finally two bases were surveyed, one a soluble amine (NEt<sub>3</sub>) and the second an inorganic base (K<sub>2</sub>CO<sub>3</sub>). Using these reagents a variety of different reaction conditions were employed in order to optimize the reaction conditions.

Initially, for the Heck coupling reaction, 5-bromonicotinic acid was used as the starting material. By synthesizing large quantities of 5-styrylpyridine-3-carboxylic acid

and 5-((E)-2-(methoxycarbonyl)vinyl)pyridine-3-carboxylic acid the goal was to use a synthetic route that limited the number of overall reactions being performed to get the final products. Once the Heck coupling method had been optimized it could be used for large-scale synthesis of 5-styrylpyridine-3-carboxylic acid and 5-((E)-2-(methoxycarbonyl)vinyl)pyridine-3-carboxylic acid, which then could be used to generate the desired nicotinamide analogues through the DPPA coupling route. However, after several attempts of using 5-bromonicotinic acid as the starting material for the Heck coupling and procedures A, B and C, it was determined that the reaction was not proceeding as expected since consistently lower yields of less than 20% were being obtained, Table 7.

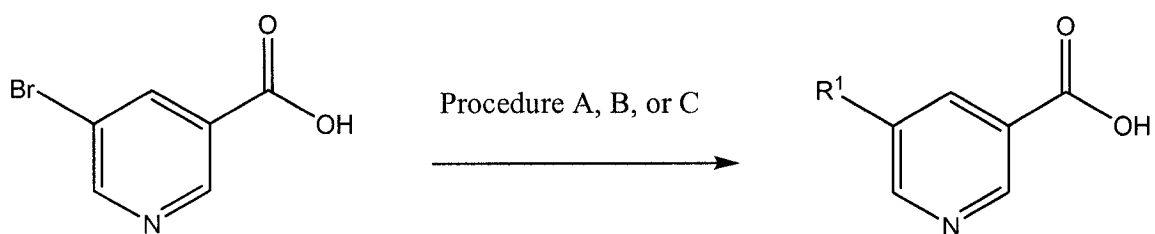
The reaction was originally performed using methyl acrylate under atmospheric pressure with refluxing THF. However, since methyl acrylate's boiling point was 80.5°C, it was hypothesized that it might have been eliminated from the reaction vessel by evaporation. More methyl acrylate was added at the 5 and 10-hour mark to alleviate this problem but this made no noticeable difference to the yield. In attempts to solve this problem the reaction was run using DMF in a sealed tube apparatus. Two reaction times of 5 and 24 h were used in order to evaluate if reaction length influenced the yields. Although the results for procedures B and C were an improvement over procedure A, the product was still not obtained in high yield. Although the concerns of evaporating methyl acrylate had been solved it appeared that there were other issues influencing the Heck reaction.

Through experimental research, it has been demonstrated that the Heck reaction tolerates both electron-withdrawing and electron-donating groups on either of the



substrates being coupled together [120, 121]. However, the rate of reaction is accelerated with electron-withdrawing groups and reduced with electron-donating groups [120, 121]. The carboxylic acid group of 5-bromonicotinic acid is an electron-withdrawing group. However under the reaction conditions of procedures A, B, or C, the triethylamine could be deprotonating the carboxylic acid to generate a carboxylate anion. This anion is more electron rich and therefore could be influencing the Heck reaction by behaving as an inductive electron-donating group, therefore resulting in reduced yields of 5-((E)-2(methoxycarbonyl)vinyl) pyridine-3-carboxylic acid by a reduction in the rate of reaction.

**Table 7.** The reagents used for the development of the Heck coupling for 5-bromonicotinic acids.

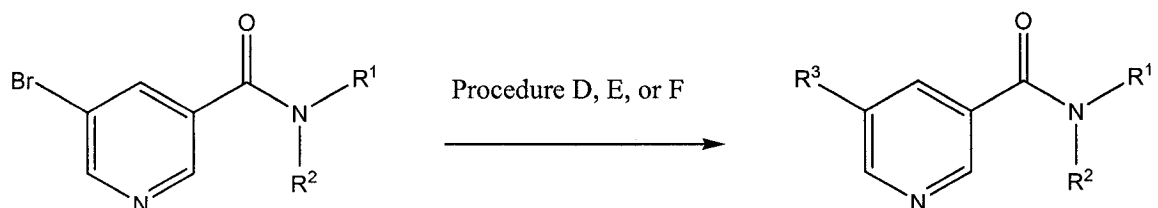


Procedure	R <sup>1</sup>	Pd Source	Ligand	Base	Solvent	Temp (°C)	Time (h)	Yield (%)
A	Methyl acrylate	Pd(OAc) <sub>2</sub>	PPh <sub>3</sub>	NEt <sub>3</sub>	THF	75	15	3
B	Methyl acrylate	Pd(OAc) <sub>2</sub>	PPh <sub>3</sub>	NEt <sub>3</sub>	DMF	125	5	10
C	Methyl acrylate	Pd(OAc) <sub>2</sub>	PPh <sub>3</sub>	NEt <sub>3</sub>	DMF	125	24	18

To overcome this synthetic difficulty, the Heck reaction was attempted using the electron-withdrawing 5-bromonicotinamide derivatives. Using the amide derivatives, the goal was to preclude the generation of the anion by the amine base, thereby preventing

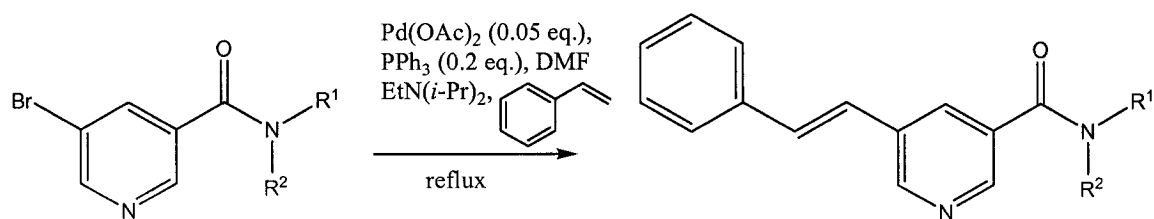
the reduction in the rate of the reaction. This synthesis was attempted using a variety of conditions in attempts to optimize the reaction (Table 8).

**Table 8.** The reagents used for the development of the Heck coupling for 5-bromonicotinamides.



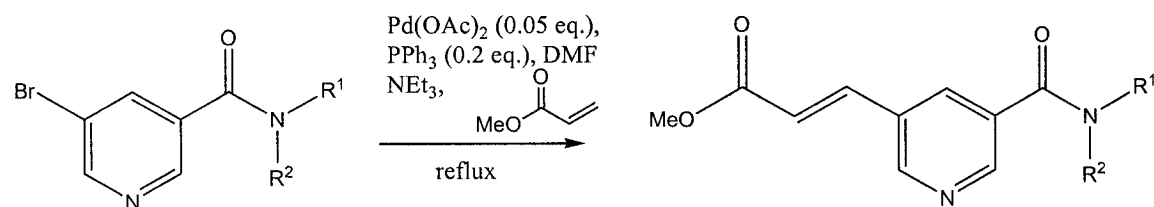
Procedure	R <sup>1</sup>	R <sup>2</sup>	R <sup>3</sup>	Pd Source	Ligand	Base	Solvent	Temp (°C)	Time (h)	Yield (%)
D	CH <sub>2</sub> C <sub>6</sub> H <sub>5</sub>	H	Methyl acrylate	Pd(OAc) <sub>2</sub>	PPh <sub>3</sub>	K <sub>2</sub> CO <sub>3</sub>	DMF	125	24	55
E	CH <sub>2</sub> C <sub>6</sub> H <sub>5</sub>	H	Methyl acrylate	Pd(OAc) <sub>2</sub>	PPh <sub>3</sub>	NEt <sub>3</sub>	DMF	125	24	70
F	CH <sub>2</sub> C <sub>6</sub> H <sub>5</sub>	H	Methyl acrylate	Pd(OAc) <sub>2</sub>	PPh <sub>3</sub>	NEt <sub>3</sub>	DMF	125	60	70

Based on the findings of the previous procedure development, DMF was chosen as the solvent, since elevated temperatures were required to promote the coupling reaction. Using the results from procedures D, E, and F it was determined that the base of choice was triethylamine and that running the reaction for longer periods of time (60 h) made no significant difference to the yield of the reaction. Using these conditions both styrene (Scheme 12) and methyl acrylate (Scheme 13) were coupled successfully to the 5-bromonicotinamide derivatives.



#	$\text{R}^1$	$\text{R}^2$	Yield (%)
22	$\text{CH}_2\text{C}_6\text{H}_5$	H	84
23	$\text{CH}(\text{CH}_3)\text{C}_6\text{H}_5$	H	82
24	$\text{CH}_2\text{C}_6\text{H}_5$	$\text{CH}_3$	79
25	$\text{C}_6\text{H}_{11}$	H	82
26	$\text{CH}_2\text{CH}_2\text{CH}_3$	H	81

**Scheme 12.** Heck coupling reaction details and yields observed for styrene.



#	$\text{R}^1$	$\text{R}^2$	Yield (%)
27	$\text{CH}_2\text{C}_6\text{H}_5$	H	70
28	$\text{CH}(\text{CH}_3)\text{C}_6\text{H}_5$	H	84
29	$\text{C}_6\text{H}_{11}$	H	82

**Scheme 13.** Heck coupling reaction details and yields observed for methyl acrylate.

#### 4.4.3 5-Bromonicotinamides And Suzuki Coupling

The Suzuki coupling method has been used extensively to introduce new C-C bonds into a wide range of organic molecules between  $\text{sp}^2$  hybridized carbons [122, 123]. Since its development in 1979, this coupling method has been employed in the

development of pharmaceuticals, materials, agrochemicals and other chemical products [124, 125]. The general reaction involves a rate-determining oxidative addition step of an alkenyl, alkynyl, benzyl or aryl halide to the palladium complex, followed by transmetallation with an organoboron reagent, and finally a reductive elimination step of the organic group to produce the coupling product and regenerate the palladium catalyst [120, 121, 126]. For the oxidative addition step, the rate is dependent on both the halide and the chemical scaffold. Reactivity of the alkyl / aryl halide decreases depending on the halide being used ( $I > OTf > Br >> Cl$ ) [122]. When electron-withdrawing groups are present on the alkyl / aryl halide they act as activating groups and increase the rate of oxidative insertion [120].

The Suzuki reaction has a variety of synthetic features that have made it a general method for the development of new C-C bonds. Some of these features include its tolerance to a broad range of functional groups including esters, ketones, amides and aldehydes, retention of stereochemistry in the product for both the boron and halide starting materials, production of non-toxic byproducts, and a reasonably high turnover rate for the palladium catalyst being used [127, 128]. This reaction also shows stereoselectivity like the Heck reaction and has been utilized for the synthesis of unsaturated products. The geometry of the double bond in both starting materials is retained in the product and is produced stereospecifically with retention of stereochemistry. This means that if the starting material is *cis*, its double bond will remain *cis* in the product and the same goes for a *trans* double bond. Although many other organometallic reagents undergo similar coupling reactions, organoboronic acids are often used in pharmaceutical laboratories and industry because of their stability and

ability to be used without any specific precautions. The advantage of using organoboronic acids is that they are thermally stable and are generally unaffected by the presence of water and oxygen making them convenient reagents for the synthesis of natural products and pharmaceuticals [120, 127]. The organoboronic acids also have a significant influence on the rate of the coupling reaction. Organoboronic acids, which are substituted with electron-withdrawing substituents, enhance the coupling reaction rate by activating the organic group allowing transfer of the organo group from the boron to the palladium catalyst [120].

Medal-mediated cross-coupling reactions are versatile synthetic techniques for introducing a variety of chemical structures. For this drug development project of nicotinamide analogues, both the Heck and Suzuki coupling techniques were employed to introduce specific structures at the 5' position. The original goal of utilizing the 5' position was to synthesize nicotinamide molecules that could maintain an extended low energy conformation. Through molecular mechanics minimizations it was understood that targeting the 5' position versus the 4', produced molecules that were linear. When the 4' position was researched with molecular mechanics calculations using aromatic substituents (phenyl and benzyl) it was found that these molecules when minimized produced structures that crowded the important points of contacts (i.e. the hydrogen bonding domain and the aryl binding site/hydrophobic pocket) making them inaccessible. In contrast, when the 5' position was substituted with the same aromatic groups, the molecules maintained an extended geometry leaving the main points of contact accessible to the active site. Through MES testing it was noted that nicotinamides that were substituted with aromatic amines had the greatest ability to prevent the development

of a seizure (see Chapter 5). Through previous testing of the nicotamide analogues, considerable activity in either the MES or PTZ test was found when the  $R^1/R^2$  groups were phenyl, benzyl, phenylethyl, or propyl. These groups were chosen because of their ability to be used as the building blocks for the synthesis of a new group of molecules in attempts to improve activity profiles.

Using the Suzuki coupling method a variety of different aromatic substituents were introduced into the 5' position of the nicotinamide analogues. The aromatic group chosen was a phenyl ring with a variety of different substitutions in the para (4') position. These substitutions included electron donating / activating groups like hydroxyl and methyl, electron donating / deactivating groups like chloride and electron withdrawing / deactivating groups like trifluoromethyl, as well as an aromatic ring with no substitutions. These substituted aromatic groups were chosen in attempts to determine the influence that different chemical factors like electron donation, steric interactions, hydrogen bonding and halogen effects have on the activity of nicotinamide molecules in the MES and PTZ tests. By changing these groups and the substituents in the  $R^1/R^2$  position, the goal was to begin to examine which chemical groups confer the greatest biological activity against the development of a seizure.

Another factor that influenced the choice of the aromatic group in the 5' position of the pyridine ring was based on a similar goal as those analogues synthesized through the Heck coupling route. By introducing an aromatic substituent, the expectation was to have improved control of the drug's half-life and limit its ability to interact with other receptors in the body. Having a drug scaffold that introduces other unique points of contact for the target receptor may help to improve its ability to be selective and limit

interactions at other undesired receptors. By introducing the substituted / unsubstituted aromatic ring into the 5' position, this may influence the ability of the nicotinamide analogues to interact at specific sites required for activity at the voltage-gated sodium channel.

The Suzuki method is a versatile palladium cross-coupling reaction that is able to tolerate a wide variety of sterically demanding substrates, which was an important consideration in the development of 5'-aryl substituted nicotinamides. Using the Suzuki cross-coupling method some of the first biaryl compounds were synthesized successfully using aryl triflates, iodoarenes and bromoarenes [121]. It was determined that steric hindrance was not a major factor that influences the formation of substituted biaryls using cross-coupling palladium methods. This reaction has also shown other advantages like being insensitive to ortho/meta/para-functional groups or heteroaromatic rings. In fact, synthetic research by Thompson in 1984, demonstrated that 5-bromonicotinate derivatives could be easily cross-coupled with substituted aryl boronic acids in yields of greater than 70% [115].

#### **4.4.3.1 Suzuki Synthetic Details**

Several methods were used in attempts to determine and optimize the coupling procedure. The most common catalyst used for Suzuki coupling is tetrakis(triphenylphosphine)palladium(0) ( $\text{Pd}(\text{PPh}_3)_4$ ) although other efficient air stable catalysts are also used like palladium(II) acetate ( $\text{Pd}(\text{OAc})_2$ ) / triphenylphosphine ( $\text{PPh}_3$ ) ligand, which is readily reduced to the active palladium(0) complex. Usually phosphine-based palladium catalysts are used because they are considered to be more stable when

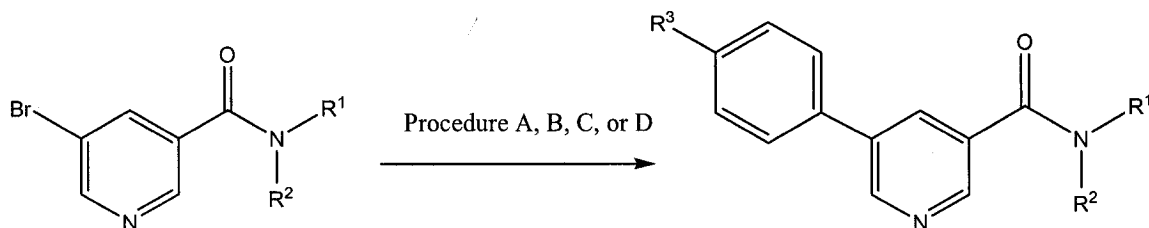
prolonged heating is required for the reaction to proceed. Both of these catalysts were used and evaluated to determine which was the most appropriate for use with nicotinamide analogues.

Organoboron compounds do not undergo transmetallation unless a base is used, this is because of their highly covalent character [126, 129]. It has been hypothesized that the boron actually forms a complex with the base and palladium catalyst to promote the transmetallation step. Different bases are often used and it has been found that weaker bases give better results with less hindered arylboronic acids [120]. The two bases that are most often utilized are sodium carbonate ( $\text{Na}_2\text{CO}_3$ ) and triethylamine ( $\text{NEt}_3$ ). Both of these bases were evaluated to determine which was the most suitable for this Suzuki coupling with nicotinamides. The reaction was run in DMF with a catalytic amount of water. DMF was the chosen solvent because these reactions generally need higher temperatures to drive the reaction forward.

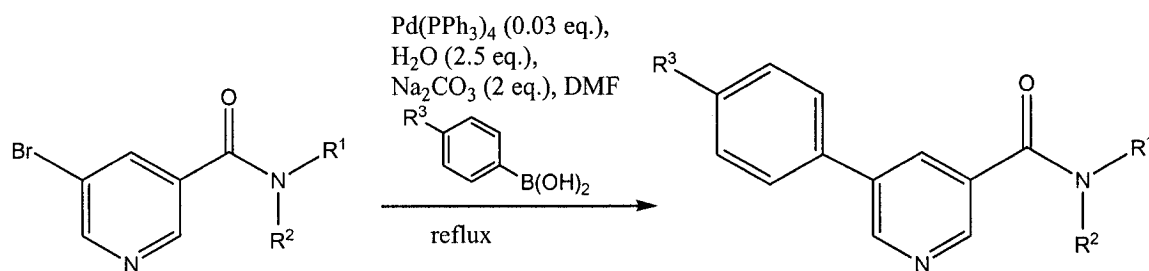
The results for the initial procedure development are presented in Table 9. Through these studies it was determined that the reaction had to be run using specific methods where each of the required components were added in a given sequence. When all the reactants were added together, yields were considerably lower than anticipated, by approximately 10 to 15%. Suzuki coupling methods can be sensitive to reaction conditions and so when the procedure developed by Heynderickx *et. al.* [130] was followed with minor modifications, the products were easily synthesized in yields of greater than 70% (Scheme 14).



**Table 9.** The reagents used for the development of the Suzuki coupling for 5-bromonicotinamides.



Procedure	$R^1$	$R^2$	$R^3$	Pd Source	Ligand	Base	Solvent	Temp (°C)	Time (h)	Yield (%)
A	$\text{CH}_2\text{C}_6\text{H}_5$	H	H	$\text{Pd}(\text{OAc})_2$	$\text{PPh}_3$	$\text{NEt}_3$	DMF	107	24	60
B	$\text{CH}_2\text{C}_6\text{H}_5$	H	H	$\text{Pd}(\text{OAc})_2$	$\text{PPh}_3$	$\text{Na}_2\text{CO}_3$	DMF	107	24	65
C	$\text{CH}_2\text{C}_6\text{H}_5$	H	H	$\text{Pd}(\text{PPh}_3)_4$		$\text{NEt}_3$	DMF	107	24	68
D	$\text{CH}_2\text{C}_6\text{H}_5$	H	H	$\text{Pd}(\text{PPh}_3)_4$		$\text{Na}_2\text{CO}_3$	DMF	107	24	81



#	$R^1$	$R^2$	$R^3$	Yield (%)
30	$\text{CH}_2\text{C}_6\text{H}_5$	H	H	81
31	$\text{CH}_2\text{C}_6\text{H}_5$	H	$\text{CH}_3$	86
32	$\text{CH}_2\text{C}_6\text{H}_5$	H	Cl	92
33	$\text{CH}_2\text{C}_6\text{H}_5$	H	$\text{CF}_3$	72
34	$\text{CH}_2\text{C}_6\text{H}_5$	H	OH	77
35	$\text{CH}(\text{CH}_3)\text{C}_6\text{H}_5$	H	H	73
36	$\text{CH}(\text{CH}_3)\text{C}_6\text{H}_5$	H	$\text{CH}_3$	89
37	$\text{CH}(\text{CH}_3)\text{C}_6\text{H}_5$	H	Cl	90
38	$\text{CH}_2\text{CH}_2\text{CH}_3$	H	Cl	75
39	$\text{CH}_2\text{CH}_2\text{CH}_3$	H	$\text{CH}_3$	76
40	$\text{C}_6\text{H}_5$	H	$\text{CH}_3$	83

**Scheme 14.** Compounds synthesized using Suzuki procedure D.

#### 4.5 Targeting The GABA<sub>A</sub>-Benzodiazepine Receptor

The previous series of analogues was designed to target the voltage-gated sodium channel; however, since nicotinamide has been shown to mediate the GABA<sub>A</sub>-benzodiazepine receptor, a series of molecules was developed in attempts to mimic the capabilities and structure of benzodiazepine derivatives. Benzodiazepines are CNS therapeutics which are used to treat a variety of disorders including epilepsy, anxiety and sleepiness [131]. The benzodiazepine binding site is located on the extracellular side of the GABA<sub>A</sub> receptor at the boundary between the  $\alpha$  and  $\gamma$  subunits [132, 133]. With no available crystal structure of the GABA<sub>A</sub> receptor bound with a benzodiazepine, it is difficult to predict the orientation and interactions between specific amino acid residues and the benzodiazepine ligand [134]. This makes the development of new drugs that target the GABA<sub>A</sub> receptor more challenging, as there are no specific chemical structures that can be built into the drug scaffold to predict or influence activity.

When GABA binds to the GABA<sub>A</sub> receptor it causes structural modifications at the benzodiazepine binding site, and it has been hypothesized that benzodiazepine binding can also cause structural changes at both GABA and benzodiazepine receptors [135, 136]. Based on this information it has been suggested that the benzodiazepine site is a flexible receptor, which is able to accommodate a variety of different structures and chemical groups [136, 137]. This means that different ligands can bind to this GABA<sub>A</sub>-benzodiazepine site in different orientations depending on which chemical contacts are crucial for binding [134]. Through examination of benzodiazepine drug scaffolds there is a considerable amount of structural diversity between the subclasses of molecules that can bind to and influence the GABA<sub>A</sub>-benzodiazepine receptor [134, 135] (Figure 19).

The primary goal for developing these nicotinamide analogues with benzodiazepine properties was to target other receptors in the CNS, so that utilizing additional channels in the CNS could control different forms of epilepsy.

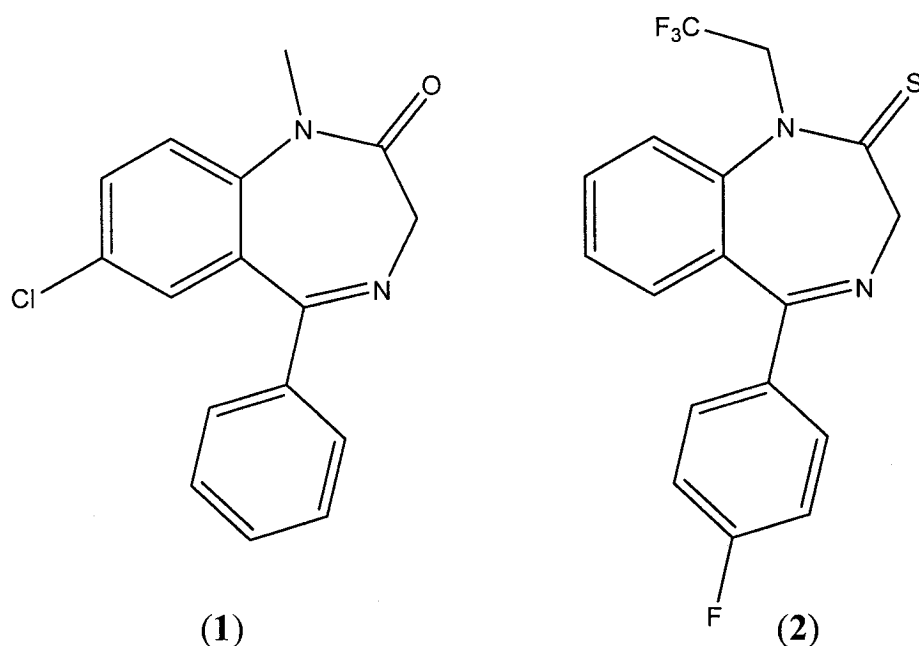


**Figure 19.** Compounds that target the benzodiazepine GABA<sub>A</sub> receptor (1) Diazepam and (2) Quazepam

One drug currently on the market, Quazepam (Figure 19), became of particular interest when it was noted that, although it had sleep/relaxation effects, it was also able to influence epilepsy. Its structure is unique from other benzodiazepines because it contains a sulfur moiety as an electron donor region instead of an oxygen or an alkene. Sulfur was chosen in attempts to strengthen the potency of the nicotinamide analogues by increasing their binding affinity for the receptor site [36]. Using this Quazepam-thio structure and the biological activity of the nicotinamides previously tested, a new series of molecules was developed for synthesis. The purpose of these analogues was to mimic

the portions of the benzodiazepine moiety that make them active molecules for the GABA<sub>A</sub> receptor, introduce a sulfide/ sulfoxide moiety at the 2' position of the pyridine ring to look at the influence of sulfur on binding, and finally to limit the tendency to develop tolerance to benzodiazepines by using a nicotinamide chemical foundation.

A benzyl group was attached to the sulfur atom since N-benzylnicotinamide was the most successful candidate in preventing the development of a seizure through the NIH screening program. By attaching the same aromatic group to the sulfur atom, the hope was to create another active pharmacophore on the nicotinamide backbone to target both the GABA<sub>A</sub>-benzodiazepine receptor and the sodium channel. The amines that were chosen for the nicotinamide structure included both alkyl and aromatic groups so that representation of different activity profiles could be addressed. The analogues were all tested as 2-(benzylthio)-N-substituted-pyridine-3-carboxamides to determine if these analogues could influence the GABA<sub>A</sub>-benzodiazepine receptor. Based on the biological data obtained from NIH, these analogues had limited activity in the PTZ model and no activity in the MES model. Although these analogues influenced the GABA<sub>A</sub> receptor, which was their initial goal, they only had limited activity and so a new series of molecules was developed in an attempt to increase bioactivity.

This next collection of molecules synthesized to target the GABA<sub>A</sub> receptor involved oxidizing the thiol in the 2-(benzylthio)-N-substituted-pyridine-3-carboxamide to a sulfoxide. All benzodiazepines derivatives contained a characteristic 7-membered ring structure. The hypothesis for using sulfoxide nicotinamides was to recreate this 7-membered ring structure but have it be established through a stabilizing hydrogen bond between the amide hydrogen the sulfoxide oxygen, instead of covalent linkages like in

benzodiazepines. Hydrogen bonding is an important intramolecular electrostatic interaction that assists in stabilizing molecular structure [36]. A hydrogen bond is considered a weak interaction with energies between 7 to 40 kJ/mol and lengths between 1.7 to 2.3 Å [36]. This pseudo 7-membered ring will hopefully allow these nicotinamide structures to bind at the GABA<sub>A</sub>-benzodiazepine receptor and influence the spread of electrical activity in the brain. Another important goal of using a pseudo 7-membered ring is to allow these compounds to have some conformational flexibility so that there are fewer effects, especially those associated with addiction, which is a common attribute of benzodiazepine drugs.

Before the 2-(benzylsulfinyl)-N-substituted-pyridine-3-carboxamide molecules were synthesized, a computational study was conducted to determine if the hypothesis of a hydrogen bond between the amide hydrogen and the sulfoxide oxygen was possible. Several amides were chosen to be studied *in silico* based on their previous MES and PTZ activity. These included 2-(benzylsulfinyl)-N-(1-phenylethyl)pyridine-3-carboxamide, N-benzyl-2-(benzylsulfinyl)pyridine-3-carboxamide, 2-(benzylsulfinyl)-N-phenylpyridine-3-carboxamide, and 2-(benzylsulfinyl)-N-propylpyridine-3-carboxamide. The molecules were minimized with molecular mechanics using the Tripos force field and Powell conjugate gradient as implemented in Sybyl 7.2 [138]. The lowest energy conformations were then examined to determine if the molecular arrangements were in the correct position to create a linear hydrogen bond and a pseudo 7-membered ring (Figure 20). Based on the calculations, all the distances between the amide hydrogen and the sulfoxide oxygen were within the distance to be considered a viable hydrogen bond; however some appear to be closer than others (Table 10). Using these calculations, 2-

(benzylsulfinyl)-N-(1-phenylethyl)pyridine-3-carboxamide and N-benzyl-2-(benzylsulfinyl)pyridine-3-carboxamide were selected to be synthesized.

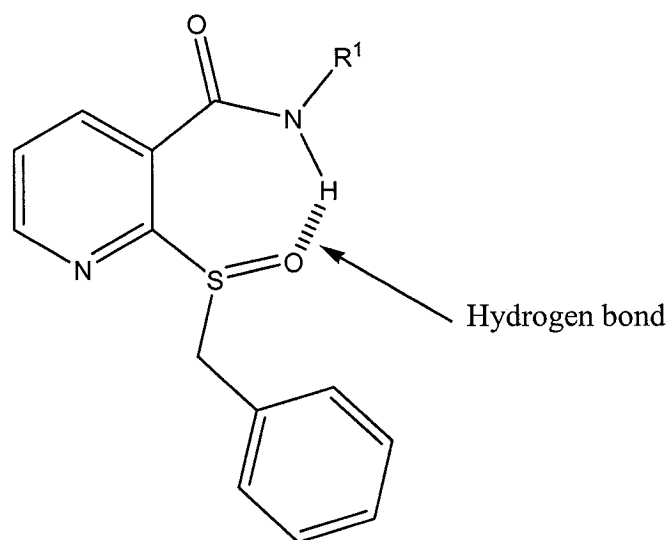


**Figure 20.** The pseudo 7-membered ring of the nicotinamide analogue showing the hydrogen bond.

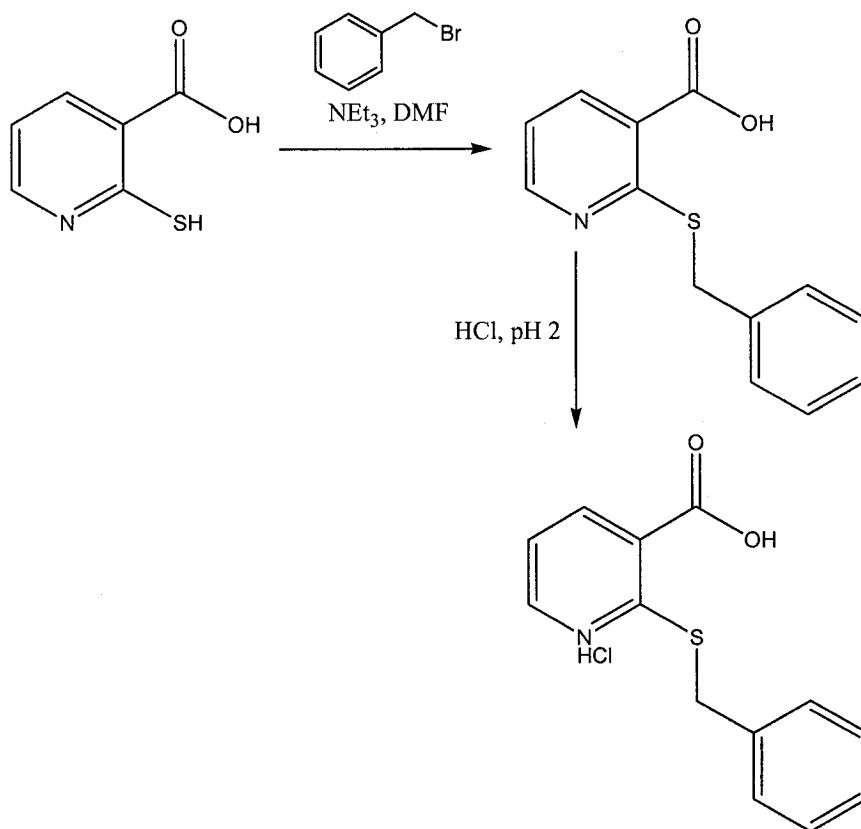
**Table 10.** The calculated hydrogen bonds for the nicotinamide analogues targeting the GABA<sub>A</sub>-benzodiazepine receptor.

Compound Name	Hydrogen Bond (Å)
2-(benzylsulfinyl)-N-(1-phenylethyl)pyridine-3-carboxamide	1.93
N-benzyl-2-(benzylsulfinyl)pyridine-3-carboxamide	2.08
2-(benzylsulfinyl)-N-phenylpyridine-3-carboxamide	2.15
2-(benzylsulfinyl)-N-propylpyridine-3-carboxamide	2.10

#### 4.5.1 Synthetic Considerations

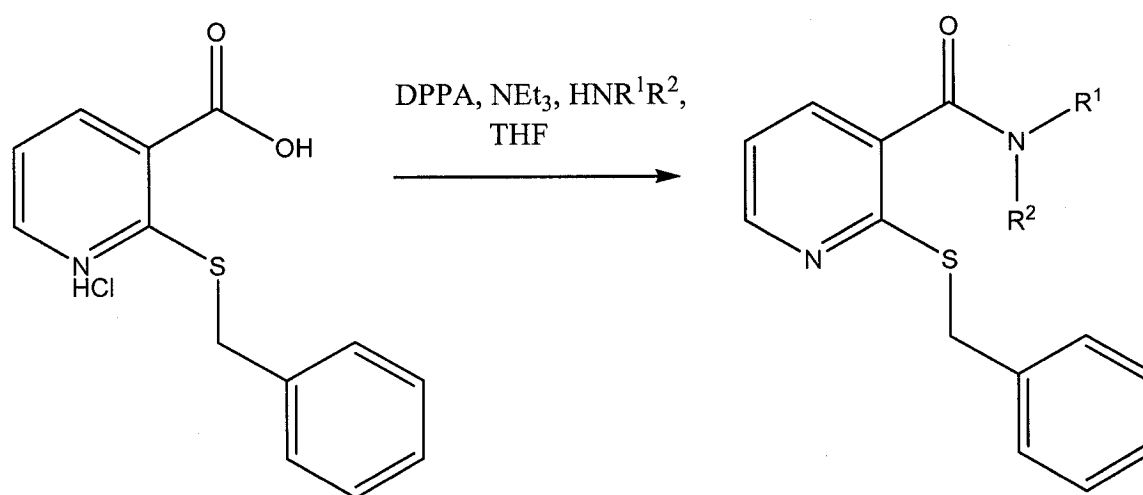
The synthesis of both the 2-(benzylthio)-N-substituted-pyridine-3-carboxamide analogues and 2-(benzylsulfinyl)-N-substituted-pyridine-3-carboxamide analogues proceeded as expected with yields of 65% or more over the three steps. The first step

involved reacting 2-mercaptopyridine-3-carboxylic acid with benzyl bromide in a nucleophilic substitution to generate 2-(benzylthio)pyridine-3-carboxylic acid, and upon acid work-up the HCl salt was produced (Scheme 15). Initially the reaction was not acidified with HCl, and a viscous liquid resulted as the product. Although this product was pure by TLC, NMR and HRMS, it was difficult to transfer from one reaction flask to another. Since this was a starting material that was going to be used in many reactions it was concluded that it would be easier for scale-up purposes if the products were produced as a solid. During the reaction work-up, the solution was acidified to a pH of 2, leading to protonation of the pyridine nitrogen, which caused the product 2-(benzylthio)pyridine-3-carboxylic acid HCl (**41**) to crash out of solution.



**Scheme 15.** Synthetic route used for the development of 2-(benzylthio)pyridine-3-carboxylic acid.

For the formation of the amide bond, two synthetic routes were attempted both the DCC and DPPA. Again, although the DCC coupling produced the correct product, yields were less than 25% for the three amides attempted. Based on the initial research into the synthesis of an amide bond, the DPPA route was utilized (Scheme 16). The yields were over 70%, therefore this DPPA procedure was used to synthesize the amide bonds.



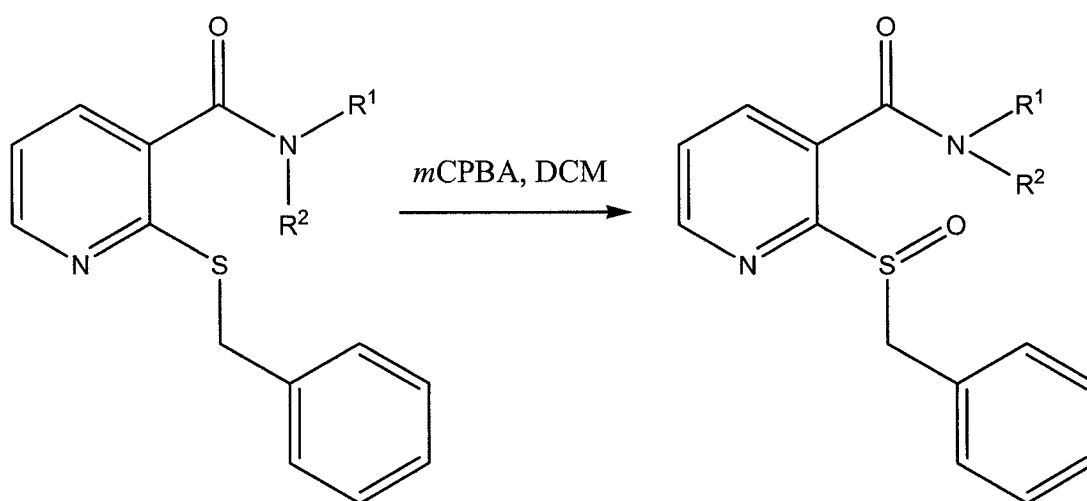
#	R <sup>1</sup>	R <sup>2</sup>	Yield (%)
42	CH <sub>2</sub> CH <sub>2</sub> CH <sub>3</sub>	H	90
43	C <sub>6</sub> H <sub>5</sub> ( <i>o</i> -CH <sub>3</sub> ) <sub>2</sub>	H	91
44	CH <sub>2</sub> C <sub>6</sub> H <sub>5</sub>	CH <sub>3</sub>	91
45	C <sub>6</sub> H <sub>11</sub>	H	85
46	C <sub>6</sub> H <sub>5</sub>	H	70
47	CH <sub>2</sub> C <sub>6</sub> H <sub>5</sub>	H	93
48	CH(CH <sub>3</sub> )C <sub>6</sub> H <sub>5</sub>	H	90

**Scheme 16.** Synthetic route used for the development of 2-(benzylthio)pyridine-3-nicotinamides.

The final step involved oxidizing the sulfide to a sulfoxide and this was accomplished using 3-chloroperoxybenzoic acid (*m*CPBA) [139]. This oxidizing agent



was chosen because it could be easily handled since it was a solid and had been used widely in the oxidation of sulfides [139-141]. Initially the incorrect product, a sulfone, was produced. It was the result of adding two equivalents of *m*CPBA too quickly and also not monitoring the reaction for completion. When the reaction was run again 1.15 equivalents of *m*CPBA were used, and it was added slowly over 5 minutes while monitoring for completion by TLC. Using this technique the sulfoxide was obtained in a 70% yield with no formation of sulfone (Scheme 17).



#	R <sup>1</sup>	R <sup>2</sup>	Yield (%)
49	CH <sub>2</sub> C <sub>6</sub> H <sub>5</sub>	H	70
50	CH(CH <sub>3</sub> )C <sub>6</sub> H <sub>5</sub>	H	81

**Scheme 17.** Synthetic route used for the development of 2-(benzylsulfinyl)pyridine-3-nicotinamides.

## 4.6 Experimental

$^1\text{H}$  and  $^{13}\text{C}$  nuclear magnetic resonance (NMR) spectra were recorded using a Bruker AC-250 MHz or AVANCE 500MHz spectrometer. Chemical shifts ( $\delta$ ) are reported as parts per million downfield from tetramethylsilane (TMS) and are calibrated using the solvent peaks or when possible, the TMS peak present in some of the deuterated solvents. Coupling constants ( $J$ ) are reported in Hz. Correlation spectroscopy techniques (HMBC, HSQC) were used in some situations to confirm structural connectivity.

High resolution mass spectrometry (HRMS) by electron impact (EI) was performed on a CEC21-100B sector mass spectrometer, and samples were analyzed as solids. The  $m^+/z$  of the molecular ion peak ( $\text{M}^+$ ) is provided along with the expected/calculated value for each of the corresponding molecular formula. The error on each of the HRMS values is  $\pm 0.0008$  amu. In situations where the compounds were not stable to EI and the molecular ion could not be detected, low resolution electrospray ionization (ESI) was used to visualize the  $[\text{M}-1]^+$ , followed by HRMS by EI on the expected fragment of the compound.

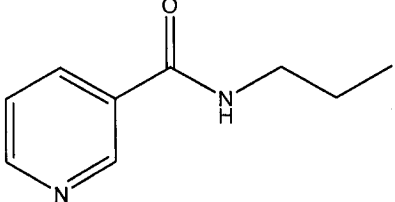
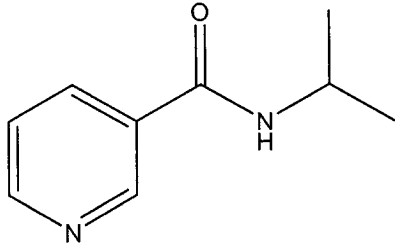
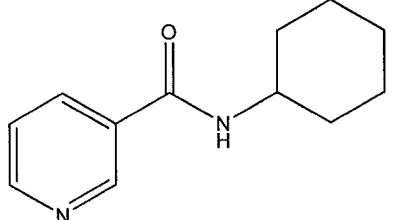
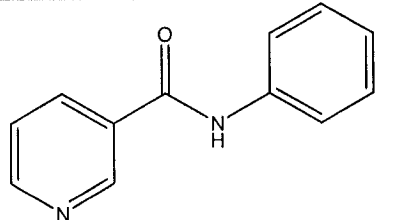
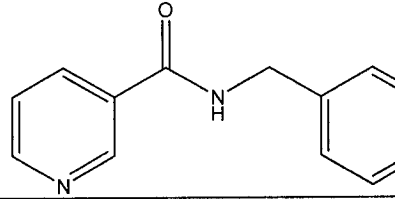
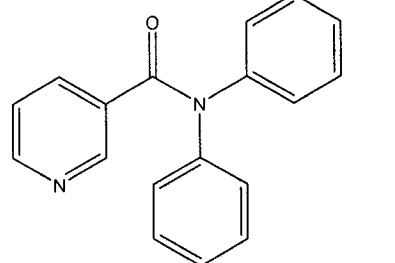
Reagents and solvents required for the reactions were obtained from commercial sources: Sigma-Aldrich, Inc. and Fluka. Melting points (mp) for the compounds synthesized were determined using a Mel-Temp II capillary apparatus and are uncorrected. Analytical thin-layer chromatography (TLC) was carried out to monitor reactions using pre-coated Brinkmann silica gel 60 F<sub>254</sub> plates with glass backing. TLC plates were visualized using UV light or, in specific situations, iodine or potassium

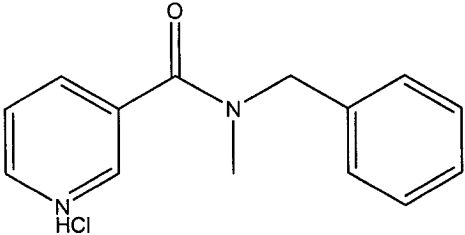
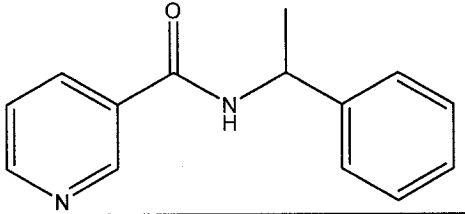
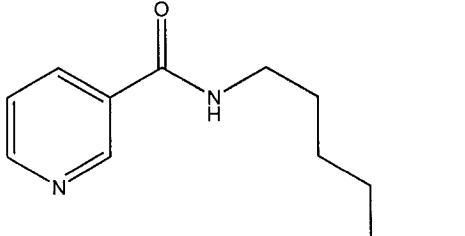
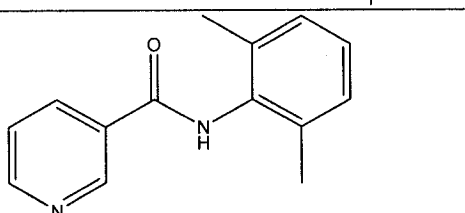
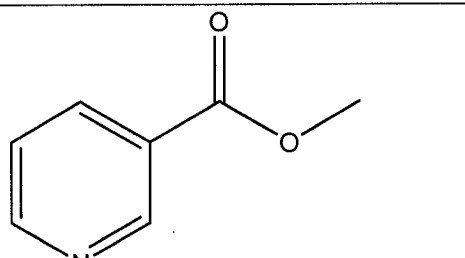
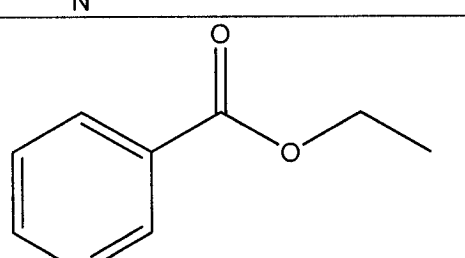
permanganate. The solvent systems used for both TLC and column chromatography are listed below.

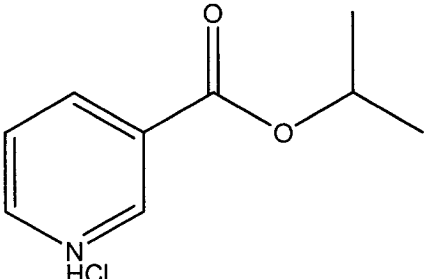
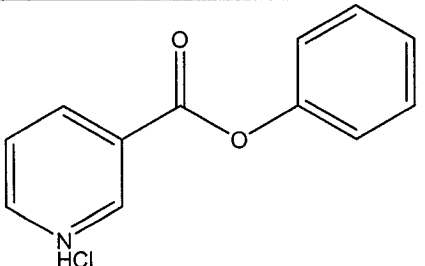
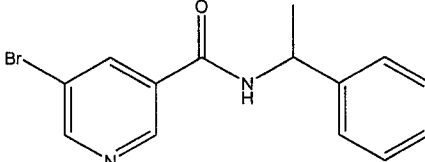
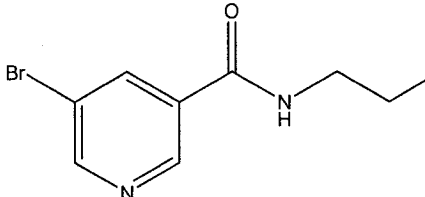
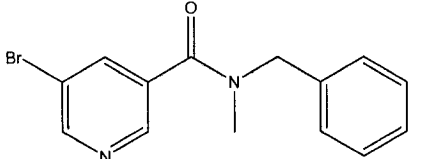
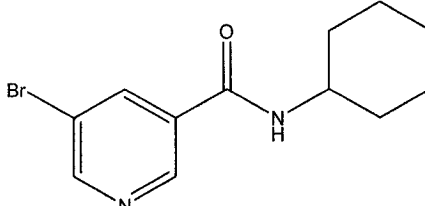
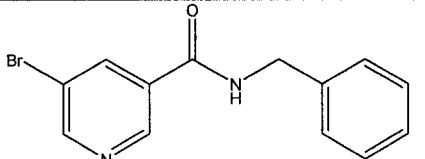
- (A) Ethyl Acetate : Methanol (20:1)
- (B) Hexane : Ethyl Acetate (2:1)
- (C) Hexane : Ethyl Acetate (1:2)
- (D) Hexane : Ethyl Acetate (1:1)
- (E) Hexane : Ethyl Acetate (5:2)
- (F) Hexane : Ethyl Acetate (1:6)
- (G) Hexane : Ethyl Acetate (3:1)
- (H) Chloroform : Ethyl Acetate (4:1)
- (I) Chloroform : Methanol (10:1)
- (J) Chloroform : Methanol (10:2.5)
- (K) Chloroform : Methanol (30:1)
- (L) Hexane : Ethyl Acetate: Acetone (7:5:1)
- (M) Hexane : Ethyl Acetate: Acetone (10:2:1)
- (N) Chloroform : Ethyl Acetate (1:1)
- (O) DCM : THF (50: 1)
- (P) Hexane : Ethyl Acetate (1:3)

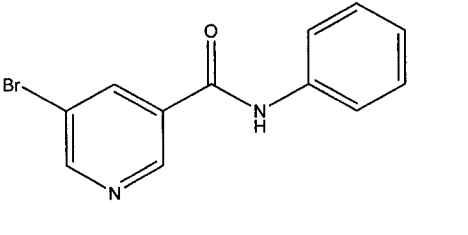
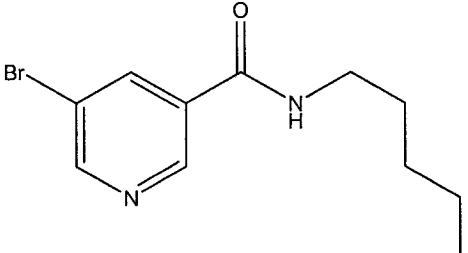
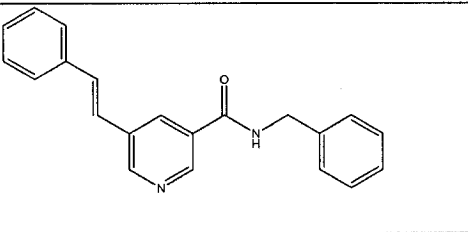
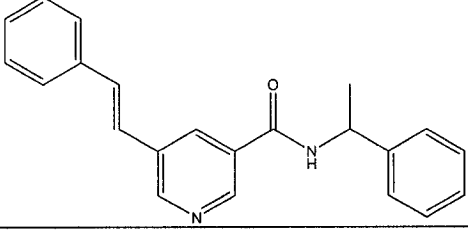
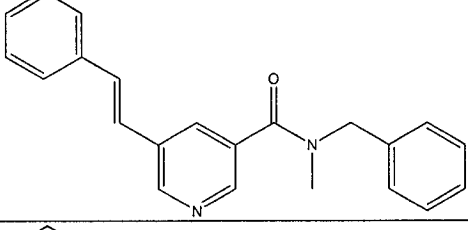
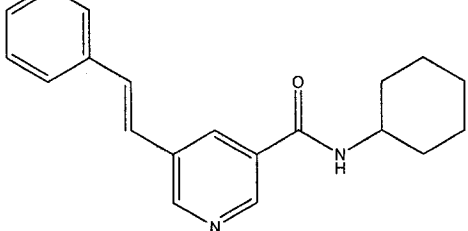
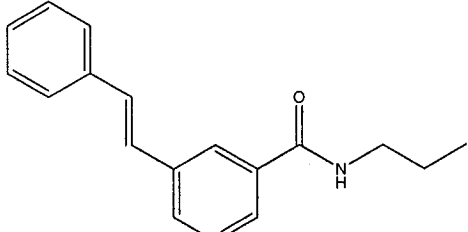
Presented below in Table 11, is a listing of all the nicotinamide analogues that were synthesized, along with their corresponding identification number and IUPAC names.

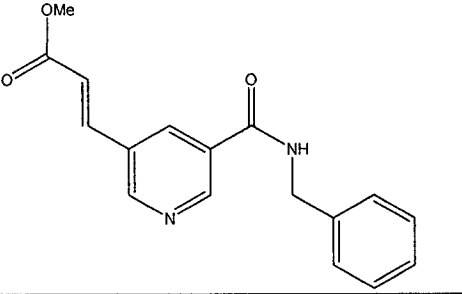
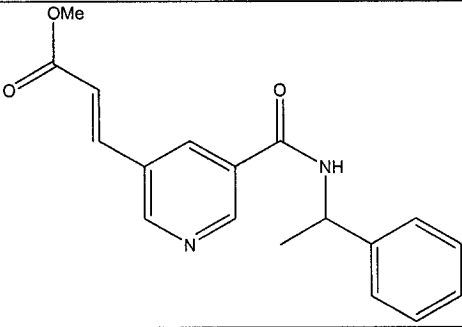
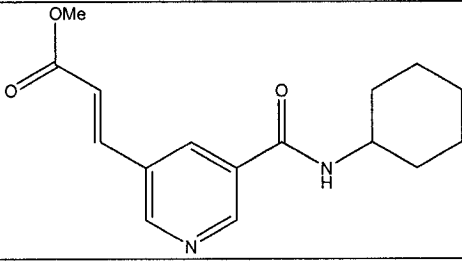
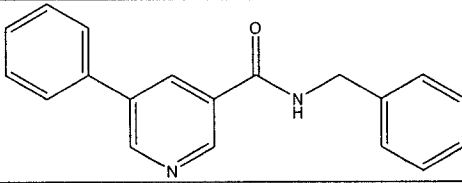
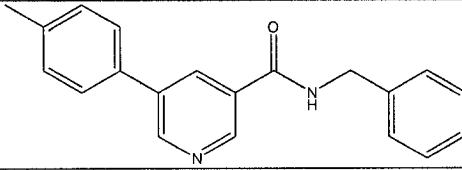
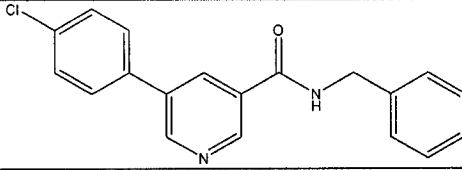
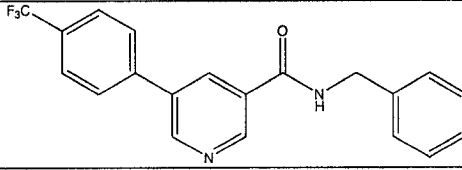
**Table 11.** The nicotinamide analogues synthesized with their corresponding identification numbers (ID) and their IUPAC names.

Compound	ID	IUPAC Name
	1	<i>N</i> -Propylnicotinamide
	2	<i>N</i> -Isopropylnicotinamide
	3	<i>N</i> -Cyclohexylnicotinamide
	4	<i>N</i> -Phenylnicotinamide
	5	<i>N</i> -Benzyl nicotinamide
	6	<i>N,N</i> -Diphenylnicotinamide

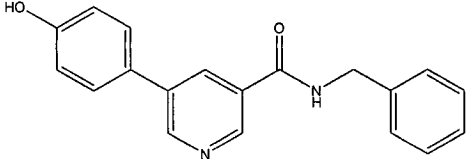
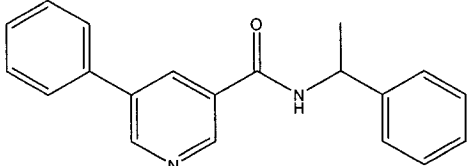
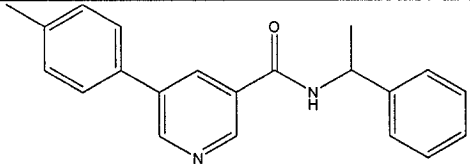
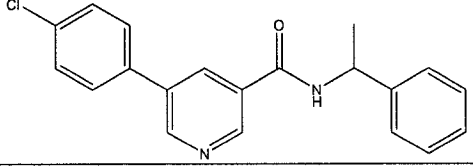
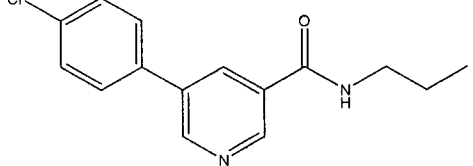
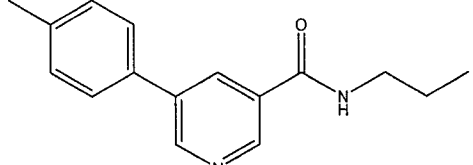
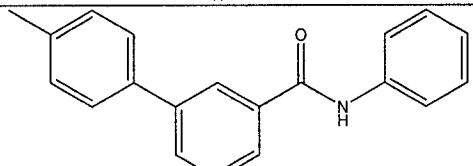
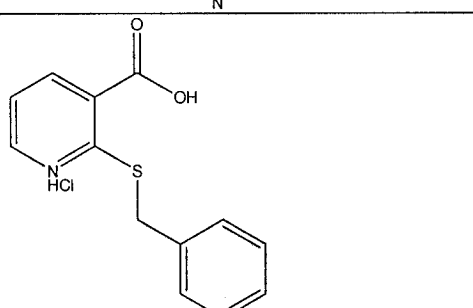
	<b>7</b>	N-Benzyl-N-methylnicotinamide HCl
	<b>8</b>	N-(1-Phenylethyl)nicotinamide
	<b>9</b>	N-Pentyl nicotinamide
	<b>10</b>	N-(2,6-Dimethylphenyl) nicotinamide
	<b>11</b>	Methyl nicotinate
	<b>12</b>	Ethyl nicotinate

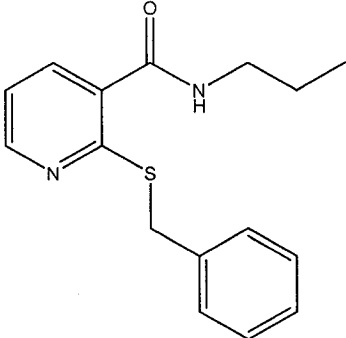
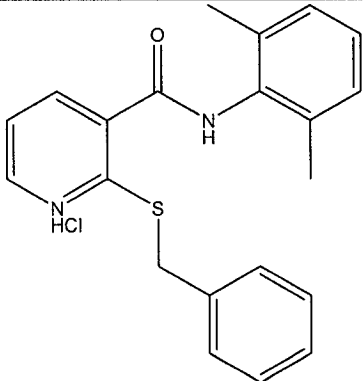
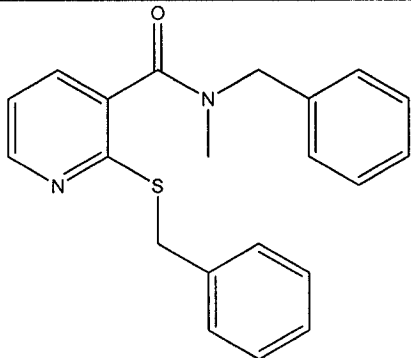
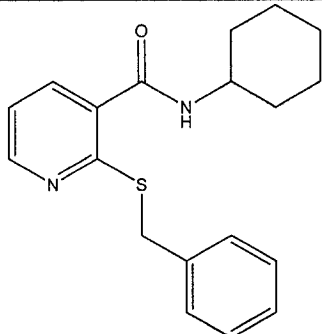
	13	Isopropyl nicotinate
	14	Phenyl nicotinate
	15	5-Bromo-N-(1-phenylethyl)pyridine-3-carboxamide
	16	5-Bromo-N-propylpyridine-3-carboxamide
	17	N-Benzyl-5-bromo-N-methylpyridine-3-carboxamide
	18	5-Bromo-N-cyclohexylpyridine-3-carboxamide
	19	N-Benzyl-5-bromopyridine-3-carboxamide

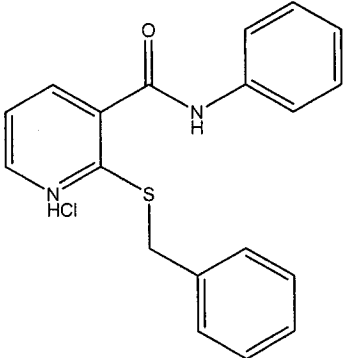
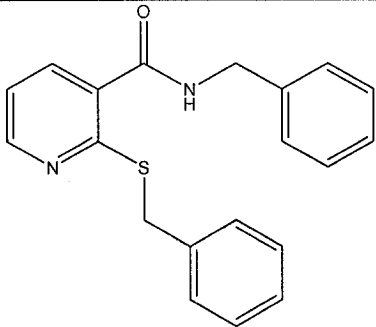
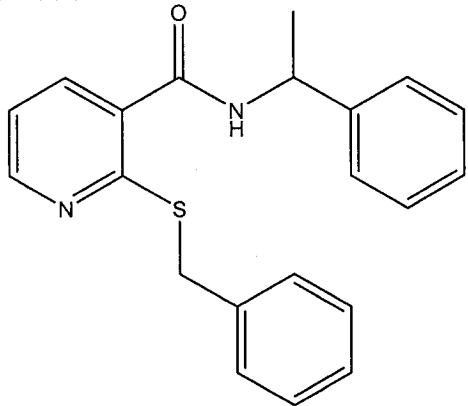
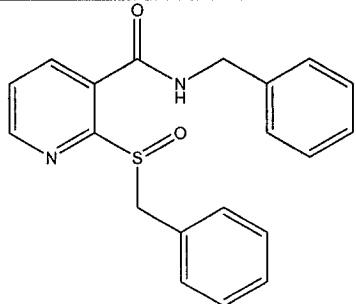
	<b>20</b>	5-Bromo-N-phenylpyridine-3-carboxamide
	<b>21</b>	5-Bromo-N-pentylpyridine-3-carboxamide
	<b>22</b>	N-Benzyl-5-styrylpyridine-3-carboxamide
	<b>23</b>	N-(1-Phenylethyl)-5-styrylpyridine-3-carboxamide
	<b>24</b>	N-Benzyl-N-methyl-5-styrylpyridine-3-carboxamide
	<b>25</b>	N-Cyclohexyl-5-styrylpyridine-3-carboxamide
	<b>26</b>	N-Propyl-5-styrylpyridine-3-carboxamide

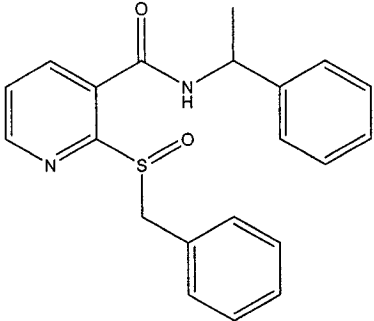
	27	(E)-Methyl-3-(5-(benzylcarbamoyl)pyridine-3-yl)acrylate
	28	(E)-Methyl 3-(5-(1-phenylethylcarbamoyl)pyridine-3-yl)acrylate
	29	(E)-Methyl 3-(5-(cyclohexylcarbamoyl)pyridine-3-yl)acrylate
	30	N-Benzyl-5-phenylpyridine-3-carboxamide
	31	N-Benzyl-5-p-tolylpyridine-3-carboxamide
	32	N-Benzyl-5-(4-chlorophenyl)pyridine-3-carboxamide
	33	N-Benzyl-5-(4-(trifluoromethyl)phenyl)pyridine-3-carboxamide



	<b>34</b>	N-Benzyl-5-(4-hydroxyphenyl)pyridine-3-carboxamide
	<b>35</b>	5-Phenyl-N-(1-phenylethyl)pyridine-3-carboxamide
	<b>36</b>	N-(1-Phenylethyl)-5-p-tolylpyridine-3-carboxamide
	<b>37</b>	5-(4-Chlorophenyl)-N-(1-phenylethyl)pyridine-3-carboxamide
	<b>38</b>	5-(4-Chlorophenyl)-N-propylpyridine-3-carboxamide
	<b>39</b>	N-Propyl-5-p-tolylpyridine-3-carboxamide
	<b>40</b>	N-Phenyl-5-p-tolylpyridine-3-carboxamide
	<b>41</b>	2-(Benzylthio)pyridine-3-carboxylic acid HCl

	42	2-(Benzylthio)- <i>N</i> -propylpyridine-3-carboxamide
	43	2-(Benzylthio)- <i>N</i> -(2,6-dimethylphenyl)pyridine-3-carboxamide HCl
	44	<i>N</i> -Benzyl-2-(benzylthio)- <i>N</i> -methylpyridine-3-carboxamide
	45	2-(Benzylthio)- <i>N</i> -cyclohexylpyridine-3-carboxamide

	46	2-(Benzylthio)- <i>N</i> -phenylpyridine-3-carboxamide HCl
	47	<i>N</i> -Benzyl-2-(benzylthio)pyridine-3-carboxamide
	48	2-(Benzylthio)- <i>N</i> -(1-phenylethyl)pyridine-3-carboxamide
	49	<i>N</i> -Benzyl-2-(benzylsulfinyl)pyridine-3-carboxamide

	<b>50</b>	2-(Benzylsulfinyl)- <i>N</i> -(1-phenylethyl)pyridine-3-carboxamide
-----------------------------------------------------------------------------------	-----------	---------------------------------------------------------------------

#### 4.6.1 Nicotinamide Derivatives: Route A (DCC coupling) – General Procedure

##### Route 1: DCC Coupling – General Procedure

A stirred solution of nicotinic acid (1.2 g, 10 mmol) and DMF (10 mL) were cooled in an ice bath. The amine derivative (1.5 eq.), triethylamine (2.5 eq.) and then the DCC (1.2 eq.) were added slowly at 0 °C and then the reaction was allowed to warm to room temperature and stirred for an additional 5 h while monitoring by TLC. Once the reaction was complete, the solution was diluted with ethyl acetate and washed three times with distilled water. The organic layer was dried using sodium sulfate, and the solvent was removed under vacuum to produce a solid. Column chromatography was used for purification using solvent system (L), (M), or (N).

##### Route 2: DCC Coupling – General Procedure

A mixture of nicotinic acid (0.1 g, 0.8 mmol), DMAP (0.1 eq.), DMF (5 mL) and the amine derivative (1.5 eq.) was stirred at room temperature, followed by the addition of DCC (1.2 eq.) and triethylamine (2.5 eq.). The mixture was stirred for 18 hours, and then the solvent was removed by rotary evaporation. The residue was combined with EtOAc (50 mL) and kept in the freezer overnight. Some of the DCU precipitated out and was

filtered off. The DCU was washed 3 times with EtOAc, the filtrates were combined with the original EtOAc mixture, washed with water (3 x 20 mL) and dried over MgSO<sub>4</sub>. The solvent was evaporated and the crude product was purified using column chromatography and solvent systems **(L)**, **(M)**, or **(N)**.

#### **4.6.2 Nicotinamide Derivatives: Route B (EEDQ coupling) – General Procedure**

To a cooled solution of nicotinic acid (1.1 g, 8.1 mmol), EEDQ (1.2 eq.), THF (20 ml) and triethylamine or diisopropylethylamine (1.5 eq.) was added the amine derivative (1.5 eq.). The solution was warmed to room temperature and stirred for 12 h while monitoring by TLC for completion. The THF was removed in vacuo resulting in a viscous liquid. Column chromatography was used for purification using solvent system **(O)** and the product was crystallized using an ethyl acetate / hexane (80: 20) mixture.

#### **4.6.3 Nicotinamide Derivatives: Route C (Nicotinyl Chloride) – General Procedure**

##### **Step 1**

A mixture of nicotinic acid (10 g, 81 mmol) and thionyl chloride (1.2 eq.) were combined in dry DMF (25 mL) and heated at reflux for 5 h. The resulting solution was cooled and filtered, and the excess thionyl chloride and DMF were removed by distillation. A viscous liquid was obtained which was dissolved in ethanol and acidified to pH 4 using 6N HCl. Solvents were removed under high vacuum to produce a crystalline product. Percent yield 85-92%.

## Step 2

To a cooled solution of nicotinyl chloride (1.3 g, 5.5 mmol) and dry THF (20 mL) was added the amine derivative (1.5 eq.) and triethylamine (2.5 eq.). The solution was warmed to room temperature and stirred for 12 h while monitoring by TLC. Once the solution had gone to completion chloroform was added and washed three times with distilled water. The organic layer was dried over sodium sulfate and the solvent was removed under vacuum. The resulting solids and viscous liquids were purified by column chromatography using solvent system (A). The resulting solids were crystallized using ethyl acetate/ hexane mixtures.

### 4.6.4 Nicotinamide Derivatives: Route D (DPPA coupling) – General Procedure

To a cooled solution of nicotinic acid (1.1 g, 8.1 mmol) and dry THF (25 mL) were added the amine derivative (1.2 eq.) and triethylamine or diisopropylethylamine (2.5 eq.). The solution was stirred for 10 min. and then DPPA (1.2 eq.) was added, and the solution was stirred at room temperature for 18 h. while being monitored by TLC. Once complete the THF was removed by evaporation, ethyl acetate was added and the solution was washed three times with sodium carbonate. The ethyl acetate layer was dried with sodium sulfate and the solvent was evaporated to viscous liquid. Column chromatography or crystallization was used to isolate the pure product. This reaction was also scaled up using nicotinic acid (10 g, 81 mmol), THF (100 mL) and the amine derivatives and triethylamine in the same molar equivalents.

***N-Propylnicotinamide (1)***

Crystalline solid (0.771 g, 85%); mp = 91-92 °C (lit. mp = 89-92°C); <sup>1</sup>H NMR (CD<sub>3</sub>OD): 1.02 (t, 3H, J=7.5), 1.69 (m, 2H), 3.39 (m, 2H), 7.57 (dd, 1H J=6.1, 7.2), 8.27 (d, 1H, J=7.2), 8.71 (d, 1H, J=6.1), 9.01 (s, 1H), 9.84 (t, 1H, J= 6.2); <sup>13</sup>C NMR (CD<sub>3</sub>OD): 11.3, 23.6, 43.1, 124.9, 130.8, 138.1, 127.5, 153.2, 167.3; HRMS: C<sub>9</sub>H<sub>12</sub>N<sub>2</sub>O calculated 164.0949 amu, found 164.0948 amu.

***N-Isopropylnicotinamide (2)***

Crystalline solid (0.811 g, 89%); mp = 86-88 °C (lit. mp = 85-87 °C); <sup>1</sup>H NMR (CD<sub>3</sub>OD): 1.21 (d, 6H, J=6.2), 3.88 (m, 1H), 7.65 (dd, 1H, J=6.1, 7.2), 8.23 (d, 1H, J=7.2), 8.85 (d, 1H, J=6.1), 9.01 (s, 1H), 10.02 (d, 1H, J=6.3); <sup>13</sup>C NMR (CD<sub>3</sub>OD): 23.5, 41.2, 124.6, 130.6, 138.3, 148.5, 153.9, 167.6; HRMS: C<sub>9</sub>H<sub>12</sub>N<sub>2</sub>O calculated 164.0949 amu, found 164.0947 amu.

***N-Cylcohexylnicotinamide (3)***

Crystalline solid (0.938 g, 82%); mp = 138-140 °C (lit. mp=140-142 °C); <sup>1</sup>H NMR (DMSO-d<sub>6</sub>): 1.45 (m, 8H), 1.75 (m, 2H), 3.54 (m, 1H), 7.59 (dd, 1H, J=6.1, 7.2), 8.32 (d, 1H, J=7.2), 8.79 (d, 1H, J=6.1), 9.02 (s, 1H), 10.01 (d, 1H, J=5.9); <sup>13</sup>C NMR (DMSO-d<sub>6</sub>): 22.9, 28.1, 33.6, 47.6, 125.1, 131.1, 138.7, 148.3, 153.8, 168.1; HRMS: C<sub>12</sub>H<sub>16</sub>N<sub>2</sub>O calculated 204.1263 amu, found 204.1266 amu.

***N*-Phenylnicotinamide (4)**

Crystalline solid (1.03 g, 91%); mp = 116-118 °C (lit. 117-119 °C); <sup>1</sup>H NMR (DMSO-d<sub>6</sub>): 7.01 (m, 1H), 7.23 (m, 2H), 7.64 (m, 3H), 8.32 (d, 1H, *J*=7.2), 8.86 (d, 1H, *J*=6.1), 9.02 (s, 1H), 9.97 (s, 1H); <sup>13</sup>C NMR (DMSO-d<sub>6</sub>): 121.6, 124.9, 125.3, 128.6, 129.2, 130.7, 138.2, 148.5, 153.3, 166.9; HRMS: C<sub>12</sub>H<sub>10</sub>N<sub>2</sub>O calculated 198.0793 amu, found 198.0781 amu.

***N*-Benzylnicotinamide (5)**

Crystalline solid (0.623 g, 82%); mp = 81-83 °C (lit. 83 °C); <sup>1</sup>H NMR (DMSO-d<sub>6</sub>): 7.06 (m, 3H), 7.19 (m, 2H), 4.32 (s, 2H), 7.57 (dd, 1H, *J*=6.1, 7.2), 8.25 (d, 1H, *J*=7.2), 8.78 (d, 1H, *J*=6.1), 9.01 (s, 1H), 10.05 (d, 1H, *J*=5.8); <sup>13</sup>C NMR (DMSO-d<sub>6</sub>): 44.5, 125.4, 126.89, 127.0, 127.1, 128.7, 131.1, 138.6, 141.8, 148.2, 154.1, 168.3; HRMS: C<sub>13</sub>H<sub>12</sub>N<sub>2</sub>O calculated 212.0949 amu, found 212.0953 amu.

***N, N*-Diphenylnicotinamide (6)**

Crystalline solid (1.20 g, 78%); mp = 151-153 °C (lit. 152-153 °C); <sup>1</sup>H NMR (DMSO-d<sub>6</sub>): 7.01 (m, 2H), 7.27 (m, 4H), 7.65 (m, 5H), 8.25 (d, 1H, *J*=7.0), 8.79 (d, 1H, *J*=6.1), 9.11 (s, 1H); <sup>13</sup>C NMR (DMSO-d<sub>6</sub>): 118.4, 119.2, 130.1, 136.3, 138.2, 140.9, 141.6, 148.34, 153.75, 167.45; HRMS: C<sub>18</sub>H<sub>14</sub>N<sub>2</sub>O calculated 274.1106 amu, found 274.1113 amu.



***N-Benzyl-N-methylnicotinamide HCl (7)***

A viscous liquid was obtained, which was dissolved in ethanol and acidified to a pH of 4 using HCl (6N). Solvents were removed by a combination of evaporation and high vacuum to produce a crystalline product. Crystalline solid (1.12 g, 85%); mp = 350 °C (dec) HCl salt; <sup>1</sup>H NMR (CD<sub>3</sub>OD): 2.91 (s, 3H), 4.22 (s, 2H), 7.07 (m, 5H), 7.56 (dd, 1H, *J*=6.1, 7.3), 8.27 (d, 1H, *J*=7.3), 8.75 (d, 1H, *J*=6.1), 9.01 (s, 1H); <sup>13</sup>C NMR (CD<sub>3</sub>OD): 34.6, 52.3, 125.2, 125.8, 127.2, 128.2, 130.1, 136.5, 137.9, 148.2, 153.1, 169.9; HRMS: C<sub>14</sub>H<sub>15</sub>ClN<sub>2</sub>O calculated 262.0878 amu, found 262.0873 amu.

***N-(1-Phenylethyl)nicotinamide (8)***

Crystalline solid (1.07 g, 85%); mp = 152-153 °C; <sup>1</sup>H NMR (DMSO-d<sub>6</sub>): 1.59 (d, 3H, *J*=6.2), 5.06 (q, 1H, *J*=6.2), 7.20 (m, 5H), 7.57 (dd, 1H, *J*=6.2, 7.2), 8.36 (d, 1H, *J*=7.2), 8.67 (d, 1H, *J*=6.2), 9.03 (s, 1H); <sup>13</sup>C NMR (DMSO-d<sub>6</sub>): 21.5, 49.6, 125.1, 126.9, 127.2, 128.6, 130.7, 138.1, 143.5, 148.2, 153.9, 167.6; HRMS: C<sub>14</sub>H<sub>14</sub>N<sub>2</sub>O calculated 226.1106 amu, found 226.1113 amu.

***N-Pentylnicotinamide (9)***

Crystalline solid (0.885 g, 82%); mp = 114-115 °C; <sup>1</sup>H NMR (DMSO-d<sub>6</sub>): 1.03 (m, 3H), 1.34 (m, 4H), 1.57 (m, 2H), 2.97 (m, 2H), 7.64 (dd, 1H, *J*=6.2, 7.2), 8.32 (d, 1H, *J*=7.2), 8.85 (d, 1H, *J*=6.2), 9.14 (s, 1H), 10.02 (t, 1H, *J*=5.8); <sup>13</sup>C NMR (DMSO-d<sub>6</sub>): 14.1, 22.5, 29.1, 29.9, 40.9, 125.1, 130.0, 139.2, 148.2, 153.5, 167.9; HRMS: C<sub>11</sub>H<sub>16</sub>N<sub>2</sub>O calculated 192.1263 amu, found 192.1259 amu.

#### ***N*-(2,6-Dimethylphenyl)nicotinamide (10)**

Peach crystalline solid (0.975 g, 86%); mp = 120-121 °C; crystallization using ethyl acetate/hexane mixture (80:20); <sup>1</sup>H NMR (DMSO-d<sub>6</sub>): 2.21 (s, 6H), 7.13 (m, 3H), 7.58 (dd, 1H, *J*=4.8, 7.8), 8.35 (d, 1H, *J*=7.9), 8.79 (dd, 1H, *J*=1.4, 4.7), 9.18 (d, 1H, *J*=1.5), 10.01 (s, 1H); <sup>13</sup>C NMR (DMSO-d<sub>6</sub>): 18.7, 124.2, 127.5, 28.4, 130.6, 135.5, 135.9, 136.2, 149.2, 152.7, 164.2; HRMS: C<sub>14</sub>H<sub>14</sub>N<sub>2</sub>O calculated 226.1106 amu, found 226.1103 amu.

#### **4.6.5 General Procedure for the Synthesis of Nicotines, Route 1**

A mixture of nicotinic acid (10 g, 8.1 mmol) and the respective alcohol derivative (45 mL) was cooled in an ice-bath and sulphuric acid (10 mL) was added slowly. The ice bath was then removed and the mixture was heated at reflux until clear (approximately 1 hour while being monitored by TLC using the solvent system (**P**)), cooled to room temperature and poured over 200 g of crushed ice and 35 g of potassium carbonate. The aqueous solution was filtered, saturated with sodium carbonate and extracted with ether. The ether layers were combined, dried with sodium sulfate, and reduced under vacuum to produce an oily residue. The oily residue was then placed under high vacuum and yellowish crystals resulted. The crude product was dissolved in the alcohol derivative and ether was added until cloudy and placed in the freezer to promote crystal formation. The final product obtained was a crystalline solid.

#### ***Methyl nicotinate* (11)**

Crystalline solid (9.44 g, 81%); mp = 110-112 °C; <sup>1</sup>H NMR (CDCl<sub>3</sub>): 3.17 (s, 3H), 8.16 (dd, 1H, *J*=5.3, 7.8), 9.00 (d, 1H, *J*=7.8), 9.20 (d, 1H, *J*=5.3), 9.33 (s, 1H); <sup>13</sup>C NMR

(CDCl<sub>3</sub>): 53.8, 127.4, 129.9, 142.3, 144.5, 145.8, 161.8; HRMS: C<sub>7</sub>H<sub>7</sub>NO<sub>2</sub> calculated 137.0477 amu, found 137.0479 amu.

#### ***Ethyl nicotinate (12)***

Crystalline solid (9.62 g, 84%); mp =124-126 °C; <sup>1</sup>H NMR (CDCl<sub>3</sub>): 1.43 (t, 3H, *J*=7.3), 4.48 (q, 2H, *J*=7.3), 8.14 (dd, 1H, *J*=4.9, 7.9), 8.97 (d, 1H, *J*=7.9), 9.16 (d, 1H, *J*=4.9), 9.32 (s, 1H); <sup>13</sup>C NMR (CDCl<sub>3</sub>): 14.1, 63.5, 127.4, 130.1, 142.2, 144.5, 145.7, 161.3; HRMS: C<sub>8</sub>H<sub>9</sub>NO<sub>2</sub> calculated 151.0633 amu, found 151.0629 amu.

#### ***Isopropyl nicotinate (13)***

Crystalline solid (4.31 g, 64%); mp =124-125 °C; <sup>1</sup>H NMR (CD<sub>3</sub>OD)δ: 1.45 (d, 6H, *J*=6.1), 5.33 (m, 1H, *J*=6.1), 8.34 (dd, 1H, *J*=5.5, 7.9), 9.05 (d, 1H, *J*=7.9), 9.12 (d, 1H, *J*=5.5), 9.28 (s, 1H); <sup>13</sup>C NMR (CD<sub>3</sub>OD): 23.9, 23.9, 69.34, 122.5, 126.1, 136.8, 150.7, 121.6, 166.23; HRMS: C<sub>9</sub>H<sub>11</sub>NO<sub>2</sub> calculated 165.0789 amu, found 165.0785 amu.

### **4.6.7 General Procedure for the Synthesis Nicotines, Route 2**

Nicotinyl chloride (1 g, 5.62 mmol) and the alcohol derivative (1.2 eq.) were combined with dry THF (25 mL) and stirred at room temperature. Triethylamine (3 eq.) was added slowly at room temperature and the reaction was monitored by TLC using solvent system (P) until complete (approximately 24 h). The solution was then extracted with water and ether, dried over sodium sulfate and reduced under vacuum. The oily residue was then placed under high vacuum and yellowish crystals resulted. The crude product was

dissolved in ethanol and then ether was added until the mixture became cloudy and then it was placed in the freezer to promote crystal formation.

#### ***Phenyl nicotinate (14)***

Crystalline solid (0.653 g, 50%); mp = 179-180 °C; <sup>1</sup>H NMR (CD<sub>3</sub>OD): 7.47 (m, 5H), 8.35 (dd, 1H, *J*=5.5, 8.0), 9.20 (d, 1H, 5.5), 9.31 (d, 1H, *J*=8.0), 9.62 (s, 1H). <sup>13</sup>C NMR (CD<sub>3</sub>OD): 121.7, 121.7, 123.8, 125.7, 127.9, 129.3, 129.3, 138.2, 151.0, 151.4, 152.8, 165.3; HRMS: C<sub>12</sub>H<sub>9</sub>NO<sub>2</sub> calculated 199.0633 amu, found 199.0632 amu.

### **4.6.8 5-Bromonicotinamide Analogues**

#### **5-Bromopyridine-3-carboxylic acid**

A mixture of nicotinic acid (0.5 g, 4.1 mmol) and thionyl chloride (3.5 eq.) were dissolved in dry DMF (25 mL) and heated at reflux for 5 h. Bromine (1.2 eq.) was then added dropwise at 70 °C, and the mixture was heated at reflux for an additional 18 h., once complete as monitored by TLC, the mixture was concentrated under vacuum to remove the volatile component. Distilled water was added to the remaining residue and the resulting mixture was stirred for 1 h at room temperature. The pH was adjusted to 4 using NaOH (6N) causing the product to precipitate out of solution. The precipitated product was collected by filtration and recrystallized from ethanol to produce the 5-bromopyridine-3-carboxylic acid (5-bromonicotinic acid). This reaction was also scaled up using nicotinic acid (10 g, 81 mmol), thionyl chloride (2.0 eq.), a catalytic amount of DMF (1 mL) and bromine (1.2 eq.).

Crystalline solid (0.685g, 83% (small scale)); mp = 180-181 °C; <sup>1</sup>H NMR (DMSO-d<sub>6</sub>): 8.41 (s, 1H), 8.89 (s, 1H), 9.17 (s, 1H); <sup>13</sup>C NMR (DMSO-d<sub>6</sub>): 113.2, 128.9, 139.8, 150.4, 151.5, 168.6; HRMS: C<sub>6</sub>H<sub>4</sub>BrNO<sub>2</sub> calculated 200.9425 amu, found 200.9431 amu.

#### **General Procedure for 5-Bromonicotinamide Syntheses: DPPA Coupling**

To a cooled solution of 5-bromonicotinic acid (1 g, 5 mmol) in dry THF (25 mL) were added the amine derivative (1.2 eq.) and triethylamine or diisopropylethylamine (2.5 eq.). The solution was stirred for 10 min, and then DPPA (1.2 eq.) was added and the solution was stirred at room temperature for 18 h while being monitored by TLC. Once complete, THF was removed by evaporation, ethyl acetate was added and washed three times with aqueous sodium carbonate. The ethyl acetate layer was dried with sodium sulfate and evaporated to produce a viscous liquid. Column chromatography or crystallization was used to separate the product.

#### ***5-Bromo-N-(1-phenylethyl) pyridine-3-carboxamide (15)***

Crystalline solid (2.25 g (starting with 2.05 g), 74%); mp = 109-111 °C; Column chromatography using solvent system (**B**); <sup>1</sup>H NMR (DMSO-d<sub>6</sub>): 1.49 (d, 3H, *J*=7.1), 5.17 (m, 1H), 7.35 (m, 5H), 8.48 (dd, 1H, *J*=1.7, 2.2), 8.86 (d, 1H, *J*=2.2), 9.01 (d, 1H, *J*=1.7), 9.09 (d, 1H, *J*=7.8); <sup>13</sup>C NMR (DMSO-d<sub>6</sub>): 22.1, 48.7, 120.0, 126.0, 126.1, 128.3, 131.4, 137.3, 144.2, 147.2, 152.4, 162.6; HRMS: C<sub>14</sub>H<sub>13</sub>N<sub>2</sub>OBr calculated 304.0211 amu, found 304.0210 amu.

***5-bromo-N-propylpyridine-3-carboxamide (16)***

Crystalline solid (1.12 g, 92%); mp = 102-104 °C; Crystallization using ethyl acetate/hexane/ether mixture (80:15:5); <sup>1</sup>H NMR (DMSO-d<sub>6</sub>): 0.91 (t, 3H, *J*=7.4), 1.55 (m, 2H), 3.25 (m, 2H), 8.41 (dd, 1H, *J*=1.7, 2.1), 8.73 (s, 1H), 8.85 (d, 1H, *J*=2.2), 8.97 (d, 1H, *J*=1.6); <sup>13</sup>C NMR (DMSO-d<sub>6</sub>): 12.0, 22.8, 41.7, 120.6, 132.3, 137.8, 147.6, 152.9, 163.8; HRMS: C<sub>9</sub>H<sub>11</sub>N<sub>2</sub>OBr calculated 242.0055 amu, found 242.0058 amu.

***N-Benzyl-5-bromo-N-methylpyridine-3-carboxamide (17)***

Crystalline solid (1.45 g, 85%); mp = 108-110 °C; Column chromatography using solvent system (C); <sup>1</sup>H NMR (DMSO-d<sub>6</sub>): 2.86 (s, 1.8H), 2.94 (s, 1.2H), 4.45 (s, 0.8H), 4.69 (s, 1.2H), 7.20 (m, 0.9H), 7.30 (m, 1.1H), 7.38 (m, 3H), 8.13 (s, 0.4H), 8.24 (s, 0.6H), 8.61 (s, 0.4H), 8.69 (s, 0.6H), 8.76 (s, 0.4H), 8.81 (s, 0.6H); <sup>13</sup>C NMR (DMSO-d<sub>6</sub>): 33.0, 36.7, 50.0, 54.1, 120.0, 126.7, 127.2, 127.4, 127.6, 128.6, 128.7, 133.7, 133.8, 136.5, 136.8, 137.1, 145.5, 146.1, 151.0, 166.5, 166.9; HRMS: C<sub>14</sub>H<sub>13</sub>N<sub>2</sub>OBr calculated 304.0211 amu, found 304.0223 amu.

***5-Bromo-N-(cyclohexyl) pyridine-3-carboxamide (18)***

Crystalline solid (0.988 g, 70%); mp = 183-184 °C; Column chromatography using solvent system (E); <sup>1</sup>H NMR (DMSO-d<sub>6</sub>): 1.15-1.31 (m, 6H), 1.74 (m, 2H), 1.84 (m, 2H), 3.76 (m, 1H), 8.41 (dd, 1H, *J*=1.7, 2.3), 8.49 (d, 1H, *J*=7.6), 8.83 (d, 1H, *J*=2.3), 8.95 (d, 1H, *J*=1.8); <sup>13</sup>C NMR (DMSO-d<sub>6</sub>): 25.4, 25.8, 32.9, 49.2, 120.6, 132.4, 137.9, 147.8, 152.9, 163.0; HRMS: C<sub>12</sub>H<sub>15</sub>N<sub>2</sub>OBr calculated 282.0368 amu, found 282.0369 amu.

***N-Benzyl-5-bromopyridine-3-carboxamide (19)***

Crystalline solid (1.21 g, 83%); mp = 107-109 °C; Crystallization using ethyl acetate/hexane mixture (80:20); <sup>1</sup>H NMR (DMSO-d<sub>6</sub>): 4.50 (d, 2H, *J*=5.9), 7.30 (m, 5H), 8.45 (dd, 1H, *J*=1.8, 2.2), 8.86 (d, 1H, *J*=2.2), 9.02 (d, 1H, *J*=1.8), 9.31 (t, 1H, *J*=5.8); <sup>13</sup>C NMR (DMSO-d<sub>6</sub>): 43.2, 120.7, 127.5, 128.0, 128.9, 131.9, 137.9, 139.6, 147.7, 153.2, 163.9; HRMS: C<sub>13</sub>H<sub>12</sub>N<sub>2</sub>OBr calculated 291.0133 amu, found 291.0131 amu.

***5-Bromo-N-phenylpyridine-3-carboxamide (20)***

Crystalline solid (1.21 g, 87%); mp = 178-180 °C; Crystallization using ethyl acetate/hexane mixture (80:20); <sup>1</sup>H NMR (DMSO-d<sub>6</sub>): 7.13 (m, 1H), 7.39 (dd, 2H, *J*=7.4, 7.7), 7.76 (d, 2H, *J*=7.7), 8.54 (dd, 1H, *J*=1.8, 2.2), 8.91 (d, 1H, *J*=2.2), 9.07 (d, 1H, *J*=1.8), 10.50 (s, 1H); <sup>13</sup>C NMR (DMSO-d<sub>6</sub>): 119.9, 120.3, 124.2, 128.7, 132.1, 137.7, 138.6, 147.3, 152.6, 162.5; HRMS: C<sub>12</sub>H<sub>9</sub>N<sub>2</sub>OBr calculated 275.9898 amu, found 275.9887 amu.

***5-Bromo-N-pentylpyridine-3-carboxamide (21)***

Crystalline solid (1.11 g, 82%); mp = 115-117 °C; Crystallization using ethyl acetate/hexane mixture (80:20); <sup>1</sup>H NMR (DMSO-d<sub>6</sub>): 1.14 (t, 3H, *J*=7.2), 1.31 (m, 2H), 1.38 (m, 2H), 1.64 (m, 2H), 3.18 (m, 2H), 8.54 (dd, 1H, *J*=1.6, 2.2), 8.79 (d, 1H, *J*=2.2), 9.04 (d, 1H, *J*=1.6), 9.13 (d, 1H, *J*=6.9), 9.13 (d, 1H, *J*=6.9); <sup>13</sup>C NMR (DMSO-d<sub>6</sub>): 15.2, 24.8, 30.6, 31.4, 43.5, 121.2, 131.9, 138.9, 146.6, 152.8, 165.6; HRMS: C<sub>11</sub>H<sub>15</sub>BrN<sub>2</sub>O calculated 270.0368 amu, found 270.0361 amu.

#### **4.6.9 Heck Coupling Procedure Development**

##### **Heck Reaction Procedure A**

5-Bromopyridine-3-carboxamide (0.25 g, 1.24 mmol), palladium acetate (0.06 mmol), and triphenylphosphine (0.31 mmol) were combined and dry THF (10 mL) was added followed by methyl acrylate (0.4 mL, 3.1 mmol) and triethylamine (0.28 mL, 3.5 mmol). The reaction was then heated at reflux for 15 h.

##### **Heck Reaction Procedure B**

5-Bromopyridine-3-carboxamide (0.25 g, 1.24 mmol), palladium acetate (0.06 mmol), and triphenylphosphine (0.31 mmol) were combined in a sealed tube, and then evacuated three times and flushed with N<sub>2</sub>. Dry DMF (10 mL) was added followed by methyl acrylate (0.4 mL, 3.1 mmol) and triethylamine (0.28 mL, 3.5 mmol). The solution was heated at 125 °C for 5 h.

##### **Heck Reaction Procedure C**

5-Bromopyridine-3-carboxamide (0.25 g, 1.24 mmol), palladium acetate (0.062 mmol), and triphenylphosphine (0.31 mmol) were combined in a sealed tube, and then evacuated three times and flushed with N<sub>2</sub>. Dry DMF (10 mL) was added followed by methyl acrylate (0.4 mL, 3.1 mmol) and triethylamine (0.28 mL, 3.5 mmol). The solution was sealed and heated at 125 °C for 24 h.



#### **Heck Reaction Procedure D**

N-Benzyl-5-bromopyridine-3-carboxamide (0.5 g, 1.72 mmol), palladium acetate (0.08 mmol), and triphenylphosphine (0.36 mmol) were combined in a sealed tube, and then evacuated and flushed with N<sub>2</sub> three times. Dry DMF (10 mL) was added followed by methyl acrylate (0.55 mL, 4.2 mmol) and potassium carbonate (0.5 g, 3.5 mmol). The solution was sealed and heated at 125°C for 24 h.

#### **Heck Reaction Procedure E**

N-Benzyl-5-bromopyridine-3-carboxamide (0.5 g, 1.72 mmol), palladium acetate (0.08 mmol), and triphenylphosphine (0.36 mmol) were combined in a sealed tube, and then evacuated and flushed with N<sub>2</sub> three times. Dry DMF (10 mL) was added followed by methyl acrylate (0.55 mL, 4.2 mmol) and triethylamine (0.2 mL, 3.5 mmol). The solution was sealed and heated at 125 °C for 24 h.

#### **Heck Reaction Procedure F**

N-Benzyl-5-bromopyridine-3-carboxamide (0.5 g, 1.72 mmol), palladium acetate (0.08 mmol), and triphenylphosphine (0.36 mmol) were combined in a sealed tube, and then evacuated and flushed with N<sub>2</sub> three times. Dry DMF (10 mL) was added followed by methyl acrylate (0.55 mL, 4.2 mmol) and triethylamine (0.2 mL, 3.5 mmol). The solution was sealed and heated at 125°C for 60h.

## Work up for Procedures A - F

For each of the procedures A, B, C, D, E and F the reactions were cooled to room temperature, ethyl acetate was added and the mixture was washed three times with water. The organic layers were combined and dried over sodium sulfate and reduced under vacuum to produce a solid residue. Column chromatography was used for purification using solvent system (F). After evaluation, Procedure F was chosen for the following Heck coupling reactions with styrene and methyl acrylate.

### Procedure F: Styrene Coupling with the 5-Bromonicotinamides

5-Bromonicotinamide (1.72 mmol), palladium acetate (0.05 eq.), and triphenylphosphine (0.2 eq.) were combined in a flask, and then evacuated and flushed with N<sub>2</sub> three times. Dry DMF (20 mL) was added followed by diisopropylethylamine (1.2 eq.) and styrene (1.2 eq.), and then the solution was heated at reflux for 18 h. The solution was cooled; ethyl acetate was added, and the mixture was washed three times with water, dried over sodium sulfate and reduced under vacuum to produce a brown solid. Column chromatography was used for purification using solvent system (C).

#### *N*-Benzyl-5-styrylpyridine-3-carboxamide (22)

Crystalline solid (0.455 g, 84%); mp = 165-166 °C; <sup>1</sup>H NMR (DMSO-d<sub>6</sub>): 4.54 (d, 2H, *J*=5.8), 7.14-7.78 (m, 12H), 8.50 (s, 1H), 8.90 (d, 1H, *J*=11.36), 8.92 (d, 1H, *J*=11.4), 9.28 (t, 1H, *J*=5.8); <sup>13</sup>C NMR (DMSO-d<sub>6</sub>): 43.3, 124.9, 127.4, 127.5, 128.0, 128.9, 129.0, 129.4, 130.4, 131.9, 132.0, 133.1, 137.1, 139.9, 147.8, 151.1, 165.4; HRMS: C<sub>21</sub>H<sub>18</sub>N<sub>2</sub>O calculated 314.1419 amu, found 314.1417 amu.

***N*-(1-Phenylethyl)-5-styrylpyridine-3-carboxamide (23)**

Crystalline solid (0.463 g, 82%); mp = 166-168°C; <sup>1</sup>H NMR (DMSO-d<sub>6</sub>): 1.62 (d, 3H, *J*=5.8), 5.13 (m, 1H), 7.14-7.82 (m, 10H), 8.52 (s, 1H), 8.89 (d, 1H, *J*=16.4), 8.91 (d, 1H, *J*=16.4), 9.08 (d, 1H, *J*=1.8), 9.13 (d, 1H, *J*=1.8), 9.31 (d, 1H, *J*=5.8); <sup>13</sup>C NMR (DMSO-d<sub>6</sub>): 21.5, 48.8, 125.4, 127.8, 128.3, 128.9, 129.2, 129.5, 130.7, 131.2, 131.8, 132.5, 133.5, 137.6, 140.4, 148.9, 152.3, 166.5; HRMS: C<sub>22</sub>H<sub>20</sub>N<sub>2</sub>O calculated 328.1576 amu, found 328.1588 amu.

***N*-Benzyl-*N*-methyl-5-styrylpyridine-3-carboxamide (24)**

Crystalline solid (0.446 g, 79%); mp = 164-166° C; <sup>1</sup>H NMR (DMSO-d<sub>6</sub>): 2.87 (s, 3H), 4.26 (s, 2H), 7.12-7.82 (m, 10H), 8.62 (s, 1H), 8.81 (d, 1H, *J*=16.5), 8.96 (d, 1H, *J*=16.5), 9.02 (d, 1H, *J*=1.7), 9.09 (d, 1H, *J*=1.7); <sup>13</sup>C NMR (DMSO-d<sub>6</sub>): 36.2, 53.6, 126.2, 127.6, 127.8, 128.2, 128.4, 128.7, 129.4, 131.4, 133.7, 134.2, 136.1, 136.5, 137.2, 148.8, 152.3, 167.1; HRMS: C<sub>22</sub>H<sub>20</sub>N<sub>2</sub>O calculated 328.1576 amu, found 328.1579 amu.

***N*-Cyclohexyl-5-styrylpyridine-3-carboxamide (25)**

Crystalline solid (0.464 g, 88%); mp = 161-163 °C; <sup>1</sup>H NMR (DMSO-d<sub>6</sub>): 1.44-1.48 (m, 8H), 1.79 (m, 2H), 3.62 (m, 1H) 7.17-7.59 (m, 5H), 8.62 (s, 1H), 8.74 (d, 1H, *J*=16.8), 8.89 (d, 1H, *J*=16.8), 9.11 (d, 1H, *J*=1.8), 9.15 (d, 1H, *J*=1.8), 9.28 (d, 1H, *J*=5.6); <sup>13</sup>C NMR (DMSO-d<sub>6</sub>): 23.6, 29.1, 33.7, 47.6, 126.9, 127.6, 128.1, 128.9, 130.5, 133.6, 133.9, 135.8, 137.4, 149.2, 153.7, 167.4; HRMS: C<sub>20</sub>H<sub>22</sub>N<sub>2</sub>O calculated 306.1732 amu, found 306.1730 amu.

***N*-Propyl-5-styrylpyridine-3-carboxamide (26)**

Crystalline solid (0.371 g, 81%); mp = 147-150 °C; <sup>1</sup>H NMR (DMSO-d<sub>6</sub>): 1.11 (t, 3H, *J*=7.3), 1.71 (m, 2H), 3.41 (m, 2H), 7.19-7.42 (m, 5H), 8.71 (s, 1H), 8.81 (d, 1H, *J*=17.1), 8.89 (d, 1H, *J*=17.1), 9.01 (d, 1H, *J*=1.8), 9.13 (d, 1H, *J*=1.8), 9.32 (t, 1H, *J*=5.8); <sup>13</sup>C NMR (DMSO-d<sub>6</sub>): 12.5, 22.4, 43.3, 126.8, 127.6, 128.2, 128.9, 131.4, 132.9, 133.8, 135.6, 136.7, 149.5, 154.7, 166.8; HRMS: C<sub>17</sub>H<sub>18</sub>N<sub>2</sub>O calculated 266.1419 amu, found 266.1413 amu.

**Procedure F: Methyl Acrylate Coupling with 5-Bromonicotinamide**

5-Bromonicotinamide (1.72 mmol), palladium acetate (0.08mmol), and triphenylphosphine (0.36 mmol) were combined in a sealed tube, and then evacuated and flushed with N<sub>2</sub> three times. Dry DMF (10 mL) was added followed by methyl acrylate (0.55 mL, 4.2 mmol) and triethylamine (0.2 mL, 3.5 mmol). The solution was sealed and heated to 125 °C. After 24 h the solution was cooled to room temperature, ethyl acetate was added and was washed three times with water. The organic layer was dried over sodium sulfate and reduced under vacuum to produce a yellow solid. Column chromatography was used for purification using solvent system (F).

***(E)*-Methyl-3-(5-(benzylcarbamoyl)pyridine-3-yl)acrylate (27)**

Crystalline solid (0.352 g, 70%); mp = 158-160 °C; <sup>1</sup>H NMR (DMSO-d<sub>6</sub>): 3.76 (s, 3H), 4.53 (d, 2H, *J*=5.9), 6.86 (d, 1H, *J*=16.2), 7.25-7.42 (m, 5H), 7.76 (d, 1H, *J*=16.2), 8.61 (s, 1H), 9.01 (d, 1H, *J*=1.7), 9.03 (d, 1H, *J*=1.7), 9.2 (t, 1H, *J*=5.9); <sup>13</sup>C NMR (DMSO-

d<sub>6</sub>): 43.3, 52.3, 121.5, 127.5, 128.0, 129.0, 130.2, 130.4, 133.7, 139.7, 141.2, 150.4, 152.6, 164.9, 166.8; HRMS: C<sub>18</sub>H<sub>16</sub>N<sub>2</sub>O<sub>3</sub> calculated 296.1161 amu, found 296.1159 amu.

***(E)-Methyl 3-(5-(1-phenylethylcarbamoyl)pyridine-3-yl)acrylate (28)***

Crystalline solid (0.448 g, 84%); mp = 162-164 °C; <sup>1</sup>H NMR (DMSO-d<sub>6</sub>): 1.64 (d, 3H, *J*=6.3), 3.74 (s, 3H), 5.10 (m, 1H), 6.69 (d, 1H, *J*=16.3), 7.19–7.36 (m, 5H), 7.79 (d, 1H, *J*=16.3), 8.72 (s, 1H), 9.19 (d, 1H, *J*=1.7), 9.24 (d, 1H, *J*=1.7), 9.38 (d, 1H, *J*=6.1); <sup>13</sup>C NMR (DMSO-d<sub>6</sub>): 23.4, 47.5, 53.1, 124.3, 125.9, 126.9, 128.8, 131.2, 134.6, 137.9, 143.5, 144.9, 148.7, 155.2, 165.7, 167.8; HRMS: C<sub>18</sub>H<sub>18</sub>N<sub>2</sub>O<sub>3</sub> calculated 310.1317 amu, found 310.1322 amu.

***(E)-methyl 3-(5-(cyclohexylcarbamoyl)pyridine-3-yl)acrylate (29)***

Crystalline solid (0.407 g, 82%); mp = 177-179°C (dec.); <sup>1</sup>H NMR (DMSO-d<sub>6</sub>): 1.42-1.52 (m, 8H), 1.82 (m, 2H), 3.51 (m, 1H), 3.81 (s, 3H), 6.78 (d, 1H, *J*=17.1), 7.73 (d, 1H, *J*=17.1), 8.69 (s, 1H), 9.21 (d, 1H, *J*=1.6), 9.24 (d, 1H, *J*=1.6), 9.34 (d, 1H, *J*=5.9); <sup>13</sup>C NMR (DMSO-d<sub>6</sub>): 24.5, 28.9, 32.4, 48.1, 51.9, 121.6, 129.8, 133.9, 137.8, 144.5, 148.8, 153.6, 164.5, 168.1; HRMS: C<sub>16</sub>H<sub>20</sub>N<sub>2</sub>O<sub>3</sub> calculated 288.1474 amu, found 288.1476 amu.

#### **4.6.10 Suzuki Coupling Procedure Development**

##### **Suzuki Reaction Procedure A**

$\text{Pd}(\text{OAc})_2$  (0.03 eq.),  $\text{PPh}_3$  (0.2 eq.) and the required boronic acid (1.5 eq.) were combined in a flask, and then evacuated and flushed with  $\text{N}_2$  three times. DMF (7 ml) was added to the mixture and it was degassed and stirred at room temperature for 30 min. Distilled water (2.5 eq.) was added and again the mixture was stirred at room temperature for 30 min.  $\text{NEt}_3$  (2 eq.) was added and the mixture was stirred for 10 min, at this point the required starting material, 5-bromonicotinamide (1eq., 1.7 mmol) was added in 3 mL of DMF, the reaction mixture was degassed and then heated to 107 °C and stirred for 24h.

##### **Suzuki Reaction Procedure B**

$\text{Pd}(\text{OAc})_2$  (0.03eq.),  $\text{PPh}_3$  (0.2eq.) and the required boronic acid (1.5 eq.) were combined in a flask, and then evacuated and flushed with  $\text{N}_2$  three times. DMF (7 ml) was added to the mixture and it was degassed and stirred at room temperature for 30 min. Distilled water (2.5 eq.) was added and again the mixture was stirred at room temperature for 30 min.  $\text{Na}_2\text{CO}_3$  (2 eq.) was added and the mixture was stirred for 10 min, at this point the required starting material, 5-bromonicotinamide (1eq., 1.7 mmol) was added in 3 mL of DMF, the reaction was degassed, an then heated to 107 °C and stirred for 24 h.

##### **Suzuki Reaction Procedure C**

The  $\text{Pd}(\text{PPh}_3)_4$  (0.03eq.) and the required boronic acid (1.5 eq.) were combined in a flask, and then evacuated and flushed with  $\text{N}_2$  three times. DMF (7 ml) was added to the

mixture and it was degassed and stirred at room temperature for 30 min. Distilled water (2.5 eq.) was added and again the mixture was stirred at room temperature for 30 min.  $\text{NEt}_3$  (2 eq.) was added and the mixture was stirred for 10 min, at this point the required starting material, 5-bromonicotinamide (1 eq., 1.7 mmol) was added in 3 mL of DMF, the reaction was degassed, and then heated to 107 °C and stirred for 24 h.

#### **Suzuki Reaction Procedure D**

$\text{Pd(PPh}_3)_4$  (0.03eq.) and the required boronic acid (1.5 eq.) were combined in a flask, and then evacuated and flushed with  $\text{N}_2$  three times. DMF (7 ml) was added to the mixture and it was degassed and stirred at room temperature for 30 min. Distilled water (2.5 eq.) was added and again the mixture was stirred at room temperature for 30 min.  $\text{Na}_2\text{CO}_3$  (2 eq.) was added and the mixture was stirred for 10 min. At this point the required starting material 5-bromonicotinamide (1eq., 1.7 mmol), was added in 3 mL of DMF, the reaction was degassed, and then heated to 107 °C and stirred for 24 h.

#### **Work up for Procedures A, B, C and D**

The reaction was monitored for completion by TLC. Once all the starting material had reacted the solution was cooled to room temperature and diluted with ethyl acetate. The solution was washed three times with sodium bicarbonate or aqueous sodium carbonate solution. The organic layers were combined, dried over magnesium sulfate and reduced in vacuo to a crude solid. Column chromatography was used for purification and the final products were crystallized using an ethyl acetate/ hexane mixture. After evaluation, Procedure D was chosen for the following Suzuki coupling reactions.

#### **Procedure D: Suzuki Coupling with the 5-Bromonicotinamides**

$\text{Pd(PPh}_3)_4$  (0.03 eq.) and the required boronic acid (1.5 eq.) were combined in a flask, and then evacuated and flushed with  $\text{N}_2$  three times. DMF (7 ml) was added and the mixture was degassed and stirred at room temperature for 30 min. Distilled water (2.5 eq.) was added and again the mixture was stirred at room temperature for 30 min.  $\text{Na}_2\text{CO}_3$  (2 eq.) was added and the mixture was stirred for 10 min, at this point the required starting material, 5-bromonicotinamide (0.500, 1.7 mmol) was added in 3 mL of DMF, the reaction was degassed and then heated to 107 °C and stirred for 18 to 48 h. depending on the reaction. TLC monitored the reaction for completion. Once all the starting material had reacted the solution was cooled to room temperature and diluted with ethyl acetate. The solution was washed three times with aqueous sodium bicarbonate or sodium carbonate solution. The organic layers were combined, dried over magnesium sulfate and reduced in vacuo to a crude solid. Column chromatography was used for purification and the final products were crystallized using an ethyl acetate hexane mixture.

#### ***N*-Benzyl-5-phenylpyridine-3-carboxamide (30)**

White solid (0.396 g, 81%); mp = 159-160 °C; Column chromatography run using eluting solvent (C);  $^1\text{H}$  NMR ( $\text{DMSO-d}_6$ ): 4.52 (d, 2H,  $J=6.1$ ), 7.19-7.34 (m, 7H), 7.77 (d, 2H,  $J=8.4$ ), 8.51 (s, 1H), 9.06 (d, 1H,  $J=2.1$ ), 9.11 (s, 1H,  $J=2.1$ ), 9.34 (t, 1H,  $J=6.1$ );  $^{13}\text{C}$  NMR ( $\text{DMSO-d}_6$ ): 43.1, 126.7, 126.9, 127.6, 128.7, 129.4, 130.2, 132.8, 133.8,



135.4, 138.9, 140.2, 147.9, 151.3, 165.8; HRMS: C<sub>19</sub>H<sub>16</sub>N<sub>2</sub>O calculated 288.1263 amu, found 288.1268 amu.

***N-Benzyl-5-p-toylpyridine-3-carboxamide (31)***

White solid (0.441 g, 86%); mp = 168-170°C; Column chromatography run using eluting solvent (C); <sup>1</sup>H NMR (DMSO-d<sub>6</sub>): 2.37 (s, 3H), 4.55 (d, 2H, *J*=5.9), 7.25-7.37 (m, 7H), 7.71 (d, 2H, *J*=8.1), 8.48 (s, 1H), 9.00 (d, 1H, *J*=2.0), 9.01 (s, 1H, *J*=2.1), 9.31 (t, 1H, *J*=5.8); <sup>13</sup>C NMR (DMSO-d<sub>6</sub>): 20.7, 42.7, 126.8, 126.8, 127.3, 128.3, 129.6, 129.7, 132.2, 133.4, 134.9, 138.0, 139.2, 147.2, 149.6, 164.7; HRMS: C<sub>20</sub>H<sub>18</sub>N<sub>2</sub>O calculated 302.1419 amu, found 302.1213 amu.

***N-Benzyl-5-(4-chlorophenyl)pyridine-3-carboxamide (32)***

White solid (0.506 g, 92%); mp = 182-184 °C; Column chromatography run using eluting solvent (C); <sup>1</sup>H NMR (DMSO-d<sub>6</sub>): 4.54 (d, 2H, *J*=5.9), 7.25 -7.37 (m, 5H), 7.60 (d, 2H, *J*=8.6), 7.86 (d, 2H, *J*=8.6), 8.52 (s, 1H), 9.04 (d, 1H, *J*=2.1), 9.05 (d, 1H, *J*=2.2), 9.31 (t, 1H, *J*=5.8); <sup>13</sup>C NMR (DMSO-d<sub>6</sub>): 42.7, 126.9, 127.3, 128.3, 128.8, 129.1, 129.7, 132.6, 133.5, 133.8, 135.2, 139.1, 147.8, 149.7, 164.5; HRMS: C<sub>19</sub>H<sub>15</sub>Cl N<sub>2</sub>O calculated 322.0873 amu, found 322.0877 amu.

***N-Benzyl-5-(4-(trifluoromethyl)phenyl)pyridine-3-carboxamide (33)***

White solid (0.436 g, 72%); mp = 160-162 °C; Column chromatography run using eluting solvent (C); <sup>1</sup>H NMR (DMSO-d<sub>6</sub>) 4.57 (d, 2H, *J*=5.6), 7.28-7.38 (m, 5H), 7.91 (d, 2H, *J*=7.9), 8.06 (d, 2H, *J*=7.9), 8.60 (s, 1H), 9.11 (s, 1H), 9.13 (s, 1H), 9.35 (t, 1H,

$J=5.6$ );  $^{13}\text{C}$  NMR (DMSO- $d_6$ ): 45.4, 123.5, 125.9, 126.5, 126.8, 127.9, 130.5, 131.5, 133.4, 134.6, 135.9, 138.7, 142.8, 148.9, 154.6, 166.9; HRMS:  $\text{C}_{20}\text{H}_{15}\text{F}_3\text{N}_2\text{O}$  calculated 356.1136 amu, found 356.1141 amu.

***N-Benzyl-5-(4-hydroxyphenyl)pyridine-3-carboxamide (34)***

Crystalline solid (0.403 g, 77%); mp = 167-168 °C; Column chromatography run using eluting solvent (C);  $^1\text{H}$  NMR (DMSO- $d_6$ ): 4.51 (d, 2H,  $J=5.8$ ), 7.24-7.39 (m, 5H), 7.57 (d, 2H,  $J=8.5$ ), 7.91 (d, 2H,  $J=8.5$ ), 8.54 (s, 1H), 9.06 (d, 1H,  $J=1.6$ ), 9.11 (d, 1H,  $J=1.6$ ), 9.27 (d, 1H,  $J=5.8$ );  $^{13}\text{C}$  NMR (DMSO- $d_6$ ): 45.5, 117.8, 126.6, 127.4, 128.9, 129.2, 129.6, 131.2, 134.5, 134.7, 135.7, 142.4, 147.8, 152.7, 157.2, 166.4; HRMS:  $\text{C}_{19}\text{H}_{16}\text{N}_2\text{O}_2$  calculated 304.1212 amu, found 304.1206 amu.

***5-Phenyl-N-(1-phenylethyl)pyridine-3-carboxamide (35)***

White solid (0.375 g, 73%); mp = 190-192°C (dec.); Column chromatography run using eluting solvent (C);  $^1\text{H}$  NMR (DMSO- $d_6$ ): 1.58 (d, 3H,  $J=7.3$ ), 5.28 (m, 1H), 7.19-7.48 (m, 8H), 7.66-7.71 (m, 2H), 8.56 (s, 1H), 9.05 (d, 1H,  $J=2.1$ ), 9.12 (d, 1H,  $J=2.1$ ), 9.21 (d, 1H,  $J=7.9$ );  $^{13}\text{C}$  NMR (DMSO- $d_6$ ): 21.5, 49.5, 126.6, 126.8, 127.2, 128.5, 129.4, 129.9, 131.3, 132.4, 133.7, 138.9, 145.5, 147.8, 151.5, 164.5; HRMS:  $\text{C}_{19}\text{H}_{18}\text{N}_2\text{O}$  calculated 302.1419 amu, found 302.1425 amu.

***N-(1-Phenylethyl)-5-p-tolylpyridine-3-carboxamide (36)***

Peach crystalline solid (0.483 g, 89%); mp = 174-177 °C; Column chromatography run using eluting solvent (C);  $^1\text{H}$  NMR (DMSO- $d_6$ ): 1.53 (d, 3H,  $J=7.1$ ), 2.39 (s, 3H), 5.23

(m, 1H), 7.24-7.44 (m, 7H), 7.69-7.73 (m, 2H), 8.48 (s, 1H), 8.99 (d, 1H,  $J=1.9$ ), 9.01 (d, 1H,  $J=2.0$ ), 9.09 (d, 1H,  $J=7.9$ );  $^{13}\text{C}$  NMR (DMSO- $d_6$ ): 20.7, 22.1, 48.5, 126.1, 126.6, 126.8, 128.2, 129.8, 129.7, 132.3, 133.4, 134.9, 137.9, 144.5, 147.3, 149.5, 163.9 ;  
HRMS:  $\text{C}_{21}\text{H}_{20}\text{N}_2\text{O}$  calculated 316.1576 amu, found 316.1581 amu.

***5-(4-Chlorophenyl)-N-(1-phenylethyl)pyridine-3-carboxamide (37)***

Crystalline solid (0.516 g, 89%); mp = 182-183°C; Column chromatography run using eluting solvent (D);  $^1\text{H}$  NMR (DMSO- $d_6$ ): 1.55 (d, 3H,  $J=7.4$ ), 5.26 (m, 1H), 7.27-7.45 (m, 7H) 7.71-7.74 (m, 2H), 8.47 (s, 1H), 9.01 (d, 1H,  $J=1.7$ ), 9.08 (d, 1H,  $J=1.7$ ), 9.19 (d, 1H,  $J=7.5$ );  $^{13}\text{C}$  NMR DMSO- $d_6$ ): 23.6, 51.4, 126.6, 127.8, 128.5, 128.9, 129.7, 131.7, 134.2, 134.5, 134.7, 135.8, 144.2, 147.6, 152.8, 166.3; HRMS:  $\text{C}_{20}\text{H}_{17}\text{ClN}_2\text{O}$  calculated 336.1029 amu, found 336.1035 amu.

***5-(4-Chlorophenyl)-N-propylpyridine-3-carboxamide (38)***

Crystalline solid (0.354 g, 75%); mp = 163-164°C; Column chromatography run using eluting solvent (C);  $^1\text{H}$  NMR (DMSO- $d_6$ ): 1.03 (t, 3H,  $J=7.8$ ), 1.69 (m, 2H), 3.42 (m, 2H), 7.51 (d, 2H,  $J=8.6$ ), 7.89 (d, 2H,  $J=8.6$ ), 8.69 (s, 1H), 9.06 (d, 1H,  $J=1.8$ ), 9.14 (d, 1H,  $J=1.8$ ), 9.21 (t, 1H,  $J=6.2$ );  $^{13}\text{C}$  NMR (DMSO- $d_6$ ): 12.5, 22.6, 44.7, 127.8, 129.5, 131.5, 134.8, 135.2, 135.7, 136.1, 148.9, 153.6, 168.2. HRMS:  $\text{C}_{15}\text{H}_{15}\text{ClN}_2\text{O}$  calculated 274.0873 amu, found 274.0871 amu

***N*-Propyl-5-*p*-tolylpyridine-3-carboxamide (39)**

Crystalline solid (0.461 g, 76%); mp=156-158°C; Column chromatography run using eluting solvent (E); <sup>1</sup>H NMR (DMSO-d<sub>6</sub>): 1.01 (d, 3H, *J*=7.8), 1.59 (m, 2H), 2.35 (s, 3H), 3.38 (m, 2H), 7.21 (d, 2H, *J*=8.5), 7.58 (d, 2H, *J*=8.5), 8.61 (s, 1H), 9.08 (d, 1H, *J*=1.8), 9.15 (d, 1H, *J*=1.8), 9.34 (t, 1H, *J*=5.9); <sup>13</sup>C NMR (DMSO-d<sub>6</sub>): 12.6, 23.6, 24.4, 43.9, 126.8, 128.9, 130.9, 133.1, 134.7, 136.8, 138.9, 145.7, 152.4, 166.9; HRMS: C<sub>16</sub>H<sub>18</sub>N<sub>2</sub>O calculated 354.1419 amu, found 354.1413 amu.

***N*-Phenyl-5-*p*-tolylpyridine-3-carboxamide (40)**

Crystalline solid (0.412 g, 83%); mp = 161-163 °C; Column chromatography run using eluting solvent (C); <sup>1</sup>H NMR (DMSO-d<sub>6</sub>): 2.38 (m, 3H), 7.13-7.1 (m, 9H), 8.49 (s, 1H), 9.01 (d, 1H, *J*=1.6), 9.09 (d, 1H, *J*=1.6), 9.26 (s, 1H); <sup>13</sup>C NMR (DMSO-d<sub>6</sub>): 25.8, 120.4, 124.6, 126.7, 128.5, 129.6, 131.6, 133.7, 134.6, 135.6, 135.9, 139.7, 146.8, 152.9, 167.4; HRMS: C<sub>19</sub>H<sub>16</sub>N<sub>2</sub>O calculated 288.1263 amu, found 288.1266 amu.

**4.6.11 Synthesis Of 2-(Benzylthio)pyridine-3-carboxylic Acid**

To a cooled solution of 2-mercaptopyridine-3-carboxylic acid (5 g, 32.3mmol) and DMF (250 mL) was added benzyl bromide (1.1 eq.) and triethylamine (2.0 eq.). The mixture was warmed to room temperature and stirred for 12 h. while monitoring by TLC. Once the reaction was complete the solution was diluted with water, and 2M HCl was added until the mixture was acidified to a pH of 2. The resulting solid was collected by filtration and crystallized from acetonitrile (CH<sub>3</sub>CN).

#### ***2-(Benzylthio)pyridine-3-carboxylic acid HCl (41)***

Peach crystalline solid (7.5 g, 83%); mp = 190-191 °C (lit. 190-193 °C); <sup>1</sup>H NMR (DMSO-d<sub>6</sub>): 4.38 (s, 2H), 7.21-7.44 (m, 6H), 8.21 (dd, 1H, *J*=1.7, 7.7), 8.69 (dd, 1H, *J*=1.5, 4.7), 13.42 (s, 1H); <sup>13</sup>C NMR (DMSO-d<sub>6</sub>): 34.4, 119.7, 123.8, 127.5, 128.9, 129.8, 138.6, 139.6, 152.5, 161.2, 166.9; HRMS: C<sub>13</sub>H<sub>12</sub>ClNO<sub>2</sub>S calculated 281.0277 amu, found 281.0279 amu.

#### **4.6.12 Synthesis Of 2-(Benzylthio)nicotinamides**

To a cooled solution of 2-(benzylthio)pyridine-3-carboxylic acid HCl (0.500 g, 1.77 mmol) in dry THF (50 mL) was added the amine derivative (1.2 eq.) and the triethylamine (3 eq.). The solution was stirred for 10 min. and then DPPA (1.2 eq.) was added and the reaction was stirred for an additional 24 h. at room temperature, while being monitored by TLC. Once the solution was complete a variety of procedures were used for further separation and purification of each compound.

#### ***2-(Benzylthio)-N-propylpyridine-3-carboxamide (42)***

Once the THF was removed by evaporation, ethyl acetate was added to the resulting viscous solution and washed three times with aqueous sodium carbonate. The organic layer was dried over sodium sulfate, concentrated and the resulting crude product was crystallized using an ethyl acetate/hexane (80:20) mixture.

Crystalline solid (0.458 g, 90%); mp = 109-111 °C; <sup>1</sup>H NMR (DMSO-d<sub>6</sub>): 0.89 (t, 3H, *J*=7.4), 1.49 (m, 2H), 3.15 (m, 2H), 4.48 (s, 2H), 7.17-7.41 (m, 6H), 7.95 (dd, 1H, *J*=1.5, 7.5), 8.66 (m, 1H), 8.74 (dd, 1H, *J*=1.5, 4.7); <sup>13</sup>C NMR (DMSO-d<sub>6</sub>): 12.1, 22.8, 34.1,

41.4, 119.7, 127.4, 128.9, 129.7, 130.6, 135.8, 138.9, 150.3, 157.4, 166.5; HRMS:

C<sub>16</sub>H<sub>18</sub>N<sub>2</sub>OS calculated 286.1139 amu, found 286.1143 amu.

***2-(Benzylthio)-N-(2,6-dimethylphenyl)pyridine-3-carboxamide HCl (43)***

Once the THF was removed by evaporation, ethyl acetate was added and the solution was washed three times with aqueous sodium carbonate. The organic layer was dried over sodium sulfate and concentrated resulting in a viscous liquid. This liquid was put under high vacuum and then diluted with methanol and acidified with 2M HCl until a pH of 3 obtained and the product crashed out of solution as a solid salt.

Crystalline solid (0.566 g, 91%); mp = 200-201 °C; <sup>1</sup>H NMR (DMSO-d<sub>6</sub>): 2.21 (s, 6H), 4.56 (s, 2H), 7.03-7.07 (m, 3H), 7.13 (dd, 1H, *J*=4.7, 8.1), 7.21-7.45 (m, 5H), 7.98 (s, 1H), 8.04 (dd, 1H, *J*=1.4, 8.1), 8.21 (dd, 1H, *J*=1.4, 4.6), 8.33 (s, 1H); <sup>13</sup>C NMR (DMSO-d<sub>6</sub>): 15.2, 39.4, 120.4, 125.8, 127.6, 127.7, 128.2, 127.4, 129.3, 131.4, 134.9, 138.1, 139.2, 145.2, 162.3, 167.8; HRMS: C<sub>21</sub>H<sub>21</sub>N<sub>2</sub>OSCl calculated 384.1063 amu, found 384.1066 amu.

***N-Benzyl -2-(benzylthio)-N-methylpyridine-3-carboxamide (44)***

To the THF solution was added ethyl acetate and it was washed three times with aqueous sodium carbonate. The organic layer was dried over sodium sulfate and concentrated to produce a viscous liquid.

Viscous liquid (0.565 g, 91%); <sup>1</sup>H NMR (DMSO-d<sub>6</sub>): 2.57 (s, 1.8H), 2.86 (s, 1.2H), 4.21 (s, 0.8H), 4.47 (s, 2H), 4.66 (s, 1.2H), 7.12-7.40 (m, 11H), 7.66 (d, 1H, *J*=7.5); <sup>13</sup>C NMR (DMSO-d<sub>6</sub>): 14.7, 21.4, 32.7, 33.9, 35.9, 49.9, 54.1, 60.4, 120.4, 120.7, 127.6, 127.7,

127.8, 127.9, 128.1, 128.4, 128.9, 129.0, 129.1, 129.2, 129.4, 129.6, 131.4, 131.9, 135.1, 135.2, 136.8, 137.4, 138.7, 138.8, 150.0, 154.2, 154.7, 167.8; HRMS: C<sub>21</sub>H<sub>20</sub>N<sub>2</sub>OS calculated 348.1296 amu, found 348.1294 amu.

***2-(Benzylthio)-N-cyclohexylpyridine-3-carboxamide (45)***

Once the THF was removed by evaporation, ethyl acetate was added and the solution was washed three times with aqueous sodium carbonate. The organic layer was dried over sodium sulfate, concentrated and the resulting crude product was crystallized from an ethyl acetate/hexane mixture (80:20).

Crystalline solid (0.493 g, 85%); mp = 152-154°C; <sup>1</sup>H NMR (DMSO-d<sub>6</sub>): 1.52 (m, 8H), 1.81 (m, 2H), 3.68 (m, 1H), 4.55 (s, 2H), 7.21 (dd, 1H, *J*=4.5, 8.3), 7.32-7.51 (m, 5H), 8.18 (dd, 1H, *J*=1.3, 8.3), 8.31 (dd, 1H, *J*=1.3, 4.5), 9.31 (d, 1H, *J*=5.8); <sup>13</sup>C NMR (DMSO-d<sub>6</sub>): 23.5, 29.3, 34.6, 39.8, 48.9, 126.1, 127.3, 127.9, 129.4, 132.6, 138.9, 139.8, 146.7, 155.2, 169.3; HRMS: C<sub>19</sub>H<sub>22</sub>N<sub>2</sub>OS calculated 326.1453 amu, found 326.1449 amu.

***2-(Benzylthio)-N-phenylpyridine-3-carboxamide HCl (46)***

The THF solution was diluted with ethyl acetate and washed three times with aqueous sodium carbonate. The organic layer was dried over sodium sulfate and concentrated to produce a viscous liquid. This liquid was put under high vacuum and then diluted with methanol and acidified with 2M HCl until a pH of 3 obtained and the product crashed out of solution as a solid salt.

Crystalline solid (0.429 g, 70%); mp= 210-212 °C; <sup>1</sup>H NMR (DMSO-d<sub>6</sub>): 4.96 (s, 2H), 6.97 (t, 1H, *J*=7.35), 7.15 (dd, 1H, *J*= 4.7, 8.1), 7.21-7.33 (m, 8H), 7.42 (t, 1H, *J*=7.7),

7.94 (s, 1H), 8.05 (dd, 1H,  $J=1.5$ , 8.1), 8.25 (dd, 1H,  $J=1.5$ , 4.7), 9.25 (s, 1H);  $^{13}\text{C}$  NMR (DMSO- $d_6$ ): 33.6, 118.2, 120.1, 122.2, 127.1, 128.4, 128.8, 128.9, 129.0, 132.5, 137.9, 139.4, 143.7, 148.6, 152.4; HRMS:  $\text{C}_{19}\text{H}_{17}\text{N}_2\text{ClOS}$  calculated 356.075 amu, found 356.0753 amu.

***N-Benzyl-2-(benzylthio)pyridine-3-carboxamide (47)***

Once the THF was removed by evaporation, the remaining solution was washed three times with sodium carbonate and the product crashed out of solution. The crude product was crystallized using an ethyl acetate/hexane mixture (80:20).

Crystalline solid (0.55 g, 93%); mp = 119-120 °C;  $^1\text{H}$  NMR (DMSO- $d_6$ ): 4.38 (s, 2H), 4.43 (d, 2H,  $J=5.8$ ), 7.22-7.40 (m, 11H), 7.84 (dd, 1H,  $J=1.6$ , 7.6), 8.55 (dd, 1H,  $J=1.6$ , 4.8), 9.04 (t, 1H,  $J=5.8$ );  $^{13}\text{C}$  NMR (DMSO- $d_6$ ): 34.2, 43.1, 119.7, 127.4, 127.9, 128.9, 129.3, 129.4, 129.7, 130.1, 136.0, 138.9, 139.7, 150.6, 157.7, 166.7; HRMS:  $\text{C}_{20}\text{H}_{18}\text{N}_2\text{OS}$  calculated 334.114 amu, found 334.1133 amu.

***2-(Benzylthio)-N-(1-phenylethyl)pyridine-3-carboxamide (48)***

Once the THF was removed by evaporation a yellow liquid was produced which was washed three times with sodium carbonate. Ethyl acetate was added to the resulting liquid and the product crashed out of solution. Column chromatography was run for purification using eluting solvent (**H**) followed by the second eluting solvent of chloroform: ethyl acetate (1:0.1) to collect the second spot on the column. The product was crystallized using an ethyl acetate/hexane mixture (80:20).



Crystalline product (0.56 g, 90%); mp = 163-164 °C; <sup>1</sup>H NMR (DMSO-d<sub>6</sub>): 1.41 (d, 3H, *J*=7.04), 4.35 (s, 2H), 5.06 (m, 1H), 7.19- 7.37 (m, 11H), 7.81 (dd, 1H, *J*=1.68, 7.58), 8.54 (dd, 1H, *J*=1.68, 4.83), 8.89 (d, 1H, *J*=7.95); <sup>13</sup>C NMR (DMSO-d<sub>6</sub>): 22.9, 34.1, 49.0, 119.7, 126.6, 127.3, 127.5, 128.8, 128.9, 129.6, 130.3, 136.1, 138.8, 145.0, 150.5, 157.5, 165.8; HRMS: C<sub>21</sub>H<sub>20</sub>N<sub>2</sub>OS calculated 348.1296 amu, found 348.1294 amu.

#### 4.6.13 Synthesis Of 2-(Benzylsulfinyl)nicotinamides

To a stirred solution of the 2-(benzylthio)-N-substituted-pyridine-3-carboxamide (0.500 g, 1.5 mmol) in DCM (25 mL) at 0 °C, meta-chloroperoxybenzoic acid (1.15 eq.) in 5 ml of DCM was added drop wise over 5 min. The solution was stirred for an additional 5 min., at 0 °C, and then washed two times with sodium carbonate, dried over sodium sulfate and then the DCM was removed under vacuum evaporation. A white solid was produced which was purified by column chromatography using eluting solvent (**I**) followed sequentially by solvent system (**J**) and (**K**) to separate all three spots. The second spot was collected since it was determined to be the product.

#### *N*-benzyl-2-(benzylsulfinyl)pyridine-3-carboxamide (49)

Crystalline product (0.364 g, 70%); mp = 189-191°C; <sup>1</sup>H NMR (DMSO-d<sub>6</sub>): 4.01 (d, 1H, *J*=12.5), 4.42 (d, 1H, *J*=12.4), 4.51 (dd, 2H, *J*=4.1, 5.5), 7.31-7.39 (m, 10H), 7.63 (dd, 1H, *J*=4.7, 7.8), 8.19 (dd, 1H, *J*=1.5, 7.8), 8.83 (dd, 1H, *J*=1.5, 4.6), 9.38 (dd, 1H, *J*=4.1, 5.5); <sup>13</sup>C NMR (DMSO-d<sub>6</sub>): 43.4, 61.5, 125.9, 127.6, 128.0, 128.5, 129.0, 129.1, 130.8, 130.9, 132.9, 137.1, 139.3, 152.1, 162.7, 165.5; HRMS: C<sub>20</sub>H<sub>18</sub>N<sub>2</sub>O<sub>2</sub>S calculated 350.1089 amu, found 350.1092 amu.

***2-(benzylsulfinyl)-N-(1-phenylethyl)pyridine-3-carboxamide (50)***

Crystalline solid (0.425 g, 81%); mp = 183-185 °C; <sup>1</sup>H NMR (DMSO-d<sub>6</sub>): 1.47 (2d, 3H, *J*=7.2), 3.98 (2d, 1H, *J*=12.5), 4.35 (2d, 1H, *J*=12.5), 5.15 (m, 1H), 7.18-7.46 (m, 10H), 7.67 (m, 1H), 8.17 (2dd, 1H, *J*=1.5, 6.6), 8.85 (2dd, 1H, *J*=1.5, 4.7), 9.26 (2d, 1H, *J*=7.9); <sup>13</sup>C NMR (DMSO-d<sub>6</sub>): 22.7, 22.9, 49.3, 49.4, 61.2, 61.3, 125.9, 126.7, 126.8, 127.5, 128.4, 128.9, 129.0, 129.1, 130.7, 131.2, 131.3, 132.7, 132.8, 137.2, 137.3, 144.4, 144.7, 151.9, 152.1, 162.5, 164.7, 164.8; HRMS: C<sub>21</sub>H<sub>20</sub>N<sub>2</sub>O<sub>2</sub> calculated 364.1245 amu, found 364.1239 amu.

## **CHAPTER 5**

### **QUANTITATIVE STRUCTURE ACTIVITY RELATIONSHIP OF THE NICOTINAMIDE ANALOGUES**

---

## 5.1 QSAR Introduction

With the development of new drug scaffolds one of the most important concepts to be evaluated is the relationship between chemical structure and bioactivity. The development of quantitative structure-activity relationship (QSAR) studies has been instrumental in the advancement of new chemical compounds since it is a rational drug design short-cut [142]. The QSAR method helps to maintain the number of developed and biologically tested molecules to a minimum, so that the cost and time investments in drug development can be kept to a minimum. When developing new compounds the primary goal is to optimize the pharmacodynamic phase, or the ability of a molecule to bind with the desired receptor. In order for a drug to influence a specific disease it must be able to bind uniquely to the required receptor so that binding elsewhere in the body can be controlled. Once biological data are available for the candidate molecules targeting the disease being studied, a QSAR can be completed. A QSAR analysis assists in identifying the chemical and structural features of a molecule that are responsible for binding to the target receptor and producing bioactivity [143, 144]. A QSAR can also be used to identify the mechanisms involved in controlling both drug efficacy and toxicity by exploiting the information available about the active and inactive compounds [143-145]. The three main classifications of QSAR studies are as follows:

- 1) 1D-QSAR (e.g., Hansch analysis)
- 2) 2D-QSAR (e.g., pattern recognition analysis)
- 3) 3D-QSAR (e.g., comparative field analysis)

QSAR studies were initially developed in the late 1960's from the research conducted by Hansch [146]. This classical QSAR analysis used the octanol/water

partition coefficient (LogP) and claimed that logP was an important molecular predictor of bioactivity [146, 147]. As computational methods developed it was determined that although logP was useful for evaluating bioactivity, it was not the only descriptor available. Many descriptors including geometric, electronic, topological, and physiochemical can be effectively determined by molecular mechanics and semiempirical calculations. Using these predictors of activity, a 2D QSAR, based on pattern recognition can be completed and used to develop and predict the activity of new drug molecules [148-151].

The 2D QSAR is a versatile technique and has been applied to a variety of different drug development projects [142, 152-155]. When performing a 2D QSAR, the molecules contained within the training-set should be diverse in both their chemical structure and biological activity so that a predictive equation for activity can be generated [144]. Each molecule in the training-set is characterized through a variety of different descriptors including bond lengths, bond angles, molecular dipoles, HOMO, LUMO, number of aromatic rings, logP, number of H-bond donors, number of H-bond acceptors, etc. Once these descriptors have been calculated, a 2D array is constructed with the training-set molecules on the vertical axis arranged in descending order of bioactivity and the molecular descriptors on the horizontal axis. The data are then evaluated to find the minimum number of descriptors required to differentiate between an active and an inactive compound, and an equation is generated [36]. Using this generated equation, new compounds can be examined to determine their hypothetical biological activity scores.

The most recent methods developed for QSAR analysis include comparative molecular field analysis (CoMFA) and comparative molecular similarity indices analysis (CoMSIA). Both define important 3D properties associated with binding to a particular receptor [156-158]. These 3D QSAR methods were developed using the pharmacophore concept which is central to rational drug discovery. The molecules in the training-sets are initially aligned based on their structure, and then molecular field descriptors are calculated for each molecule and stored as points on a grid in 3D space. Using this spatial information, the biological activity is correlated with the 3D arrangement of specific functional groups like those which are electron donating, electron withdrawing, aromatic, hydrophobic, bulky, etc [36, 152]. This information helps to predict a blueprint of the receptor binding pocket based on the contacts which appear to be critical for bioactivity.

Although a 3D QSAR pharmacophore model is useful for determining the specific arrangement of chemical groups for an active molecule, it is a difficult QSAR model to calculate when you have a structurally diverse library of compounds [152]. When the compounds being studied have different functional elements, structurally aligning the entire database becomes almost impossible. The 2D QSAR method is more suitable for general drug development such as database searching and virtual screening [159]. The 2D QSAR methods are computationally time efficient and produce models that are predictive and comparable to those obtained by 3D methods [152]. Since the nicotinamide library is diverse in both the functional groups used, the scaffold placements of these groups as well the biological targets for epilepsy, a 2D QSAR method was used.

## **5.2 Computational Methods**

### **5.2.1 QSAR Equation Overview**

The objective of this study was to develop equations that could be used to classify nicotinamide analogues into either biologically active or inactive for both the MES and PTZ tests, based upon specific structural features. Generation of a QSAR equation involves following a general procedure. The first step is to identify the molecules to be included in the training-set and to input their molecular structures and biological activity data. Using the previously synthesized nicotinamides (Table 1: Compounds **1-20**, **22**, **27** and **41-50**) from Chapter 3, with their known biological activities for both the MES and PTZ tests, a training-set was developed to calculate the 2D QSAR equations. Once this was completed, a conformational search was performed for each of the molecules in the training-set. All the molecules included in the training-set were energy-minimized using molecular mechanics, and a variety of molecular descriptors were computed for each of the nicotinamide analogues in the training-set. The molecular descriptors were initially chosen based on their ability to describe the significant structural features of the nicotinamide compounds and can be grouped into several categories including electronic, topological, structural, spatial and physiochemical. After the dependent and independent variables have been identified, statistical methods were used to generate a QSAR equation and to identify the minimum number of descriptors needed to differentiate active compounds from those with no bioactivity. These statistical methods are important for determining the predictive capabilities of a QSAR equation. Using the partial least squares (PLS) method for regression analysis, an equation is developed which expresses the dependent variable of bioactivity in terms of the calculated independent descriptors.

Once an equation is generated it is then validated to identify molecular outliers and then can be used to predict the biological activity of new compounds whose activities are unknown.

### 5.2.2 Computational Application

Optimization of the nictotinamide training-set was preformed on a Silicon Graphics workstation using the Sybyl 7.1 software package. The compounds were minimized to find the lowest energy conformations using molecular mechanics with the Tripos force field (1) and the Powell conjugate gradient method. The general Tripos force field equation (1) and equation terms are shown below.

$$E_{\text{Total}} = \sum E_{\text{str}} + \sum E_{\text{bend}} + \sum E_{\text{oop}} + \sum E_{\text{tors}} + \sum E_{\text{vdw}} + \sum E_{\text{elec}} \quad (1)$$

**E<sub>str</sub>** : Energy of a bond stretched or compressed from its equilibrium bond length.

**E<sub>bend</sub>** : Energy of bending bond angles from their equilibrium values.

**E<sub>oop</sub>** : Energy of bending planar atoms out of the plane.

**E<sub>tors</sub>** : Torsional energy due to twisting about bonds.

**E<sub>vdw</sub>** : Energy due to van der Waals non-bonded interactions.

**E<sub>elec</sub>** : Charges calculated using a Gasteiger and electrostatic energy calculated using a Coulomb potential.

Once a molecule is built and its energy has been minimized, generally a conformational search is in order to map out the various low energy conformations. Conformational analysis consists of moving the atoms of a molecule in such a way as to reduce the total energy of the system based on the force field equation. When this is carried out from the same starting point the same low energy conformation will always



be calculated. Although a minimum is calculated when starting from an input structure, it is a local energy minimum and not necessarily the global minima for the molecule.

Grid searching is a conformational search tool, which maps out all the low energy conformations on the potential energy surface that are available to a molecule. Grid search systematically moves along the potential energy surface changing the starting positions in an attempt to find the global minimum. Using a grid search the global minimum was calculated for all the molecules in the nicotinamide library. This was accomplished by systematically rotating specific bonds in each of the nicotinamide molecules by 30° through 360°. By moving these selected bonds all the low energy positions on the potential energy surface were calculated for the nicotinamide analogues.

When the lowest energy conformations had been determined, an aligned database was constructed using a minimized nicotinamide framework (Figure 21). For each molecule in the library the lowest calculated energy conformation was used, so long as it overlapped with the nicotinamide framework. When alignment was not possible, the next most lowest energy conformation that could overlap with the scaffold, and was within a maximum of 5 kcal/mol from the lowest energy calculated, was chosen.

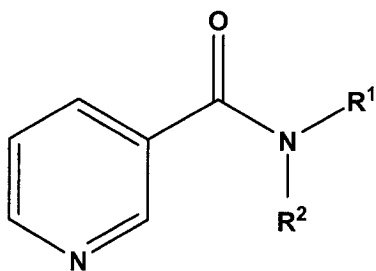


**Figure 21.** The nicotinamide framework used to align the nicotinamide training-set.

After the nicotinamide database had been constructed, a 2D QSAR equation was calculated using Cerius<sup>2</sup> and optimized for each of the biological tests. The default descriptor sets available in the Cerius<sup>2</sup> software package were used to describe each of the molecules in the nicotinamide database (Table 12). Both the conformational, electronic, spatial, and structural descriptors were calculated from the low energy conformations determined by the molecular mechanics calculations. The topological descriptors were determined using graph-theory calculations (where each molecular structure is represented as a graph with the atoms as vertices and covalent chemical bonds as edges), and the only physiochemical/ thermodynamic descriptor used was logP, which was calculated computationally based on experimentally derived values. The logP calculated in Cerius2 is an atom-based approach (AlogP98), where each atom is assigned to a particular atom class and each atom descriptor provides an additive or subtractive quantity to the overall logP value [160].

**Table 12.** List of descriptors used for 2D QSAR calculation

**Conformational Descriptors**

Lowest energy conformer (LowEne)  
 Energy (Eng)  
 Energy and Low energy difference (EPenalty)

**Electronic Descriptors**

Sum of partial charges (Charge)  
 Sum of atomic polarizabilities (Apol)  
 Dipole moment (Dipole)  
 Highest occupied molecular orbital (HOMO)  
 Lowest unoccupied molecular orbital (LUMO)

**Spatial Descriptors**

Radius of gyration (RadofGyr)  
 Molecular area (Area)  
 Molecular density (Density)  
 Molecular volume (Vm)  
 Principal moment of inertia (PMI)

**Structural Descriptors**

Molecular weight (MW)  
Number of rotatable bonds (Rotlbonds)  
Number of hydrogen-bond acceptor groups (Hbond\_ac)  
Number of hydrogen-bond donor groups (Hbond\_do)

**Topological Descriptors**

Zagreb topological indices (Zagreb)  
Molecular flexibility index (PHI)  
Werner index (Werner)

**Physiochemical/ Thermodynamic Descriptors**

Log of the partition coefficient (lipophilicity) atom-type value (AlogP98)

**5.3 QSAR****5.3.1 Data Analysis**

Regression analysis is used to develop an equation that describes the dependent variables (biological activity) in terms of calculated independent variables. The equation that is generated can then be used to predict the activity of new molecules and aid in the development of drugs with improved biological activity. For this QSAR study, partial least squares (PLS) was utilized to determine the relationship between the biological activity and the structural/physiochemical properties of the nicotinamide molecules in the training-set. For PLS, a linear multiple-term equation was generated where both the dependent and independent variables were transformed into linear combinations using the original descriptors. The main objective was to maximize variance and correlate the dependent variables with the independent variables and was usually used when the independent variables were correlated. Once the QSAR equations were generated, they were then validated using the cross-validation leave-one-out test. In this process each compound was removed from the training-set in sequence and then, using the generated equation, the compounds activity was predicted and compared to the original value. The

smaller the difference between the predicted and the actual activity, the more precise the QSAR equation was. When the cross-validation was complete an  $r^2$  value was calculated which provided insight into the predictive power of the calculated QSAR equation using the PLS method.

Using the 21 descriptors chosen, the QSAR equations for the voltage-gated sodium channel and the GABA<sub>A</sub>-benzodiazepine receptor were generated and the results indicated a predictive significance. In order for the model to be chemically significant, the number of descriptors needs to be reduced so that only descriptors that were not directly correlated be included in the equations. Data reduction techniques were employed to determine the independent variables that were required to predict activity.

### **5.3.2 Descriptor Reduction**

Once the 21 descriptors had been calculated for each of the molecules in the nicotinamide training-set and the 2D-QSAR equations had been generated, data reduction was used to reduce the number of descriptors to only those required. Using data reduction the goal was to increase the statistical significance of the QSAR equation by using the minimum number of independent variables to describe the dependent variable of bioactivity. For these results, correlation matrices were used to determine if there was any correlation between the independent variables [161]. The correlation matrix was a calculated table that showed the correlation values between each of the independent variables. The calculated values could then be used to improve the generated QSAR equation by removing those descriptors that provided redundant information. If two descriptors in the equation were strongly correlated, which was indicated by correlation

values close to 1 or  $-1$ , only one of the correlated descriptors was required to adequately define the QSAR equation [144, 161]. Through a series of correlation analyses the number of descriptors was reduced from 21 to 11 and at each step PLS and cross-validation was used for statistical analysis. The equations that were generated with the 11 significant terms also had cross-validation that was predictive. The equations are as follows:

**Voltage-gated sodium channel ( $r^2 = 0.58$ )**

$$\begin{aligned} \text{Activity} = & 0.000255 \text{ Apol} + 0.864 \text{ Dipole} + 2.634 \text{ RadofGyr} - 0.000854 \text{ Area} - \\ & 0.000566 \text{ MW} + 0.00339 \text{ Vm} - 0.758 \text{ Density} + 0.000473 \text{ PMI} + 0.253 \text{ Rotlbonds} \\ & - 0.449 \text{ Hbond\_ac} + 1.059 \text{ Hbond\_do} + 0.034 \text{ AlogP98} - 15.871 \end{aligned}$$

**GABA<sub>A</sub>-benzodiazepine receptor ( $r^2 = 0.65$ )**

$$\begin{aligned} \text{Activity} = & -4.55 \times 10^{-5} \text{ Apol} - 0.00335 \text{ Dipole} - 0.0931 \text{ RadofGyr} - 0.00205 \text{ Area} \\ & - 0.00234 \text{ MW} - 0.00252 \text{ Vm} + 2.664 \text{ Density} - 0.000155 \text{ PMI} - 0.0580 \\ & \text{Rotlbonds} + 0.143 \text{ Hbond\_ac} + 0.0709 \text{ Hbond\_do} - 0.0566 \text{ AlogP98} + 0.991 \end{aligned}$$

Inspection of these equations indicates the importance of specific chemical features that are required to bind with the active site and influence biological activity. The descriptors that appear to influence activity include those from the electronic, physiochemical, spatial and structural categories. Based on the equations, the size of the molecule, that is the molecular area (Area), density (Density) and volume (Vm)

contribute to influencing activity. These terms are spatial descriptors that define the molecule and are directly related to the binding and transport of the molecule. The actual size of the active site pocket is one of the controlling factors for determining the activity of a molecule. If a molecule is too large it will be unable to fit into the active site and interact effectively with the residues required. In contrast, if the molecule is too small, it will be able to fit into the binding pocket but will be unable to interact with all the amino acid residues needed for bioactivity. Calculation of these spatial descriptors can be used to help indicate those molecules with bioactivity versus those molecules without.

The ability of the nicotinamide analogues to bind to the voltage-gated sodium channel and the GABA<sub>A</sub>-benzodiazepine receptor is dependent on the molecules ability to form binding interactions with the active site. This is often influenced by the formation of hydrogen bonds either as hydrogen bond donors or hydrogen bond acceptors. Both of these terms (H-bond donor and H-bond acceptor) are included in and influence the QSAR equations. This ability to form hydrogen bonds affects how a molecule docks into the active site and determines which residues are required to be in close contact. Other important descriptors that influences the binding ability are the atomic polarizability term (Apol) and the dipole moment (Dipole) of the molecule. The atomic polarizability term describes the relative tendency of the electrons around an atom to be distributed based on the electronegativity of the atoms in the molecule as well as the influence of external ions or dipoles. Within the active site, the bulk of the interactions used to bind molecules with receptors are dipole-dipole and ion- dipole. The polarizability descriptor and the dipole moment of the molecules is crucial because it accounts for the ability of these molecules to produce transient electron distributions and form these interactions based on partial

charges. Molecules that lack these abilities for polarization and hydrogen bonding may have lower bioactivity values based on the inability to bind with the active site pocket.

Other important descriptors in the QSAR equations are the spatial descriptors, which are used to establish the 3D shape of the molecules being studied. The descriptors included in the QSAR are the radius of gyration (RadofGyr) and the principal moment of inertia (PMI) and both are dependent on the conformation and orientation of the molecule in space. The principal moment of inertia is the angular mass of the molecule and is used to quantify its rotational inertia. The radius of gyration describes the distribution of the molecule in 3D space which is dependent on the molecule's center of mass. Both of these values are used to develop and characterize the overall shape of molecules, which influences its ability to fit into the active site pocket.

Other important descriptors that are significant for predicting activities in the QSAR equation are the logP value (AlogP98), a physiochemical descriptor and molecular weight (MW), a structural descriptor. These descriptors are influential because they help to indicate and determine which molecules will have the ability to cross the BBB and interact with the required receptors in the brain. In order for drugs to influence epilepsy they must be able to penetrate the BBB. Having these terms in the QSAR equation is crucial as it helps to determine which molecules will have bioactivity based on their ability to get into the brain.

## 5.4 Biological Testing

When developing new treatments to target epilepsy, there are a variety of *in vivo* biological tests available which can assess the ability of new drug candidates to influence the biological processes involved in epilepsy. Since epilepsy is a complex brain disease, it is characterized by a variety of symptoms as well as the CNS regions that are susceptible to sudden electrical discharges. Through extensive examination of specific symptoms and brain imaging, different classifications of epilepsy have been determined and well documented (as presented in Chapter 1). These types of epilepsy include simple partial seizures, complex partial seizures, generalized tonic-clonic seizures and absence seizures. In order to evaluate the ability of new drug candidates to target epilepsy, a variety of different seizure models are utilized. The biological tests performed include the maximal electroshock induced-seizure model (MES), the subcutaneous pentylenetetrazole (Metrazol) induced-seizure (PTZ) model and the six-Hertz psychomotor test. These biological tests along with preliminary neurotoxicity studies were completed at NIH in Bethesda, MD, USA, through their anticonvulsant drug development program (ADD), on the nicotinamide compounds that were synthesized (Table 13).

### (1) Maximal Electroshock Induced-Seizure Model (MES) [26]

This biological model is used to study the effects of new drug candidates on generalized tonic-clonic seizures and voltage dependent sodium channels. For this test, an electrical stimulus (50 mA in mice, 150 mA in rats; 60 Hz) is delivered via corneal electrodes primed with a drop of electrolyte solution (9 % aqueous sodium chloride) to



the eyes and is used to induce an electrical stimulation in the brain leading to the development of a seizure [162]. The electrical stimulus is 0.2 s in duration and is administered after the test compound has been administered interperitoneally. Upon electrical stimulation the animals are observed for 30 min to see if any seizure activity develops. For this test the animals are examined at varying test compound doses of 30, 100 and 300 mg/kg, and at different time intervals of ½ hour and 4 hours, following injection of the test compound. The compounds being tested are considered to have protection against MES-induced seizures if they are able to halt hind-leg tonic extensions, which are normally observed by those animals having a MES-induced seizure.

## **(2) Subcutaneous Pentylenetetrazole (Metrazol) Induced-Seizure Model (PTZ) [26]**

This biological model is used to study the effects of new drug candidates on absence seizures and the GABA<sub>A</sub>-benzodiazepine receptors. Pentylenetetrazole (PTZ) is a chemical that induces seizure activity by acting as a GABA antagonist. The test compound is administered interperitoneally, while the PTZ (85 mg/kg in mice and 70 mg/kg in rats) is injected subcutaneously after the test compound has been administered. After injection of the PTZ the animals are observed for 30 min to see if any seizure activity develops. The absence of clonic limb spasms for greater than 5 seconds indicates that the test drugs may offer protection from PTZ-induced seizures. For this test the animals are examined at varying dosages of the test compound, 30, 100 and 300 mg/kg and at different time intervals of a ½ hour and 4 hours after drug administration.

### **(3) Six-Hertz Psychomotor Seizure Test [26]**

The MES and PTZ biological tests are useful for identifying novel anticonvulsant compounds. However, they may not detect compounds that would be effective against therapy-resistant epilepsy [163]. The six-hertz psychomotor test was developed as an alternate biological test and has been successful in identifying new anticonvulsant drugs including levetiracetam (Keppra<sup>®</sup>), which was actually found to be completely inactive in both the MES and PTZ epilepsy models, even at high dosages [164-167]. This example illustrates the importance of using the correct screening model to find novel anticonvulsant agents. For the 6 Hz psychomotor seizure test, the seizures are induced using a low frequency current (32 mA, 6 Hz), a long duration (3 s) that is delivered through corneal electrodes, in a similar manner to the MES protocol, to produce psychomotor seizures [163]. These 6 Hz seizures observed in rats and mice actually involved a minimal clonic phase, which later was followed by automatistic behaviours. These characteristics closely resemble human partial or limbic epilepsy [168-170]. Based on epilepsy research conducted in the ADD program at NIH, the 6 Hz test is only utilized when compounds are found to be inactive in both the MES and PTZ tests [26].

For this experiment, the animals are initially treated with the test compound (200 mg/kg) intraperitoneally, followed by the 6 Hz current delivered at specified time intervals of 0.25, 0.5, 1.0, and 4.0 hours. Animals that do not display a minimal clonic phase and /or automatistic behaviours are considered to be protected by an active test compound.

#### **(4) Neurotoxicity Tests [26]**

The final group of tests that were completed at NIH include neurotoxic evaluation of the test compounds. Toxicity is measured using a standardized rotarod test which evaluates the ability of the test animals to maintain balance for one minute on a rod rotating at 6 rpm. The animals are tested for neurotoxicity at the variable dosages of 30, 100 and 300 mg/kg and at time intervals of ½ hour and 4 hours. If an animal is unable to stay on the rotarod for 3 consecutive trials or there is observation of neurologic abnormalities like a change in gait or stance, display of a tremor, increase in activity, somnolence, stupor and/ or other neuronal impairments, the animal is considered to be suffering from neuronal impairment.

**Table 13.** The chemical structure and identification numbers (ID#) for the synthesized nicotinamides analogues.

ID #	X	R <sup>1</sup>	R <sup>2</sup>	R <sup>3</sup>	R <sup>4</sup>	R <sup>5</sup>	R <sup>6</sup>
1	N	CH <sub>2</sub> CH <sub>2</sub> CH <sub>3</sub>	H	H	H	H	H
2	N	CH(CH <sub>3</sub> ) <sub>2</sub>	H	H	H	H	H
3	N	C <sub>6</sub> H <sub>11</sub>	H	H	H	H	H
4	N	C <sub>6</sub> H <sub>5</sub>	H	H	H	H	H
5	N	CH <sub>2</sub> C <sub>6</sub> H <sub>5</sub>	H	H	H	H	H
6	N	C <sub>6</sub> H <sub>5</sub>	C <sub>6</sub> H <sub>5</sub>	H	H	H	H
7	N	CH <sub>2</sub> C <sub>6</sub> H <sub>5</sub>	CH <sub>3</sub>	H	H	H	H
8	N	CH(CH <sub>3</sub> ) C <sub>6</sub> H <sub>5</sub>	H	H	H	H	H
9	N	CH(CH <sub>2</sub> ) <sub>3</sub> CH <sub>3</sub>	H	H	H	H	H
10	N	C <sub>6</sub> H <sub>3</sub> ( <i>o</i> -CH <sub>3</sub> ) <sub>2</sub>	H	H	H	H	H
11	O	CH <sub>3</sub>	n/a	H	H	H	H
12	O	CH <sub>2</sub> CH <sub>3</sub>	n/a	H	H	H	H
13	O	CH(CH <sub>3</sub> ) <sub>2</sub>	n/a	H	H	H	H
14	O	C <sub>6</sub> H <sub>5</sub>	n/a	H	H	H	H
15	N	CH(CH <sub>3</sub> ) C <sub>6</sub> H <sub>5</sub>	H	H	H	Br	H
16	N	CH <sub>2</sub> CH <sub>2</sub> CH <sub>3</sub>	H	H	H	Br	H
17	N	CH <sub>2</sub> C <sub>6</sub> H <sub>5</sub>	CH <sub>3</sub>	H	H	Br	H
18	N	C <sub>6</sub> H <sub>11</sub>	H	H	H	Br	H
19	N	CH <sub>2</sub> C <sub>6</sub> H <sub>5</sub>	H	H	H	Br	H
20	N	C <sub>6</sub> H <sub>5</sub>	H	H	H	Br	H
21	N	CH(CH <sub>2</sub> ) <sub>3</sub> CH <sub>3</sub>	H	H	H	Br	H
22	N	CH <sub>2</sub> C <sub>6</sub> H <sub>5</sub>	H	H	H	Styryl	H
23	N	CH(CH <sub>3</sub> ) C <sub>6</sub> H <sub>5</sub>	H	H	H	Styryl	H
24	N	CH <sub>2</sub> C <sub>6</sub> H <sub>5</sub>	CH <sub>3</sub>	H	H	Styryl	H
25	N	C <sub>6</sub> H <sub>11</sub>	H	H	H	Styryl	H
26	N	CH <sub>2</sub> CH <sub>2</sub> CH <sub>3</sub>	H	H	H	Styryl	H
27	N	CH <sub>2</sub> C <sub>6</sub> H <sub>5</sub>	H	H	H	Methyl acrylate	H
28	N	CH(CH <sub>3</sub> ) C <sub>6</sub> H <sub>5</sub>	H	H	H	Methyl acrylate	H
29	N	C <sub>6</sub> H <sub>11</sub>	H	H	H	Methyl acrylate	H
30	N	CH <sub>2</sub> C <sub>6</sub> H <sub>5</sub>	H	H	H	C <sub>6</sub> H <sub>5</sub>	H

ID #	X	R <sup>1</sup>	R <sup>2</sup>	R <sup>3</sup>	R <sup>4</sup>	R <sup>5</sup>	R <sup>6</sup>
31	N	CH <sub>2</sub> C <sub>6</sub> H <sub>5</sub>	H	H	H	<i>p</i> -(CH <sub>3</sub> )-C <sub>6</sub> H <sub>4</sub>	H
32	N	CH <sub>2</sub> C <sub>6</sub> H <sub>5</sub>	H	H	H	<i>p</i> -(Cl)-C <sub>6</sub> H <sub>4</sub>	H
33	N	CH <sub>2</sub> C <sub>6</sub> H <sub>5</sub>	H	H	H	<i>p</i> -(CF <sub>3</sub> )-C <sub>6</sub> H <sub>4</sub>	H
34	N	CH <sub>2</sub> C <sub>6</sub> H <sub>5</sub>	H	H	H	<i>p</i> -(OH)-C <sub>6</sub> H <sub>4</sub>	H
35	N	CH(CH <sub>3</sub> ) C <sub>6</sub> H <sub>5</sub>	H	H	H	C <sub>6</sub> H <sub>5</sub>	H
36	N	CH(CH <sub>3</sub> ) C <sub>6</sub> H <sub>5</sub>	H	H	H	<i>p</i> -(CH <sub>3</sub> )-C <sub>6</sub> H <sub>4</sub>	H
37	N	CH(CH <sub>3</sub> ) C <sub>6</sub> H <sub>5</sub>	H	H	H	<i>p</i> -(Cl)-C <sub>6</sub> H <sub>4</sub>	H
38	N	CH <sub>2</sub> CH <sub>2</sub> CH <sub>3</sub>	H	H	H	<i>p</i> -(Cl)-C <sub>6</sub> H <sub>4</sub>	H
39	N	CH <sub>2</sub> CH <sub>2</sub> CH <sub>3</sub>	H	H	H	<i>p</i> -(CH <sub>3</sub> )-C <sub>6</sub> H <sub>4</sub>	H
40	N	C <sub>6</sub> H <sub>5</sub>	H	H	H	<i>p</i> -(CH <sub>3</sub> )-C <sub>6</sub> H <sub>4</sub>	H
41	O	H	n/a	S-CH <sub>2</sub> C <sub>6</sub> H <sub>5</sub>	H	H	H
42	N	CH <sub>2</sub> CH <sub>2</sub> CH <sub>3</sub>	H	S-CH <sub>2</sub> C <sub>6</sub> H <sub>5</sub>	H	H	H
43	N	C <sub>6</sub> H <sub>3</sub> ( <i>o</i> -CH <sub>3</sub> ) <sub>2</sub>	H	S-CH <sub>2</sub> C <sub>6</sub> H <sub>5</sub>	H	H	H
44	N	CH <sub>2</sub> C <sub>6</sub> H <sub>5</sub>	CH <sub>3</sub>	S-CH <sub>2</sub> C <sub>6</sub> H <sub>5</sub>	H	H	H
45	N	C <sub>6</sub> H <sub>11</sub>	H	S-CH <sub>2</sub> C <sub>6</sub> H <sub>5</sub>	H	H	H
46	N	C <sub>6</sub> H <sub>5</sub>	H	S-CH <sub>2</sub> C <sub>6</sub> H <sub>5</sub>	H	H	H
47	N	CH <sub>2</sub> C <sub>6</sub> H <sub>5</sub>	H	S-CH <sub>2</sub> C <sub>6</sub> H <sub>5</sub>	H	H	H
48	N	CH(CH <sub>3</sub> ) C <sub>6</sub> H <sub>5</sub>	H	S-CH <sub>2</sub> C <sub>6</sub> H <sub>5</sub>	H	H	H
49	N	CH <sub>2</sub> C <sub>6</sub> H <sub>5</sub>	H	S(O)- CH <sub>2</sub> C <sub>6</sub> H <sub>5</sub>	H	H	H
50	N	CH(CH <sub>3</sub> ) C <sub>6</sub> H <sub>5</sub>	H	S(O)- CH <sub>2</sub> C <sub>6</sub> H <sub>5</sub>	H	H	H

## 5.5 Biological Results

Once all the biological test results were received, each of the molecules in the training-set were assigned activity codes so that the biological results could be standardized for the QSAR study. These codes were determined based on several factors, including the number of animals that were protected against the development of a seizure, the nicotinamide dosage required for this protection, and finally the neurotoxicity results. A numerical scale was developed, ranging from 0 to 4, as shown in Table 14, and the compounds were divided into groups using ratios to represent the number of animals protected over the number of animals tested. The biological results and assigned activity codes for the training-set are displayed in Table 15.

**Table 14.** Activity codes and the corresponding animal protection ratios and dosages.

Activity Code	Ratios	Dosage of test compound (mg/kg)
0	0/4	300
1	1-2/4	300
2	>2/4	300
3	>2/4	100
4	>2/4	30

Through inspection of the biological data in Table15, several trends were noted in the activity profiles for targeting either the voltage gated sodium channel or the GABA<sub>A</sub> channel.

### 5.5.1 Voltage Gated Sodium Channel: Maximal Electroshock Seizure Model (MES)

The utilized pharmacophore model predicted by Dimmock *et al.* [79, 80] involving a hydrogen bonding domain (HBD), an aryl binding site/hydrophobic pocket (HP) and an electron donor region (D) for targeting the fast inactivated state of the sodium channel appeared to play an important role in the structure-activity relationships (SAR). It was clearly evident that when an aromatic group was utilized in the R<sup>1</sup> and/or R<sup>2</sup> position (Table 15: Compounds **4**, **5**, **7**, **8**, and **10**) the molecules had a greater ability to control seizure activity in the MES model compared to those compounds that had short alkyl chains (Table 15: Compounds **1**, **2**).

Compound **5** (N-benzylnicotinamide), when tested in the MES assay showed the most promising ability to prevent the development of a seizure of the R<sup>1</sup>/R<sup>2</sup> substituted nicotinamides. For this compound an ED<sub>50</sub> was calculated in a rat model using both the MES and PTZ tests. The preliminary results, presented in Table 16, show that five of the eight animals were protected from the development of a seizure at a dosage of 30 mg/kg. It was also determined that increasing the dosage of compound **5** does not result in an increase in the percentage of protected animals.

**Table 15.** Biological testing results and activity codes for nicotinamide analogues in the QSAR training-set. The ratios indicated the number of animals protected over the number of animal tested.

Dosage (mg/kg)	MES Testing												PTZ Testing										Toxicity						Activity Scores	
	30				100				300				30				100				300				100		300		MES	PTZ
	0.5	4.0	0.5	4.0	0.5	4.0	0.5	4.0	0.5	4.0	0.5	4.0	0.5	4.0	0.5	4.0	0.5	4.0	0.5	4.0	0.5	4.0	0.5	4.0	0.5	4.0	0.5	4.0		
Time (hrs)																														
ID Codes																														
1	0/1	0/1	0/3	0/3	0/1	0/1	0/1	0/1	0/1	0/1	0/1	0/1	0/1	0/1	0/1	0/1	0/1	0/1	0/1	0/1	0/1	0/1	0/1	0/1	0/1	0/1	0/1	0/1	0	2
2	0/1	0/1	0/3	0/3	0/1	0/1	0/1	0/1	0/1	0/1	0/1	0/1	0/1	0/1	0/1	0/1	0/1	0/1	0/1	0/1	0/1	0/1	0/1	0/1	0/1	0/1	0/1	0/1	0	0
3	0/1	0/1	0/3	0/3	0/1	0/1	0/1	0/1	0/1	0/1	0/1	0/1	0/1	0/1	0/1	0/1	0/1	0/1	0/1	0/1	0/1	0/1	0/1	0/1	0/1	0/1	0/1	0/1	0	0
4	0/1	0/1	3/3	0/3	1/1	0/1	0/1	0/1	0/1	0/1	0/1	0/1	0/1	0/1	0/1	0/1	0/1	0/1	0/1	0/1	0/1	0/1	0/1	0/1	0/1	0/1	0/1	0/1	3	0
5	4/4	1/1	2/3	0/3	1/1	1/1	0/1	0/1	0/1	0/1	0/1	0/1	0/1	0/1	0/1	0/1	0/1	0/1	0/1	0/1	0/1	0/1	0/1	0/1	0/1	0/1	0/1	0/1	4	0
6	0/1	0/1	0/3	0/3	0/1	0/1	0/1	0/1	0/1	0/1	0/1	0/1	0/1	0/1	0/1	0/1	0/1	0/1	0/1	0/1	0/1	0/1	0/1	0/1	0/1	0/1	0/1	0/1	0	1
7	0/1	0/1	0/3	0/3	1/1	0/1	0/1	0/1	0/1	0/1	0/1	0/1	0/1	0/1	0/1	0/1	0/1	0/1	0/1	0/1	0/1	0/1	0/1	0/1	0/1	0/1	0/1	0/1	1	2
8	0/1	0/1	3/3	0/3	1/1	1/1	0/1	0/1	0/1	0/1	0/1	0/1	0/1	0/1	0/1	0/1	0/1	0/1	0/1	0/1	0/1	0/1	0/1	0/1	0/1	0/1	0/1	0/1	3	0
9	0/1	0/1	1/3	0/3	1/1	0/1	0/1	0/1	0/1	0/1	0/1	0/1	0/1	0/1	0/1	0/1	0/1	0/1	0/1	0/1	0/1	0/1	0/1	0/1	0/1	0/1	0/1	0/1	2	1
10	0/1	0/1	3/3	0/3	1/1	1/1	0/1	0/1	0/1	0/1	0/1	0/1	0/1	0/1	0/1	0/1	0/1	0/1	0/1	0/1	0/1	0/1	0/1	0/1	0/1	0/1	0/1	0/1	3	1
11	0/1	0/1	0/3	0/3	0/1	0/1	0/1	0/1	0/1	0/1	0/1	0/1	0/1	0/1	0/1	0/1	0/1	0/1	0/1	0/1	0/1	0/1	0/1	0/1	0/1	0/1	0/1	0/1	0	0
12	0/1	0/1	0/3	0/3	0/1	0/1	0/1	0/1	0/1	0/1	0/1	0/1	0/1	0/1	0/1	0/1	0/1	0/1	0/1	0/1	0/1	0/1	0/1	0/1	0/1	0/1	0/1	0/1	0	1
13	0/1	0/1	0/3	0/3	0/1	0/1	0/1	0/1	0/1	0/1	0/1	0/1	0/1	0/1	0/1	0/1	0/1	0/1	0/1	0/1	0/1	0/1	0/1	0/1	0/1	0/1	0/1	0/1	0	0
14	0/1	0/1	0/3	0/3	0/1	0/1	0/1	0/1	0/1	0/1	0/1	0/1	0/1	0/1	0/1	0/1	0/1	0/1	0/1	0/1	0/1	0/1	0/1	0/1	0/1	0/1	0/1	0/1	0	0
15	0/1	0/1	0/3	0/3	1/1	0/1	0/1	0/1	0/1	0/1	0/1	0/1	0/1	0/1	0/1	0/1	0/1	0/1	0/1	0/1	0/1	0/1	0/1	0/1	0/1	0/1	0/1	0/1	1	0
16	0/1	0/1	1/3	0/3	1/1	0/1	0/1	0/1	0/1	0/1	0/1	0/1	0/1	0/1	0/1	0/1	0/1	0/1	0/1	0/1	0/1	0/1	0/1	0/1	0/1	0/1	0/1	0/1	2	3
17	0/1	0/1	0/3	0/3	0/1	0/1	0/1	0/1	0/1	0/1	0/1	0/1	0/1	0/1	0/1	0/1	0/1	0/1	0/1	0/1	0/1	0/1	0/1	0/1	0/1	0/1	0/1	0/1	0	3
18	0/1	0/1	0/3	0/3	0/1	0/1	0/1	0/1	0/1	0/1	0/1	0/1	0/1	0/1	0/1	0/1	0/1	0/1	0/1	0/1	0/1	0/1	0/1	0/1	0/1	0/1	0/1	0/1	0	2
19	0/1	0/1	2/3	0/3	1/1	1/1	0/1	0/1	0/1	0/1	0/1	0/1	0/1	0/1	0/1	0/1	0/1	0/1	0/1	0/1	0/1	0/1	0/1	0/1	0/1	0/1	0/1	0/1	3	1
20	0/1	0/1	0/3	0/3	0/1	0/1	0/1	0/1	0/1	0/1	0/1	0/1	0/1	0/1	0/1	0/1	0/1	0/1	0/1	0/1	0/1	0/1	0/1	0/1	0/1	0/1	0/1	0/1	0	2
22	0/1	0/1	0/3	0/3	0/1	0/1	0/1	0/1	0/1	0/1	0/1	0/1	0/1	0/1	0/1	0/1	0/1	0/1	0/1	0/1	0/1	0/1	0/1	0/1	0/1	0/1	0/1	0/1	0	0



	MES Testing						PTZ Testing						Toxicity						Activity Scores			
	30		100		300		30		100		300		30		100		300		MES	PTZ		
Dosage (mg/kg)	0.5	4.0	0.5	4.0	0.5	4.0	0.5	4.0	0.5	4.0	0.5	4.0	0.5	4.0	0.5	4.0	0.5	4.0	7/4	7/4		
Time (hrs)	0.5	4.0	0.5	4.0	0.5	4.0	0.5	4.0	0.5	4.0	0.5	4.0	0.5	4.0	0.5	4.0	0.5	4.0		1/4		
ID Codes																						
27	0/1	0/1	0/3	0/3	0/1	0/1	0/1	0/1	1/5	0/1	0/1	0/1	0/1	0/1	1/4	1/2	6/8	0/4	2/4	1/2	0	1
41	0/1	0/1	0/3	0/3	0/1	0/1	0/1	0/1	0/1	0/1	4/5	0/1	0/1	0/1	0/4	0/2	0/8	0/4	2/4	1/2	0	2
42	0/1	0/1	0/3	0/3	0/1	0/1	0/1	0/1	0/1	0/1	0/1	0/1	0/1	0/1	0/4	0/2	0/8	0/4	0/4	0/2	0	0
43	0/1	0/1	0/3	0/3	0/1	0/1	0/1	0/1	0/1	0/1	0/1	0/1	0/1	0/1	0/4	0/2	1/8	0/4	0/4	0/2	0	0
44	0/1	0/1	0/3	0/3	0/1	0/1	0/1	0/1	0/1	0/1	0/1	0/1	0/1	0/1	1/4	0/2	0/8	0/4	0/4	0/2	0	0
45	0/1	0/1	0/3	0/3	0/1	0/1	0/1	0/1	0/1	0/1	0/1	0/1	0/1	0/1	0/4	0/2	4/8	2/4	1/4	1/2	0	0
46	0/1	0/1	0/3	0/3	0/1	0/1	0/1	0/1	0/1	0/1	0/1	0/1	0/1	2/4	0/2	2/8	0/4	1/4	0/2	0	0	0
47	0/1	0/1	0/3	0/3	0/1	0/1	1/5	0/1	1/1	0/1	0/1	0/1	0/1	0/1	0/4	0/2	0/8	1/4	1/4	1/2	0	1
48	0/1	0/1	0/3	0/3	0/1	0/1	0/1	0/1	0/1	0/1	1/1	0/1	1/1	0/1	0/4	0/2	1/8	1/4	0/4	1/2	0	1
49	0/1	0/1	0/3	0/3	0/1	0/1	0/1	0/1	0/1	0/1	0/1	0/1	0/1	0/1	0/4	0/2	0/8	1/4	0/4	0/2	0	0
50	0/1	0/1	0/3	0/3	0/1	0/1	3/5	0/1	0/1	0/1	0/1	0/1	0/1	0/1	0/4	0/2	1/8	0/4	0/4	0/2	0	4

**Table 16.** The ED<sub>50</sub> value results for N-benzylnicotinamide (**5**) in the both the MES and PTZ tests.

Test	Time (Hrs)	ED50
MES	1	<30
PTZ	0.25	<100
TOX	0	>125

Test	Dosage (mg/kg)	Animal Deaths	Protective Ratio
MES	3	0	0/8
MES	7.5	0	3/8
MES	15	0	2/8
MES	30	0	5/8
MES	40	0	5/8
MES	80	0	4/8
MES	125	0	4/8
PTZ	12.5	0	2/8
PTZ	25	0	3/8
PTZ	50	0	2/8
PTZ	100	0	6/8

For this R<sup>1</sup>/R<sup>2</sup> substituted series, it was determined that when larger alkyl groups, like pentyl (Table 15: Compound **9**) were used activity values increased. This may be a result of both chain length and the alkyl group's space-filling capacities, which allow the compound to fit into the receptor pocket and bind [79, 80]. When both the R<sup>1</sup> and R<sup>2</sup> positions were substituted with phenyl groups (Table 15: Compound **6**) activity was lost, this was possibly due to steric interactions between the two phenyl groups and the binding pocket in the sodium channel.

The second region to be biologically researched involved the introduction of different groups to the R<sup>5</sup> position on the nicotinamide scaffold. Replacement of the hydrogen with bromine was the first alteration. It was clearly evident from the biological results that this chemical alteration made a significant contribution to the activity profile by either increasing or decreasing bioactivity. For those compounds with an aromatic

group in the R<sup>1</sup>/R<sup>2</sup> position bioactivity in the MES screen decreased, while PTZ bioactivity results improved. Introduction of a bromine, which is more electronegative than hydrogen (Br = 2.8, H = 2.1), means that the bromo group should have a negative partial charge compared to the original compound with the hydrogen. This chemical alteration may have decreased the binding ability of the nicotinamide molecules for the voltage gated sodium channel, while increasing their binding affinity at the GABA<sub>A</sub> channel. The brominated compounds **16** and **19**, both displayed sedation capabilities indicating that these compounds may be exerting their effect on the GABA<sub>A</sub> channel by binding to a similar location like the general anesthetic etomidate [171].

From the initial biological results using methyl acrylate (compound **27**) an electron withdrawing group, and styrene (compound **22**) an electron donating group in the R<sup>5</sup> position limited biological activity was noted for both MES and PTZ tests. For both of these compounds the R<sup>1</sup> group initially chosen was a benzyl group. This group was selected based on the previous MES biological activity seen for both N-benzylnicotinamide (**5**) and N-benzyl-5-bromopyridine-3-carboxamide (**19**). These compounds (**22** and **27**) were synthesized using a Heck coupling. After the compounds bioactivity was determined these molecules were energy minimized using molecular mechanics to examine their low energy conformations. In both chemical situations the lowest energy conformations had the predicted trans double bond; however, instead of being extended so that the bioactive face, was exposed the receptor the molecules were folded into a helical shape. In the case of N-benzyl-styrylpyridine-3-carboxamide (**22**) the phenyl/ pyridine rings appeared stacked and were most likely held in this position through pi-pi stacking interactions. For (E)-methyl-3-(5-(benzylcarbamoyl)pyridine-3-

yl)acrylate (**27**) the lowest energy conformation determined through molecular mechanics was similar to **22**, with pi-pi stacking between the phenyl/pyridine rings and the methyl acrylate in a trans coiled conformation and not extended. Although these biological results were not as promising as hoped, new compounds in this Heck coupling series and Suzuki coupling series have been synthesized with other aromatic and non-aromatic moieties in the R<sup>1</sup>/R<sup>2</sup> position.

### 5.5.2 GABA<sub>A</sub>-Benzodiazepine Receptors: Pentylenetetrazole Seizure Model (PTZ)

The hypothesis for targeting GABA<sub>A</sub> channel was to create a novel nicotinamide series that could bind to, and influence, the GABA<sub>A</sub>-benzodiazepine receptor. Ten compounds were created and tested in both the biological assays (Compounds **41-50**) and the results are presented in Table 15. The compounds tested included both a thio and sulfoxide functional group in the R<sup>3</sup> position as well as aromatic and non-aromatic groups in the R<sup>1</sup> and R<sup>2</sup> positions. Very little protective activity against the development of a seizure was observed in either of the MES and PTZ tests when R<sup>1</sup> or R<sup>2</sup> was not an aromatic substituent, however, when an aromatic substituent was used minimal activity was observed. This can be seen with compounds **46**, **47** and **48**, which had activity in the MES and PTZ. Since it had limited activity in the PTZ test, N-benzyl-2-(benzylthio)pyridine-3-carboxamide (**47**) was also screened in the 6 Hz assay, but no protective activity was detected (Table 17). Only two molecules were tested with R<sup>3</sup> as a sulfoxide group and it was found that activity was structure dependent. In the case of N-benzyl-2-(benzylsulfinyl)pyridine-3-carboxamide (**49**) no activity was seen, but 2-(benzylsulfinyl)-N-(1-phenylethyl)pyridine-3-carboxamide (**50**) had maximum protection

in the PTZ test (Table 15) as well as in the 6 Hz assay (Table 17). The only difference between the two molecules was a methyl group, however, it made a huge impact on seizure protection. Each of the molecules was minimized using molecular mechanics, and it was clearly evident that when R<sup>1</sup> is the N-(1-phenylethyl) free rotation around the amide bond was restricted due to steric effects. This helped the molecule to maintain the low energy conformation of a pseudo-7-membered ring, which was originally hypothesized to be crucial for bioactivity in the PTZ test. When R<sup>1</sup> was a N-benzyl group free rotation about the amide bond could occur more readily therefore bioactivity in the PTZ assay was reduced, presumably because a pseudo-7-membered ring was not the only contributing low energy conformation of the molecule. To further test this hypothesis of steric control, new nicotinamide molecules with bulky space filling substituents in the R<sup>1</sup> position need to be synthesized and biologically tested in the PTZ assay.

**Table 17.** The results for the 6 Hz psychomotor test at varying time intervals. The ratios indicated the number of animals protected over the number of animal tested.

6 Hz Test		Time (h)				
ID Codes	Dosage (mg/kg)	0.25	0.5	1.0	2.0	4.0
47	100	0/4	0/4	0/4	0/4	0/4
50	100	0/4	0/4	0/4	2/4	0/4

### 5.5.3 Neurotoxicity

Many of the compounds tested displayed no appreciable neurotoxic side effects and were well tolerated, even at the highest dosage of 300 mg/kg. All the neurotoxicity results are presented in Table 15. This may be a result of several important design factors including, ability of the nicotinamide analogues to be selective for the target receptors initially chosen. Secondly, the compound's metabolism is controlled so that the compounds have a reasonable half-life and do not remain in circulation for an extended period of time, and, finally, the metabolites of the nicotinamide analogues are not able to interact and influence new receptors. In the instances where toxic side-effects were observed, few animal deaths were the final result. The toxicity concerns were all observed at the highest dosage of 300 mg/kg, and included ataxia, myoclonic jerks, loss of righting reflex, inability to grasp the rotorod and sedation. Although these results are not desired, they do indicate that many of these compounds are capable of crossing the BBB and influencing the processes controlled by the CNS. All the animal deaths that occurred, were the result of continuous tonic clonic seizures, indicating that it may be a result of an extended half-life or inability to control neuronal excitation. Those compounds that led to animal death were compounds **7**, **20** and **44**.

## 5.6 Conclusions

Through these QSAR studies two mathematical equations were developed, one to represent those molecules targeted towards voltage-gated sodium channels and one for the benzodiazepine site on the GABA<sub>A</sub> channel. These equations have been instrumental in attempting to identify the chemical components of the nicotinamide analogues, which are required for biological activity. Based on the results, it has been determined that there is a connection between the components of the nicotinamide chemical scaffold and the biological findings. The specific chemical qualities that appear to be required include an amide bond region, an aromatic moiety or bulky hydrophobic alkyl group, and an electron donor region. The results obtained from this study have helped to develop an initial predicative model of nicotinamides' influence on the process of epilepsy. Using the NIH results and calculated 2D QSAR equations an optimized structure of a biologically active nicotinamide compound for both voltage-gated sodium channel and GABA<sub>A</sub>-benzodiazepine could be developed.

## **CHAPTER 6**

### **DIHYDROURACILS**

---



## 6.1 Introduction

Since neurotransmitters are central to information processing within the central and peripheral nervous systems, they are crucial molecular platforms in normal brain function and in the pharmacological manipulation of abnormal brain function. Historically, the most important neurotransmitters have been small molecules (acetylcholine, norepinephrine, dopamine), which have provided fundamental insights into normal neurochemistry and disease

Amongst small molecule neurotransmitters, amino acid neurotransmitters are major players.  $\alpha$ -Amino acids (e.g. the excitatory glutamate and inhibitory glycine transmitters) and  $\gamma$ -amino acids (e.g. the inhibitory  $\gamma$ -aminobutyric acid [GABA] transmitter) contribute to the most fundamental processes of the brain (arousal, sleep, consciousness) and to the disorders (epilepsy, stroke, dementia) that affect these processes. Structurally, amino acid neurotransmitters are extremely simple molecules possessing an anionic carboxylate on one end and a cationic ammonium on the other end. In  $\alpha$ -amino acids, the carboxylate and ammonium termini are separated by a 2.5 Å one-carbon bridge; in  $\gamma$ -amino acids the carboxylate and ammonium termini are separated by a 5.1 Å three-carbon bridge.

On the basis of structural arguments, it is reasonable to hypothesize that a structurally intermediate  $\beta$ -amino acid, with a carboxylate-ammonium separation formed by a 3.8 Å two-carbon bridge, should also be a neurotransmitter (see Figure 22). Indeed, from a biomolecular perspective, the existence of a  $\beta$ -amino acid neurotransmitter geometrically juxtaposed between  $\alpha$ - and  $\gamma$ -amino acid neurotransmitters would be biologically logical within an analogue series of information transmitting

neurochemicals. Moreover, functionally, such a structurally intermediate amino acid neurotransmitter would afford additional opportunities to fine tune the careful balance between excitatory and inhibitory processes within the brain. Thus, on theoretical grounds, the existence of a  $\beta$ -amino acid neurotransmitter seems not only logical, but also desirable.

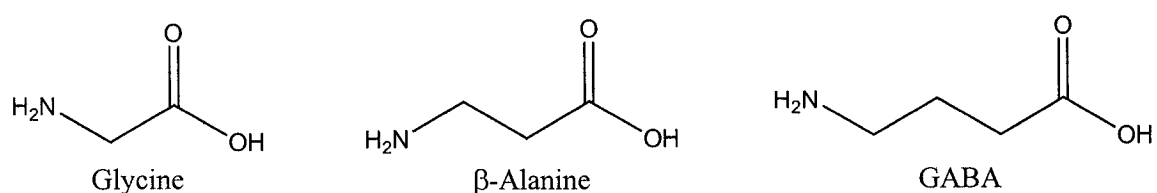


**Figure 22.**  $\beta$ -Alanine is a structural hybrid between the neurotransmitters glycine and GABA.

Structurally,  $\beta$ -alanine is the simplest possible  $\beta$ -amino acid, having no substituents on its central two-carbon bridge [172]. Fortuitously,  $\beta$ -alanine is one of four naturally occurring  $\beta$ -amino acids (including taurine) endogenous to humans. Moreover, despite not being used in the synthesis of any enzyme or protein, it is considered to be the only  $\beta$ -amino acid with any physiological significance.  $\beta$ -Alanine does occur within the human central nervous system (CNS) and some authors have suggested that it might function as a neuromodulator [173]. Within muscle,  $\beta$ -alanine exists as a component of the dipeptide carnosine ( $\beta$ -alanyl-histidine). In non-neural tissues, it occurs in many forms: as a free amino acid, as part of coenzyme A's pantothenic acid moiety, as a product of L-aspartate and uracil metabolism, and as a by-product of aspartic acid decarboxylation by gut microbes [174].

The purpose of this review is to analyze  $\beta$ -alanine neurochemistry and to ascertain whether  $\beta$ -alanine has the properties necessary to be a neurotransmitter. To approach this analysis, the review is structured in three parts: Part A reviews the known biochemistry of  $\beta$ -alanine; Part B determines if these biochemical data are sufficient to classify  $\beta$ -alanine as a neurotransmitter; and Part C examines the implications of classifying  $\beta$ -alanine as a neurotransmitter.

## **6.2 Part A – Overview Of $\beta$ -Alanine Neurochemistry**

### **6.2.1 $\beta$ -Alanine Synthesis**

$\beta$ -Alanine is produced by three main biosynthetic pathways: a product of L-aspartate decarboxylation by gut microbes [175] (Figure 23); a by-product of the interchangeable reaction of pyruvate to L-alanine (Figure 24); and a product of deamination and carboxylation of the pyrimidine uracil [174] (Figure 25).

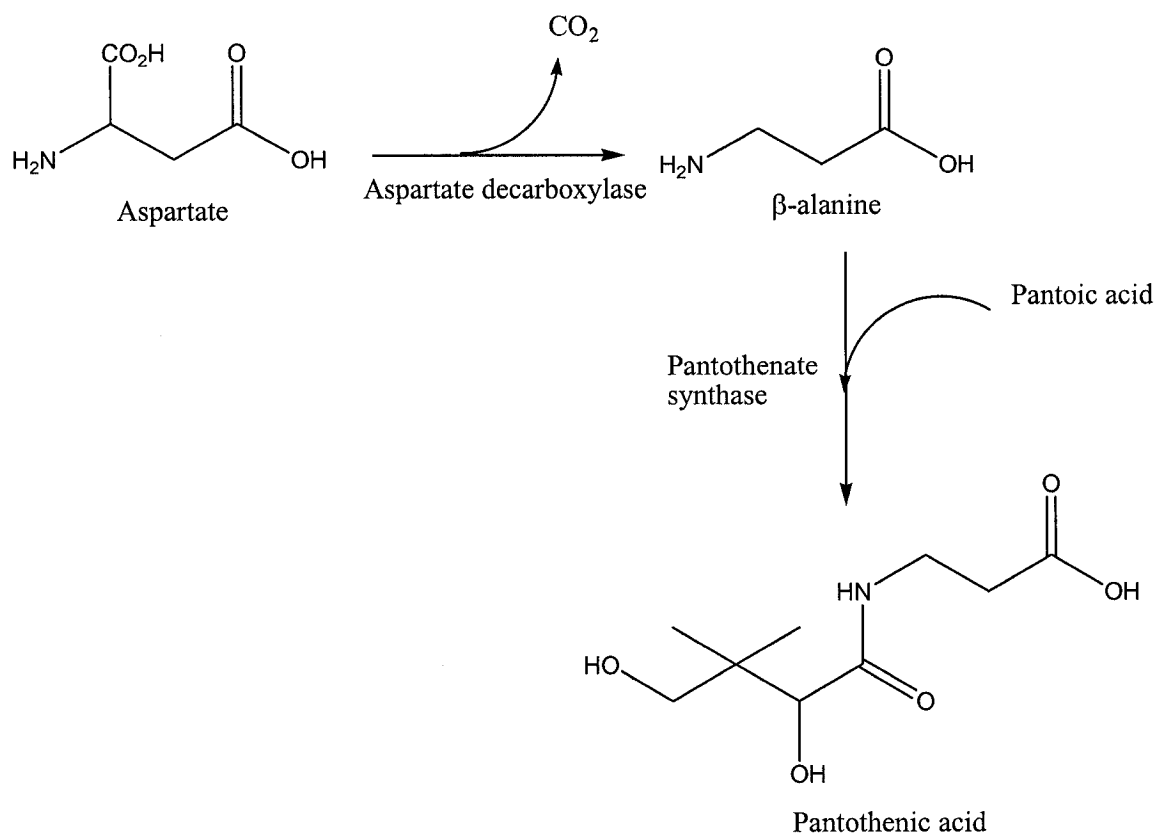


**Figure 23.** Decarboxylation of L-aspartate to β-alanine by gastrointestinal microbes.

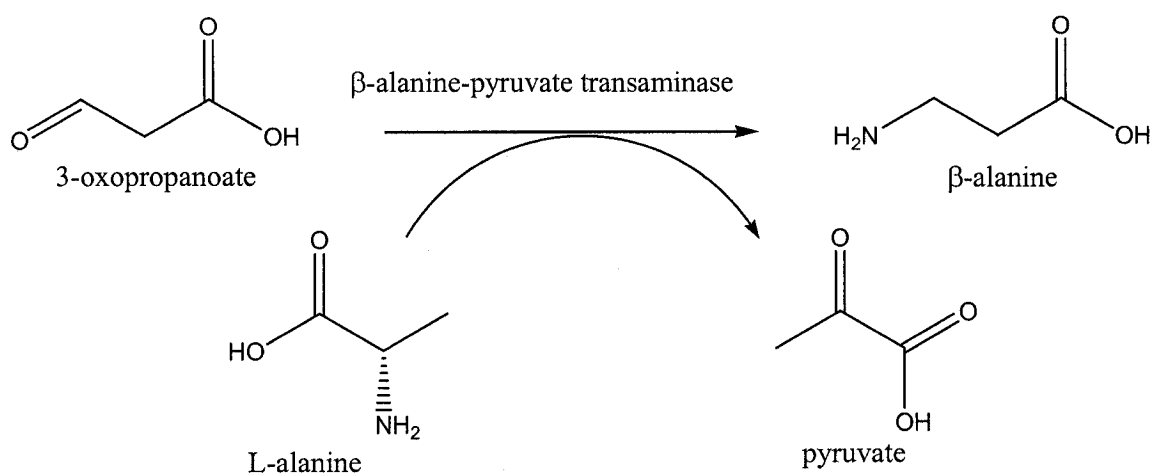


**Figure 24.** β-Alanine is a metabolic by-product of the interchangeable reaction of L-alanine and pyruvate.

Though  $\beta$ -alanine biosynthesis can occur via any of these three pathways, not all pathways occur equally in all organ systems. For example, although the biosynthesis of  $\beta$ -alanine from aspartate does occur in the brain, it does not appear that aspartate decarboxylation is the major source of  $\beta$ -alanine within brain. Indirect evidence lends support for neuronal formation of  $\beta$ -alanine via uracil.

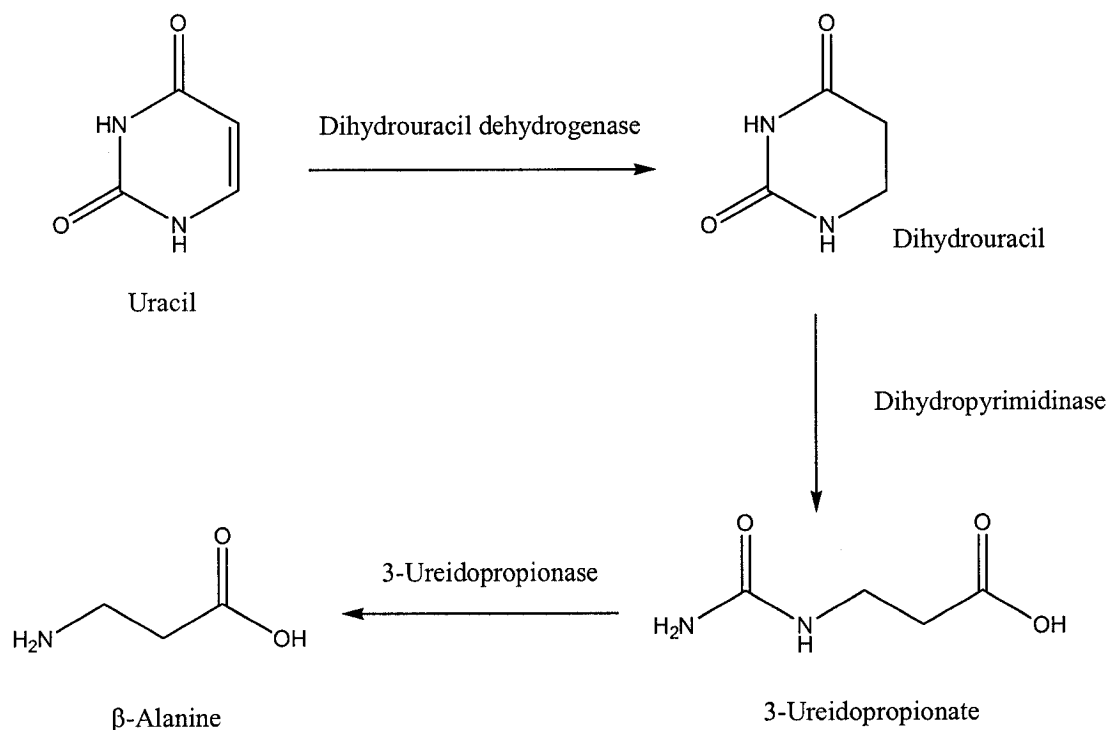


**Figure 25.** Pyrimidine metabolic pathway used for the metabolism of uracil to  $\beta$ -alanine.

#### 6.2.1.1 $\beta$ -Alanine Synthesis From Uracil

$\beta$ -Amino acids can be produced from the pyrimidine metabolic cycle through the degradation of uracil and thymine (Figure 25). Both uracil and thymine are reduced to dihydro derivatives that are hydrolyzed to produce  $\beta$ -ureido compounds [176]. These intermediates then undergo further hydrolysis yielding specific  $\beta$ -amino acids. The

metabolism of uracil results in  $\beta$ -alanine while thymine metabolism produces  $\beta$ -aminoisobutyric acid. Uracil and thymine are degraded in four steps with the first three steps in both pathways being controlled by the same enzymes. The enzymes involved in this metabolism include dihydropyrimidine dehydrogenase (DPD, 1.3.1.2), dihydropyrimidinase (DHP, 3.5.2.2),  $\beta$ -ureidopropionase (UP, 3.5.1.6, new name *N*-carbamoyl- $\beta$ -alanine amidohydrolase or  $\beta$ -alanine synthase), and the amino transferases (*R*)-(-)- $\beta$ -aminoisobutyratepyruvate aminotransferase (BAIBPAT, 2.6.1.40),  $\beta$ -alanine-pyruvate aminotransferase (BAPAT, 2.6.1.18) and  $\beta$ -alanine- $\alpha$ -ketoglutarate aminotransferase (BAKAT, 2.6.1.19). The aminotransferase used for the metabolism of  $\beta$ -alanine to malonate semialdehyde is  $\beta$ -alanine- $\alpha$ -ketoglutarate aminotransferase (BAKAT); (*R*)-(-)- $\beta$ -aminoisobutyratepyruvate aminotransferase (BAIBPAT) is used for the metabolism of  $\beta$ -aminoisobutyrate [177].

Malonate semialdehyde formed from  $\beta$ -hydroxypropionate is converted to  $\beta$ -alanine in the brain [178, 179]. GABA-transaminase (GABA-T) is equally reactive towards GABA and  $\beta$ -alanine, both for their metabolism and biosynthesis, based on the reversible action of this enzyme [180]. Using GABA-T for the reverse transamination of malonate semialdehyde, biosynthesis of  $\beta$ -alanine in the CNS can occur [174, 181, 182]. The endogenous concentration and release of  $\beta$ -alanine is influenced by GABA-T, indicating that this enzyme is also involved in the CNS synthesis of  $\beta$ -alanine [174, 180, 181].

Enzyme abnormalities of the DPD and DHP enzymes of the pyridine metabolic pathway cause serious neurological disorders, including epilepsy. These deficiencies in the key metabolic enzymes suggest the important regulatory roles that  $\beta$ -alanine has on

the CNS [177]. In an individual with a DPD deficiency, carnosine is metabolized in attempts to maintain  $\beta$ -alanine homeostasis, especially in the CNS [183]. However, despite these homeostatic adjustments,  $\beta$ -alanine concentrations are still 2-3 times lower than in individuals with no DPD deficiency [183]. Abnormalities in the BAKAT and BAPAT aminotransferases cause an accumulation of  $\beta$ -alanine diffusely throughout the body tissues since it cannot be metabolized to malonic acid semialdehyde correctly [177]. These altered concentration levels of  $\beta$ -alanine in the body are relevant because patients that display enzyme defects in DPD, DHP, BAKAT or BAPAT have been shown to have cerebral dysfunction [177].

### **6.2.2 $\beta$ -Alanine Transport**

$\beta$ -Alanine is distributed throughout blood plasma, muscle tissue and the CNS [184-200]. Since it is both a metabolic precursor and product, regulation of this  $\beta$ -amino acid is crucial to maintaining correct physiological concentrations. Various  $\beta$ -alanine transport systems have been identified in the human placenta, kidney, liver, brain and skeletal muscle. However, currently it is not known whether there is a single sodium dependent  $\beta$ -amino acid transport system or multiple ones. Available human transport data indicate that even if multiple transporters are involved, they have similar properties and mechanisms of action [201].

In the renal and intestinal systems, transport of  $\beta$ -alanine across the brush-border membrane is dependent on both sodium and chloride ions [202-206]. One chloride ion and multiple sodium ions are required for the transport of  $\beta$ -alanine across the membrane, and a net transfer of positive charges occurs based on stoichiometry. This transporter is

inhibited by taurine, hypotaurine, and  $\gamma$ -aminoisobutyric acid, which may also use this  $\beta$ -alanine transporter (as well as their own unique transporter) to traverse the membrane; however, this shuttle is unaffected by other amino acids [192, 201].  $\beta$ -Alanine transport is symmetric: when anions are present in the extracellular space,  $\beta$ -alanine is taken up into the cells; when anions are present in the intracellular space,  $\beta$ -alanine is effluxed out of the cell [207]. Although different anions (bromide, thiocyanate, nitrate, iodide and fluoride) have been used to test transport capabilities of the  $\beta$ -alanine shuttle, chloride has been shown to be the most effective [208].

In the kidney the epithelial surface of the renal proximal tube is responsible for maintaining  $\beta$ -alanine homeostasis. During dietary reduction of  $\beta$ -alanine, the proximal tubule increases absorption of this  $\beta$ -amino acid, and when  $\beta$ -alanine is in excess it allows an increase in  $\beta$ -alanine excretion [188, 209]. The uptake of  $\beta$ -alanine by the sodium dependent transporter in the proximal tubule is drastically reduced by the presence of taurine (a sulfur containing  $\beta$ -amino acid), which competes for this same transport system. When other amino acids are applied, they also compete with  $\beta$ -alanine but with a lower affinity than taurine [191].

In the gastrointestinal system, transport of  $\beta$ -alanine across the epithelial cell layer is not only dependent on sodium and chloride, but also on pH. When cells were acidified to pH = 6.0, the absorption and accumulation of  $\beta$ -alanine across the brush-border membrane was increased. When sodium-free conditions were used while maintaining pH = 6, there was still significant absorption of  $\beta$ -alanine. When the pH of the membrane environment was increased to 7.5, the absorption of  $\beta$ -alanine in a sodium-free environment did not occur. Based on these data, a proton dependent, but sodium-



independent,  $\beta$ -amino acid transporter has been identified in the acidic regions of the intestinal tract [189, 210].

Skeletal muscle is dependent on both sodium and chloride ions for the transport of  $\beta$ -alanine. One chloride ion and two sodium ions are required for the transport of one  $\beta$ -alanine molecule. During cellular differentiation of muscle tissue, there is no apparent change in the affinity for  $\beta$ -alanine between myoblasts and myotubes [201]. Kinetic data for the transport of  $\beta$ -alanine by muscle cells are comparable to the data obtained from other systems, like the brush-boarder membranes of the intestinal and renal system. Like the previous systems,  $\beta$ -alanine transport is highly specific and is highly dependent on the chloride anion compared to the other anions tested [201].

The uptake of  $\beta$ -alanine in murine brain slices and synaptosomes is sodium-dependent and similar to the uptake of hypotaurine, taurine, and GABA [211-217]. Two sodium ions are required for the transport of one  $\beta$ -alanine molecule; sodium ions act as allosteric effectors for the transport of the  $\beta$ -amino acid. For the transport of GABA and hypotaurine, two sodium ions are also required. For taurine, a minimum of three sodium ions are needed for transport in brain slices and synaptosomes [211-214, 218-220]. Taurine has no effect on the transport and uptake of  $\beta$ -alanine, indicating that these amino acids are not transported exclusively on the same carrier system. Murine brain cDNA has been identified and a taurine/  $\beta$ -alanine transporter has been cloned [221]. Based on the results of Kontro [222],  $\beta$ -alanine demonstrates transport mechanisms that are characteristic for those of a neurotransmitter [222].

### 6.2.3 $\beta$ -Alanine Transport In The CNS

Within the CNS there are several important transporters that  $\beta$ -alanine utilizes and influences. GABA transporters (GAT) are distributed throughout the CNS and are used to transport a variety of different molecules [223]. GABA transporters are expressed in both brain (GAT-1 and GAT-4) and peripheral tissues (GAT-2 and GAT-3). GAT-1 is found in both neural and glial cells. It transports GABA, but is inhibited by nipecotic acid (a  $\beta$ -alanine derivative) [224]. Both GAT-3 and GAT-4 are able to transport  $\beta$ -alanine with high affinity. GAT-3 is also responsible for the transport of GABA, subsequently inhibiting the transport of  $\beta$ -alanine [224, 225]. The GAT-3 transporter is localized in the cellular elements of both glia and the meninges, and may play a role during CNS development and maturation [9, 12, 226]. Like GAT-1, GAT-4 is concentrated in the CNS, more specifically in the brainstem as compared to the cerebellum and cerebral cortex. It has a high affinity for both GABA and  $\beta$ -alanine, suggesting a role in maintaining specific CNS levels of these two endogenous substances [224, 227]. Since  $\beta$ -alanine is transported by GAT-3 and GAT-4 at high rates, the transport of GABA is controlled by the presence of  $\beta$ -alanine in the CNS. GAT-2 transports  $\beta$ -alanine, and  $\beta$ -alanine inhibits GABA uptake by GAT-2 [12, 226]. GAT-2 is located in both brain and peripheral nervous tissue, and its location changes during development. It has the ability to regulate GABA and  $\beta$ -alanine concentrations in the cerebrospinal fluid and is insensitive to nipecotic acid [226].

The GAT proteins are not the only known routes for the transport of  $\beta$ -alanine in the CNS. Taurine transporters have also been identified and are distinguishable from GAT-3 and GAT-4. The uptake of  $\beta$ -alanine by both GAT-3 and GAT-4 is inhibited by

GABA, but the taurine transporter is not influenced by GABA concentrations. The uptake of  $\beta$ -alanine by the taurine transporter is inhibited by low concentrations of taurine, but high concentrations of taurine are a necessity to inhibit  $\beta$ -alanine transport by GAT-3 and GAT-4 [224].

Studies with isolated rat brain have shown that  $\beta$ -alanine can also be transported in membrane vesicles. Using an artificially generated ion gradient,  $\beta$ -alanine uptake is dependent on the concentration of both  $\text{Na}^+$  and  $\text{Cl}^-$  ions [228]. When these gradients are manipulated, the amount of  $\beta$ -alanine that is transported into and out of cells changes. Using a  $\text{Na}^+$  gradient, more  $\beta$ -alanine is present outside the cells; when a  $\text{Cl}^-$  gradient is imposed, more  $\beta$ -alanine is present inside the cells.  $\beta$ -Alanine uptake into membrane vesicles is inhibited by the presence of GABA [228].

#### **6.2.4 $\beta$ -Alanine Receptors**

Multiple CNS receptors have been shown to respond to endogenous  $\beta$ -alanine. This is not surprising given that  $\beta$ -alanine is structurally intermediate between  $\alpha$  and  $\gamma$  amino acids.

The two glycine receptors in the CNS are the strychnine-sensitive glycine receptor (primarily located in the brainstem and spinal cord) and the strychnine-insensitive glycine subsite on the NMDA receptor (located throughout the brain) [1, 229-232]. Glycine shows inhibitory effects at the strychnine-sensitive site and excitatory effects at the strychnine-insensitive site. Glycine binding to the strychnine-sensitive site, produces an inward conductance of chloride ions across the neuronal membrane [229, 233, 234]. Amino acids like  $\beta$ -alanine and taurine ( $K_d$  values 5-20  $\mu\text{M}$ ) have the ability

to bind to the strychnine-sensitive glycine receptor and act in an inhibitory fashion [233, 235, 236]. The order for agonist potency at the glycine receptor is glycine >  $\beta$ -alanine > taurine [225, 233, 237]. At active concentrations,  $\beta$ -alanine can behave as a full agonist for the glycine receptor by inducing currents with identical amplitude to glycine. Taurine, however, is not able to evoke the same amplitude as glycine and is considered a partial agonist at the glycine receptor [237, 238]. Since  $\beta$ -alanine activates the strychnine-sensitive glycine receptor it helps to control neuronal excitation [239].

$\beta$ -Alanine has also shown the ability to bind to, and influence the strychnine-insensitive glycine subsite on the NMDA receptor [240]. Pullan and Powel [241] found that  $\beta$ -alanine was recognized by both the strychnine-sensitive and strychnine-insensitive glycine receptors.  $\beta$ -Alanine was able to displace [3H]glycine binding to the NMDA receptor in models using hippocampal and cortical synaptic membranes [241]. Ogita *et al.* [242] examined the ability of specific amino acids structurally related to glycine and glycine containing peptides to inhibit glycine binding to the NMDA receptor. They found that  $\beta$ -alanine had the ability to bind to the NMDA receptor thereby inhibiting any further binding of glycine [242].

The principal inhibitory neurotransmitter is  $\gamma$ -aminobutyric acid (GABA). GABA has several receptors (GABA-A, GABA-B, GABA-C) distributed in varying locations. Both the GABA-A and GABA-B receptors are located in the CNS while the GABA-C receptor is found primarily in the retina [243, 244]. GABA-A receptors are fast acting and hyperpolarize the neuron by increasing the inward flow of chloride anions [245]. GABA-B receptors are slow acting as they decrease calcium entry into the neuron by increasing potassium conductance. In addition to being activated by GABA, the GABA-

A receptor is also activated by  $\beta$ -alanine [225, 238, 246] . The amplitude of the  $\beta$ -alanine response in the cerebellum and brainstem is similar to GABA, suggesting that  $\beta$ -alanine can change the membrane potential of neurons in the CNS when released and applied to synaptic receptors [247-251]. Additional research has focused on  $\beta$ -alanine as a neuromodulator in the visual system [243, 252, 253].  $\beta$ -Alanine is released in the optic nerve in a calcium-dependent manner, and when calcium-free conditions are applied  $\beta$ -alanine release is suppressed [243, 254]. Within the visual system  $\beta$ -alanine acts as an agonist at the GABA-C receptor, increasing membrane sodium conductance [255].

$\beta$ -Alanine has important effects not only in the CNS but also on the spinal cord dorsal root ganglia.  $\beta$ -Alanine influences the final step in the ventral root-dorsal root potential as sensory information is relayed from the periphery to the CNS [256]. There are three distinct neutral amino acid receptors in the primary afferent terminals and optimal activity is obtained when the amino acid carboxyl and amino termini are separated by a two to three carbon chain length, as in GABA and  $\beta$ -alanine [257]. The receptors identified include a GABA-like receptor, a glycine-like receptor and a  $\beta$ -alanine/taurine receptor. These distinct receptors were demonstrated by analyzing the effects of the convulsants (e.g. picrotoxin, bicuculline and strychnine) on spinal cord receptors [257].

### **6.2.5 $\beta$ -Alanine: Chemical Neuroanatomy**

$\beta$ -Alanine is widely distributed throughout the brain [173, 258-264]. Average concentrations within the brain have been found to be between 0.03-0.08 mM [265-267]. Examination of  $\beta$ -alanine concentration in rat brain shows that  $\beta$ -alanine has regional

differences [187]. Midbrain has the highest concentration (0.108  $\mu\text{mol/g}$  frozen weight); the cortex has just over half this value (0.065  $\mu\text{mol/g}$ ), while the cerebellum contains the lowest concentration (0.039  $\mu\text{mol/g}$ ).

Autoradiography studies have found  $\beta$ -alanine is localized in both neurons and glia [254, 268-271]. Hosli and Hosli [268], found that there was a greater proportion of labelled neurons in the brainstem than the spinal cord and that [ $^3\text{H}$ ] $\beta$ -alanine accumulation in the cerebellum was almost entirely in glial cells; this is consistent with available biochemical data [173]. In the retina, both glial and neuronal localization of  $\beta$ -alanine has been observed, and the total radioactivity is higher than found in other brain regions [254, 269, 270, 272]. Radioactivity appears in the inner nuclear layer, and is mainly localized in selected amacrine cells as well as in the inner plexiform layer [254, 272]. Some ganglion cells were moderately radioactive. However, this may have been due to a general, low-affinity amino acid uptake. There was also slight, if any, radioactivity in layers outside of the inner nuclear layer. This distribution is conserved in cats, rats, guinea pigs, humans and monkeys, and these results are similar for those found with [ $^3\text{H}$ ]GABA [269].

It has been shown that  $\beta$ -alanine is localized at synaptic regions of the inner and outer mouse retina (Figure 26). Intense staining was noted throughout the inner plexiform layer where bipolar and ganglion cells make synaptic contact with one another and with inhibitory interneurons called amacrine cells. Intense staining was also noted around cell bodies within the ganglion cell layer. Modest punctate staining was also noted in the outer plexiform layer of the retina, where photoreceptors make reciprocal synaptic contact with inhibitory horizontal cells and send output via bipolar cells. Such

patterns of staining were consistent with a role for  $\beta$ -alanine as a retinal neurotransmitter.

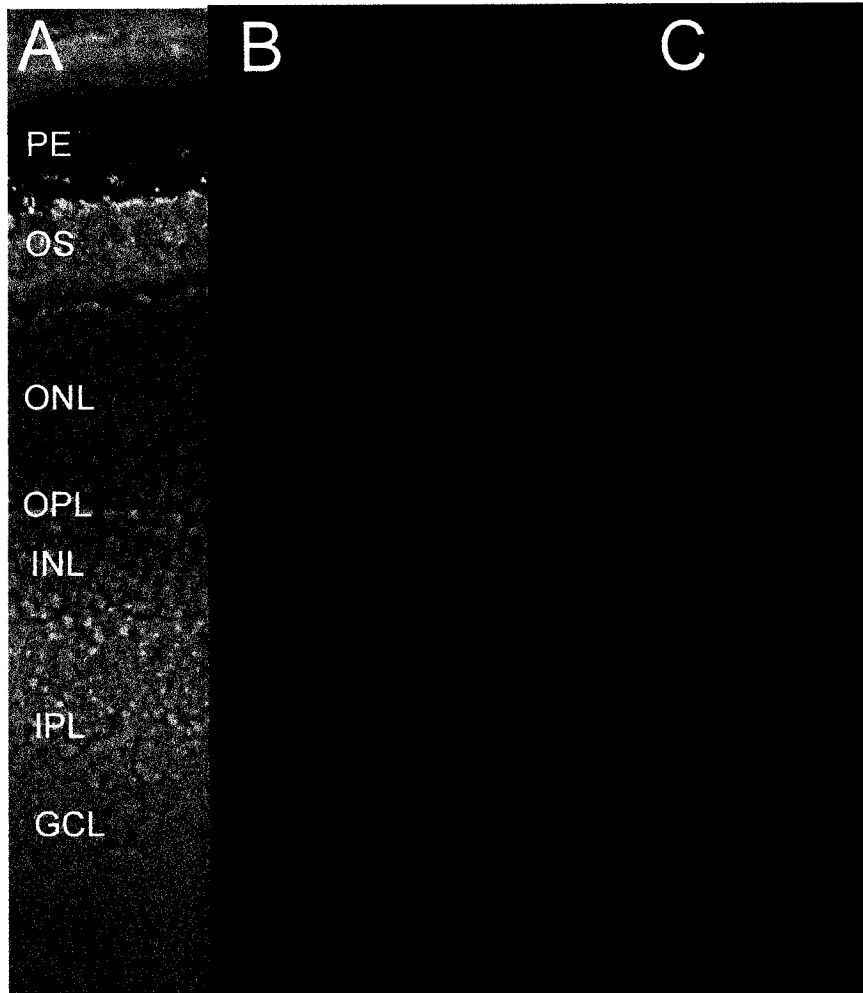


**Figure 26.** Immunohistochemical analysis of  $\beta$ -alanine localization in mouse retina. **A.** Cresyl violet-stained image of a 14  $\mu$ m thick retinal section showing the synaptic and cell body layers of the retina. GCL – ganglion cell layer; IPL – inner plexiform layer; INL – inner nuclear layer; OPL – outer plexiform layer; ONL – outer nuclear layer; OS – outer segments; PE – pigment epithelium. **B.** Laser scanning confocal microscope (LSCM) image of a 14  $\mu$ m retinal cross-section stained with an antibody against  $\beta$ -alanine. Regions of intense staining are seen throughout the two synaptic layers of the retina (IPL and OPL), as well as around ganglion cell bodies (GCL). **C.** Control staining with secondary antibody only shows staining of ellipsoid region of photoreceptors between the ONL and the OS, as well as modest staining of PE and OPL (Staining methods available in Appendix A).

These data provide evidence for the existence of free  $\beta$ -alanine in brain. However,  $\beta$ -alanine also exists as a component of other neurochemicals, including carnosine and pantothenic acid.

#### **6.2.6 $\beta$ -Alanine In Carnosine**

The largest concentration of  $\beta$ -alanine in the body is located as part of the dipeptide carnosine, which is formed in skeletal muscle where its main function is to activate the myosin enzyme ATPase [273] (Figure 27). Carnosine is synthesized from  $\beta$ -alanine and L-histidine in an ATP-dependent reaction using the enzyme carnosine synthase (CS, 6.3.2.11) [274-276]. The cofactor for carnosine synthase is zinc, and when elevated levels of carnosine occur, it is frequently associated with a zinc deficiency. When there is a deficiency of carnosine synthase, the body is unable to convert carnosine back into L-histidine and  $\beta$ -alanine. This trait has been associated with neurologic deficits [277, 278]. When carnosine levels are elevated in the plasma and urine, mental retardation can occur [279]. Carnosine modulates the immune response by increasing the release of interleukin-1 beta from neutrophils, acting to suppress neutrophil apoptosis [280]. Another important physiological role of carnosine is its involvement in the metabolism of calcium by inhibiting calcium uptake by the mitochondria. This response is due to its ability to chelate divalent cations including calcium and nickel [281]. Carnosine can also form a complex with  $Zn^{2+}$  thereby protecting the gastric system through an antioxidant mechanism [282]. With this ability to complex cations, carnosine has been shown to prevent neurotoxicity that is caused by accumulation of zinc and copper in the CNS, making carnosine an endogenous neuroprotective agent [283].



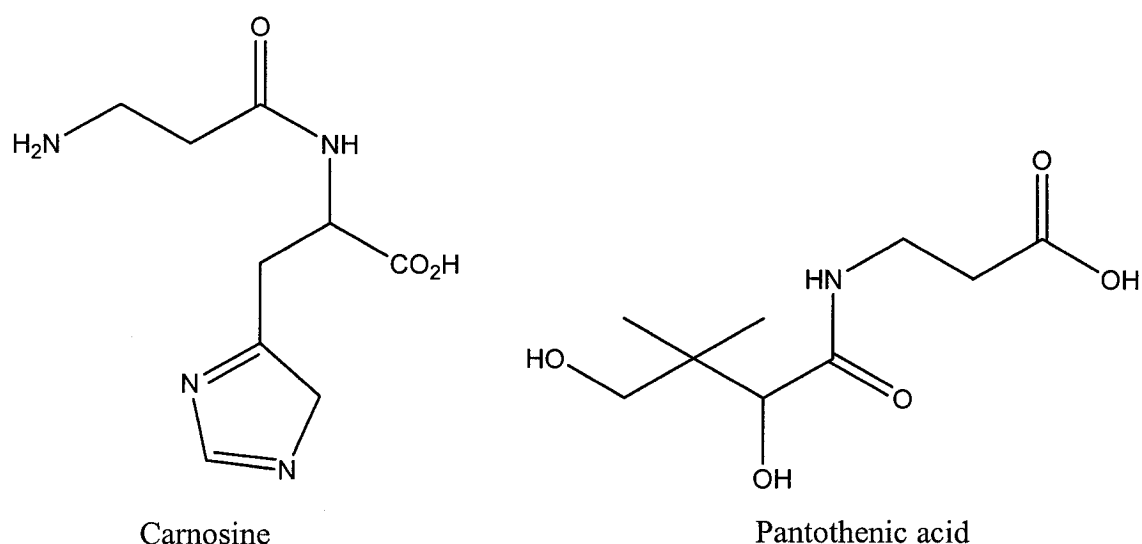


**Figure 27.** Carnosine and pantothenic acid chemical structure.

Studies with histidine-free diets have been pursued to monitor the effects of histidine deprivation of carnosine levels [284]. Urinary excretion of  $\beta$ -alanine increased when histidine was provided in the diet and was most likely a product of carnosine metabolism. Other studies on thoroughbred horses have noted that carnosine biosynthesis is influenced by the concentration of endogenous  $\beta$ -alanine. When the levels of  $\beta$ -alanine are increased through dietary supplementation, carnosine biosynthesis is increased, and when  $\beta$ -alanine levels are lowered, there is a reduction in the amount of carnosine that is produced [190]. When  $\beta$ -alanine concentrations are elevated in the diet there is an adaptive increase in the amount of  $\beta$ -alanine that is transported across the gastrointestinal tract [190].

### 6.2.7 $\beta$ -Alanine In Pantothenic Acid

Pantothenic acid is a water soluble B vitamin, synthesized by plants and microorganisms. It is an important dietary supplement for humans (Figure 27). Pantothenic acid is produced in an ATP-dependent condensation of  $\beta$ -alanine and (R)-pantoate. Its main metabolic role in the body is its incorporation into the coenzyme A molecule. Coenzyme A is an acyl carrier protein (ACP) and is involved in the  $\beta$ -oxidation of fatty acids, the citric acid cycle, glyceride synthesis, and pyruvate oxidation.

### 6.2.8 $\beta$ -Alanine Inactivation And Breakdown

The two primary methods of  $\beta$ -alanine inactivation are enzymatic degradation and reuptake via neurons or glia. Though  $\beta$ -alanine is nearly as good as GABA as a substrate for GABA transaminase it does not appear to be routinely metabolized via this route in the brain [254, 285, 286].

There is, however, ample evidence, for both low- and high-affinity  $\beta$ -alanine uptake mechanisms. Studies by Schon *et al.* [286] show that  $\beta$ -alanine uptake by a high-affinity sodium-dependent process does occur in the sensory ganglia and cerebral cortex, and GABA is a potent inhibitor of  $\beta$ -alanine uptake, and vice versa. Cummins *et al.* [287] found that in astrocytes, there is no inhibition of  $\beta$ -alanine uptake by GABA. Both the accumulation of  $\beta$ -alanine and inhibition of GABA uptake, however, were only by the glial uptake system and not by neurons. Since  $\beta$ -alanine did not accumulate in neurons in these areas, its uptake may be a consequence of its similarity to GABA versus an actual use as a neurotransmitter in these areas [254, 288]. Though there was evidence of high-affinity uptake for  $\beta$ -alanine, it was not found to influence the uptake of GABA in rat

CNS tissue [289], and only a moderate influence was noted on glycine uptake in either spinal cord or cerebral cortex [290]. In guinea pigs, it was reported that  $\beta$ -alanine only had a moderate influence on the uptake of GABA by cerebral cortex slices [291]. There is also evidence in fish, chicken and rat that  $\beta$ -alanine may use both GABA and glycine transporter systems and that this transport is ATP-dependent [292].

Studies in the retina found that  $\beta$ -alanine is taken up and retained by specific neurons in a manner similar to the uptake and retention of glycine and GABA [254]. For metabolism in retina,  $\beta$ -alanine uses the same transport system as GABA, and to a much lesser extent that of glycine [269, 288, 293]. Studies using different, simple, amino acids (in order of increasing carbon chain length: glycine,  $\beta$ -alanine, GABA,  $\delta$ -aminovaleric acid) found that certain amacrine cells selectively accumulate simple-amino acids and that retinal analyses of GABA,  $\beta$ -alanine,  $\delta$ -aminovaleric acid, and  $\epsilon$ -aminocaproic acid are virtually indistinguishable from each other [270]. The longer chain simple-amino acids ( $\delta$ -aminovaleric acid and  $\epsilon$ -aminocaproic acid) have no demonstrable inhibitory effects. Therefore, it is probable that the uptake mechanism is sensitive to the amino acid structure, and these molecules are being taken up because of their similarity to the uptake mechanism's regular substrate. The uptake mechanism is also sensitive to the carbon chain length, with GABA having the highest tissue-medium ratios, and  $\beta$ -alanine and the longer simple-amino acids having smaller ratios. Therefore, within the retina,  $\beta$ -alanine uptake into cells is primarily due to an affinity with the GABA-uptake mechanism. In conclusion,  $\beta$ -alanine has a complex, but surprisingly well understood neurochemistry. Ample data provide insights into the synthesis, transport, binding and breakdown of this  $\beta$ -amino acid.

### **6.3 Is $\beta$ -Alanine A Neurotransmitter?**

There are multiple important criteria that must be satisfied for an endogenous chemical substance to be designated as a neurotransmitter [173, 294]. These criteria were established by Werman [294] and have been used for the identification and verification of several important neurotransmitters including acetylcholine, GABA and glycine.

These criteria are as follows:

- (1) Presence of the transmitter molecule within neural tissue
- (2) Capacity for storage of the transmitter molecule within neural tissue
- (3) Specific release mechanism and specific site of action
- (4) Presence of a synthesizing enzyme(s)
- (5) Presence of metabolic precursors
- (6) Presence of inactivating enzymes
- (7) Identical action between endogenous and exogenous application
- (8) Pharmacological identity with other agents

#### **6.3.1 Presence And Storage Of The Transmitter Molecule In Neural Tissue**

For a chemical substance to be active in the CNS it must first be available either through synthesis or by transport across the blood-brain barrier (BBB). As discussed in Part A,  $\beta$ -alanine is synthesized via three main biosynthetic pathways: a product of L-aspartate decarboxylation; a by-product of the interchangeable reaction of pyruvate to L-alanine; and a product of deamination and carboxylation of the pyrimidine uracil (Figure 28).

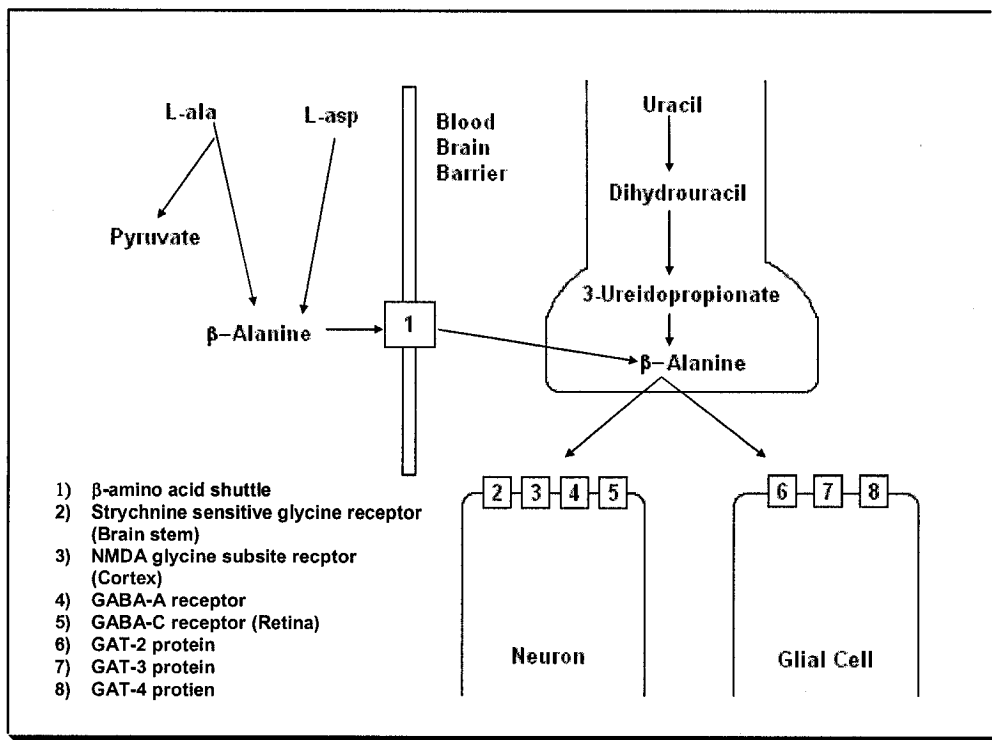


**Figure 28.** The receptors, proteins, and distribution of β-alanine in the CNS

In addition to being synthesized within the CNS, β-alanine is also transported into the brain. β-Alanine is the only naturally occurring β-amino acid to be effectively transported across the BBB by a high affinity active transporter [227, 291, 295]. β-Alanine is carried across the BBB into the CNS via a taurine-sensitive β-amino acid transporter in a  $\text{Na}^+$  and  $\text{Cl}^-$  dependent manner [185, 197, 296]. This transporter is highly selective for β-amino acids because neither L-glutamic acid (transported by the anionic amino acid transporter) nor L-phenylalanine, (transported by the large neutral amino acid transporter), affects the movement of β-alanine across the BBB via this transporter [185, 292, 297, 298]. β-Alanine may also cross the BBB by passive diffusion [287, 299].

Due to both biosynthesis and transport into the brain, β-alanine is present in the CNS in a sufficient amount to have a neurotransmitter role. In fact, it is stored in an equal

or greater concentration compared to other important neurotransmitters including acetylcholine, dopamine and norepinephrine [173]. In the CNS,  $\beta$ -alanine acts as a depressant or inhibitor of neuronal activity with a rapid onset and a potency comparable to that of the neurotransmitter GABA [300].  $\beta$ -Alanine concentration has already been shown to be regionally variable, being highest in the midbrain with the concentration in the cortex and cerebellum being lower [187]. This concentration variation between locations of the CNS is similar to variable concentrations for GABA [226]. This is a significant observation since it establishes regional distribution of  $\beta$ -alanine in the CNS, which is an important attribute of a neurotransmitter substance [187].

### **6.3.2 Specific Release Mechanism And Specific Receptor (Site Of Action)**

Since  $\beta$ -Alanine is a structural analogue between two major inhibitory neurotransmitters (GABA and glycine), it is not surprising that  $\beta$ -alanine interacts with multiple receptors.  $\beta$ -Alanine has five recognized receptor sites: glycine co-agonist site on the NMDA complex (strychnine-insensitive); the glycine receptor site (strychnine-sensitive); the GABA-A receptor; GABA-C (GABA- $\rho$ ) receptor; and the GAT protein-mediated glial GABA uptake [186, 301]. Numerous studies demonstrate the ability of  $\beta$ -alanine to bind to the GABA-A, and the strychnine-insensitive site or glycine site on the NMDA receptor [302-304]. Based on radioligand binding assays,  $\beta$ -alanine is more potent in binding to the benzodiazepine and GABA-A receptor than taurine [186].  $\beta$ -Alanine is also an effective agonist at the glycine receptor, inhibiting neuronal firing through increased chloride conductance [233, 268, 305, 306]. Although research has indisputably shown the capability of  $\beta$ -alanine to bind to known CNS receptors, it has

been concluded that  $\beta$ -alanine may also possess its own distinctive receptor in the CNS [262]. Parker *et al.* [307], using messenger RNA from chick and rat brains, found that this mRNA induced greater activation responses to low concentrations of  $\beta$ -alanine compared to those obtained from high concentrations of GABA and glycine. These results indicate that the activation response did not arise from either the GABA or glycine receptors. Based on their findings they concluded that a distinct mRNA codes for the  $\beta$ -alanine CNS receptor [307].

### **6.3.3 Presence Of Precursors, Synthesizing Enzymes, And Inactivating Enzymes**

For an endogenous molecule to be further considered as a neurotransmitter, it has to have biological precursors and enzymes available for its synthesis and inactivation [308]. Multiple biosynthetic precursors for  $\beta$ -alanine have been identified and include malonate semialdehyde, aspartate, and uracil [180, 309]. In pig brain, liver and kidney, malonate semialdehyde formed from  $\beta$ -hydroxypropionate is converted to  $\beta$ -alanine, making it available in the CNS either with or without transport across the BBB [178]. Moreover,  $\beta$ -alanine is a better substrate for GABA-transaminase (GABA-T) than GABA, allowing for it to be metabolically broken down to yield malonic semi-aldehyde which is converted to carbon dioxide and acetate in the liver [174, 181, 258, 285, 310]. GABA-T is a reversible enzyme with reactivity towards  $\beta$ -alanine and malonate semialdehyde, through a reverse transamination of malonate semialdehyde.  $\beta$ -Alanine accumulates rapidly in the brain and can quickly be transported and metabolized [311].

$\beta$ -Alanine levels are carefully regulated and controlled.  $\beta$ -Alanine synthase involved in the conversion of uracil to  $\beta$ -alanine is present in brain. This enzyme is

allosterically controlled by the substrate and product and is the irreversible step in the uracil metabolic pathway [312]. The CNS also has a high concentration of aspartate (between 2-4  $\mu\text{mol/g}$  of tissue) which has been shown to also act as a precursor for  $\beta$ -alanine [313, 314], through the decarboxylation of aspartate.

#### **6.3.4 Identical Action, Pharmacological Identity**

When exogenous  $\beta$ -alanine is applied to synaptic preparations, it mimics the action of endogenous  $\beta$ -alanine through an inhibitory action by hyperpolarizing neurons [290, 315]. Pharmacological identity is defined as the ability of other agents to interact at the post-synaptic level in a similar fashion to the naturally occurring neurotransmitter.  $\beta$ -Alanine exerts pharmacological actions on both GABAergic and glutamatergic processes. By binding at the glycine co-agonist site on the NMDA receptor,  $\beta$ -alanine acts to decrease glutamatergic excitation, while increasing GABAergic inhibition by binding to the glial GABA uptake site [240, 242, 316]. It has also been shown that the depressant effects of  $\beta$ -alanine are antagonized by strychnine, picrotoxin and bicuculine in the CNS [257].

#### **6.3.5 $\beta$ -Alanine Is A Neurotransmitter**

Part A provided a comprehensive review of  $\beta$ -alanine neurochemistry. Part B demonstrated that these neurochemical data support the conclusion that  $\beta$ -alanine satisfies the eight selection criteria of Werman for being a small molecule neurotransmitter (Figure 28).



## **6.4 Implications Of $\beta$ -Alanine As A Neurotransmitter**

### **6.4.1 Exposure To $\beta$ -Alanine Or $\beta$ -Alanine Derivatives**

Part B data are compatible with  $\beta$ -alanine being a neurotransmitter – a molecule that influences information processing within the human brain. Moreover, it is a molecule that can be readily absorbed and transported into the CNS. Accordingly, human exposure to  $\beta$ -alanine, either deliberately or accidentally, through food additives, cosmetics or environmental contaminants, becomes a potentially relevant issue.

#### **6.4.1.1 Non-Pharmacologic Exposure To $\beta$ -Alanine Or $\beta$ -Alanine Derivatives**

**Oral Exposure:** It has been suggested that the anaerobic working capacity of tissues can be increased by ingesting either  $\beta$ -alanine, or a mixture of  $\beta$ -alanine and creatine [317]. By increasing the concentration of  $\beta$ -alanine in the body, the hope is to increase the synthesis of  $\beta$ -alanylhistidine dipeptides, subsequently increasing the accumulation of creatine in the body's tissues. Because of this supposition,  $\beta$ -alanine is sometimes included in multi-vitamin preparations, especially those targeted at consumers who wish to augment muscle bulk or strength. In addition to being an additive in so-called body-building dietary supplements,  $\beta$ -alanine is sometimes also used as a component of artificial sweeteners [318] and as a flavoring in alcoholic beverages and juices [319-321].

**Topical Exposure:** Since  $\beta$ -alanine is readily absorbed and distributed throughout the human body, an appreciation of topical exposure to  $\beta$ -alanine is also relevant. An examination of the patent literature reveals that topically applied  $\beta$ -alanine is present in many facets of daily life. Many skin creams marketed for the treatment of wrinkles and

aging contain  $\beta$ -alanine. When targeting the aging process via wrinkle reduction, one of the main goals is to use substances, like  $\beta$ -alanine, that are agonists for the chloride channel, especially in cutaneous tissue [322-324]. By interacting with these specific receptors,  $\beta$ -alanine causes “relaxation or slackening” of the skin, leading to visual reduction of fine lines. These treatments are either delivered topically or through a localized injection [325, 326].  $\beta$ -Alanine is also a component of some liquid cleansers suitable for use on skin.  $\beta$ -Alanine derivatives are a useful group of detergents since they are inexpensive to produce, have excellent foaming properties and yield little irritation [327-329]. These  $\beta$ -alanine detergents are frequently formulated as an amide type anionic carboxylate surfactant having either a N-lauryl- $\beta$ -alanine or N-myristoyl- $\beta$ -alanine form [327, 330, 331].

As a common chemical component of antiperspirants,  $\beta$ -alanine is one of the preferred amino acid buffers. Water soluble antiperspirants are frequently prepared as a combination of a basic aluminum-poly compound, a zirconium compound, and an organic buffer which includes the use of  $\beta$ -alanine [332, 333].  $\beta$ -Alanine is also a key component of certain hair dyes and shampoos. For use in hair dyes,  $\beta$ -alanine is a component of the vehicle polymer solution [334]. This polymer is used in sufficient amount to increase the “body and hold” of the hair [335]. As a component of hair shampoo,  $\beta$ -alanine is used to “revive” unwashed oily hair [336, 337].

**Indirect Exposure:** The  $\beta$ -alanine structure has also been used in the pulp and paper industry to provide novel resins and undercoatings in photo-lithographic plates. Paper resins are produced by reacting branched water soluble poly- $\beta$ -alanine with glyoxal to produce a resin, which gives paper strength when dry or wet [338, 339]. On

lithographic plates,  $\beta$ -alanine is used as a hydrophilic undercoating [340, 341]. Large quantities of these paper products end up in the environment through our waste stream.

#### **6.4.1.2 Pharmacologic Exposure To $\beta$ -Alanine Or $\beta$ -Alanine Derivatives**

*Central Nervous System Indications:* A number of neuroactive drug molecules incorporate the  $\beta$ -alanine moiety into their overall structure (see Figure 9). These include such diverse agents as etomidate, tiagabine, methylphenidate, clorazepate, cocaine and mefanamic acid. Etomidate functions via a  $\beta$ -alaninergic mechanism, exerting its general anaesthetic effects via interactions with the GABA-A receptor. Tiagabine is an anticonvulsant that also functions via a  $\beta$ -alaninergic mechanism by interacting with the glial GABA uptake transporter mechanism.

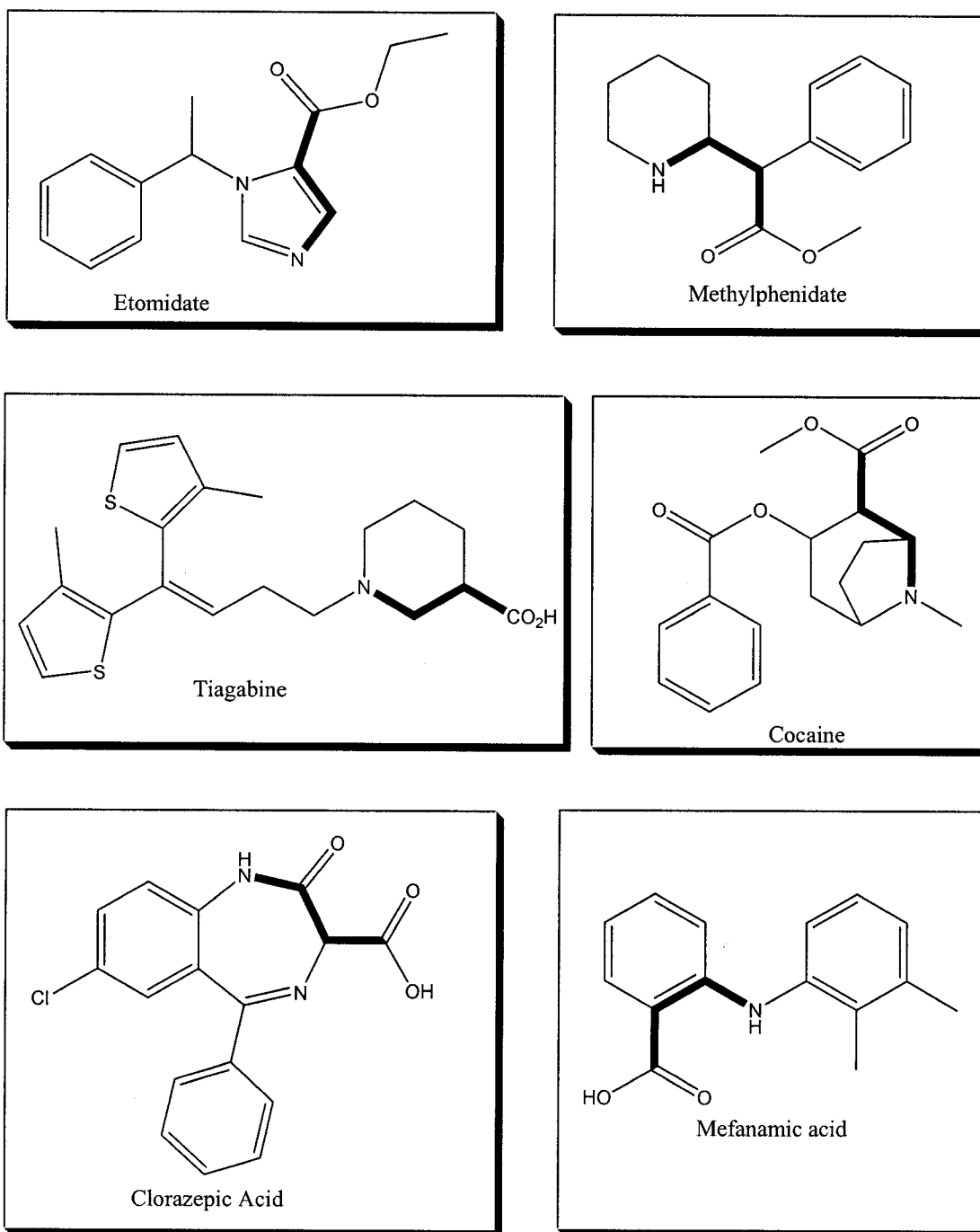


**Figure 29.** Current drugs that contain the  $\beta$ -alanine scaffold in their chemical structure.  $\beta$ -Alanine scaffold is the bolded portion of each molecule.

Clorazepate (clorazepic acid) is used for the management of both anxiety disorders and as an adjunctive therapy for the treatment of partial seizures. Clorazepate is a benzodiazepine and influences the CNS by binding to the benzodiazepine site on the GABA-A receptor.

Methylphenidate (Ritalin) is used as a CNS stimulant for the treatment of children suffering from attention-deficit disorders and for narcolepsy. This drug blocks the uptake of dopamine by both carrier proteins and transporters in the central adrenergic neurons. Cocaine is a compound that has local anaesthetic properties by reversible binding to an inactivating sodium channels and by binding to the dopamine, serotonin and norepinephrine transport proteins, preventing their uptake into the pre-synaptic neurons. It has also been shown that cocaine exerts indirect actions on other neuromodulatory systems like the GABAergic and glutamatergic systems. Mefenamic acid is a nonsteroidal anti-inflammatory drug (NSAID) that is used for the treatment of mild to moderate pain and rheumatoid arthritis. Mefenamic acid inhibits prostaglandin synthetase by binding to the COX-1 and COX-2 receptors.

***Non-Central Nervous System Indications:*** There are numerous drug therapies that contain  $\beta$ -alanine or one of its structural analogues to treat a variety of human disease conditions.

The  $\beta$ -alanine molecule has been proposed as a potential treatment for cancer, more specifically melanoma. Specific treatment compositions include  $\beta$ -alanine as the major chemical constituent (30 to 50% by weight) as well as ascorbic acid, nicotinic acid, ribose and deoxyribose [342].

Specific substituted  $\beta$ -alanine derivatives have been devised as cell adhesion inhibitors for treatment of asthma, allergies and other autoimmune, inflammatory diseases [343]. These  $\beta$ -alanine derivatives are antagonists of VLA-4, a leukocyte adhesion molecule of the beta 1 integrin family, thereby inhibiting the cell adhesion mediated process [343].

It has also been shown that amidinophenyl pyrrolidiny  $\beta$ -alanine urea analogues have pharmaceutical potential as antithrombotics to reduce blood coagulation and platelet activation [344]. Another pharmaceutically active  $\beta$ -alanine analogue, 3(R)-2-(piperidin-4-yl)ethyl-2-piperidone-1-acetyl-3(R)-methyl- $\beta$ -alanine, has been evaluated as an inhibitor of thromboxane formation [345].

CCK (cholecystokinin) antagonist pro-drugs (novel peptoid analogues of  $\alpha$ -substituted trp-phe derivatives) that contain  $\beta$ -alanine building blocks have been developed [346]. These CCK antagonist pro-drugs have been suggested as possible therapeutics for such diverse disorders as gastric hypersecretion, gastrin dependent tumors, obesity, psychosis, and opioid withdrawal [346].

#### **6.4.2 $\beta$ -Alanine Is Widely Distributed In Our Environment**

Thus,  $\beta$ -alanine exposure is widely distributed through both pharmacologic and non-pharmacologic routes of administration. Non-pharmacologically,  $\beta$ -alanine is a constituent of food additives, cosmetics, hair care products and through the environmental waste stream. Pharmacologically, it is used as a “nutritional supplement” and as a molecular component of both neurological and non-neurological drugs. Because of the ease of systemic absorption and biodistribution, this widespread environmental

availability of  $\beta$ -alanine, a neurotransmitter substance, could conceivably have implications.

## **6.5 $\beta$ -Alanine As A Neurotransmitter Conclusions**

$\beta$ -Alanine is structurally intermediate between  $\alpha$ -amino acids (glycine, glutamate) and  $\gamma$ -amino acids (GABA). As demonstrated in this review,  $\beta$ -alanine satisfies the prerequisite criteria for being a neurotransmitter:  $\beta$ -alanine occurs naturally in the CNS, is released by electrical stimulation, has binding sites, and inhibits neuronal excitability.  $\beta$ -Alanine has 5 recognized receptor sites: glycine co-agonist site on the NMDA complex (strychnine-insensitive); glycine receptor site (strychnine sensitive); GABA-A receptor; GABA-C receptor; and blockade of GAT protein-mediated glial GABA uptake. Multiple studies have verified the dual action of  $\beta$ -alanine on glutamatergic and GABA processes.  $\beta$ -Alanine binding has been identified throughout the hippocampus, limbic structures, and neocortex. Also, an active transport shuttle capable of transporting  $\beta$ -alanine and related analogues across the blood-brain barrier (BBB) has been identified.

Thus,  $\beta$ -alanine is a small molecule neurotransmitter and should join the ranks of the other amino acid neurotransmitters. The role of  $\beta$ -alanine in epilepsy, consciousness, stroke and other disorders requires greater clarification.  $\beta$ -Alanine as a molecular platform for rational drug design should likewise be considered. These realizations open the door for a more comprehensive exploitation and explanation of  $\beta$ -alanine's neurochemistry.

## **6.6 Dihydrouracils And $\beta$ -Alanine: Potential Anti-Epileptogenic Treatments**

Previous extensive research has been performed to determine a direction to take in the search for new neurological drugs to both treat and prevent the development of epilepsy after head trauma. It was found that  $\beta$ -alanine and its biochemical precursors (e.g. dihydrouracil) were unexplored territory that showed great potential. Research performed by DeFeudis and Martin del Rio found that  $\beta$ -alanine exerted depressant effects on the neurons in the mammalian CNS by acting as an inhibitory neurotransmitter that is released upon electrical stimulation. It exhibits both GABA-like inhibitory effects as well as having the affinity to bind at the glycine site on the NMDA receptor. By observation it can be noted that  $\beta$ -alanine is a structural hybrid between GABA and glycine hence it is not surprising that it shows inhibitory neural properties (Figure 22) [301].

$\beta$ -Alanine is one of the metabolites produced when dihydrouracil is broken down in the body via pyrimidine catabolism (Figure 25). Uracil and dihydrouracil are readily available in the body, and are formed when RNA is degraded, therefore they are considered to be pro-drugs since they are metabolized into other usable substrates [174]. It has been postulated that uracil and dihydrouracil are also natural depressants of brain activity and are involved in the mediation of sleep [179, 309, 347].

### **6.6.1 The BBB and Metabolites Of The Pyrimidine Pathway**

Although both dihydrouracil and  $\beta$ -alanine derivatives show the capacity to act as inhibitory transmitters of neural activity [348], they must also be able to cross the blood-brain barrier (BBB) in order to cause CNS pharmacological effects. In previously



conducted studies it has been found that neither GABA nor glycine could cross the BBB [314]. So treatments involving the elevation of GABA levels by providing GABA directly are not reasonable methods to be employed when attempting to control epilepsy.  $\beta$ -Alanine, when administered parenterally, suppresses seizures suggesting its capability to cross the BBB [187, 222, 296]. Several studies have suggested the presence of a transporter in the brain capillaries called the  $\beta$ -shuttle allows  $\beta$ -alanine and other  $\beta$ -amino acids to cross the BBB via high- affinity active transport [186, 292, 296, 349]. Dihydrouracil, the precursor for  $\beta$ -alanine, does not appear to have the ability to cross the BBB. Studies conducted where dihydrouracil was radioactively labelled with  $^{15}\text{N}$  found that the majority of it was excreted in the urine. However, as previously mentioned, since dihydrouracil is the primary precursor for  $\beta$ -alanine and other potential  $\beta$ -amino acids, structural alterations of dihydrouracil could potentially led to the development of an active pro-drug. Moreover, with the appropriate substituents, dihydrouracils might be modified to cross the BBB by passive diffusion or an active transport shuttle.

#### **6.6.2 CNS Receptors And Dihydrouracils**

$\beta$ -Amino acids and potentially the metabolites of the pyrimidine pathway could inhibit neurons by binding to multiple receptor sites in the CNS, therefore producing neural protective effects against the development of epilepsy [30]. Pyrimidine metabolic products should show their impact as anti-epileptogenic compounds in three main capacities. First, they could increase GABAergic inhibition by binding to the GABA<sub>A</sub> receptor producing inhibitory neurotransmitter effects [186]. These metabolic products could also be able to act as antagonist, blocking glutamatergic excitation through binding

to the glycine sub-site on the NMDA receptor [229-232]. Finally, they could bind to the glial GABA transporter, blocking GABA uptake. An ability to act as a GAT-2 and -3 inhibitor, could increase the lifetime of endogenous GABA in the synapse [224, 227]. It is these unique properties of dihydrouracil and  $\beta$ -alanine, metabolic products of the pyrimidine pathway, that allows them to act simultaneously to decrease neuronal hyperexcitability, which is important to their ability to act as anti-epileptogenic drugs.

Although the structure of the GABA site on the GABA receptor has not been resolved, experimental results support the notion of a large receptor site. While  $\beta$ -alanine is similar to both GABA and glycine, structurally it is intermediate between the two having a different carbon chain length and structural properties. GABA is a larger molecule than  $\beta$ -alanine, having a carbon chain of four in comparison to  $\beta$ -alanine whose carbon chain contains three and in contrast  $\beta$ -alanine has a longer carbon chain than glycine, which is composed of two carbons. These differences in length can lead to variability in both folding structure and three-dimensional shape, ultimately affecting how the molecules fit into their corresponding receptors. Based on previous research it has been noted that bulky substituents on the N<sup>1</sup> and N<sup>3</sup> positions of uracil and the  $\beta$  position of the  $\beta$ -amino acids correspond with anticonvulsant activity (Figure 30). When the group is an aryl ring or a bulky alkyl chain, the ability of the analogues to suppress seizure activity is increased [348, 350]. The concept of bulky substituents and their influence on neuronal activity is an important direction to address in the synthesis of dihydrouracil analogues, since it is an unexploited research area and would offer further insight into which receptors are targeted in the CNS.

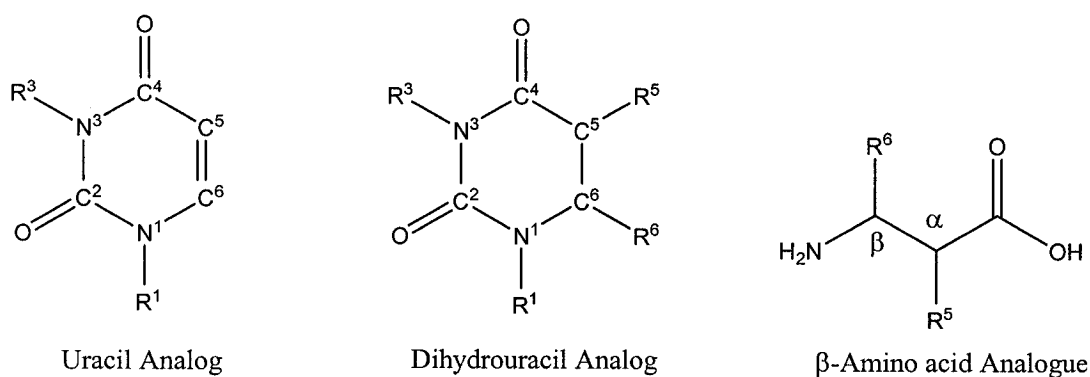


**Figure 30.** The uracil, dihydrouracil, and  $\beta$ -amino acid derivatives.

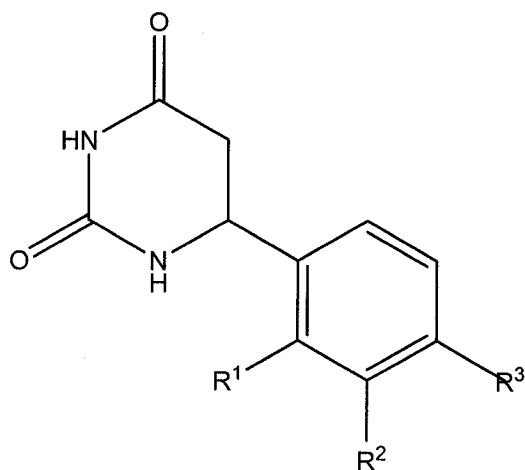
The ability of the metabolites of the pyrimidine pathway to suppress seizure activity may be due to the corresponding  $\beta$ -amino acid metabolite or due to the uracil or dihydrouracil intermediate [351]. Binding pockets that are accessible have the ability to accommodate molecules both larger and smaller than the endogenous ligands making them accessible to a wide range of derivatives. If the dihydrouracil analogues are able to bind to the GABA receptor, they offer advantages over the corresponding  $\beta$ -amino acids. Since they are rigid molecules, they would be less likely to bind with many different receptors in the body, reducing the potential of side effects.

Since dihydrouracil is a metabolic precursor for  $\beta$ -alanine it could be a lead compound for the delivery of various  $\beta$ -amino acids to the CNS. Specific enzymatic steps break down dihydrouracil and various intermediate products result that could cross the BBB and also exhibit neuronal suppression. By utilizing rational drug design to synthesize substituted dihydrouracil derivatives as a pro-drug approach and testing their biological activity in the available anti-ictogenic and anti-epileptogenic models, the ability of dihydrouracil to prevent both seizure activity and halt the underlying pathology of epilepsy development can be analyzed.

## 6.7 Dihydrouracil Analogues

A series of dihydrouracil compounds were rationally designed, synthesized and biologically tested to determine their activity and potential to act as new therapeutic agents. The primary goal of this project was to synthesize a series of dihydrouracils that are the metabolic precursors to  $\beta$ -amino acids (previously developed in our laboratory) that have already demonstrated anti-epileptogenic activity in animal testing models [348, 350, 352, 353]. Uracils have been used as a pro-drug approach, since they can be metabolized by the body into other active compounds such as  $\beta$ -alanine [348, 350]. The goal of this project was to eventually develop and synthesize a range of dihydrouracils such that a library of analogues was available to provide research into the connection between structure and biological activity as pertaining to epilepsy (Table 18). These analogues will be determined using a comprehensive diversity study based on previous uracil research, while accounting for important biological interactions of the compounds to prevent potential toxic/mutagenic effects [354].

**Table 18.** Representative dihydrouracil derivatives to be developed as anticonvulsants and anti-ictogenics, with a variety of substitutions in R<sup>1</sup>, R<sup>2</sup> and R<sup>3</sup> positions. The Y indicates, that Yes these molecules will be synthesized.

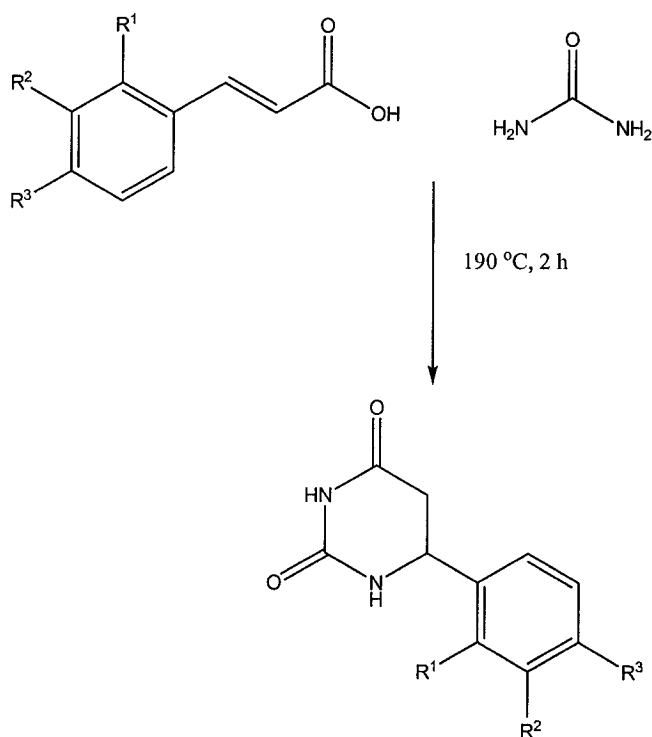


R <sup>1</sup>	R <sup>2</sup>	R <sup>3</sup>	Synthesized
CH <sub>3</sub>	H	H	Y
H	CH <sub>3</sub>	H	Y
H	H	CH <sub>3</sub>	Y
H	H	NO <sub>2</sub>	Y
H	H	OCH <sub>3</sub>	Y

The first series of dihydrouracil analogues to be synthesized will be a group of 6-aryl substituted dihydrouracil analogues. This direction was initially chosen based on the results from the  $\beta$ -substituted- $\beta$ -amino acids. When 6-aryl substituted dihydrouracil analogues are metabolized they produce  $\beta$ -substituted amino acids. In previous research it was found that aryl groups in the  $\beta$ -position of  $\beta$ -amino acids produced increased ability to both prevent the development of seizures and halt the biochemical process leading to the development of epilepsy.

### 6.7.1 6-Aryl Substituted Dihydrouracil Analogues: Route A

In the case of this research into the development of dihydrouracils for the treatment and prevention of epilepsy, synthetic routes which could potentially be useful in medicinal chemistry were examined. The first method that was explored synthetically for the synthesis of 6-aryl substituted dihydrouracil analogues involved the condensation of urea and the appropriate functionalized cinnamic acid (Scheme 18) [355].



**Scheme 18.** Synthetic scheme for the synthesis of 6-aryl-substituted dihydrouracil analogues using Route 1.

Although this scheme led to the synthesis of pure 6-aryl substituted dihydrouracil analogues, the yields were quite low, ranging from 8-11 %. The major impurities that

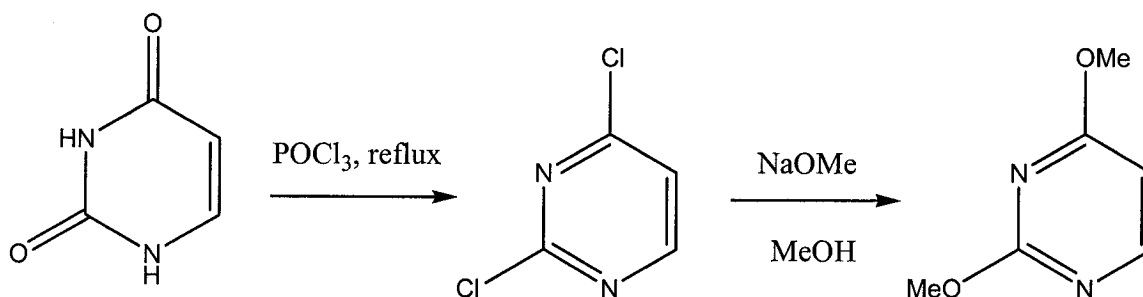
could be characterized were unreacted cinnamic acid and the uncyclized intermediate cinnamoyl urea. The reaction conditions like temperature and time was altered, but this led too no overall improvement in the final yields. Another attempt was to separate the cinnamoyl urea since it appeared on TLC to be the major product of the reaction. It was thought that upon separation, that pure cinnamoyl urea could be experimented with in order to ascertain condition that would promote cyclization.

By treating the cinnamoyl urea with sodium hydride, cyclization could be promoted by creating a better nitrogen nucleophile for attack on the  $\alpha$ ,  $\beta$  unsaturated system through a Michael addition mechanism. Crystallization using ethanol/water, 95% ethanol and THF were attempted to isolate and purify the cinnamoyl urea from the reaction mixture, but all were unsuccessful and a mixture of products still resulted. Column chromatography was used to separate the cinnamoyl urea, but complications with decomposition of the cinnamoyl urea on the column occurred, therefore the cinnamoyl urea could not be recovered successfully. Although it has not been synthetically attempted, treatment of the mixture containing the cinnamoyl urea with the NaH could promote formation of the cyclized product.

Upon examination of Route A, it was apparent that although this route produced the desired products, the yields were too low to make it a viable route for medicinal chemistry. For biological testing gram quantity amounts were required and this synthetic route made it difficult to even obtain 100 mg. Optimization of the scheme was unproductive and so a new route for the synthesis 6-aryl substituted dihydrouracil was researched.

### 6.7.2 6-Aryl Substituted Dihydrouracil Analogues: Route B

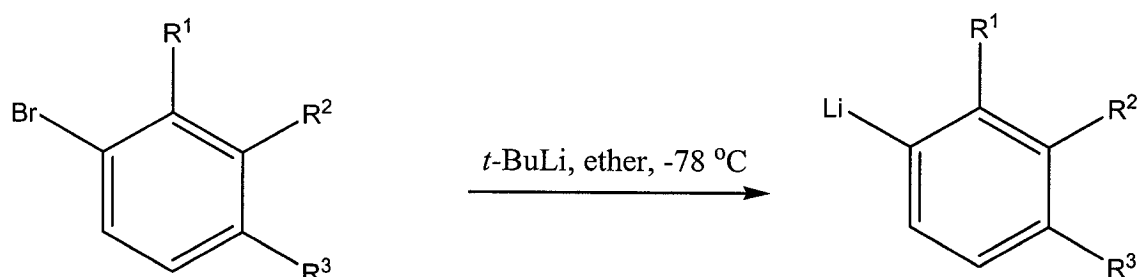
The new route that was developed was no longer dependent on the cyclization technique used in Route 1. This technique involved using an intermediate, 2,4-dimethoxypyrimidine (Scheme 19) [356]. Once the intermediate was synthesized it could then be treated with specific organolithium reagents and upon acidic work up the required 6-aryl substituted dihydrouracil analogues could be produced [357-359] (Schemes 19, 20, 21).



**Scheme 19.** The first two steps of synthetic Route 2 used for the synthesis of the 2,4-dimethoxypyrimidine intermediate.

Synthesis of 2,4-dichloropyrimidine was completed on both small and large scales, with yields of approximately 95%. The next step which formed the 2,4-dimethoxypyrimidine intermediate was also completed with yields of 90% or greater, making these initial steps synthetically useful to produce large amounts of the starting material so that a variety of 6-aryl substituted dihydrouracil analogues could be produced successfully.



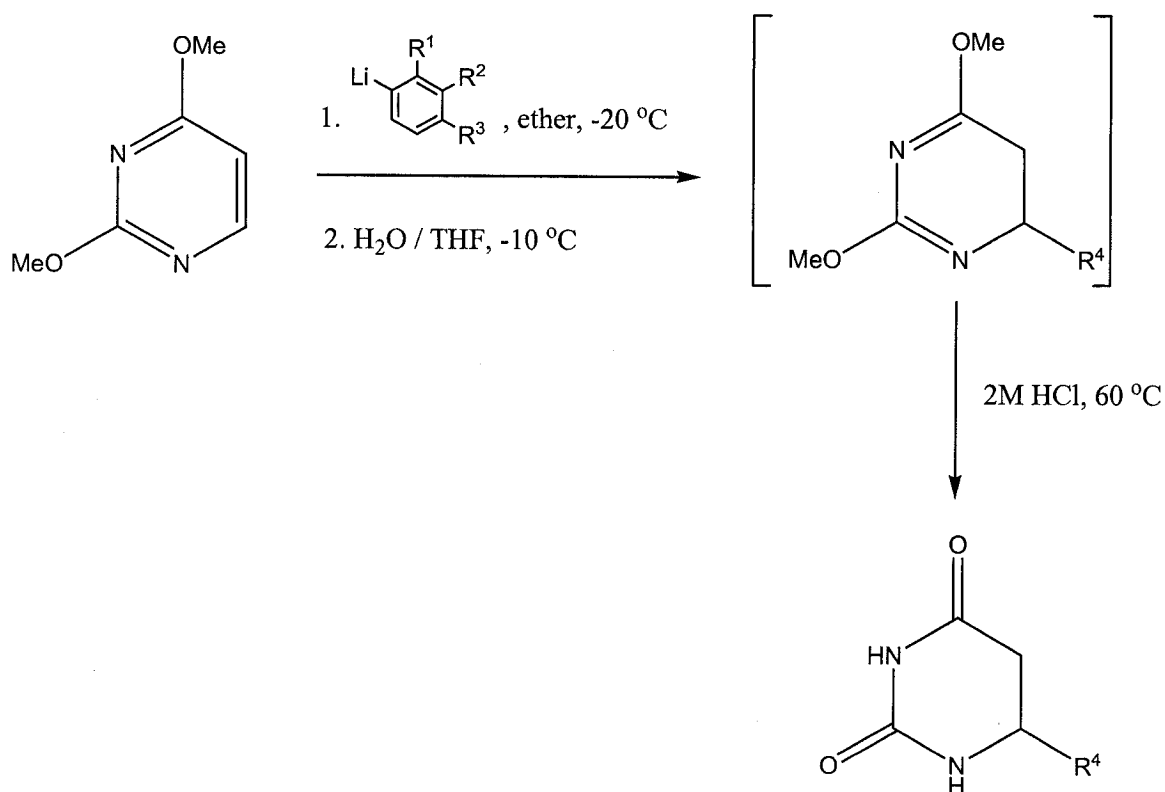


Brominated Compound	R <sup>1</sup>	R <sup>2</sup>	R <sup>3</sup>
2-bromotoluene	CH <sub>3</sub>	H	H
3-bromotoluene	H	CH <sub>3</sub>	H
4-bromotoluene	H	H	CH <sub>3</sub>
4-bromoanisole	H	H	OCH <sub>3</sub>
4-bromo-3-methylanisole	H	CH <sub>3</sub>	OCH <sub>3</sub>

**Scheme 20.** Synthetic route used for the synthesis of the lithioarene intermediates.

Halogen-metal exchange reactions using *tert*-butyllithium have been well established for use with substituted aryl bromides [360, 361]. Through more recent work it has been demonstrated that this reaction is tolerant for haloarenes that are substituted with electron-withdrawing groups or electron-donating groups [362-364]. This reaction is synthetically useful as long as the substituents on the haloarene are not reactive towards alkyl or aryllithium reagents [365]. Halogen-metal exchange reactions help to maintain procedural simplicity and also demonstrate selectivity, allowing for a specific lithioarene intermediate to be created. Using these lithioarene intermediates, application to a one-flask procedure could be achieved, allowing for different intermolecular and intramolecular reactions to be attempted [366]. Using this method a variety of lithioarene intermediates presented in Scheme 20, were synthesized and reacted with 2,4-

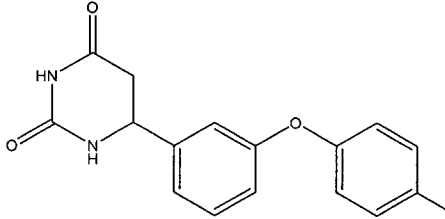
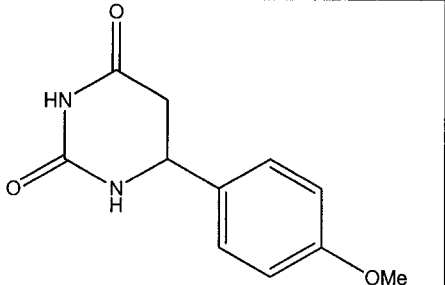
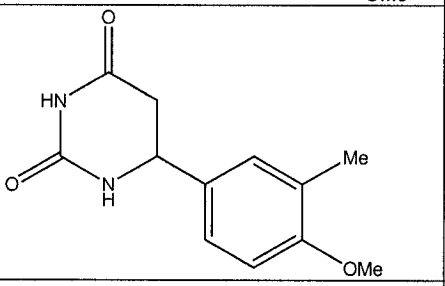
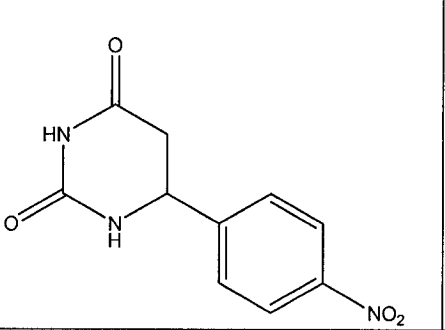
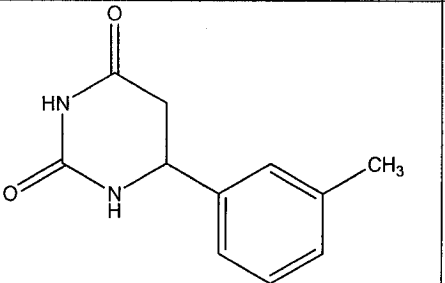
dimethoxypyrimidine to produce the final 6-aryl substituted dihydrouracil products (Scheme 21).

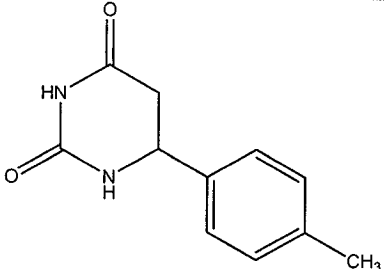
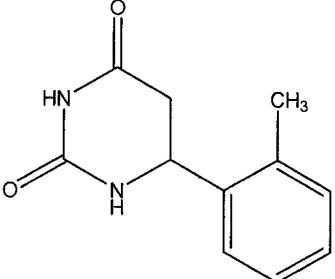


**Scheme 21.** The synthetic route used to synthesize the 6-aryl substituted dihydrouracil analogues.

All the 6-aryl substituted dihydrouracil analogues that were synthesized using Route A and/or Route B are presented in Table 19, including structures, identification numbers and IUPAC names.

**Table 19.** The 6-aryl substituted dihydrouracil analogues synthesized using Route A and/or Route B, with their respective identification numbers (ID).

Compound	ID	IUPAC Name
	1	6-(3-(4-Chlorophenoxy)-phenyl)-5,6-dihydropyrimidine-2,4-dione
	2	6-(4-Methoxyphenyl)-5,6-dihydropyrimidine-2,4-dione
	3	6-(4-Methoxy-3-methylphenyl)-5,6-dihydropyrimidine-2,4-dione
	4	6-(4-Nitrophenyl)-5,6-dihydropyrimidine-2,4-dione
	5	6-( <i>meta</i> -Tolyl)-5,6-dihydropyrimidine-2,4-dione

	6	6-( <i>para</i> -Tolyl)-5,6-dihydropyrimidine-2,4-dione
	7	6-( <i>ortho</i> -Tolyl)-5,6-dihydropyrimidine-2,4-dione

The results of using Route B to synthesize the 6-aryl substituted dihydrouracil analogues produced yields that were substantially better than those obtained from Route A. The yields ranged from 50 to 68% and allowed much larger quantities of the final product to be produced using reasonable amounts of the starting materials. Route A in theory was a useful synthesis because it involved a single condensation/cyclization step to produce the final product. However in, comparison Route B, which involved several steps, was more labour and time intensive. That said, by comparison of the yields (Table 20) it can be clearly seen that Route B is more suited to the pharmaceutical development of 6-aryl substituted dihydrouracil analogues.

**Table 20:** The yields obtained for the synthesis of 6-aryl substituted dihydrouracil analogues using Route A and Route B.

Compound ID	Route A Yield (%)	Route B Yield (%)
1	8	63
2	10	68
3	8	66
4	N/A	50
5	9	67
6	8	67
7	11	63

## 6.8 Dihydrouracils: Biological Results

The biological tests performed included the maximal electroshock induced-seizure model (MES) and the subcutaneous pentylenetetrazole (Metrazol) induced-seizure (PTZ) model. These biological tests along with preliminary neurotoxicity studies were completed at NIH in Bethesda, MD, USA, through their anticonvulsant drug development program (ADD). The results presented in Table 21, with the activity code legend in Table 22. The protocols used for each of these biological tests and neurotoxicity studies were the same as those presented Chapter 5.

**Table 21.** Biological testing results and activity codes for 6-aryl substituted dihydrouracil analogues. The ratios indicated the number of animals protected over the number of animal tested.

Dosage (mg/kg)	MES Testing						PTZ Testing						Toxicity				Activity Scores	
	30		100		300		30		100		300		30		100		300	
	0.5	4.0	0.5	4.0	0.5	4.0	0.5	4.0	0.5	4.0	0.5	4.0	0.5	4.0	0.5	4.0	0.5	4.0
Time (hrs)																		
ID Codes																		
1	0/1	0/1	1/3	2/3	0/1	0/1	0/1	0/1	0/1	0/1	0/1	0/1	0/1	0/1	0/2	0/8	0/4	0/2
2	0/1	0/1	0/3	0/3	0/1	0/1	0/1	0/1	0/1	0/1	0/1	0/1	0/1	0/1	0/4	0/2	0/4	0/2
3	0/1	0/1	0/3	0/3	0/1	0/1	0/1	0/1	0/1	0/1	0/1	0/1	0/1	0/1	0/4	0/2	0/4	0/2
4	0/1	0/1	3/3	0/3	0/1	0/1	0/1	0/1	0/1	0/1	1/1	0/1	0/1	0/4	0/8	0/4	2/4	0/2
5	0/1	1/1	3/3	0/3	1/1	0/1	0/1	0/1	3/6	1/6	1/1	0/1	0/1	0/4	0/2	0/8	4/4	0/2
6	0/1	0/1	2/3	0/3	1/1	0/1	0/1	0/1	0/1	0/1	0/1	0/1	0/1	0/4	0/2	1/8	3/4	1/2
7	0/1	1/1	1/3	0/3	1/1	0/1	0/1	0/1	0/1	0/1	0/1	0/1	0/1	0/4	0/2	2/8	4/4	0/2
														0/4	0/2	0/8	4/4	0/2
																	3	3
																	0	0
																	3	0
																	3	0
																	3	0

**Table 22.** Activity codes and the corresponding animal protection ratios and dosages.

Activity Code	Ratios	Dosage of test compound (mg/kg)
0	0/4	300
1	1-2/4	300
2	>2/4	300
3	>2/4	100
4	>2/4	30

### 6.8.2 Biological Discussion

Of the compounds tested, 6-aryl substituted dihydrouracil analogues **1**, **2**, **3**, **4** and **5** all had bioactive  $\beta$ -amino acid metabolites, which have previously displayed anti-epileptogenic activity [348]. Although these dihydrouracil compounds have only been tested in the anti-ictogenic models, it can already be seen that they display bioactivity for protection against the development of a seizure. Compounds **1**, **3** -**7** (Table 21) all displayed some biological activity in either or both of the biological tests, indicating that they may be able to influence the voltage gated sodium channel and the GABA<sub>A</sub> receptor. This activity may be a result of the dihydrouracil analogue and not the  $\beta$ -amino acid metabolite.

In order to further test the hypothesis that dihydrouracils can be used to target epileptogenesis, they need to be further evaluated in the anti-epileptogenic bioactivity screens. Based on the limited biological results, it appears that there may be some correlation between the anti-ictogenic properties of dihydrouracil and its  $\beta$ -amino acid metabolite's antiepileptogenic properties. Through this project groundwork has been laid for further research into the ability of dihydrouracil analogues to act as "bioactive" pro-drugs. Meaning they have the ability to influence epilepsy, both as a dihydrouracil analogue (anti-ictogenic properties) and as a  $\beta$ -amino acid metabolite (antiepileptogenic properties).

## 6.9 Experimental: Dihydrouracil Derivatives

$^1\text{H}$  and  $^{13}\text{C}$  nuclear magnetic resonance (NMR) spectra were recorded using a Bruker AC-250 MHz or AVANCE 500MHz spectrometer. Chemical shifts ( $\delta$ ) are reported as parts per million downfield from tetramethylsilane (TMS) and are calibrated using the solvent peaks or when possible, the TMS peak present in some of the deuterated solvents. Coupling constants ( $J$ ) are reported in Hz. Correlation spectroscopy techniques (HMBC, HSQC) were used in some situations to confirm structural connectivity.

High resolution mass spectrometry (HRMS) by electron impact (EI) was performed on a CEC21-100B sector mass spectrometer, and samples were analyzed as solids. The  $m^+/z$  of the molecular ion peak ( $\text{M}^+$ ) is provided along with the expected/calculated value for each of the corresponding molecular formula. The error on each of the HRMS values is  $\pm 0.0008$  amu. In situations where the compounds were not stable to EI and the molecular ion could not be detected, low resolution electrospray ionization (ESI) was used to visualize the  $[\text{M}-1]^+$ , followed by HRMS by EI on the expected fragment of the compound.

Reagents and solvents required for the reactions were obtained from commercial sources: Sigma-Aldrich, Inc. and Fluka. Melting points (mp) for the compounds synthesized were determined using a Mel-Temp II capillary apparatus and are uncorrected. Analytical thin-layer chromatography (TLC) was carried out to monitor reactions using pre-coated Brinkmann silica gel 60 F<sub>254</sub> plates with glass backing. TLC plates were visualized using UV light or, in specific situations, iodine or potassium permanganate. The solvent system used was (A) ethanol and ethyl acetate (3:2).



### 6.9.1 Synthesis Of 6-Aryl Substituted Dihydrouracils: Route A

A mixture of cinnamic acid derivative (0.50 g, 3.4 mmol) and urea (1.0 g, 1.7 mmol) were heated to 190 °C for 2 hours. The resulting yellow oil was then taken up in water and heated at reflux for 2 hours. The reaction was cooled to room temperature, and the solid cinnamoyl urea was removed by filtration. The filtrate was then extracted with ether 5 times and the organic layer was dried over sodium sulfate. The solvent was removed under reduced pressure and the product was crystallized from methanol.

#### Preparation of specific cinnamic acid starting materials for Route A [367]

##### *4-Methoxy-3-methyl cinnamic acid*

4-Methoxy-3-methylbenzaldehyde (1.95 mL, 13.2 mmol), malonic acid (1.35 g, 13.2 mmol) were combined with ammonium acetate (2.00 g, 26.4 mmol) in dry ethanol and heated at reflux for 8 h. The solid  $\beta$ -amino acid that formed was collected by filtration and the filtrate was evaporated under reduced pressure to produce a yellowish solid. The solid was crystallized from water and ethanol.

Yellow crystalline product (1.89g, 75%); mp = 161-163 °C;  $^1\text{H}$  NMR (DMSO- $d_6$ ): 2.23 (s, 3H), 3.76 (s, 3H), 6.39 (d, 1H,  $J=16.5$ ), 7.05 (d, 1H,  $J=16.4$ ), 7.48-7.50 (m, 3H);  $^{13}\text{C}$  NMR (DMSO- $d_6$ ): 15.8, 54.6, 115.8, 117.6, 123.5, 124.7, 128.5, 129.2, 146.5, 158.2, 167.3.

### ***3-(4-Chlorophenoxy)-cinnamic acid***

3-(4-Chlorophenoxy)-benzaldehyde (4.0 mL, 20 mmol), malonic acid (10.5 g, 100 mmol), and morpholine (3 mL, 4 mmol) were in 10 mL of pyridine and heated at 60 °C for 10 h. The reaction was then cooled to room temperature and stirred for an additional 48 h. After this the reaction mixture was poured over a 1% aqueous solution of HCl and stirred for 2 h at 0 °C. The solid that formed was collected and purified by crystallization from ethanol.

Crystalline solid (4.67 g, 85%); mp = 162-164 °C (lit. mp = 163-164 °C); <sup>1</sup>H NMR (DMSO-d<sub>6</sub>): 6.52 (d, 1H, *J*=16.3), 6.97-7.05 (m, 5H), 7.19-7.25 (m, 3H), 7.64 (d, 1H, *J*=16.3); <sup>13</sup>C NMR (DMSO-d<sub>6</sub>): 112.4, 115.8, 116.9, 118.4, 119.2, 126.5, 128.2, 129.2, 133.6, 148.3, 156.4, 157.9, 167.2.

## **6.9.2 6-Aryl Substituted Dihydrouracil Analogues: Route B**

### **Step 1: Preparation of 2,4-dichloropyrimidine**

A mixture of uracil (10 g, 89 mmol) and phosphorus oxychloride (40 mL) were refluxed at 100-110 °C for 2.5 h. The solution was cooled to room temperature and a brown solution was obtained. The excess phosphorus oxychloride was removed by distillation and a viscous mixture resulted. This mixture was then slowly poured over 85 g of ice, and then 10 ml of ether was added. The ether layer was removed, and the resulting mixture was extracted with ether (25 mL) 5 times. The combined ether layers were washed with saturated aqueous sodium carbonate and dried with sodium sulfate. The ether was then removed and a crude crystalline product was obtained. The product was crystallized from hexane.

Cream coloured powder (12.13 g, 95%); mp = 61-62 °C (lit. mp = 61-62 °C); <sup>1</sup>H NMR (DMSO-d<sub>6</sub>): 7.38 (d, 1H, *J*=6.2), 8.76 (d, 1H, *J*=6.2); <sup>13</sup>C NMR (DMSO-d<sub>6</sub>): 121.3, 159.9, 161.3, 163.8.

### **Step 2: Preparation of 2,4-dimethoxypyrimidine**

A solution of 2,4-dichloropyrimidine (10 g, 67 mmol) in 50 mL of dry methanol was added slowly to a stirring solution of 3.2 g of sodium in 60 ml of dry methanol. The mixture was heated at reflux for 10 min, cooled and filtered. The collected sodium chloride was rinsed three times with ether and combined with the filtrate, which was then rotary evaporated. An oily residue resulted which was dissolved in 40 mL of ether. The solution was washed with two 20 mL portions of 30% aqueous sodium hydroxide and then water. The ether layers were combined dried with sodium sulfate and reduced under vacuum.

Crude residue (8.45 g, 90 %); mp = n/a; <sup>1</sup>H NMR (DMSO-d<sub>6</sub>) δ: 3.69 (s, 3H), 3.72 (s, 3H), 7.42 (d, 1H, *J*=6.3), 8.89 (d, 1H, *J*=6.3); <sup>13</sup>C NMR (DMSO-d<sub>6</sub>): 53.2, 54.4, 121.3, 159.9, 161.3, 163.8.

### **Step 3: General Procedure for 6-substituted-dihydropyrimidine-2,4-diones** **Organolithium reagent preparation**

A mixture of the brominated compound (Table 23) and dry diethylether (50 mL) were combined and maintained under a nitrogen atmosphere. The solution was cooled to -78 °C, and tert-butyllithium (1.2 mL, 12 mmol) was added slowly over the course of 1 h by a dropping funnel. The solution was then stirred for an additional 1 h at -78 °C. The

resulting solution containing the organolithium reagent  $R^4\text{-Li}$  was then utilized in the next step of the reaction.

**Table 23.** The amount of each brominated compound that was used in Route B for the organolithium preparation.

Brominated Compound	MW (g/mol)	Moles used (mmol)	Mass (g)
2-bromotoluene	171.03	6.1	1.05
3-bromotoluene	171.03	6.5	1.11
4-bromotoluene	171.03	6.1	1.04
4-bromoanisole	187.03	5.7	1.06
4-bromo-3-methylanisole	201.06	5.6	1.13

### General preparation of 6-substituted-dihydropyrimidine-2,4-diones

To a stirred solution of the organolithium reagent  $R^4\text{-Li}$  (5 mmol) in ether (50 mL) under nitrogen at  $-78\text{ }^{\circ}\text{C}$  a solution of 2,4-dimethoxypyrimidine (5.6 mmol) in ether (5 mL) was added dropwise over 10 min. The mixture was then stirred at  $-20\text{ }^{\circ}\text{C}$  for 1 h and then slowly warmed to room temperature and stirred for an additional 2 h. The solution was then quenched with water (2 mL) in THF (5 mL) at  $-10\text{ }^{\circ}\text{C}$  and the solution was concentrated to a volume of 25 mL on the rotary evaporator. A solution of the crude product in 2M HCl was heated at  $60\text{ }^{\circ}\text{C}$  for 2.5 h to promote hydrolysis and generate the 6-substituted dihydrouracil compound. The solution was then cooled and the 6-substituted dihydrouracil precipitated from solution and was isolated by filtration. The product was crystallized from methanol.

### 6-(3-(4-Chlorophenoxy)-phenyl)-5,6-dihydropyrimidine-2,4-dione (1)

Crystalline solid [Route A: (0.405 g, 8%) from 3-(4-chlorophenoxy)-cinnamic acid];

[Route B: (0.995 g, 63%)]; mp =  $206\text{--}208\text{ }^{\circ}\text{C}$ ; (lit. mp =  $201\text{--}203\text{ }^{\circ}\text{C}$ );  $^1\text{H}$  NMR (DMSO-

d<sub>6</sub>): 2.64 (dd, 1H  $J$ = 7.2, 16.1), 2.86 (dd, 1H,  $J$ =6.3, 16.1), 2.87 (dd, 1H,  $J$ =7.2, 20.5), 4.68 (s, 1H), 7.04-7.45 (m, 8H) <sup>13</sup>C NMR (DMSO-d<sub>6</sub>): 38.6, 49.7, 51.2, 117.5, 118.6, 121.2, 122.7, 128.1, 130.4, 131.3, 144.7, 14.7, 156.9, 167.2; HRMS: C<sub>16</sub>H<sub>13</sub>ClN<sub>2</sub>O<sub>3</sub> calculated 316.0615 amu, found 316.0624 amu.

***6-(4-Methoxyphenyl)-5,6-dihydropyrimidine-2,4-dione (2)***

Crystalline solid [Route A: (0.033 g, 10%) from 4-methoxy cinnamic acid]; [Route B: (0.748 g, 68%)]; mp = 219-220 °C (lit. mp = 216-217 °C); <sup>1</sup>H NMR (DMSO-d<sub>6</sub>): 2.62 (dd, 1H,  $J$ =10.3, 23.5), 2.85 (dd, 1H,  $J$ =8.7, 23.5), 3.42 (m, 1H), 3.76 (s, 3H), 7.03 (d, 2H,  $J$ =12.4), 7.21 (d, 2H,  $J$ =12.4); <sup>13</sup>C NMR (DMSO-d<sub>6</sub>): 41.5, 45.7, 57.8, 125.2, 126.8, 139.4, 143.7, 156.6, 172.4; HRMS: C<sub>11</sub>H<sub>12</sub>N<sub>2</sub>O<sub>3</sub> calculated 220.0848 amu, found 220.0852 amu.

***6-(4-Methoxy-3-methylphenyl)-5,6-dihydropyrimidine-2,4-dione (3)***

Crystalline solid [Route A: (0.064 g, 8%) from 3-methyl-4-methoxy cinnamic acid]; [Route B: (0.772 g, 66%)]; mp = 201-203 °C; (lit. mp = 201-203 °C); <sup>1</sup>H NMR (DMSO-d<sub>6</sub>): 2.24 (s, 3H), 2.66 (dd, 1H,  $J$ =8.3, 20.4), 2.87 (dd, 1H,  $J$ =7.2, 20.5), 3.91 (s, 3H), 4.68 (m, 1H), 7.03 (m, 3H); <sup>13</sup>C NMR (DMSO-d<sub>6</sub>): 17.3, 38.9, 51.3, 55.3, 112.1, 125.4, 126.7, 129.8, 134.5, 155.6, 158.1, 169.7; HRMS: C<sub>12</sub>H<sub>14</sub>N<sub>2</sub>O<sub>3</sub> calculated 234.1004 amu, found 223.1012 amu.

***6-(4-Nitrophenyl)-5,6-dihydropyrimidine-2,4-dione (4)***

*6-phenyl-5,6-dihydropyrimidine-2,4-dione* was prepared using [Route A (0.045 g, 7%) from cinnamic acid] and [Route B (0.582 g, 60%) from bromobenzene]; mp = 218-220 °C (lit. mp = 217-218 °C); <sup>1</sup>H NMR (DMSO-d<sub>6</sub>): 2.78 (dd, 1H, *J*=8.3, 16.9), 2.92 (dd, 1H, *J*=7.2, 16.9), 4.89 (m, 1H), 7.48-7.53 (m, 5H)].

*6-phenyl-5,6-dihydropyrimidine-2,4-dione* (0.350 g, 1.45 mmol), was dissolved in 10 mL of a 1:1 volume ratio solution of HNO<sub>3</sub> and H<sub>2</sub>SO<sub>4</sub> and stirred at room temperature for 30 min. The reaction mixture was poured over 25 g of ice and a yellow precipitate formed. The precipitate was collected by filtration and crystallized from an ethanol: water mixture (2:1).

Yellow crystalline product [Route B: (0.176 g, 50%)] mp = 254-257 °C (lit. mp = 254-256 °C); <sup>1</sup>H NMR (DMSO-d<sub>6</sub>): 2.68 (dd, 1H, *J*=7.1, 17.2), 2.93 (dd, 1H, *J*= 6.7, 17.2), 4.86 (m, 1H), 7.64 (d, 2H, *J*=11.8), 8.32 (d, 2H, *J*=11.8); <sup>13</sup>C NMR (DMSO-d<sub>6</sub>): 43.4, 45.9, 121.6, 128.2, 144.4, 148.7, 153.6, 172.8; HRMS: C<sub>10</sub>H<sub>9</sub>N<sub>3</sub>O<sub>4</sub> calculated 235.0593 amu, found 235.0584 amu.

***6-meta-Tolyl-5,6-dihydropyrimidine-2,4-dione (5)***

Crystalline solid [Route A: (0.066 g, 9%) from 3-methyl cinnamic acid]; [Route B: (0.684 g, 67%)] mp = 200-202 °C; <sup>1</sup>H NMR (DMSO-d<sub>6</sub>): 2.33 (s, 3H), 2.64 (dd, 1H, *J*=6.6, 16.4), 2.83 (dd, 1H, *J*=5.8, 16.4), 3.45 (m, 1H), 7.21-7.34 (m, 4H); <sup>13</sup>C NMR (DMSO-d<sub>6</sub>): 22.4, 39.5, 42.3, 124.2, 127.8, 128.8, 129.6, 138.8, 141.3, 154.9, 171.1; HRMS: C<sub>11</sub>H<sub>12</sub>N<sub>2</sub>O<sub>2</sub> calculated 204.0899 amu, found 204.0889 amu.

***6-para-Tolyl-5,6-dihydropyrimidine-2,4-dione (6)***

Crystalline solid [Route A: (0.055 g, 8%) from 4-methyl cinnamic acid]; [Route B: (0.685 g, 67%)]; mp = 201-203 °C; <sup>1</sup>H NMR (DMSO-d<sub>6</sub>): 2.42 (s, 3H), 2.64 (ss, 1H, *J*=6.7, 16.3), 2.85 (dd, 1H, *J*=5.7, 16.3), 3.53 (m, 1H), 7.42 (d, 2H, *J*=8.2) 7.56 (d, 2H, *J*=8.2); <sup>13</sup>C NMR (DMSO-d<sub>6</sub>): 22.3, 39.4, 44.5, 125.8, 127.2, 138.8, 142.4, 155.1, 171.3; HRMS: C<sub>11</sub>H<sub>12</sub>N<sub>2</sub>O<sub>2</sub> calculated 204.0899 amu, found 204.0898 amu.

***6-ortho-Yolyl-5,6-dihydropyrimidine-2,4-dione (7)***

Crystalline solid [Route A: (0.076 g, 11%) from 2-methyl cinnamic acid]; [Route B: (0.643 g, 63%)]; mp = 201-203 °C; <sup>1</sup>H NMR (DMSO-d<sub>6</sub>): 2.52 (s, 3H), 2.74 (dd, 1H, *J*=6.6, 16.1), 2.83 (dd, 1H, *J*=5.7, 16.1), 3.54 (m, 1H), 7.17-7.31 (m, 4H); <sup>13</sup>C NMR (DMSO-d<sub>6</sub>): 20.1, 39.7, 41.7, 124.5, 128.1, 129.8, 138.9, 142.6, 155.1, 171.5; HRMS: C<sub>11</sub>H<sub>12</sub>N<sub>2</sub>O<sub>2</sub> calculated 204.0899 amu, found 204.0893 amu.

## **CHAPTER 7**

### **ENZYMES IN THE PYRIMIDINE METABOLIC PATHWAY**

---



## 7.1 Introduction

One of the main difficulties with computer-aided drug development is predicting the important interactions between the proteins of interest and the drug candidate molecules. The binding affinity of a drug molecule for a receptor pocket is dependent on the 3-dimensional (3D) structure of a protein's binding pocket [368]. In order for a drug molecule to influence a specific disease it must be able to bind to the receptor of interest and fit into the binding pocket.

Due to advances in X-ray crystallography and NMR spectroscopy, information regarding the 3D structures of therapeutically relevant proteins has increased dramatically [369]. Through X-ray crystallography the structures of the active sites for specific proteins have become available and the goal now is to predict the binding strength and conformation of ligand molecules with their respective receptors [370]. With an increase in the available information about the structure of proteins, the development of computer-based methods for the development of new drugs has increased. Having the crystal structure of an enzyme allows for evaluation of the active site pocket which is important for determining the residues that are required for binding a specific ligand. Crystal structures also provide information regarding the size of a pocket and the placement of other important residues within the active site like hydrogen bond donor and acceptors, salt bridges and pi-pi interactions. These considerations are important for determining the specific binding points and recognition sites for the ligand [368]. Along with these advances in the methods of enzyme structure elucidation, there has also been an increase in the interest of using computational methods to screen ligand

databases for development of lead compounds in the pharmaceutical industry [369, 371, 372].

The use of computational methods to study enzymes has become an important research tool, especially in the development of new drug candidates. Over the last decade, research has concentrated on the development of computational methods to accurately predict or model the structural information of receptor sites [373]. By using this information about the active site, the goal is to calculate and critically evaluate the ability of ligands to dock with a specific enzyme receptor. The formation of intermolecular complexes between the protein's receptor site and a specific molecule has been widely accepted as the main mode for determining a drug's ability to influence the function of a protein. However, when using molecular docking to study protein-ligand interactions there are several hurdles that need to be evaluated.

One of the problems with computational docking is dealing with the conformational flexibility of both the ligand and the receptor [374]. When determining possible docking conformations most conventional ligands that are studied have approximately 30 degrees of freedom. However the problem resides with the protein being studied, which contains a minimum of at least a 1000 degrees of freedom [375, 376]. These degrees of freedom arise from the rotatable bonds contained within a molecule or protein. Most ligands have 3-15 rotatable bonds, while most receptor sites have 1000-2000, therefore modeling the flexibility of a protein during ligand binding is beyond the capabilities of the current computational methods [375].

Advances in computational chemistry now allow for energy calculations of both the ligand and the interactions between the ligand and the protein [375, 377]. By

calculating the atomic level interactions between a protein and a ligand the values obtained can be utilized as a tool for the development of new pharmaceutical agents [373, 378]. The accuracy of these calculations is dependent on both the energy calculation method with the computational time required [379, 380]. The goal is to maintain a balance between computational expense, ranging from a few seconds to several days, and the accuracy of the method chosen to evaluate the energy of interaction [375]. The docking methods that are currently available use simplified scoring functions so that the energy evaluations can be determined quickly and effectively, so that the best structures will be selected and ranked [373]. Calculating the docking energy using scoring functions is both efficient and selective. The efficiency of the model means that the calculations are determined in an acceptable amount of time and selectivity enable the scoring function to determine the difference between correctly and incorrectly docked structures [375]. An accurate and efficient prediction of a binding constant for protein-ligand interactions is important for structure-based drug development. When ligands interact and bind to biological molecules they interfere with its specific biochemical pathways either through enzyme inhibition or modulation [369].

## **7.2 Project Goals**

FlexX, a suite in Sybyl 7.2 [138], is a docking program that uses an incremental construction function to bind the ligand with the receptor in a low energy conformation. Using the FlexX program, the goal of this project was to evaluate the ability of the enzymes of the pyrimidine pathway to metabolize specific derivatives of uracil and dihydrouracil to their corresponding  $\beta$ -amino acid metabolites. Since uracil and

dihydrouracil are metabolic precursors, it is hypothesized that they can act as pro-drugs for specific  $\beta$ -amino acids. However, in order to be a viable pro-drug approach, these derivatives of the natural substrates must be metabolized by the pyrimidine metabolic pathway. Using computational docking methods, the goal was to test the hypothesis that the enzymes in the pyrimidine pathway can metabolize a diverse range of uracil and dihydrouracil derivatives to specific  $\beta$ -amino acids. This hypothesis was tested in silico using the FlexX program which calculates the strength of protein-ligand.

The goal of the FlexX suite is to compute low-energy conformations of the ligand within the active site quickly and effectively. The interactions that are modeled include: polar (hydrogen bonds and charge-charge) and non-polar (hydrophobic). In both circumstance these interactions are geometrically restrictive, so that small changes from ideal produce large changes in interaction energy, in return, this leads to rapid calculation times enabling large libraries of compounds to be screened effectively.

### **7.3 Background Information: FlexX Program**

Using FlexX, the receptor is a rigid structure that is usually defined by a 3D X-ray crystallography study. This program attempts to reconstruct the bound ligand in the defined receptor site through several important steps. The first step involves placing a rigid base fragment, usually a complete ring structure, into the active site followed by the reconstruction of the ligand through the addition of the required fragments [368]. FlexX uses a scoring function that is a variation on the Böhm equation, with the addition of several important scoring and penalty terms, so that deviations of a molecule from ideal geometry can be accounted for [373, 381, 382]. The main goal of FlexX is to compute

low-energy conformation of the ligand with the active site receptor, using an algorithm for fragment placement. This algorithm predicts a small number of positions for the base molecular fragment in a few seconds and is dependent on pattern recognition techniques [370]. The positioning of the molecular fragment into the active site is dependent on the localized hydrogen bonds, salt bridges and hydrophobic interactions [370]. Several different steps are involved in the FlexX procedure of docking molecules into a active site [368-370, 382].

### **7.3.1 Input Data**

The first step involves providing the program with an appropriate description of the protein. This information about the key active site residues involved in recognition is used to define the receptor pocket. The physiochemical properties of the receptor pocket are then calculated and are presented as atom labels. These properties include the chemical element, the number of bound hydrogens and their relative positions, hybridization of the atom, partial charge on the atom and the van der Waals radius of each atom. Using this information all the possible interactions and their geometries are calculated. A file is then created and defined as the receptor description file (RDF). This RDF also defines any ambiguities of the protein data bank file and adds the hydrogens and charges to the entire protein structure.

The ligands chosen to be docked into the active site are described as sets of atoms with bonds between them. Like the active site, physiochemical properties are used to label each of the atoms in the molecule. The low energy conformation of each of these ligand molecules is determined using a discrete model of conformational flexibility,

meaning that the bond lengths, bond angles and torsions for double or triple bonds are fixed. In the case of single bonds and ring systems, suitable torsional angles are used and are represented as sets of atoms.

### 7.3.2 Molecular Interactions

When determining how to position the fragment into the active site a variety of localized interactions are included. Hydrogen bonds, salt bridges, and hydrophobic contacts are the key interactions that are modeled in this process. Each of these interactions is represented by both an interaction centre (IC) and interaction surface (IS) which is defined by the chemical group and its geometry (Figure 31).

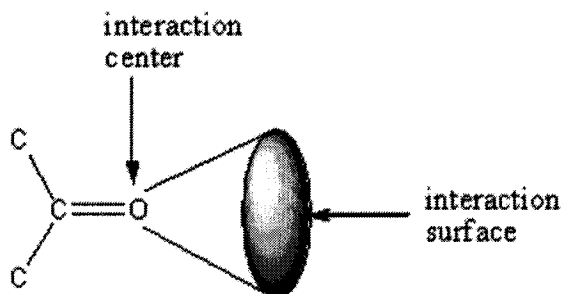


**Figure 31.** Model showing how a carbonyl is represented in the FlexX suite, with its calculated interaction centre (IC) and interaction surface (IS).

In order for there to be an interaction between two chemical groups, the interaction centre of group A must be contained within the interaction surface of group B and vice versa as well, the interaction types must be chemically compatible. These interactions include H-bond acceptors with H-bond donors, metal acceptors with a metal centre, and an aromatic ring, methyl or amide with an aromatic ring centre. In order for a

hydrogen bond to occur the interaction centers do not have to be directly across from one another, but must be contained within the interaction surface (Figure 32).

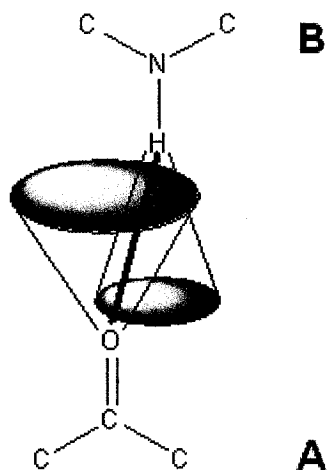


**Figure 32.** A hydrogen bond interaction between Group A (carbonyl) and Group B (amine) where each of the IC is contained on the required IS.

FlexX then estimates the free energy of binding for these protein-ligand interactions, by using an equation that is a modification of Böhm's empirical free energy function used in the de novo program LUDI [368, 381, 382].

#### **Böhm's free energy of binding function [382]**

$$\Delta G_{\text{binding}} = \Delta G_0 + \Delta G_{\text{hb}} \sum_{\text{h-bonds}} f(\Delta R \Delta \alpha) + \Delta G_{\text{ionic}} \sum_{\text{ionic int.}} f(\Delta R \Delta \alpha) + \Delta G_{\text{lipo}} |A_{\text{lipo}}| + \Delta G_{\text{rot}} \text{NROT} \quad (1)$$

#### **FlexX free energy of binding function [369]**

$$\Delta G_{\text{binding}} = \Delta G_0 + \Delta G_{\text{rot}} \times N_{\text{rot}} + \Delta G_{\text{hb}} \sum_{\text{neutral h-bonds}} f(\Delta R \Delta \alpha) + \Delta G_{\text{ionic}} \sum_{\text{ionic int.}} f(\Delta R \Delta \alpha) + \Delta G_{\text{aro}} \sum_{\text{aro int.}} f(\Delta R \Delta \alpha) + \Delta G_{\text{lipo}} \sum_{\text{lipo.cont.}} f^*(\Delta R) \quad (2)$$

This FlexX equation can be divided into three main sections. In the first section ( $\Delta G_0 + \Delta G_{\text{rot}} \times N_{\text{rot}}$ ), the  $\Delta G_0$  is a fixed term and the ( $\Delta G_{\text{rot}} \times N_{\text{rot}}$ ) term considers how ligand binding affects the loss of entropy to the system. The second section of the equation ( $\Delta G_{\text{hb}} \sum_{\text{neutral h-bonds}} f(\Delta R \Delta \alpha) + \Delta G_{\text{ionic}} \sum_{\text{ionic int.}} f(\Delta R \Delta \alpha) + \Delta G_{\text{aro}} \sum_{\text{aro int.}} f(\Delta R \Delta \alpha)$ ) considers how contributions from hydrogen bonds, ionic interactions like salt bridges and aromatic groups influence the free energy of binding. In this equation (2), these parameters are all adjusted by the penalty function  $f(\Delta R \Delta \alpha)$ , which penalizes deviations for an ideal geometry in the protein-ligand complex. For each of the functions the  $\Delta R$  is calculated by the equation  $\Delta R = R - R_0$ , where  $R$  is a calculated value for each of the atom centers and  $R_0$  is the calculated ideal value for each of these interactions. The final part of the equation ( $\Delta G_{\text{liipo}} \sum_{\text{liipo.cont.}} f^*(\Delta R)$ ) is the lipophilic energy contribution, and is a modification of Böhm's value, which is estimated using the grid method. For FlexX this value is calculated as a sum of all atom-atom contacts between the protein and the ligand. When these distances are not ideal the value is penalized by the  $f^*(\Delta R)$  function, where the ideal lipophilic distance is calculated using van der Waals radii plus 0.3 Å.

$f^*(\Delta R) =$	0	$\Delta R > 0.6 \text{ \AA}$
	$1 - (\Delta R - 0.2/0.4)$	$0.2 \text{ \AA} < \Delta R < 0.6 \text{ \AA}$
	1	$-0.2 \text{ \AA} < \Delta R < 0.2 \text{ \AA}$
	$1 - (-\Delta R - 0.2/0.4)$	$-0.6 \text{ \AA} < \Delta R < -0.2 \text{ \AA}$
	$\Delta R + 0.6/0.2$	$\Delta R < -0.6 \text{ \AA}$



### 7.3.3 Docking Algorithm

The final step in this protein-ligand procedure involves base fragment selection, base fragment placement and incremental reconstruction of the ligand in the active site. Ligand fragmentation occurs at each of the acyclic, single and rotatable bonds in the molecule to generate the ligand base fragment. The FlexX program considers double bonds, triple bonds, and bonds to amine and methyl groups as acyclic bonds that are not rotatable [368, 369, 383]. Once the base fragment has been selected the remaining portions of the molecule are separated into small fragments. A desirable base fragment is one that yields low-energy docking solutions through specificity and placement. By using the FlexX algorithm the main objective is to create interactions between the ligand and the protein so that the required points line up in the 3D space of the receptor. For docking purposes, the base fragment and active site are composed of interaction centers and surfaces. The goal of placing the base fragment in the receptor is to find a sufficient number of favorable and specific interactions between the base fragment and the active site residues. Transforming the ligand fragment into the receptor involves mapping three interaction centers of the ligand with three interaction spheres of the active site [368, 369, 383]. This means that the number of interaction groups has to be maximized while the number of base fragment conformations needs to be minimized so that fragment placement can be accomplished efficiently using the docking algorithm.

The FlexX receptor is defined as a set of interaction points and the base fragment is transformed into the active site by superimposing three interaction sites from the base fragment onto three reciprocal interaction sites in the receptor (Figure 33). Once these transformations have been recognized, they are examined to make sure the

ligand does not collide with other parts of the receptor. This is used so that impossible placements of the ligand are removed. The last step in base fragment placement involves calculating the interaction energies for all non-overlapping ligand placements [368, 369, 383].

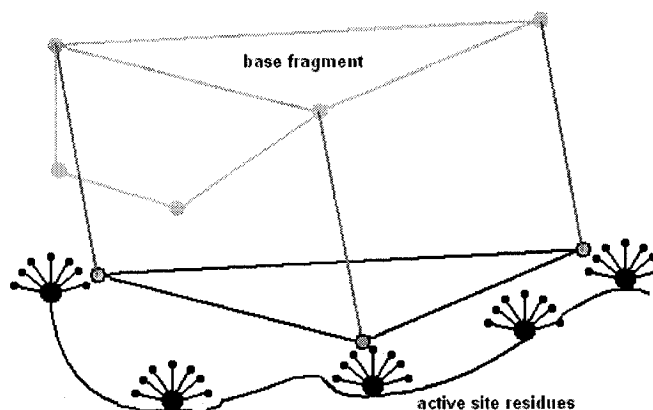


**Figure 33.** Description of the receptor pocket where the active site residues are represented as black interaction surfaces and the ligand base fragment is represented as grey interaction surfaces. In order for the ligand base fragment to dock with the receptor active site residues there must be three reciprocal interactions between the two.

The remaining ligand fragments are then added in a step by step fashion, and at each incremental step a specified number of partial solutions that are optimal are selected and carried forward to the next fragment addition. Each of these solutions is scored using the free energy of binding equation (Equation 2). For each of the fragments to be placed correctly into defined active site, the FlexX algorithm looks for matching interaction centres. This is accomplished by examining all the interaction groups of the fragments and then scanning the active site for all the corresponding interaction sites. After a series of placements for the base fragments have been determined and ranked, the remaining fragments of the ligand are added to the various base choices in all possible orientations

[368, 369, 383]. The fragments are added sequentially in the same order to all base fragment conformations, and the attachment of a new fragment is dependent on the previous placements. The first interactions that are considered are hydrogen bonds and salt bridges since they are directional and geometrically defined.

All of the base ligand placements and fragment additions are carried out using the box-hashing technique, which is used to increase the speed of the algorithm. The box hashing technique involves placing a cubic grid that covers the 3D space over the receptor area. Each cube has a defined coordinate, and each atom of the system is stored in the cube where the center of the atom is contained [384]. This system is then used as a way to check if a ligand atom overlaps with the receptor. A ligand is placed in the grid system, and the radius of each of the ligand atoms is defined as the sum of the van der Waals radii of the ligand atom and the largest atom contained in the receptor. The grid is then examined to determine which cubes have receptor atoms intersecting the ligand atom's radius, and then a box is used to surround this area and define it as a ligand-receptor overlap region. This increases the speed of the algorithm because only those receptor atoms that intersect the ligand atom area are evaluated and scored for docking interaction capabilities. Once a ligand has been completely reconstructed, the smallest  $\Delta G_{\text{binding}}$  that has been calculated for each of the ligands is determined and used to rank each of the ligands being tested from lowest to highest  $\Delta G_{\text{binding}}$ .

## 7.4 Computational Methods

The crystal structures of the enzymes dihydrouracil dehydrogenase (DHD), dihydropyrimidinase (DHP) and 3-ureidopropionase/  $\beta$ -alanine synthase ( $\beta$ -AS) were all obtained from the Research Collaboratory for Structural Bioinformatics (RCSB) Protein Data Bank (PDB) [385]. It was found that crystal structures were not available for the human enzymes but were found for *Sus scrofa* (DHD), *Thermus sp.* (DHP) and *Saccharomyces Kluyveri* ( $\beta$ -AS). For each of the proteins in the pyrimidine metabolic pathway, a receptor description file (rdf) was generated manually. This file is important since it contains the assigned physiochemical information about the amino acids of the protein, like atom types, bond types, interaction groups, as well protonation and formal charges for the atoms. This information is required by the FlexX program to resolve ambiguities in the PDB file. The FlexX program also requires a definition of the amino acids for the active site of the protein. Each of the active sites are defined by all the key residues required for metabolic activity as well as all those residues within a 6.5 Å radius. This distance was chosen because it included the entire receptor pocket that is needed for to correctly model docking. The program also identifies all the residues in the pocket that are accessible to water molecules, meaning they are on the Connolly surface of the protein.

Since the crystal structure for the human enzyme cannot be obtained, the amino acid sequences for each of these enzymes were aligned against the human sequences to determine homology and generate an alignment score. The amino acid sequences obtained from Entrez and ClustalW were used to align and score each of the sequences [386, 387].

ClustalW is a multiple alignment program that can be used for DNA and protein sequences. This program involves three main steps. To begin, the sequences are aligned and compared generating an initial starting score or distance. A matrix is generated between the pairs of sequences and a dendrogram is created. A dendrogram is tree diagram that is used to illustrate how individual data points, like amino acids, form relationship clusters. This dendrogram is used to construct a multiple sequence alignment where the most closely related sequence pairs are aligned first. The numerical value for the alignment is generated by assigning positive score values to pairs of aligned amino acid residues, and smaller or negative score to amino acid mismatches. The parameters that influence the alignment score are gap penalties, gap-extension penalties and amino acid substitutions. Those amino acids that are considered to have similar chemical properties are assigned a positive value, but this value is considerable less than that obtained from identical matches.

The complete amino acid sequences were available for the human enzymes of the pyrimidine metabolic pathway, as well as for all the required crystal structures. Once the alignment was complete the amino acid sequence was examined to confirm that the active sites were conserved, and that a reasonable alignment score had been obtained. For the first two enzymes dihydrouracil dehydrogenase (DHD) and dihydropyrimidinase (DHP) a large positive alignment score was obtained and the active site residues were conserved in both situations. The alignment percentages calculated were found to be 94% and 33% for DHD and DHP respectively. However for the 3-ureidopropionase/  $\beta$ -alanine synthase ( $\beta$ -AS) a negative alignment scores and alignment percentage (-2.7 %) were calculated, which indicated that there was little to no sequence homology between these

two enzymes. Although they react with the same substrates there was no conservation of the active site between the two enzymes, indicating that possible different residues are involved in metabolizing 3-ureidopropionate.

Using this alignment information it was determined that the first two enzymes in the pathway could be used to examine the ability, *in silico*, of this enzymatic pathway to metabolize derivatives of uracil and dihydouracil. Since the final enzyme in the pathway from *Saccharomyces kluyveri*, was not homologous to the human sequence it was not used as part of this study.

#### **7.4.1 Dihydrouracil Dehydrogenase (DHD)**

This enzyme is the first in the pyrimidine three-step pathway leading to  $\beta$ -alanine and is the rate-limiting enzyme. DHD is a cytosolic, NADPH-dependent enzyme that catalyzes the reduction of uracil and thymine to 5,6-dihydropyrimidines [388-390]. The enzyme is a homodimer (2 x 111 kDa) with each subunit having 1025 amino acids, with one FAD, one FMN and four iron-sulfur [4Fe-4S] clusters. It has been determined that there is a high sequence homology and reaction mechanism between the human, bovine and pig enzymes. The enzyme contains 5 distinct domains which were determined upon examination of the enzymes 3D crystal structure. The first domain (residues 27-172) is a  $\alpha$ -helical region and contains two of the iron-sulfur clusters. Regions 2 (residues 173-286, 442-524) and 3 (287-441) are responsible for binding the FAD and NADPH [388-390]. The pyrimidine binding site and the FMN are located in region 4 (residues 525-847) on the top portion of  $\alpha_8/\beta_8$  barrel. The final region 5 (residues 1-26, 848-1025) contains the remaining two iron-sulfur residues. Through the 3D arrangement of these

domains into the homodimeric enzyme, the formation of the required electron-transfer chains between the FAD and iron-sulfur clusters can occur [388-390]. The key active site residues are asparagine (Asn, N) 668, 736, 609, threonine (Thr, T) 737 and cysteine (Cys, C) 671 (Figure 34). This structure elucidation was determined by examining the crystal structure of the pig (*Sus scrofa*) liver DHD enzyme.

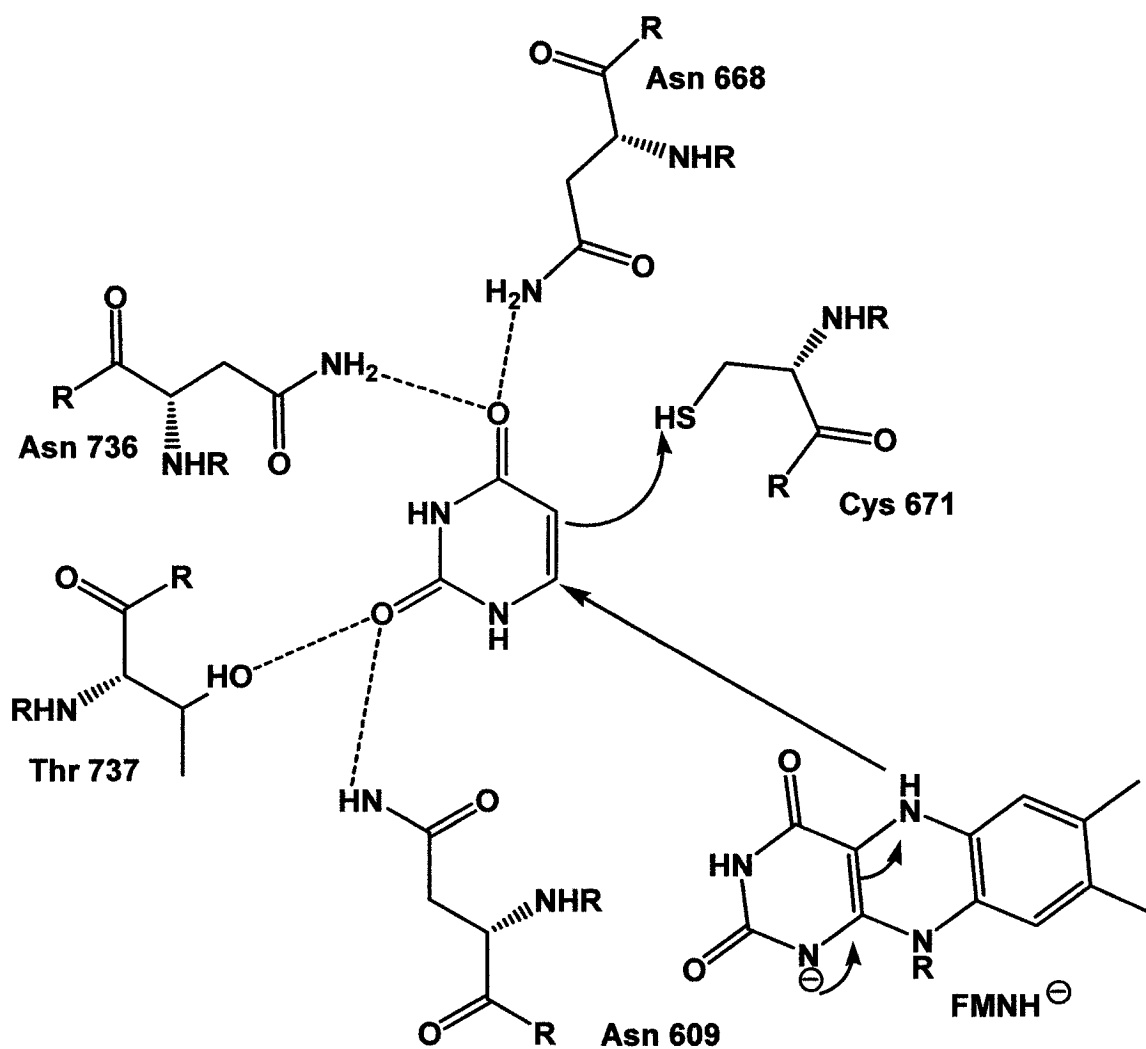


**Figure 34.** The active residues and cofactors of dihydrouracil dehydrogenase (DHD) involved in metabolizing uracil to dihydrouracil.

# Dihydrouracil Dehydrogenase (DHD) ClustalW Alignment

Sequence 1: Human\_DHD 1025 aa

Sequence 2: SusScrofa\_DHD 1025 aa

Alignment Score 6012

Perfect Alignment Score 6390

Alignment Percentage 94%

Human	MAPVLSKDSADIESILALNPRTQTHATLCSTSAKKLDKKHWKRNPDKNCFNCEKLENNFD	60
SusScrofa	MAPVLSKDVADIESILALNPRTQSHAALHSTLAKKLDKKHWKRNPDKNCFHCEKLENNFG	60
Human	DIKHTTLGERGALREAMRCLKCADAPCQKSCPTNLDIKSFITSIANKNYYGAAKMIFSDN	120
SusScrofa	DIKHTTLGERGALREAMRCLKCADAPCQKSCPTHLDIKSFITSISNKNYYGAAKMIFSDN	120
Human	PLGLTCGMVCPTSDLCVGGCNLYATEEGPINIGGLQQFATEVFKAMSIQIRNPSPLPPE	180
SusScrofa	PLGLTCGMVCPTSDLCVGGCNLYATEEGSINIGGLQQFASEVFKAMNIPQIRNPCLPSQE	180
Human	KMSEAYSAKIALFGAGPASISCSAFLARLGYS DITIFEKQEYVGGGLSTSEIPQFRLPYDV	240
SusScrofa	KMPEAYSAKIALLGAGPASISCSAFLARLGYS DITIFEKQEYVGGGLSTSEIPQFRLPYDV	240
Human	VNFEIELMKDLGVKIIICGKSLSVNEMTLSTLKEKGYKAAFIGIGLPEPNKDAIFQGLTQD	300
SusScrofa	VNFEIELMKDLGVKIIICGKSLSENEITLNTLKEEGYKAAFIGIGLPEPKTDDIFQGLTQD	300
Human	QGFYTSKDFLPLVAKGSKAGMCACHSPLPSIRGVVIVLGAGDTAFDCATSALRCGARRVF	360
SusScrofa	QGFYTSKDFLPLVAKSSKAGMCACHSPLPSIRGAVIVLGAGDTAFDCATSALRCGARRVF	360
Human	IVFRKG FVNIRAVPEEMELAKEEKCEFLPFLSPRKVIVKGG RIVAMQFVRTEQDET GKWN	420
SusScrofa	LVFRKG FVNIRAVPEEVELAKEEKCEFLPFLSPRKVIVKGG RIVAVQFVRTEQDET GKWN	420
Human	EDEDQM VHLKADVVISAFGSVLSDPKVKEALSPIKFNRWGLPEVDPETMQTSEAWVFAGG	480
SusScrofa	EDEDQIVHLKADVVISAFGSVLRDPKVKEALSPIKFNRWDLPEVDPETMQTSEPWFVAGG	480
Human	DVVGLANTTVESVNDGKQASWYIHKYVQSQYGASVSAKPELPLFYTPIDLVDISVEMAGL	540
SusScrofa	DIVGMANTTVESVNDGKQASWYIHKYIQAQYGASVSAKPELPLFYTPVDLVDISVEMAGL	540
Human	KFINPFGLASATPATSTSMIRRAFEAGWGFALTKTFSLDKDIVTNVSPRIIRGTTSGPMY	600
SusScrofa	KFINPFGLASAAPTTSSSMIRRAFEAGWGFALTKTFSLDKDIVTNVSPRIVRGTTSGPMY	600
Human	GPGQSSFLNIELISEKTAAYWCQSVTELKADFPDNIVIASIMCSYNKNDWTELAKKSEDS	660
SusScrofa	GPGQSSFLNIELISEKTAAYWCQSVTELKADFPDNIVIASIMCSYNKNDWMELSRKAEAS	660
Human	GADALELNLSCPHGMGERGMGLACGQDPELVRNICRWVRQAVQIPFFAKLTPNVTDIVSI	720
SusScrofa	GADALELNLSCPHGMGERGMGLACGQDPELVRNICRWVRQAVQIPFFAKLTPNVTDIVSI	720
Human	ARAAKEGGANGVTATNTVSGLMGLKSDGTPWPAVGIAKRTTYGGVSGTAIRPIALRAVTS	780
SusScrofa	ARAAKEGGADGVATNTVSGLMGLKADGTPWPAVGAGKRTTYGGVSGTAIRPIALRAVTT	780



Human	IARALPGFPILATGGIDSAESGLQFLHSGASVLQVCSAIQNQDFTVIEDYCTGLKALLYL	840
SusScrofa	IARALPGFPILATGGIDSAESGLQFLHSGASVLQVCSAVQNQDFTVIQDYCTGLKALLYL	840
Human	KSIEELQDWDGQSPATVSHQKGKVPRIAEELMDKKLPSFGPYLEQRKKIIAENKIRLKEQ	900
SusScrofa	KSIEELQGWGQSPGTESHQKGKVPRIAEELMGKKLPNFGPYLEQRKKIIAEKMRLEQ	900
Human	NVAFSPLKRSCFIPKRPIPTIKDVIGKALQYLGTFGELSNVEQVAMIDEEMCINCCKCY	960
SusScrofa	NAAFPLERKPFIPKKPIPAIKDVIGKALQYLGTFGELSNIEQVVAVIDEEMCINCCKCY	960
Human	MTCNDSGYQAIQFDPETHLPTITDTCGCTLCLSVCPIDCIKMVSRTTPYEPKRGVPLS	1020
SusScrofa	MTCNDSGYQAIQFDPETHLPTVTDTCGCTLCLSVCPIIDCIRMVSRTTPYEPKRGVPLA	1020
Human	VNPVC	1025
SusScrofa	VNPVC	1025

#### 7.4.2 Dihydropyrimidinase (DHP)

The DHP enzyme is the second enzyme required for the catabolism of uracil to  $\beta$ -alanine. DHP is involved in catalyzing the reversible hydrolysis of 5,6-dihydrouracil to N-carbamyl- $\beta$ -alanine [391-394]. This enzyme is a tetramer, with each subunit composed of 458 amino acids. It is a metal-dependent enzyme with the cofactor being zinc ( $\text{Zn}^{2+}$ ), but it has been found that it can be substituted by other divalent transition metals like manganese ( $\text{Mn}^{2+}$ ) and cobalt ( $\text{Co}^{2+}$ ). Removal of the  $\text{Zn}^{2+}$  leads to disassembly of the tetramer into its monomers. Through sequence homology it has been found that DHP from different species show approximately a 30% similarity with the human sequence. For the reported 3D structure, each of the monomers in the homotetramer consists of a  $(\alpha/\beta)_8$ -barrel flanked by  $\beta$ -sheet domains and additional helices [391-394]. The  $(\alpha/\beta)_8$ -barrel is located between residues 55 and 344. The  $(\alpha/\beta)_8$ -barrel is extended through the  $\alpha$ -helices and the  $\beta$ -sheet domain, which consists of two mixed antiparallel/ parallel sheets and contains both the C- and N-terminus. The active site is located on one side of the  $(\alpha/\beta)_8$ -barrel away from the  $\beta$ -rich domain at the

hydrophobic cleft. In the active site a lysine residue and a hydroxyl group bridge the binuclear zinc center. Within the active site there is a key water residue within close proximity of the two zincs ions, such that its pKa is lowered. This allows for nucleophilic attack of the water on the carbonyl carbon (C4) of the N3 amide bond, leading to generation of the N-carbamyl- $\beta$ -alanine. The key active site residues are histidine (His, H) 60, 62, 183, 239 and aspartic acid (Asp, D) 312 [391-394] (Figure 35). This structure was determined by examining the crystal structure obtained from a bacterium, *Thermus* *sp.*

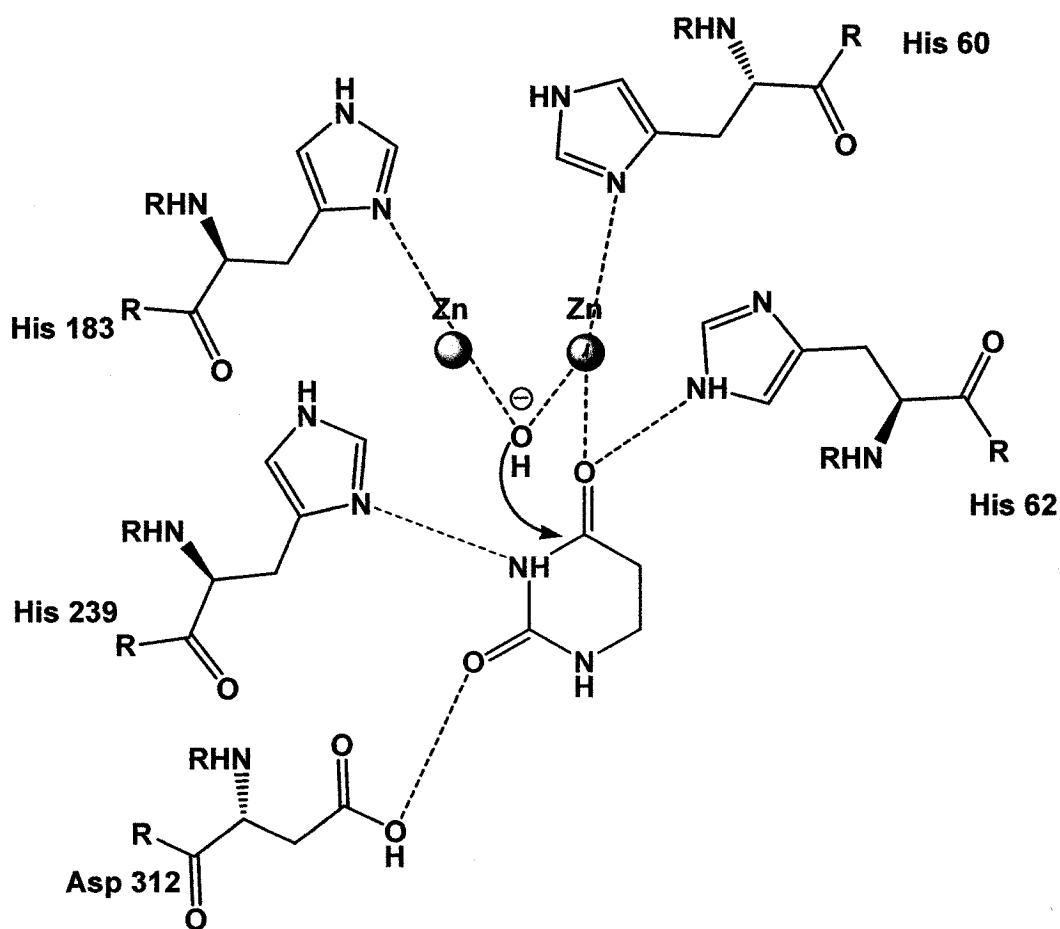


**Figure 35.** The active residues and zinc cofactors of dihydropyrimidinase (DHP) involved in metabolizing dihydrouracil to 3-ureidopropionate.

### Dihydropyrimidinase (DHP) ClustalW Alignment

Sequence 1: Human DHP 519 aa

Sequence 2: Thermus sp. DHD 458 aa

Alignment Score 1082

Perfect Alignment Score 3276

Alignment Percentage 33 %

```
Human      MAAPSRLLIRGGRVVNDDFSEVADVLVEDGVVRALGHDLLPPGGAPAGLRVLDAAAGKLV 60
Thermus    -----PLLIKNGEIIITADSRKADIYAEGETITRIGQNLEAP-----PGTEVIDATGKYVF 51

Human      PGGIDTHTHMQFFPMGSRSIDDFHQGTAAALSGGTTMIIDFAIPQKGGSLIEAFETWRSW 120
Thermus    PGFIDPHVHIYLPFMATFAKDTHETGSKAALMGGTTTYIEMCCPSRNDDALEGYQLWKSK 111

Human      ADPKVCCDYSLHVAVTWSDQVKEEMKILVQDKGVNSFKMFEMAYKDLYMVTDLLEYEAFS 180
Thermus    AEGNSYCDYTFHMAVSKFDEKTEGQLREIVAD-GISSFXIFLSYKNFFGVDDGEMYQTLR 170

Human      RCKEIGATAQVHAENGDLIAEGAKKMLALGITGPEGHELCPPEAVEAEATLRAITIASAV 240
Thermus    LAKELGVITVAHCENAELVGRLLQQLLSEGKTGPEWHEPSRPEAVEAEGTARFATFLETT 230

Human      NCPLYIVHVMSKSAAKVIADARRDGKVVEGPIAASLGTDGTHYWNKEWHHAHHVMGPP 300
Thermus    GATGYVVHLSCKPALDAAMAAKARGVPIYIESVIPHFLLDKT-YAERGGVEAMKYIMSP 289

Human      LRPDPSTPDFLMNLLANDDLTTTGTDNCTFNTCQKALGKDDFTKI PNGVNGVEDRMSVIW 360
Thermus    LR-DKRNQKVLWDALAQQGFIDTVGTDHCPDTEQKLLGKEAFTAI PNGIPAIEDRVNLLY 348

Human      EKGVHSGKMDENRFVAVTSTNAAKIFNLYPRKGRIAVGSDADIVIWDPKGTRTISAKTHH 420
Thermus    TYGVSRGRLDIHRFVDAASTKAAKLFGLFPRKGTTI AVGSDADLVVYDPQYRGTISVKTQH 408

Human      QAVNFNIFEGMVCHGVPLVTISRGVVVEAGVFSVTAGDGKFI PRKPF AEYIYKRKIQRD 480
Thermus    VNNDYNGFEGFEIDGRPSVTVRGKVAVRDQGQFVGEKGWGKLLRREP MYF----- 458

Human      RTCTPTPVERAPYKGEVATLKSRVTKEDATAGTRKQ AHP 519
Thermus    -----
```

#### 7.4.3 3-Ureidopropionase/ $\beta$ -Alanine Synthase ( $\beta$ -AS)

This is the final enzyme in the pyrimidine metabolic pathway. 3-

Ureidopropionase /  $\beta$ -alanine synthase ( $\beta$ -AS) is an aminohydrolase enzyme that acts on the substrate N-carbamyl- $\beta$ -alanine to produce  $\beta$ -alanine, carbon dioxide and ammonia [395]. This enzyme is a homodimer, where each unit is composed of 455 amino acids and two domains; the catalytic domain and the dimerization domain. The catalytic domain

(residues 2-246, 365-455) has a three layer  $\alpha/\beta/\alpha$ - stacking structure, and the dimerization domain (residues 247-364) folds into a four-stranded antiparallel sheet flanked on one side by two  $\alpha$ -helices. The active site is located between these two domains and again utilizes a di-zinc center for the activation of water to catalyze the hydrolysis of the bond between the carbon of the carbonyl moiety and the nitrogen of  $\beta$ -alanine [395]. The key active site residues include arginine (Arg, R) 322, asparagine (Asn, N) 309, and histidine (His, H) 262, as well as the residues for the di-zinc center, glycine (Gly, G) 396, glutamine (Gln, Q) 229, glutamic acid (Glu, E) 159, 160, histidine (His, H) 114, 226, 397, 421 and aspartic acid (Asp, D) 125 [395] (Figure 36). These structural studies were completed on the crystal structure obtained from *Saccharomyces kluyveri*, which shares only a limited sequence homology to humans (<10%).

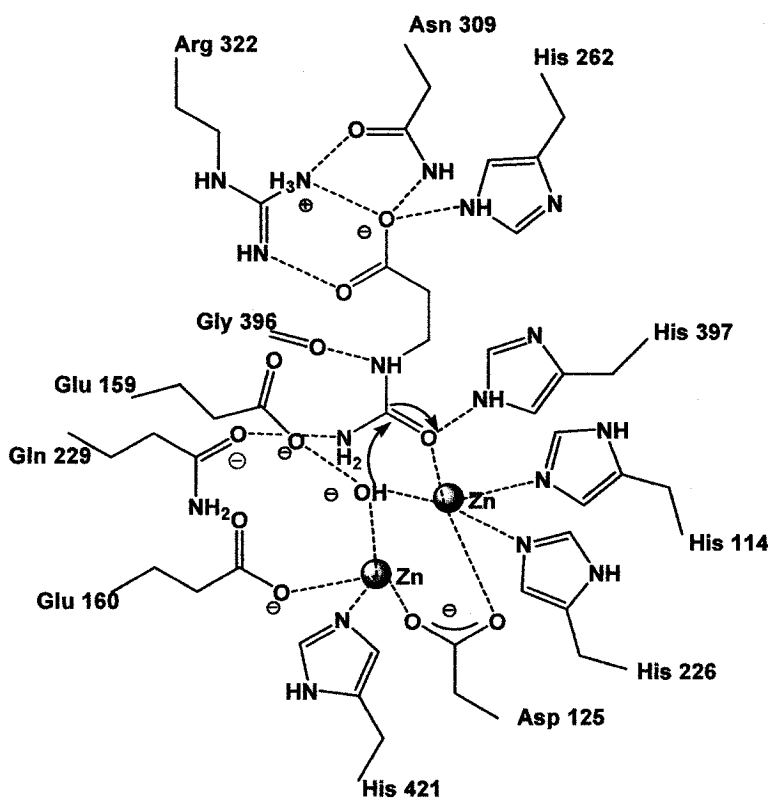


**Figure 36.** The active residues and zinc cofactors of 3-ureidopropionase/  $\beta$ -alanine synthase ( $\beta$ -AS) involved in metabolizing 3-ureidopropionate to  $\beta$ -alanine.

### 3-Ureidopropionase/ $\beta$ -Alanine synthase ( $\beta$ -AS) ClustalW alignment

Sequence 1: Human  $\beta$ -AS 384 aa

Sequence 2: Saccharomyces Kluyveri 455 aa

Alignment Score -67

Perfect Alignment Score 2453

Alignment Percentage -2.7 %

```

Human      ---MAGAEWKSLEECLEKHLPLPDLQEVKRVLYGKELRKLDLPREAFEAASRE-----DF  52
Sacch.     MSKDVSSSTITTVSASPDGTLNLPAAAPLS-IASGRNLNQITLETGSQFGGVARWQGESHF  59

Human      ELQGYAFEAAEEQLR-----RPRIVHVGLVQNRIP-----LPANAPVAEQVSA  95
Sacch.     GMRRLAGTALDGAMRDWFTNECESLGCKVKVDKIGNMFAVYPGKNGGKPTATGSHLDTQP  119

Human      LHRRIKAIVEVAAMCGVNIICFQEAWTMPFAFCTREKLP--WTEFAESAEDGPTTRFCQK  153
Sacch.     EAGKYDGILGVLAGLEVLRTFKDNNYVPNYDVCVVVWFNEEGARFARSCTGSSVWSDLS  179

Human      LAKNHDMVVVS-----PILERDSEHGDLWNTAVVISNSGAVLGKTRKNHIPRVGDFNES  208
Sacch.     LEEAYGLMSVGEDKPESVYDSLKNIGYIGDTPASYKENEIDAHFELHIEQGPILEDENKA  239

Human      TYMEGNLGHVPVFQTQFGRIAVNICYG----RHHPLNWLMSINGAEIIFNPS---ATIG  261
Sacch.     IGIVTGVQAYNWQKVTVHGVGAHAGTTPWRLRKDALLMSSKMIVAASEIAQRHNGLFTCG  299

Human      ALSESLWPIEARNAAIAN-----HCFTCAINRVGTEHFPNEFTSGDG-----KKA  306
Sacch.     IIDAKPYSVNIIPGEVSFTLDFRHPSDDLATMLKEAAAEFDRLIKINDGGALSYESL  359

Human      HQDFGYFYGSSYVAAPDSSRTPGLSRSRDGLLVAKLDLNLCCQVN-----  351
Sacch.     QVSPAVNFHEVCIECVSRSAFAQFKKDQVRQIWSGAGHDSCQTAPHVPTSMIFIPSKDGL  419

Human      --DVWNFKMTGRYEMYARELAEAVKSNYSPTIVKE-  384
Sacch.     SHNYEYSSPEEIENGFKVLLQAIINYDNYRVIRGH  455

```

## 7.5 Results And Discussion

A series of uracil derivatives (Figure 37) and dihydrouracil derivatives (Figure 38) with known epileptic activities were chosen. They were all energy-minimized using the Tripos force field and Powell conjugate gradient in Sybyl 7.2 [138], and were then docked with their respective active sites of DHD and DHP enzymes using FlexX. The free energies of binding ( $\Delta G_{\text{binding}}$ ) were calculated for each of the protein-ligand complexes, and then the solutions were ranked from lowest to highest  $\Delta G_{\text{binding}}$ . For each

of these sets of calculations, pentane, which was added as a control molecule, was docked into the active sites. Since the enzymes of the pyrimidine metabolic pathway do not metabolize pentane, it was used as a control molecule to ensure that the enzyme models being used could in fact assess the ability of the natural substrate and its derivatives to bind with the active site. For each of the calculations no  $\Delta G_{\text{binding}}$  could be calculated for pentane and no points of interaction were found to exist between the active site and the pentane ligand.

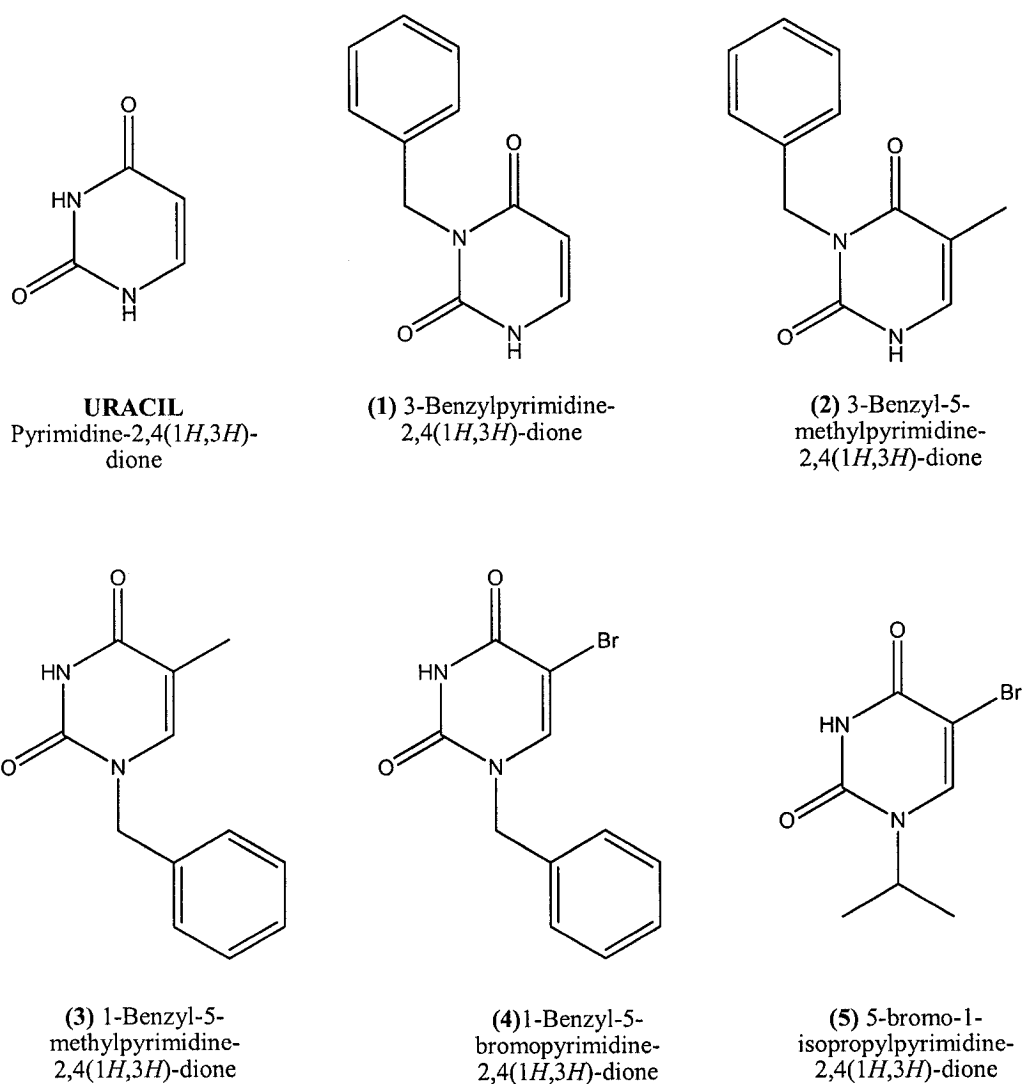


**Figure 37.** The structure of the uracil derivatives that were docked with the DHD enzyme active site using the FlexX program.

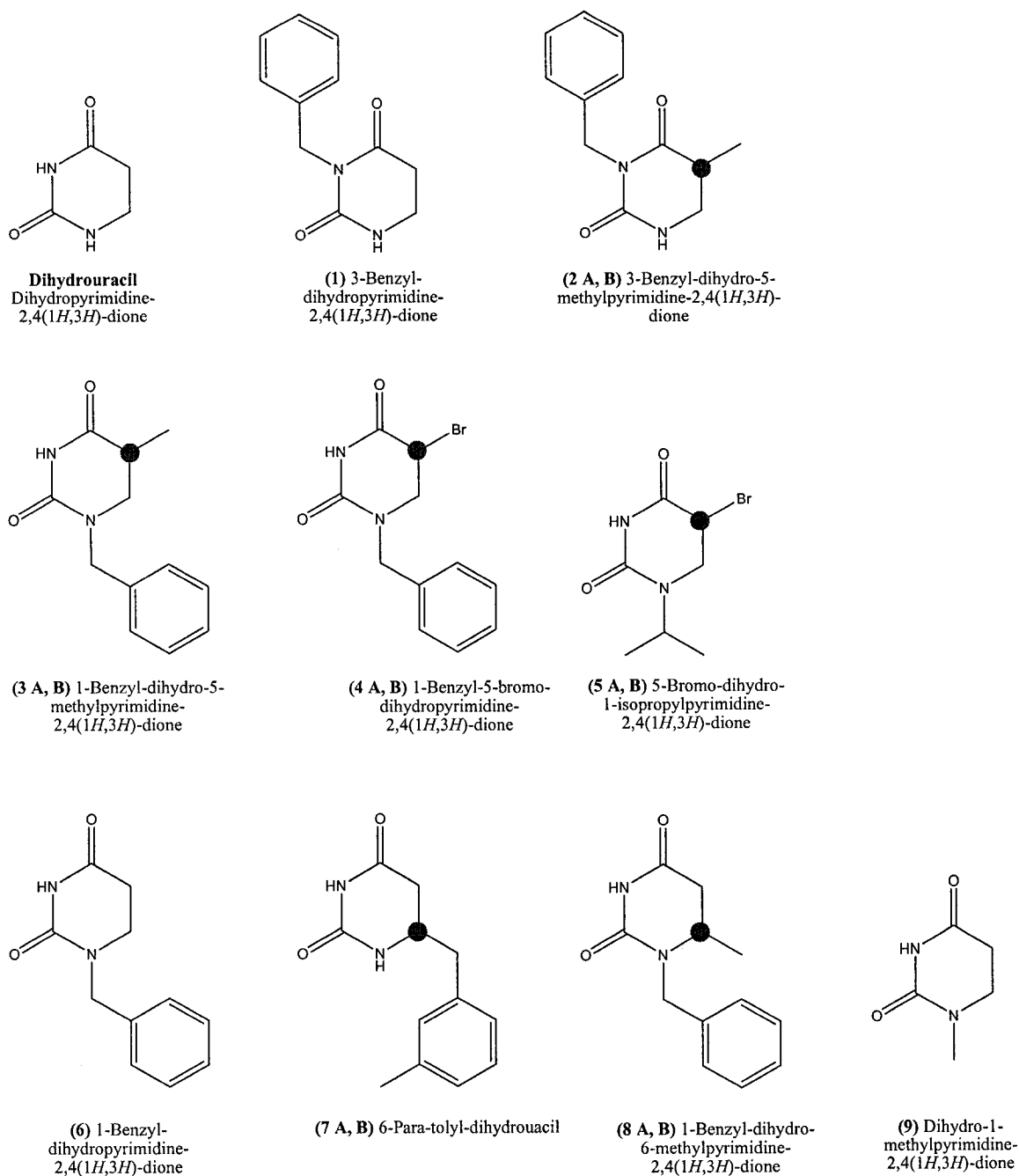


**Figure 38.** The structure of the dihydrouacil derivatives that were docked with the DHP enzyme active site using FlexX program. The black dots over the specific molecular location indicate those chemical centres that can have either an R or S configuration.

Based on the calculated  $\Delta G$  values shown in Table 24, derivatives of uracil show the ability to dock with the active site of the DHD enzyme and may be metabolized to the corresponding dihydrouracil analogues. This was particularly important since the goal behind developing these drug candidates was to use them as a pro-drug for the development of specific  $\beta$ -amino acids. In order to be a viable pro-drug the uracil derivatives must be metabolized by the enzymes of the pyrimidine metabolic pathway.

**Table 24.** Relative docking energies for uracil derivatives in the DHD enzyme

Ranking	Compound #	$\Delta G$ (kJ/mol)	$\Delta G$ (kcal/mol)
1	4	-19.422	-4.639
2	Uracil	-19.219	-4.590
3	3	-16.727	-3.995
4	1	-15.677	-3.744
5	2	-15.401	-3.679
6	5	-10.542	-2.518

The values that were calculated for these docking calculations with the DHD enzyme, show that the  $\Delta G_{\text{binding}}$  values for the derivatives of uracil were not significantly different than the  $\Delta G_{\text{binding}}$  for the natural substrate, uracil. For the derivatives tested the values were all within a 5 kJ/mol (2 kcal/mol) range, and do not vary considerably from the energy value obtained for uracil. These results support the hypothesis that the first enzyme in the pyrimidine metabolic pathway, DHD, may be able to dock and metabolize a diverse range of uracil derivatives.

The molecules have a variety of substituents at different locations, including N<sup>1</sup>, N<sup>3</sup> and C<sup>5</sup>. Through inspection of the 3D structure of the active site pocket it was



observed that this pocket was not constricted and contained flexible pockets that could accept substitution on the uracil ring, but would still allow the active site residues to influence the required bonds. Upon overlap of the docked structures with the active site, it was noted that each of the compounds bound to the active site in the geometry required for metabolism, based on the previous research [388-390]. By examining the molecules independently it was found that each of them was placed in the active site with the same orientation and that substitution at the N<sup>1</sup> and N<sup>3</sup> positions was accommodated by the localized pockets.

For the next enzyme in the series, DHP, all the uracils that were tested with DHD were converted to their corresponding dihydrouracils and an additional four dihydrouracils were included. These new dihydrouracil molecules were chosen since they were shown to have biological activity in the MES and PTZ testing.

Again the results indicated that, although there are differences in the calculated  $\Delta G_{\text{binding}}$  values, they do not vary substantially from the natural substrate, dihydrouracil. The values calculated for  $\Delta G_{\text{binding}}$ , were all within a 5 kcal/mol range with dihydrouracil having one of the lowest  $\Delta G_{\text{binding}}$  energies (Table 25).

**Table 25.** Relative docking energies for dihydrouracil derivatives in the DHP enzyme

Ranking	Compound #	$\Delta G$ (kJ/mol)	$\Delta G$ (kcal/mol)
1	9	-20.504	-4.897
2	5 R	-19.924	-4.759
3	6	-18.270	-4.364
4	Dihydrouracil	-18.009	-4.301
5	3 R	-15.599	-3.726
6	4 B	-15.442	-3.688
7	1	-15.034	-3.591
8	5 S	-13.788	-3.293
9	4 R	-12.606	-3.011
10	7 S	-12.315	-2.941
11	3 S	-11.835	-2.827
12	2 R	-11.435	-2.731
13	7 R	-8.553	-2.043
14	8 S	-7.434	-1.776
15	2 S	-6.728	-1.607
16	8 R	-2.839	-0.678

Again the dihydrouracil derivatives had a variety of substitutions at different chemical locations, including N<sup>1</sup>, N<sup>3</sup>, C<sup>5</sup> and C<sup>6</sup>. Through inspection of the 3D structure of the active site pocket of DHP it was determined that there was a large accessible pocket indicating that it could be possible to accept a variety of substitutions on the dihydrouracil ring. Upon overlap of the docked dihydrouracil structures with the active site pocket, it was found that each of the compounds bound with the active site residues in the geometry required for metabolism [391-394].

For each of the molecules both the R and S configurations were utilized and tested independently. Although each of the configurations of the molecules had a

different  $\Delta G_{\text{binding}}$ , there was no noticeable preference for R versus S. Through these calculations it was also revealed that although the  $\Delta G_{\text{binding}}$  values were different for the R and S configurations of each molecule, they showed a tendency to be grouped. This is apparent with compounds 4 A/ B and 8 A/B. For 4B, it was ranked 6<sup>th</sup> with an energy of -3.688 kcal/mol, and for 4A it ranked 9<sup>th</sup> with an energy of -3.011 kcal/mol, both being ranked in the middle section. However, for compound 8B it ranked 14<sup>th</sup> with an energy of -1.776 kcal/mol and 8A ranked 16<sup>th</sup> with an energy of -0.678 kcal/mol, meaning that both ranked in the bottom quarter. Presumably this means that although these compounds have different configurations it does not appear to affect their ability to bind to the active site residues of the DHP enzyme. For dihydrouracils 7 and 8 they were biologically tested as a racemate and based on these *in silico* results neither had a significant advantage over the other for binding to the DHP active site for metabolism to 3-ureidopropionase derivative.

## 7.6 Conclusions

Through these *in silico* docking studies using FlexX, a diverse group of uracil and dihydrouracil analogues that can dock into the active sites of the DHD and DHP enzymes in a homologous way to the endogenous ligands, have been found. Through this research it can be inferred that the analogues may be subject to metabolism by the pyrimidine metabolic pathway. The results obtained help to support the hypothesis that a diverse group of uracil and dihydrouracil analogues can be used as pro-drugs to produce specific  $\beta$ -amino acids using the described endogenous metabolic pathway.

By using the computational method FlexX, we have been able to study and access the ability of the enzymes of the pyrimidine metabolic pathway to metabolize analogues of uracil and dihydrouracil. The binding affinity of the molecule for the receptor pocket and the 3D structure of the protein's binding pocket are important factors for developing new therapeutic molecules. *In silico* research has been instrumental for determining the receptor pocket size and the intermolecular complexes that are formed between the DHD and DHP enzymes and their specific uracil and dihydrouracil ligands. This project is particularly important and will be used to further the development of new  $\beta$ -amino acid pro-drugs to target epilepsy.

## **CHAPTER 8**

### **MOLECULAR MODELLING OF PHENYTOIN AND DIHYDROURACILS**

---

## 8.1 Introduction

Epilepsy is the second most common neurologic disorder, affecting 300,000 individuals of all ages in Canada. Drugs that are currently on the market often fail to adequately control the symptoms associated with epilepsy and have adverse side effects [396]. In order to develop drugs that can improve upon those available, an understanding of the mechanism of action for epilepsy is crucial, as well as a determination of the bioactive face (pharmacophore).

In molecular modelling, a “pharmacophore” (i.e., the “bioactive” face of the drug) is a set of features that is common to a group of known active molecules. These features include hydrogen bond donors and acceptors, hydrophobic and hydrophilic regions, and positively and negatively charged groups [37]. For drug molecules, a three dimensional (3D) pharmacophore indicates the spatial arrangement between the above-mentioned groups. The arrangement is often expressed as a distance or distances between the pharmacophore units as well as angle measurements [37, 39]. Once a pharmacophore has been determined, it can be used to suggest the activity for other classes of molecules. However, difficulties can arise in trying to determine the combination and spatial positioning of the pharmacophore units. An assumption that is inherent when determining the active face of a molecule is that all molecules with a similar pharmacophore bind in a similar manner to the target site [38].

Of the anticonvulsant drugs that have been conventionally used, phenytoin (5,5-diphenylhydantoin) (Figure 39) has been a primary treatment for the suppression of seizure activity in epileptic patients [397]. Its main mechanism of action is to bind to the fast-inactivated state of the neuronal sodium channel, thereby preventing the continuous

spread of aberrant electrical activity [398]. Despite their clinical importance, hydantoin derivatives have associated side effects due to the toxicophore unit in their structure. These side effects range from uncomfortable and inconvenient, through to life threatening. Due to these complications, the need for new treatments that can maintain seizure suppression while reducing unwanted side effects is greatly needed [396].

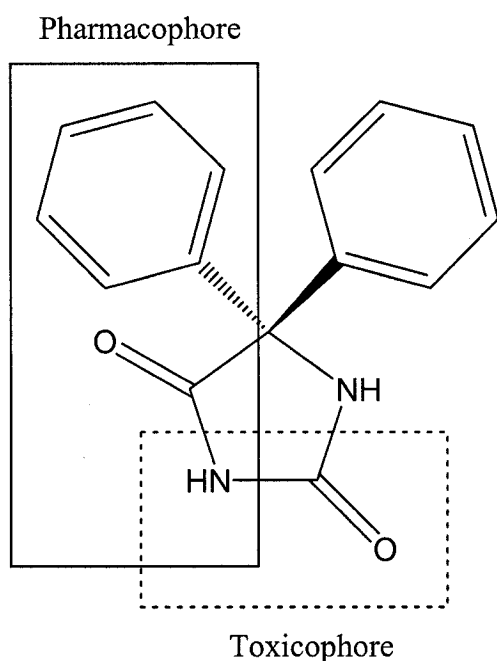


**Figure 39.** Phenytoin (5,5-diphenylhydantoin) and its respective pharmacophore and toxicophore units.

After an extensive literature review, dihydrouracil analogues (Figure 40) were chosen (based on their receptor properties) as suitable molecular platforms for the development of new epilepsy treatments.

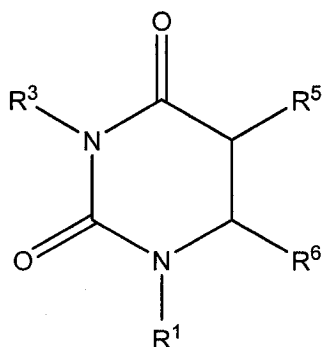


**Figure 40.** Dihydrouracil analog where the R groups can be a variety of substituents.

## 8.2 Computational Methods

In order to calculate the distances and angles, the hydantoin and dihydrouracil derivatives first had to be energy minimized. This was accomplished using a variety of techniques so that a comparison could be made in order to determine the optimal lengths and angles of the molecules. The programs utilized were molecular mechanics (AMBER, with a conjugate gradient for minimization), semi-empirical (AM1) and *ab initio* (Hartree-Fock / 6-31G\*). The AMBER calculations were completed using Hyperchem 7.5 software [399] and the semi-empirical and *ab initio* values were calculated using CHEM 3D 8.0 [63].

## 8.3 Calculated Results: Phenytoin And Dihydrouracil

The results obtained from the calculations (bond lengths and bond angles) using molecular mechanics, semi-empirical and *ab initio* are provided below in Table 26 and with Figure 41, Figure 42, and Figure 43 available for angle and atom explanation.



**Table 26.** The calculated results for phenytoin, 5-phenyldihydrouracil and 6-phenyl dihydrouracil. Angles are all expressed in degrees and the distances in angstroms.

GROUPS	AMBER	AM1	6-31G*
<b>Phenytoin</b>			
Angle 1	96.974	101.834	99.655
Angle 2	110.120	106.845	106.874
Angle 3	109.982	110.912	113.443
Angle 4	110.086	108.567	105.612
Angle 5	112.838	111.634	114.423
<b>Phenytoin Phenyl 1</b>			
C4-Aromatic Distance	3.845	3.693	3.704
O4-Aromatic Distance	4.204	4.042	4.037
N3-Aromatic Distance	4.710	4.570	4.554
H3--Aromatic Distance	5.543	5.365	5.331
<b>Phenytoin Phenyl 2</b>			
C4-Aromatic Distance	3.845	3.823	3.843
O4-Aromatic Distance	4.214	4.193	4.242
N3-Aromatic Distance	4.710	4.751	4.693
H3-Aromatic Distance	5.543	5.585	5.534
<b>5-Phenyl Dihydrouracil</b>			
Angle 1	116.536	115.1	114.961
Angle 2	124.579	124.4	127.778
Angle 3	118.255	118.3	114.766
Angle 4	122.789	120.6	123.134
Angle 5	111.441	112.3	110.000
Angle 6	110.260	112.3	109.656
C4-Aromatic Distance	3.755	3.779	3.822
O4-Aromatic Distance	3.781	3.822	3.885
N3-Aromatic Distance	5.068	5.075	5.088
H3-Aromatic Distance	5.798	5.826	5.830
<b>6-Phenyl Dihydrouracil</b>			
Angle 1	116.365	117.9	115.011
Angle 2	124.178	122.9	126.723
Angle 3	118.226	119	115.444
Angle 4	122.705	122.1	125.075
Angle 5	110.319	112.5	108.208
Angle 6	109.897	113.2	112.689
C4-Aromatic Distance	5.267	5.136	4.294
O4-Aromatic Distance	6.261	6.117	4.954
N3-Aromatic Distance	5.636	5.598	5.601
H3-Aromatic Distance	6.641	6.591	6.329
C2-Aromatic Distance	5.005	5.025	4.499
O2-Aromatic Distance	5.866	5.931	5.402
N1-Aromatic Distance	3.696	3.714	3.779
H1-Aromatic Distance	3.521	3.648	4.135

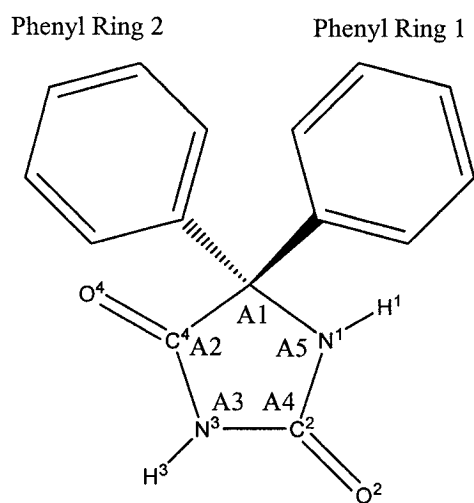


**Figure 41.** Phenytoin with the phenyl rings, angles (A1, A2, A3, A4, A5) and atoms labelled for comparison with the calculated results.

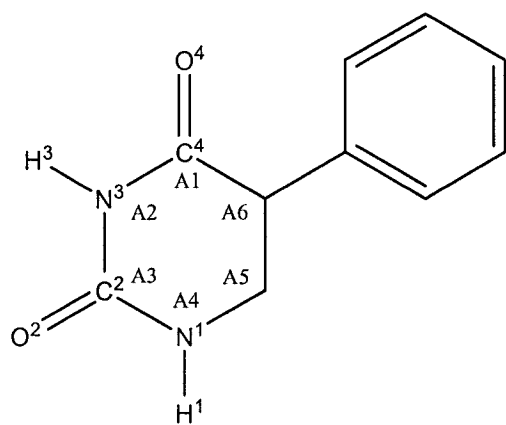


**Figure 42.** 5-Phenyl dihydouracil with the angles (A1, A2, A3, A4, A5, A6) and atoms labelled for comparison with the calculated results.

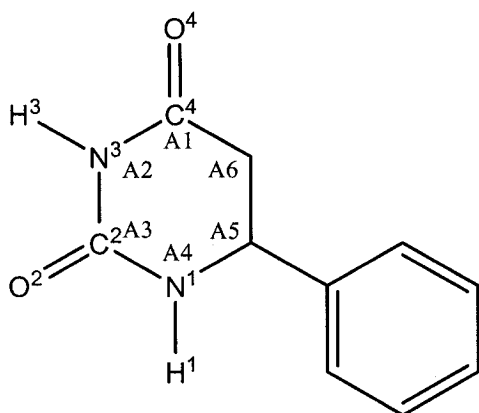


**Figure 43.** 6-Phenyl dihydrouracil with the angles (A1, A2, A3, A4, A5, A6) and atoms labelled for comparison with the calculated results.

#### 8.4 Pharmacophore Discussion

Some of the important points were to compare the pharmacophore unit of phenytoin with that of the dihydrouracil derivatives and to observe if the lengths between the aromatic ring moiety and the amide bond were consistent. Another important aspect of this study was to determine if the toxicophore face of phenytoin was also apparent in the dihydrouracil structure based on ring size and angles [371]. Through previous toxicity studies on rats, it had been found that uracil, dihydrouracil and  $\beta$ -alanine derivatives had a much higher toxicity threshold than phenytoin, potentially indicating the absence of the toxicophore [348, 350]. The final direction of this study was to compare the results between all the energy evaluation techniques and to determine if molecular mechanics could provided statistically similar results to those calculated with semi-empirical and *ab initio*.

#### 8.4.1 Minimization Techniques

The molecular mechanics calculations were completed using the AMBER force field. This force field was chosen since the MM2 force field was unable to minimize phenytoin and the dihydrouracil derivatives due to the torsion angles in the ring structures. AMBER uses a general torsion parameter that is dependent only on the two atoms that comprise the central bond and not the atoms at the terminals [38]. MM2, however, uses the three terms, the central atoms and the terminal atoms, thus making calculations more intense. However since AMBER is able to assign atom types to carbon atoms at the junction between five- and six-membered rings [38], AMBER minimizations could deal with carbon atoms at the junctions in the phenytoin and dihydrouracils rings.

For the semi-empirical calculations the Austin Model 1 (AM1) was utilized since it eliminates the tendency to overestimate repulsions of atoms separated by distances equal to the sum of their van der Waals radii. AM1 parameterization includes terms for carbon (four terms), hydrogen (three terms), nitrogen (three terms) and oxygen (two terms) [38]. By including these Gaussian terms, the number of parameters per atom is increased, improving upon deficiencies with core repulsion and proper atom characterization [38]. The calculations and minimizations using AM1 were completed successfully and did not encounter any parameterization hurdles like the initial MM2 calculations.

The final minimization technique used was an *ab initio* molecular orbital calculation. The STO 6-31G\* basis set was used. In *ab initio* calculations it is common to replace the Slater type orbitals (STO) with functions based upon Gaussians. The general

basis set equation is STO-nG, where n is the number of Gaussian functions used to represent each Slater type orbital [38]. For these calculations, a split valence was used since the core orbitals do not affect chemical properties like the valence orbitals. In this basis set, six Gaussian functions were used to describe the core orbitals. Six Gaussians also described the valence orbitals, with the contracted part by two and the diffuse part by one. Polarization was also applied in the basis set calculations allowing for the mixing of orbitals resulting in a more flexible representation of the molecular orbitals [38]. By addition of these functions and increasing the number of Gaussians, the complexity of the calculation is increased as well as the accuracy.

By comparing the results for each energy evaluation technique found in Table 5, it can be noted that, although each technique varies in its computational time, the results obtained for the distances and angles are all very similar with little variability. The distances for phenytoin, 5-phenyl dihydrouacil, and 6-phenyl dihydrouacil are all within approximately  $0.1 \text{ \AA}$  of each other when comparing the results of each technique. The angles, although still similar, have a larger range of variability between each of the methods. This can be reasoned by the notion that bond lengths are relatively fixed, but ring angles have the ability to be manipulated and still present a minimized conformation with the correct bond lengths. Angles are more flexible and the difference of two or three degrees over  $360^\circ$  is still relative to a change of  $0.1 \text{ \AA}$  in bond lengths.

### 8.4.2 Pharmacophore

Based on the results in comparing the energy evaluation techniques for the molecules, it was concluded that molecular mechanics is a useful tool for evaluating and comparing pharmacophore and toxicophore regions in a molecule. As previously mentioned, the pharmacophore and toxicophore regions both represent sites of activity in a molecule, one with positive effects on a disease and the other promoting unwanted side effects by interacting undesirably with an active site, DNA or with other regions in the body. When attempting to develop new drug treatments, the main goals are to maintain the active component of the drug while eliminating associated toxic side effects. This can only be accomplished by determining the key molecular features of the active face of the molecule as well as those of the toxic effects [371].

Shown in Figure 39 are the pharmacophore and toxicophore of phenytoin. The distances between the aromatic ring (phenyl ring 1) and the carbonyl carbon ( $C^4$ ) and oxygen ( $O^4$ ) as well as the amide nitrogen ( $N^3$ ) and hydrogen ( $H^3$ ) have been determined using AMBER and are presented in Table 26 and Figure 44. These values were found to be  $C^4$ -Aromatic 3.846 Å,  $O^4$ -Aromatic 4.204 Å,  $N^3$ -Aromatic 4.710 Å, and  $H^3$ -Aromatic 5.537 Å.

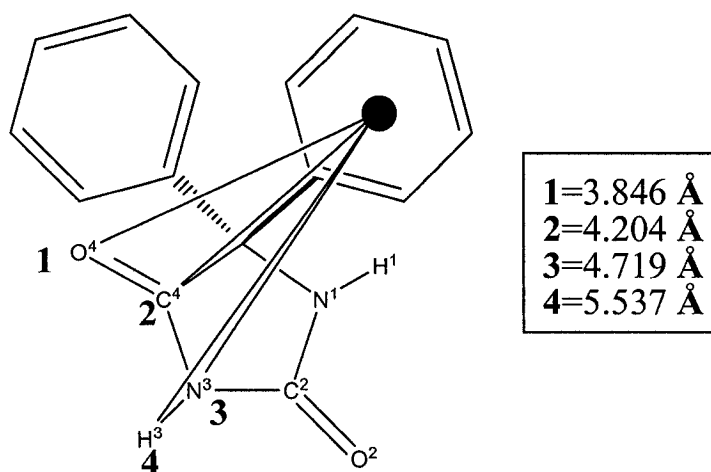


**Figure 44.** Phenytoin with the calculated distance between the atoms and the centroid of the aromatic ring (phenyl 1) determined using AMBER.

These distances were also calculated for 5-phenyl dihydrouacil and 6-phenyl dihydrouacil using AMBER and are presented in Table 26. For 5-phenyl dihydrouacil the distances are C<sup>4</sup>-Aromatic 3.755 Å, O<sup>4</sup>-Aromatic 3.781 Å, N<sup>3</sup>-Aromatic 5.068 Å, and H<sup>3</sup>-Aromatic 5.798 Å . For 6-phenyl dihydrouacil the distances are C<sup>4</sup>-Aromatic 5.267 Å, O<sup>4</sup>-Aromatic 6.261 Å, N<sup>3</sup>-Aromatic 5.636 Å, and H<sup>3</sup>-Aromatic 6.641 Å (Figure 45).

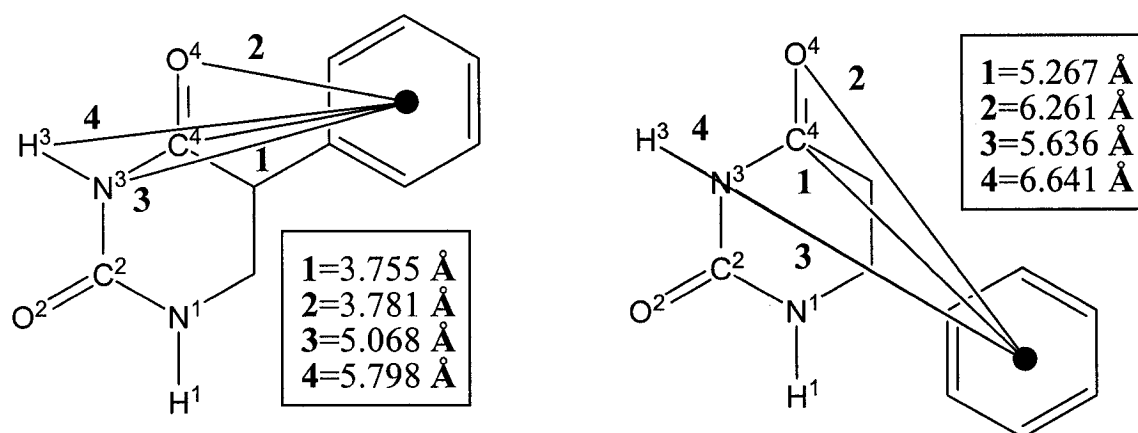


**Figure 45.** 5-Phenyl dihydrouracil and 6-phenyl dihydrouracil with the calculated distance between the atoms and the centroid of the aromatic ring determined using AMBER.

By inspection of these results it can be seen that positioning of the phenyl group is important. When the phenyl ring is in the six position of dihydrouracil, the distances calculated far exceed those determined for phenytoin. When the phenyl ring is in the five position of the dihydrouracil, the distances are quite similar to those of phenytoin. Based on these calculations, 5-phenyldihydrouracil analogue has a similar active face as phenytoin. When the structures are overlapped, the amide bond and aromatic rings in both structures occupy similar regions in space. Based on this information the amide bond, the aromatic ring and the distance between them are important components of the pharmacophore required to bind to the fast-inactivated state of the neuronal sodium channels. Although the distances in 5-phenyldihydrouracil are not exactly the same as those of phenytoin, active sites are not ridged structures and have the ability to accommodate variability in size and 3D shape [400]. Many drugs that are ligand mimics are not identical in shape or size to the natural ligand. However, they are still able to



bind to the active site and elicit biological activity [401]. In many situations it has become apparent that drugs often show a stronger binding affinity for the active site.

#### **8.4.3 Toxicophore**

Biological testing has shown that dihydrouracil compounds have lower toxicity than phenytoin [350]. Based on this information it can be proposed that dihydrouracil analogues do not contain the toxicophore face that is associated with phenytoin. By comparing of the two molecules it can be observed that although they each contain two distinct amide bonds, phenytoin is a five-membered ring system and dihydrouracils are a six membered ring system. Upon comparison of the angles in Figure 46 and Figure 47, the toxicophore face comprised of the angles A3 and A4 varies between the two molecules. The variability in the angles between phenytoin and 5-phenyl dihydrouracil is approximately 10 to 12 degrees. This difference in angles and ring size affects the 3D geometric shape that the molecule retains when it is in its lowest energy conformation [402]. By altering this shape the toxic effects associated with phenytoin do not appear to be a problem with dihydrouracil.

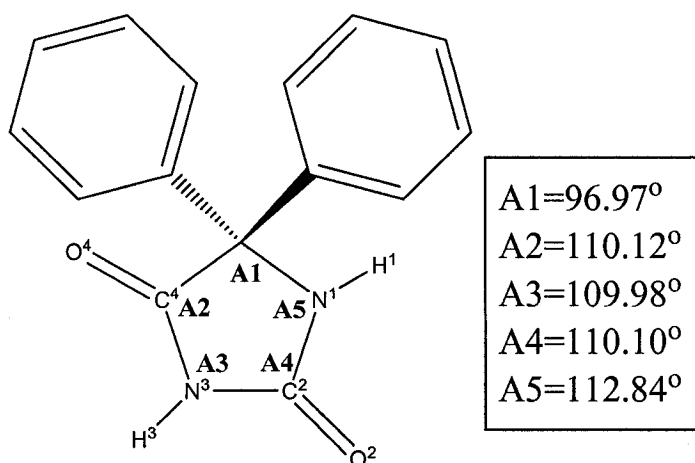


**Figure 46.** The AMBER calculated bond angles of the phenytoin ring, when A3 and A4 are the angles of interest for the toxicophore face.

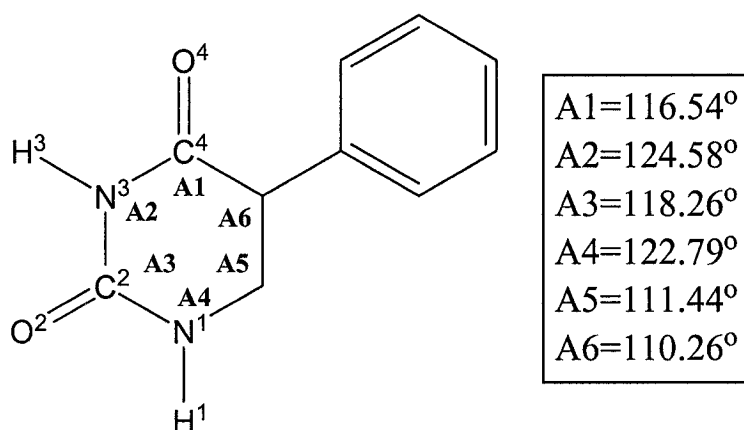


**Figure 47.** The AMBER calculated bond angles of the 5-phenyl dihydrouracil ring, when A3 and A4 are the angles of interest for the toxicophore face.

## 8.5 Conclusions

Based on these minimization results it can be clearly seen that, although molecular mechanics does not obtain the exact results as those found with the more rigorous *ab initio* calculations, they are still similar enough to allow for comparison between molecular structures. Since *ab initio* is a computationally expensive technique and molecular mechanics offers similar results it would be more practical when minimizing a large library of compounds. The AMBER calculations (angles, bond length, molecular distances) can be readily used to determine and search for specific pharmacophore units in molecules.

Although there are metabolic routes available in the body for degradation of dihydrouracil to  $\beta$ -alanine, which has known anticonvulsant activity, it may be that dihydrouracil can cross the BBB and bind to the fast-inactivated state of the neuronal sodium channels in a similar fashion to that of phenytoin. This may be one of the sources of activity of the dihydrouracil analogues, and the others may result from the metabolism of dihydrouracil to its active  $\beta$ -alanine derivative. This pro-drug approach has the capacity to act at several different receptors depending on its metabolic form, therefore allowing for a “first pass effect” followed by a continued protection once fully broken down. By allowing the drug to act at numerous receptors, the possibility of extended protection and lower dosage is possible with dihydrouracils, which may in turn prevent possible dose- dependent toxicity effects. Since dihydrouracil compounds vary slightly in their overall 3D structure when compared to phenytoin, the toxicophore that is associated with the hydantoin derivatives may be manipulated enough in the dihydrouracils so that both the short- and long-term side effects are reduced.

Therefore, in conclusion, studies on hydantoins show that a  $\text{-N(H)-C(=O)-X-}$  **Aromatic** pharmacophore is necessary for anticonvulsant activity mediated via the voltage gated sodium channel. Dihydrouracils contain this pharmacophore with analogous geometric features to hydantoins. Therefore, in theory, dihydrouracils should have anticonvulsant activity prior to being metabolized to the  $\beta$ -amino acids. In this regard, dihydrouracils could be “bioactive” pro-drugs, with the pro-drug exerting a pharmacologic effect prior to metabolic activation.

## **CHAPTER 9**

### **CONCLUSIONS**

---

## 9.1 Summary

The main objective of this thesis was to design novel therapeutics to target epilepsy. Using rational drug design, two new classes of molecules were developed to target the biological processes of ictogenesis and epileptogenesis. The drug scaffolds were generated using specific endogenous molecules that were considered to be involved in influencing the CNS and the biochemical cascades associated with the development of a seizure and/or seizure focus.

## 9.2 Endogenous Anti-Ictogenics

Nicotinamide, an endogenous molecule, was used as the chemical scaffold around which 50 nicotinamide analogues were developed. These compounds were developed to target two different receptors, the voltage-gated sodium channel and the GABA<sub>A</sub> benzodiazepine receptor, which are both involved in controlling the process of ictogenesis. Nicotinamide has scaffold properties that show strong similarities to the experimentally determined phenytoin pharmacophore (-N(H)-C(=O)-X-aromatic). Using this pharmacophore, novel nicotinamide analogues were developed and synthesized. Through the biological results it was found that nicotinamide analogues have the ability to influence the process of ictogenesis by influencing the voltage-gated sodium channel and the GABA<sub>A</sub> benzodiazepine receptor. By allowing the nicotinamide analogues to interact at numerous receptors the goal was to have a novel drug that can target different types of epilepsy, therefore being a broad-spectrum comprehensive treatment.

### 9.3 Anti-Ictogenics/Antiepileptogenics: A Novel “Bioactive” Pro-drug

Dihydrouracil analogues can be endogenously metabolized to produce  $\beta$ -amino acid derivatives, which have been shown to influence the process of epileptogenesis. By using dihydrouracil as a pro-drug approach, the goal was to develop a series of 6-aryl dihydrouracil analogues, which could be metabolized to the specific  $\beta$ -aryl- $\beta$ -amino acids that have previously shown antiepileptogenic properties.

Upon examination of the anti-ictogenic biological testing it was determined that dihydrouracil analogues have the ability to act as anti-ictogenics. This anticonvulsant activity was theoretically a result of the dihydrouracil analogues influencing the voltage-gated sodium channel prior to being metabolized to  $\beta$ -amino acids. Due to this capability, dihydrouracils are a “bioactive” pro-drug, meaning the pro-drug exerts a pharmacologic effect prior to metabolic activation. This concept is a novel development in the area of drug design.

### 9.4 Future Directions

After consideration of the projects completed for this thesis, the next goal would be to continue to pursue the development of new nicotinamide analogues to target ictogenesis. Based on the results of the QSAR analysis, having an aromatic/bulky group in the  $R^1/R^2$  position is important for the development of molecules with bioactivity. Using this nicotinamide as the base scaffold, the next direction that will be to target both the voltage-gated sodium channel and the GABA<sub>A</sub>-benzodiazepine receptor and investigate the introduction of other substituents to the 2' position of the pyridine ring. Through the initial biological screening it was found experimentally that this position had

the ability to influence the GABA<sub>A</sub>-benzodiazepine receptor. The next goal would be further optimize the 2-(benzylsulfinyl)nicotinamides, in attempts to determine which groups are required for activity. These chemical alterations would include substituting the benzyl moiety with EWG and EDG's as well as introducing a variety of aromatics to the nitrogen of the amide bond (Figure 48, Compound 1).

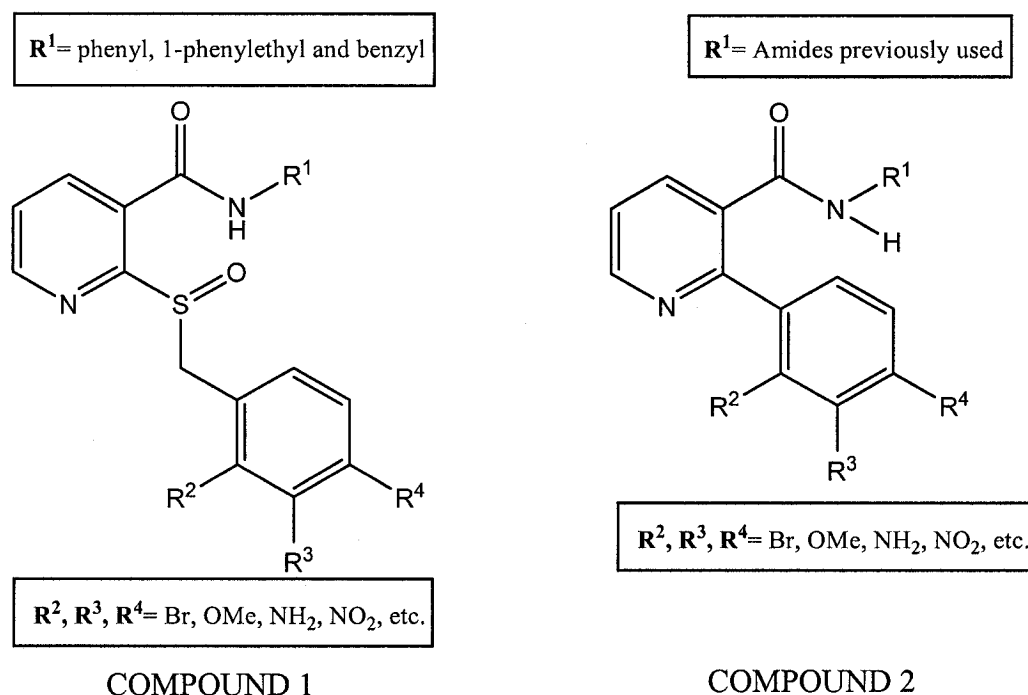


**Figure 48.** The scaffold of the next compounds to be developed in the nicotinamide series.

Other alterations to the 2' position should include the introduction of a substituted phenyl group (Figure 48, Compound 2). By targeting this position the hope is to develop an analogue that will have the ability to interact with two distinct receptors in the CNS, leading to the development of a compound that has the ability to treat various types of epilepsy.



## APPENDIX

---

### Methods Used To Produce Figure 26

Experiments completed by Kelly Stevens and Steven Barnes, Department of Physiology & Biophysics, Dalhousie University

Mouse eyes were fixed in 4% paraformaldehyde overnight at 4 °C and then placed in a 30% sucrose solution for 1-2 days at 4 °C. Following fixation, individual eyes were embedded in Tissue-Tek OCT compound (Sakura Finetek Inc., Torrance, CA). The entire retina was transversely cut on a Leica Cryocut 3000 freezing cryostat into 14 µm thick sections. Retinal sections were mounted on Superfrost Plus slides (silane treated glass microscope slides). The following procedures were carried out at room temperature. First, sections were rinsed with phosphate-buffered saline (PBS) and 3% Triton X-100 and then incubated in a solution of PBS containing 10% normal goat serum for 1 hour. The sections were then placed in fresh PBS containing the primary antibody rabbit anti-β-alanine (QED Bioscience Inc., San Diego CA) at 1:500 dilution overnight at 4 °C. The retinal sections were rinsed for 10 min in PBS and then incubated in the secondary antibody, AlexaFluor 546-conjugated goat anti-rabbit IgG (H+L) (Molecular Probes, Burlington ON) for 1 h at room temperature. Sections were then rinsed in PBS (3 x 10 min) at room temperature and coverslipped with 0 thickness coverslips. The control for staining specificity was performed by omitting the primary antibody. β-Alanine immunoreactive retinal sections were visualized with a laser-scanning confocal microscope (Nikon C-1) in 1 µm optical sections with a 40x oil immersion lens.

## REFERENCES

---

1. Engel, J. and Pedley, T. A., *Epilepsy: A Comprehensive Textbook*, Lippincott-Raven, Philadelphia, 1997.
2. Dam, M., *A Practical Guide to Epilepsy*, Pergamon Press Inc., New York, 1991.
3. Siegel, G., Agranoff, B., Albers, R. W. and Molinoff, P., *Basic Neurochemistry*, Raven Press, New York, 1989.
4. Treiman, D. M., *Epilepsia*, **2001**, 42 Suppl 3, 8.
5. Caldwell, J. H., Schallen, K., Lasher, R., Peles, E. and Levinson, R. S., *Proc. Nat. Acad. Sci.*, **2000**, 97, 5616.
6. French, J., Leppik, I. and Dichter, M. A., *Anti-epileptic Drug Development Advances in Neurology*, Lippincott-Raven, Philadelphia, 1998.
7. Wallance, R. H., Wang, D. W., Singh, R., Scheffer, I. E., Phillips, H. A., Saar, K., Reis, A., Sutherland, G., Berkovic, S. F., George, A. and Mulley, J. C., *Nature Genet.*, **1998**, 19, 366.
8. Carter, A. J., *Drugs of the Future*, **1992**, 17, 595.
9. Jursky, F. and Nelson, N., *J. Neurosci. Res.*, **1999**, 55, 394.
10. Bengzon, J., Okabe, S., Lindvall, O. and McKay, R. D., *Eur. J. Neurosci.*, **1999**, 11, 916.
11. Sutula, T., He, X. X., Cavazos, J. and Scott, G., *Science*, **1988**, 239, 1147.
12. Tamura, S., Nelson, A., Tamura, A. and Nelson, N., *J. Biol. Chem.*, **1995**, 270, 28712.
13. Pardridge, W. M., *Annu. Rep. Med. Chem.*, **1984**, 20, 305.
14. Cecchelli, R., Dehouck, B., Descamps, L., Fenart, L., Buee-Scherrer, V. V., Duhem, C., Lundquist, S., Rentfel, M., Torpier, G. and Dehouck, M. P., *Adv. Drug. Deliv. Rev.*, **1999**, 36, 165.
15. Riviello, J. J., *Curr. Neurol. Neurosci. Rep.*, **2003**, 3, 325.
16. Glass, M. and Drgunow, M., *Brain Res. Brain. Res. Rev.*, **1995**, 21, 29.
17. Wasterlain, C. G. and Shirasaka, Y., *Brain Dev.*, **1994**, 16, 279.

18. Mattson, R. H., Petroff, O. A., Rothman, D. and Behar, K., *Acta. Neuronal Scandinavia (Supp)*, **1995**, 162, 27.
19. Kwan, P., Sills, G. J. and Brodie, M. J., *Pharmacol. Ther.*, **2001**, 90, 21.
20. Avanzini, G., Regesta, G., Tanganelli, P. and Avoli, M., *Molecular and Cellular Targets for Anti-Epileptic Drugs*, John Libbey and Company Inc., New York, 1997.
21. Brodie, M. J. and Dichter, M. A., *Seizure*, **1997**, 6, 159.
22. Olsen, R. W. and Avoli, M., *Epilepsia*, **1997**, 38, 399.
23. Dichter, M. A. and Brodie, M. J., *New Engl. J. Med.*, **1996**, 334, 1583.
24. French, J., Edrich, P. and Cramer, J., *Epilepsia Res.*, **2001**, 47, 77.
25. McLean, M. J. and McDonald, R. L., *J. Pharmacol. Exp. Ther.*, **1983**, 227, 779.
26. Stables, J. P. and Kupferberg, J., The NIH anticonvulsant drug development (ADD) program: Preclinical anticonvulsant screening program, In *Molecular and Cellular Targets for Anti-epileptic Drugs*, John Libbey and Company, New York, 1997, 191.
27. Bernard, C., Cossart, R., Hirsch, J. C., Esclapez, M. and Ben-Ari, Y., *Epilepsia*, **2000**, 41 Suppl 6, S90.
28. Leeson, P. D. and Iversen, L. L., *J. Med. Chem.*, **1994**, 37, 4053.
29. Dichter, M. A., *Epilepsia (Suppl 9)*, **1997**, 38, 2.
30. Thompson, K., Anantharam, V., Behrstock, S., Bongarzone, E., Campagnoni, A. and Tobin, A. J., *Exp. Neurol.*, **2000**, 161, 481.
31. Dragunow, M., *Neurosci. Biobehav. Rev.*, **1986**, 10, 229.
32. Bajorek, J. G., Lee, R. J. and P., L., *Adv. Neurol.*, **1986**, 44, 489.
33. Bajorek, J. G., Lee, R. J. and Lomax, P., *Ann. Neurol. (Suppl)*, **1984**, 16, 31.
34. Drews, J., *Science*, **2000**, 287, 1960.
35. Wess, G., Urmann, M. and Sickenberger, B., *Angew. Chem. Int. Ed. Engl.*, **2001**, 40, 3341.
36. Nogrady, T. and Weaver, D. F., *Medicinal Chemistry: A Molecular and Biochemical Approach*, Oxford University Press Inc., Oxford, 2005.
37. Patani, G. A. and LaVoie, E. J., *Chem. Rev.*, **1996**, 96, 3147.

38. Leach, A. R., *Molecular Modelling Principles and Applications*, Prentice Hall, Harlow, 2001.
39. Pickett, S. D., Mason, J. S. and McLay, A. M., *J. Chem. Info. Comp. Sci.*, **1996**, *36*, 1214.
40. Lipinski, C. A., Lombardo, F., Dominy, B. and Feeney, P., *Adv. Drug Deliv. Rev.*, **1997**, *23*, 3.
41. Smith, D., Absorption and distribution as factors in drug design, In *Medicinal Chemistry into the Millennium*, Royal Society of Chemistry, Cambridge, 1998, 331.
42. Shaw, J. E., *Annu. Rep. Med. Chem.*, **1980**, *15*, 302.
43. Sinkula, A. A., *Annu. Rep. Med. Chem.*, **1975**, *10*, 306.
44. Henderson, N. L., *Annu. Rep. Med. Chem.*, **1983**, *18*, 275.
45. Poznansky, M. J. and Juliano, R. L., *Pharmacol. Rev.*, **1984**, *36*, 277.
46. Bodor, N., Novel approaches to the design of safer drugs: soft drugs and site-specific delivery systems, In *Advanced Drug Research*, Academic Press, New York, 1984, 255.
47. Beck, L. R. and Pope, V. Z., *Drugs*, **1982**, *27*, 528.
48. Merritt, H. H., *Arch. Neurol. Psychiat.*, **1938**, *39*, 1003.
49. Dichter, M. A., *Adv. Neurol.*, **1998**, *76*, 1.
50. Coddington, P. W., Lee, T. A. and Richardson, J. F., *J. Med. Chem.*, **1984**, *27*, 649.
51. Weaver, D. F., *Seizure*, **1993**, *1*, 223.
52. Boyd, W. J., *Biochem. J.*, **1933**, *26*, 1838.
53. French, G., *Arch. Pharm.*, **1905**, *243*, 684.
54. Finkbeiner, H. L. and Stiles, M., *J. Am. Chem. Soc.*, **1963**, *85*, 616.
55. Finkbeiner, H. L., *J. Org. Chem.*, **1965**, *30*, 3414.
56. Aschan, O., *Chem. Ber.*, **1883**, *16*, 1544.
57. Fischer, E., *Chem. Ber.*, **1900**, *33*, 2370.
58. Dunnivant, W. R. and James, F. L., *J. Am. Chem. Soc.*, **1956**, *78*, 2740.

59. Close, W. J., Doub, L. and Spielman, M. A., *J. Med. Chem.*, **1961**, 5, 1.
60. Lyon, A. P., Wainman, D., Marone, S. and Weaver, D. F., *Seizure*, **2004**, 13, 82.
61. Lyon, A. P., Wainman, D., Marone, S. and Weaver, D. F., *Can. J. Neurol. Sci.*, **2005**, 32, 97.
62. Turski, L., Ikonomidou, C., Turski, W. A., Bortolotto, Z. A. and Cavalheiro, E. A., *Synapse*, **1989**, 3, 154.
63. Chem 3D Ultra, Version 8.0, Chem Office, 2004.
64. Fujiwara, H., Bose, A. K., Manhas, M. S. and van der Veen, J. M., *J. Chem. Soc. Perkin Trans. II.*, **1979**, 653.
65. Fujiwara, H. and van der Veen, J. M., *J. Chem. Soc. Perkin Trans. II.*, **1979**, 659.
66. Robinson, R. and Jencks, W. P., *J. Am. Chem. Soc.*, **1965**, 87, 2470.
67. Crowley, C. L., Payne, C. M. and Bernstein, H., *Cell Death Differ.*, **2000**, 7, 314.
68. Petley, A., Macklin, B., Renwick, A. G. and Wilkin, T. J., *Diabetes*, **1995**, 44, 152.
69. Parkhomets, P. K., Kuchmerovaskaya, T. M., Donchenko, G., Chichkovakaya, G. and Klimenko, A., *Ukrain. Bio. Zhur.*, **1995**, 67, 3.
70. Kryshanovskii, G. and Shandra, A., *Fam. Tok.*, **1985**, 48, 21.
71. Bourgeois, B. F. D., Dodson, W. E. and Ferrendelli, J. A., *Epilepsia*, **1983**, 24, 238.
72. Kryshanovskii, G., Shandra, A., Godlevskii, L. and Nikushkin, E., *Byu. Eks. Bio. Med.*, **1982**, 94, 61.
73. Kryshanovskii, G., Shandra, A. and Godlevskii, L., *Byu. Eks. Bio. Med.*, **1984**, 98, 150.
74. Maitre, M., Ciesielski, L., Lehmann, A., Kempf, E. and Mandel, P., *Biochem. Pharm.*, **1974**, 23, 2807.
75. Braslavskii, V., Shchhavelev, V., Kryshanovskii, G., Nikushkin, E. and Germanov, S., *Byu. Eks. Bio. Med.*, **1982**, 94, 39.
76. Spivak, J. L. and Jackson, D. L., *Johns Hopkins Med. J.*, **1977**, 140, 295.
77. Kertesz, S. G., *Mayo Clin. Proc.*, **2001**, 76, 315.
78. Carpenter, K. J. and Lewin, W. J., *J. Nutr.*, **1985**, 115, 543.

79. Dimmock, J. R., Sidhu, K. K., Thayer, R. S., Mack, P., Duffy, M., Reid, R., Quail, J. W., Pugazhenth, U., Ong, A., Bikker, J. and Weaver, D. F., *J. Med. Chem.*, **1993**, 36, 2243.
80. Dimmock, J. R., Puthucode, R. N., Smith, J., Hetherington, M., Quail, J. W., Pugazhenth, U., Lechler, T. and Stables, J. P., *J. Med. Chem.*, **1996**, 39, 3984.
81. Pandeya, S., Yogeeswari, P. and Stables, J. P., *Eur. J. Med.*, **2000**, 2000, 879.
82. Puthucode, R. N., Pugazhenth, U., Quail, J. W., Stables, J. P. and Dimmock, J. R., *Eur. J. Med. Chem.*, **1998**, 33, 595.
83. Dimmock, J. R., Vashishtha, S. C. and Stables, J. P., *Eur. J. Med. Chem.*, **2000**, 35, 241.
84. Murray, W. J. and Keir, L. B., *J. Med. Chem.*, **1977**, 15, 591.
85. Iwaanami, S., Takashima, M., Hirata, Y., Hasegawa, O. and Usuda, S., *J. Med. Chem.*, **1981**, 24, 1224.
86. Sergusa, J., Garcia, I., Borja, L., Tarrus, E. and Bakke, O., *J. Pharm. Pharmacol.*, **1981**, 33, 214.
87. Schulze-Delrieu, K., *N. Engl. J. Med.*, **1981**, 305, 28.
88. Clark, C., Wells, M., Samson, R., Norris, G., Dockens, R. and Ravis, W., *J. Med. Chem.*, **1984**, 27, 779.
89. Braun, M. and Waldmuller, D., *Synthesis*, **1989**, 856.
90. Tunoori, A., White, J. and Georg, G., *Org. Lett.*, **2000**, 2, 4091.
91. Neises, B. and Steglich, W., *Angew. Chem. Int. Ed. Engl.*, **1978**, 17, 522.
92. Seitz, L. E., Suling, W. and Reynolds, R. C., *J. Med. Chem.*, **2002**, 45, 5604.
93. Kim, Y. K., Lee, S. J. and Ahn, K. H., *J. Org. Chem.*, **2000**, 65, 7807.
94. Dugas, H. and Penney, C. L., *Bioorganic Chemistry; A Chemical Approach to Enzyme Action*, Springer-Verlag, New York, 1981.
95. Zacharie, B., Connolly, T. P. and Penney, C. L., *J. Org. Chem.*, **1995**, 60, 7072.
96. Belleau, B. and Malek, G., *J. Am. Chem. Soc.*, **1968**, 90, 1651.
97. Kitagausa, D. and Tokujiro, K., *Chem. Pharm. Bulletin*, **1987**, 35, 294.
98. Stanovik, B., *J. Heterocycl. Chem.*, **1980**, 17, 733.

99. Parmer, S., Ali, B. and Dwivedi, C., *J. Med. Chem.*, **1972**, *15*, 846.
100. Sonntag, N. O., *Chem. Rev.*, **1953**, *52*, 237.
101. Shioiri, T., Ninomiya, K. and Yamada, S., *J. Am. Chem. Soc.*, **1972**, *94*, 6203.
102. Qian, L., Sun, Z., Deffo, T. and Mertes, K., *Tetrahedron Lett.*, **1990**, *31*, 6469.
103. Cazaux, L., Duriez, M., Picard, C. and Tisnes, P., *Tetrahedron Lett.*, **1989**, *30*, 1369.
104. Gilman, H. and Broadbent, H. S., *J. Am. Chem. Soc.*, **1948**, 2755.
105. Wojtczak, A., Cody, V., Luft, J. R. and Pangborn, W., *Acta. Crystallogr. D.*, **2001**, *57*, 1061.
106. Auffinger, P., Hays, F. A., Westhof, E. and Shing Ho, P., *Proc. Nat. Acad. Sci.*, **2004**, *48*, 16789.
107. van Pée, K. H. and Unversucht, S., *Chemosphere*, **2003**, *52*, 299.
108. Gerebtzoff, G., Liblatter, X., Fischer, H., Frentzel, A. and Seelig, A., *Chembiochem*, **2004**, *5*, 676.
109. Böhm, H. J., Banner, D., Bendels, S., Kansy, M., Kuhn, B., Müller, K., Obst-Sander, U. and Stahl, M., *Chembiochem*, **2004**, *5*, 637.
110. Smith, D. H., van de Waterbeem, H. and Walker, D. K., *Pharmacokinetics and Metabolism in Drug Design, Methods and Principles in Medicinal Chemistry*, Wiley-VCH, Weinheim, 2001.
111. Lommerse, J. P. M., Stone, A. J., Taylor, R. and Allen, F. H., *J. Am. Chem. Soc.*, **1996**, *118*, 3108.
112. Chou, Y., Davey, D. D., Eagen, K. A., Greidel, B. D., Karanjawala, R., Phillips, G. B., Sacchi, K. L., Shaw, K. J., Wu, S. C., Lentz, D., Liang, A. M., Trinh, L., Morrissey, M. M. and Kochanny, M. J., *Bioorg. Med. Chem. Lett.*, **2003**, *13*, 507.
113. Bachman, G. B. and Micucci, D. D., *J. Am. Chem. Soc.*, **1948**, *70*, 2381.
114. Mikroyannidis, J. A., Barberis, V. P., Ding, L. and Karasz, F. E., *J. Poly. Sci. Part A: Poly. Chem.*, **2004**, *42*, 3212.
115. Thompson, W. J. and Gaudino, J., *J. Org. Chem.*, **1984**, *49*, 5237.
116. Yao, Q., Kinnew, E. P. and Yng, Z., *J. Org. Chem.*, **2004**, *68*, 7528.
117. Heck, R. F. and Nolley, J. P., *J. Org. Chem.*, **1972**, *37*, 2320.

118. Littke, A. F. and Fu, G. C., *J. Am. Chem. Soc.*, **2001**, *123*, 6989.
119. Haberli, A. and Leumann, C. J., *Org. Lett.*, **2001**, *3*, 489.
120. Miyaura, N. and Suzuki, A., *Chem. Rev.*, **1995**, *95*, 2457.
121. Miyaura, N., Yanagi, T. and Suzuki, A., *Synth. Commun.*, **1981**, *11*, 513.
122. Navarro, O., Kelly, R. A. and Nolan, S. P., *J. Am. Chem. Soc.*, **2003**, *125*, 16194.
123. Suzuki, A., Metal-Catalyzed Cross Coupling Reactions, Chapter 2, In Wiley-VCH, Weinheim, Germany, 1998,
124. Parry, P. R., Wang, C., Batsanov, A. S., Bryce, M. R. and Tarbit, B., *J. Org. Chem.*, **2002**, *67*, 7541.
125. Miyaura, N. and Suzuki, A., *J. Chem. Soc., Chem. Commun.*, **1979**, 866.
126. Suzuki, A., *Pure & App. Chem.*, **1985**, *57*, 1149.
127. Wallow, T. I. and Novak, B. M., *J. Org. Chem.*, **1994**, *59*, 5034.
128. Oh-e, T., Miyaura, N. and Suzuki, A., *J. Org. Chem.*, **1993**, *58*, 2201.
129. Matos, K. and Soderquist, J. A., *J. Org. Chem.*, **1998**, *63*, 461.
130. Heynderickx, A., Samat, A. and Guglielmetti, R., *Synthesis*, **2002**, *2*, 213.
131. Doble, A. and Martin, I. L., The GABA<sub>A</sub>/ Benzodiazepine Receptor as a Target for Psychoactive Drugs, Landes, Austin, TX, 1996.
132. Smith, G. B. and Olsen, R. W., *Trends Pharmacol. Sci.*, **1995**, *16*,
133. Sigel, E. and Buhr, A., *Trends Pharmacol. Sci.*, **1997**, *18*, 425.
134. Kucken, A. M., Teissere, J. A., Seffinga-Clark, J., Wagner, D. A. and Czajkowski, C., *Mol. Pharmacol.*, **2003**, *63*, 289.
135. Teissere, J. A. and Czajkowski, C., *J. Neurosci.*, **2001**, *21*, 4977.
136. Squires, R. F., GABA and benzodiazepine receptors, CRC Press, Inc., Boca Raton, Florida, 1987.
137. Olsen, R. W. and Venter, J. C., Benzodiazepine/ GABA receptors and chloride channels, In *Receptor Biochemistry and Methodology*, Alan R. Liss, Inc., New York, 1986,
138. SYBYL 7.2 Molecular Modeling Software, Version 7.2, 1994.



139. Jana, N. K. and Verkade, J. G., *Org. Lett.*, **2003**, 5, 3787.
140. Madesclaire, M., *Tetrahedron*, **1986**, 42, 5459.
141. Wilson, S. R., Phillips, L. R., Pelister, Y. and Huffman, J. C., *J. Am. Chem. Soc.*, **1979**, 101, 7373.
142. Lopez-Rodriguez, M. L., Morcillo, M. J., Fernandez, E., Rosado, M. L., Pardo, L. and Schaper, K., *J. Med. Chem.*, **2001**, 44, 198.
143. Dunn, W. J. and Wold, S., Pattern recognition techniques in drug design, In *Comprehensive Medicinal Chemistry*, Oxford, Pergamon Press, 1990, 173.
144. Knight, J. L. and Weaver, D. F., *Seizure*, **1998**, 7, 347.
145. Bocker, A., Derksen, S., Schmidt, E., Teckentrup, A. and Schneider, G., *J. Chem. Inf. Model*, **2005**, 45, 807.
146. Hansch, C. and Fujita, T., *J. Am. Chem. Soc.*, **1964**, 86, 1616.
147. Hansch, C., Steward, A. R., Anderson, S. M. and Bentley, D., *J. Med. Chem.*, **1967**, 11, 1.
148. Wold, S., Dunn, W. J. and Hellberg, S., Pattern recognition as a tool for drug design, In *Drug Design: Fact or Fiction*, Academic Press, London, 1984, 95.
149. Wold, S. and Dunn, W. J., *J. Chem. Info. Comp. Sci.*, **1983**, 23, 6.
150. Stuper, A. J. and Jurs, P. C., *J. Am. Chem. Soc.*, **1975**, 97, 187.
151. Kirschner, G. L. and Kowalski, B. R., The application of pattern recognition to drug design, In *Drug Design*, Academic Press, New York, 1979, 73.
152. Shen, M., LeTiran, A., Xiao, Y., Golbraikh, A., Kohn, H. and Tropsha, A., *J. Med. Chem.*, **2002**, 45, 2811.
153. Trapani, G., Latrofa, A., Franco, M., Altomare, C., Sanna, E., Usala, M., Biggio, G. and Liso, G., *J. Med. Chem.*, **1998**, 41, 1846.
154. Lopez-Rodriguez, M. L., Rosado, M. L., Benhamu, B., Morcillo, M. J., Fernandez, E. and Schaper, K., *J. Med. Chem.*, **1997**, 40,
155. Shen, M., Beguin, C., Golbraikh, A., Stables, J. P., Kohn, H. and Tropsha, A., *J. Med. Chem.*, **2004**, 47, 2356.
156. Cramer, R. D., Patterson, D. E. and Bunce, J. D., *J. Am. Chem. Soc.*, **1988**, 110, 5959.
157. Klebe, G., Abraham, U. and Mietzner, T., *J. Med. Chem.*, **1994**, 37, 4130.

158. Bohm, M., Sturzebecher, J. and Klebe, G., *J. Med. Chem.*, **1999**, 42, 458.
159. Tropsha, A., Cho, S. J. and Zheng, W., "New tricks for an old dog": Development and application of novel QSAR methods for rational drug design of combinatorial chemical libraries and database mining, ACS Symposium Series 719: American Chemical Society, 1999, Washington, DC.
160. Ghose, A. K., Viswanadhan, V. N. and Wendoloski, J. J., *J. Phys. Chem.*, **1998**, 102, 3762.
161. Todeschini, R., Cazar, R. and Collina, E., *Chemo. Int. Lab. Sys.*, **1992**, 15, 51.
162. Piredda, S. G., Woodhead, J. H. and Swinyard, E. A., *J. Pharmacol. Exp. Ther.*, **1985**, 232, 741.
163. Barton, M. E., Klein, B. D., Wolf, H. H. and White, H. S., *Epilepsy Res.*, **2001**, 47, 217.
164. Abou-Khalil, B., Nasreddine, W., Fakhoury, T., Atkinson, D. and Beydoun, A., *Epilepsia*, **1996**, 169.
165. Cameron, N., Penovich, P. E., Ritter, F. J. and Espe-Lillo, J., *Epilepsia*, **1996**, 37 (S5), 169.
166. Shorvon, S., Janz, D., Loiseau, P., Lowenthal, A., Bielen, E. and Johnscer, G., *Epilepsia*, **1996**, 37 (S5), 170.
167. van Rijckevorsel, K., Debrabandere, L. and Deberdt, W., *Epilepsia*, **1996**, 37 (S5), 169.
168. Toman, J. E. P., Everett, G. M. and Richards, R. K., *Tex. Rep. Biol. Med.*, **1952**, 10, 96.
169. Toman, J. E. P., *Neurology*, **1951**, 1, 444.
170. Brown, L. B., Zha, C., c, Van Dyke, C. C., Brown, G. B. and Brouillette, W. J., *J. Med. Chem.*, **1999**, 42, 1537.
171. Krasowski, M. D. and Harrison, N. L., *Cell. Mol. Life Sci.*, **1999**, 55, 1278.
172. Sriver, C. R., Pueschel, S. and Davies, E., *New Eng. J. Med.*, **1966**, 274, 635.
173. DeFeudis, F. V. and Martin del Rio, R., *Gen. Pharmacol.*, **1977**, 8, 177.
174. Hayaishi, O., Nishizuka, Y., Tatibana, M., Takeshita, M. and Kuno, S., *J. Biol. Chem.*, **1961**, 236,
175. Cronan, J. E., *J. Bacteriol.*, **1980**, 141, 1291.

176. Traut, T. W. and Loechel, S., *Biochemistry*, **1984**, 23, 2533.
177. Van Gennip, A. H., Abeling, N. G., Vreken, P. and Van Kuilenburg, A. B., *J. Inher. Metab. Dis.*, **1997**, 20, 203.
178. Kupiecki, F. P. and Coon, M. J., *J. Biol. Chem.*, **1957**, 229, 743.
179. Greier, A. and Yamasaki, S., *J. Neurochem.*, **1956**, 1, 93.
180. Kihara, M., Misu, Y. and Kubo, T., *Life Sci.*, **1988**, 42, 1817.
181. Baxter, C. and Roberts, E., *J. Biol. Chem.*, **1958**, 233, 1135.
182. Chambliss, K. L., Gray, R. G., Rylance, G., Pollitt, R. J. and Gibson, K. M., *J. Inherit. Metab. Dis.*, **2000**, 23, 497.
183. Van Kuilenburg, A. B., Stroomer, A. E., Van Lenthe, H., Abeling, N. G. and Van Gennip, A. H., *Biochem.*, **2004**, 379, 119.
184. Chen, Z., Wu, J., Baker, G. B., Parent, M. and Dovichi, N. J., *J. Chromatog. A*, **2001**, 914, 293–298.
185. Komura, J., Tamai, I., Senmaru, M., Terasaki, T., Sai, Y. and Tsuji, A., *J. Neurochem.*, **1996**, 67, 330.
186. Williams, M., Risley, E. A. and Totaro, J. A., *Life Sci.*, **1979**, 26, 557.
187. Martin Del Rio, R., Munoz, L. M. and DeFreudis, F. V., *Exp. Brain Res.*, **1977**, 28, 225.
188. Chesney, R. W., Zelikovic, I., Dabbagh, S., Friedman, A. and Lippincott, S., *J. Exp. Zool.*, **1988**, 248, 25.
189. Thwaites, D. T., McEwan, G. T., Brown, C. D., Hirst, B. H. and Simmons, N. L., *J. Biol. Chem.*, **1993**, 268, 18438.
190. Dunnett, M. and Harris, R. C., *Equine Vet. J. Suppl.*, **1999**, 30, 499.
191. Jessen, H., *Biochim. Biophys. Acta.*, **1994**, 1194, 44.
192. Miyamoto, Y., Balkovetz, D. F., Leibach, F. H., Mahesh, V. B. and Ganapathy, V., *FEBS Lett.*, **1988**, 231, 263.
193. Abe, T., Kurozumi, Y., Yao, W. and Ubuka, T., *J. Chromatogr. B*, **1998**, 712, 43.
194. Castets, J. C., Parvy, P., Allard, D. and Huang, Y., *Tijd. Belg. Veren. Labor.*, **1980**, 1, 33.

195. Chang, J. Y., Martin, P., Bernasconi, R. and Braun, D. G., *FEBS Lett.*, **1981**, 132, 117.
196. Christensen, H., *J. Biol. Chem.*, **1964**, 239, 3584.
197. Christensen, H., Hess, B. and R., R. T., *Cancer Res.*, **1954**, 14, 124.
198. Drescher, M. J., Medina, J. E. and Drescher, D. G., *Anal. Biochem.*, **1981**, 116, 280.
199. Ferraro, T. N. and Hare, T. A., *Brain Res.*, **1985**, 338, 53.
200. Grove, J., Schechter, P. J., Tell, G., Koch-Weser, J., Sjoerdsma, A., Warter, J. M., Marescaux, C. and Rumbach, L., *Life Sci.*, **1981**, 28, 2431.
201. Bakardjiev, A. and Bauer, K., *Eur. J. Biochem.*, **1994**, 225, 617.
202. Turner, J., *J. Biol. Chem.*, **1986**, 261, 16060.
203. Holopainen, I., *Neurochem. Res.*, **1988**, 13, 853.
204. Holopainen, I. and Kontro, P., *Neurochem. Res.*, **1986**, 11, 207.
205. Hofmann, U., Schwab, M., Seefried, S., Marx, C., Zanger, U. M., Eichelbaum, M. and Mürdter, T. E., *J. Chromatogr. B*, **2003**, 791, 371–380.
206. Pasieka, A. E. and Thomas, M. E., *Clin. Biochem.*, **1969**, 2, 423.
207. Munck, L. K. and Munck, B. G., *Am. J. Physiol.*, **1992**, 262, G609.
208. Miyamoto, Y., Nakamura, H., Hoshi, T., Ganapathy, V. and Leibach, F. H., *Am. J. Physiol.*, **1990**, 259, G372.
209. Cocuzza, S. and Lumare, A., *Minerva Pediatrica*, **1966**, 18, 1486.
210. Chang, K. J., *Adv. Exp. Med. Biol.*, **2000**, 483, 571.
211. Wheeler, D. D. and Hollingsworth, R. G., *J. Neurosci. Res.*, **1979**, 4, 265.
212. Kontro, P., *Neurochem. Res.*, **1982**, 7, 1391.
213. Kontro, P. and Oja, S. S., *Neuroscience*, **1978**, 3, 761.
214. Kontro, P. and Oja, S. S., *J. Neurochem.*, **1981**, 37, 297.
215. Martin, D. L. and Smith, A. A., *J. Neurochem.*, **1972**, 19, 841.
216. Logan, W. J. and Snyder, S. H., *Brain Res.*, **1972**, 42, 413.

217. Orendanz, L. M., DeFeudis, F. V. and Fando, J. L., *Neuropharmacology*, **1977**, 16, 537.
218. Wheeler, D. D., *Pharmacology*, **1980**, 21, 141.
219. Wheeler, D. D., *J. Neurosci. Res.*, **1980**, 5,
220. Larsson, O., Hertz, L. and Schousboe, A., *J. Neurosci. Res.*, **1980**, 5, 469.
221. Liu, Q. R., Lopez-Corcuera, B., Nelson, H., Mandiyan, S. and Nelson, N., *Proc. Natl. Acad. Sci.*, **1992**, 89, 12145.
222. Kontro, P., *Neuroscience*, **1983**, 8, 153.
223. Itouji, A., Sakai, N., Tanaka, C. and Saito, N., *Mol. Brain Res.*, **1996**, 37, 309.
224. Liu, Q. R., Lopez-Corcuera, B., Mandiyan, S., Nelson, H. and Nelson, N., *J. Biol. Chem.*, **1993**, 268, 2106.
225. Mori, M., Gahwiler, B. H. and Gerber, U., *J. Physiol.*, **2002**, 539, 191.
226. Borden, L., *Neurochem. Int.*, **1996**, 29, 335.
227. Sidhu, H. S. and Wood, J. D., *Neuropharmacology*, **1986**, 26, 555.
228. Zafra, F., Aragon, M. C., Valdivieso, F. and Gimenez, C., *Neurochem Res.*, **1984**, 9, 695.
229. Rajendra, S., Lynch, J. W. and Schofield, P. R., *Pharmacol. Ther.*, **1997**, 73, 121.
230. McDonald, J. W., Penney, J. B., Johnston, M. V. and Young, A. B., *Neuroscience*, **1990**, 35, 653.
231. Beyer, C., Banas, C., Gomora, P. and Komisaruk, B. R., *Pharmacol. Biochem. Behav.*, **1988**, 29, 73.
232. Schmieden, V., Kuhse, J. and Betz, H., *Science*, **1993**, 262, 256.
233. Betz, H., *TINS*, **1987**, 10, 113.
234. Rajendra, S., Lynch, J. W., Pierce, K. D., French, C. R., Barry, P. H. and Schofield, P. R., *Neuron*, **1995**, 14, 169.
235. Laube, B., Langosch, D., Betz, H. and Schmieden, V., *Neuroreport*, **1995**, 6, 897.
236. Tremblay, N., Warren, R. and Dykes, R. W., *Neuroscience*, **1988**, 26, 745.
237. Boehm, S., Harvey, R. J., von Holst, A., Rohrer, H. and Betz, H., *J. Physiol.*, **1997**, 504, 683.

238. Choquet, D. and Korn, H., *Neurosci. Lett.*, **1988**, 84, 329.
239. Krishtal, O. A., Osipchuk, Y. V. and Vrublevsky, S. V., *Neurosci. Lett.*, **1988**, 84, 271.
240. Tan, C. Y. K., Wainman, D. and Weaver, D., *Bioorg. Med. Chem.*, **2003**, 11, 113.
241. Pullan, L. M. and Powel, R. J., *Neurosci Lett*, **1992**, 148, 199.
242. Ogita, K., Suzuki, T. and Yoneda, Y., *Neuropharmacology*, **1989**, 28,
243. Sandberg, M. and Jacobson, I., *J. Neurochem*, **1981**, 12, 1353.
244. Enz, R., *Biol. Chem.*, **2001**, 382, 1111.
245. Barker, J. L., McBurney, R. N. and MacDonald, J. F., *J. Physiol.*, **1982**, 322, 365.
246. Shen, W., Mennerick, S., Covey, D. and Zorumki, C., *J. Neurosci.*, **2000**, 20, 3571.
247. Brown, D. A. and Scholfield, C. N., *Br. J. Pharmacol.*, **1979**, 65, 339.
248. DeFeudis, F. V., *Fr. Experientia.*, **1978**, 34, 1314.
249. Horikoshi, T., Asanuma, A., Yanagisawa, K., Anzai, K. and Goto, S., *Mol. Brain. Res.*, **1989**, 4, 97.
250. Curtis, D. R., Duggan, A. W., Felix, D., Johnston, G. A. R. and McLennan, G., *Brain Res.*, **1971**, 33, 57.
251. Brown, D. A. and Galvan, M., *Br. J. Pharmac.*, **1979**, 65, 347.
252. Henke, H., Schenker, M. T. and Cuenod, M., *J. Neurochem.*, **1976**, 26, 125.
253. Tebecis, A. K., *Brain Res.*, **1973**, 63, 31.
254. Ehinger, B., *Brain Res.*, **1972**, 46, 297.
255. Zhang, J. and Slaughter, M. M., *J. Neurophysiol.*, **1995**, 74, 1583.
256. Barker, J. L., Nicoll, R. A. and Padjen, A., *J. Physiol.*, **1975**, 245, 537.
257. Barker, J. L., Nicoll, R. A. and Padjen, A., *J. Physiol.*, **1975**, 245, 521.
258. Roberts, E. and Bregoff, H., *J. Biol. Chem.*, **1953**, 210, 393.
259. Berkman, M. Z., Palaoge, S., Erbeni, T. and Erbeni, A., *Neurosurgery*, **1998**, 42, 1992.

260. Lehmann, A. and Hansson, E., *Neurochem. Res.*, **1987**, *12*, 797.
261. Nadi, N. S., McBride, W. J. and Aprison, M. H., *J. Neurochem.*, **1977**, *28*, 453.
262. Orendanz, L. M., Ambrosio, E., Fernandez, I. and Montero, M. T., *Neurochemical Res.*, **1988**, *13*, 1133.
263. Perry, T. L., Hansen, S., Berry, K., Mok, C. and Lesk, D., *J. Neurochem.*, **1971**, *18*, 521.
264. Shank, R. P. and Campbell, G., *J. Neurosci.*, **1984**, *4*, 58.
265. Tallan, H. H., Moore, S. and Stein, W. H., *J. Biol. Chem.*, **1954**, *211*, 927.
266. Lajtha, A. and Marks, N., *Dis. Nerv. Syst.*, **1969**, *30*, Suppl. 36.
267. Yoshino, Y. and Elliott, K. A., *Can. J. Biochem.*, **1970**, *48*, 1175.
268. Hosli, E. and Hosli, L., *Neuroscience*, **1980**, *5*, 145.
269. Bruun, A. and Ehinger, B., *Exp. Eye Res.*, **1974**, *19*, 435.
270. Ehinger, B. and Lindberg-Bauer, B., *Brain Res.*, **1976**, *113*, 535.
271. Kelly, J. S. and Weitsch-Dick, F., *NATO Advanced Study Institute Series, Series A: Life Sciences*, **1978**, *A16 (Amino Acids Chem. Transm.)*, 103.
272. Ehinger, B. and Falck, B., *Exp Eye Res.*, **1970**, *10*, 352.
273. Nagai, K., Suda, T., Kawasaki, K. and Mathuura, S., *Surgery*, **1986**, 815.
274. Kalyanker, G. D. and Meiser, A., *J. Biol. Chem.*, **1959**, *234*, 3210.
275. Winnick, R. E. and Winnick, T., *Biochim. Biophys. Acta.*, **1959**, *31*, 47.
276. Gallant, S., Semyonova, M. and Yuneva, M., *Biochem.*, **2000**, *65*, 866.
277. Wisniewski, K., *Neuropediatrics*, **1981**, *12*, 143.
278. Fleisher, L. D., *Pediatr. Res.*, **1980**, *14*, 269.
279. Murphey, W. H., *Pediatr. Res.*, **1973**, *7*, 601.
280. Tan, K. M. and Candlish, J. K., *Clin. Lab. Haematol.*, **1998**, *20*, 239.
281. Daniel, R. L., Osbaldeston, N. J. and McCormack, J. G., *Biochem. Soc. Trans.*, **1992**, *20*, 131.
282. Yoshikawa, T., *Free Radic. Res. Commun.*, **1991**, *14*, 289.

283. Horning, M. S., Blakemore, L. J. and Trombley, P. Q., *Brain Res.*, **2000**, 852, 56.
284. Kriengsinyos, W., Raffi, M., Wykes, L. J., Ball, R. O. and Pencharz, P. B., *Am. Soc. Nutrit. Sci.*, **2002**, 132, 3340.
285. Beart, P. M. and Johnston, G. A. R., *Brain Res.*, **1973**, 49, 459.
286. Schon, F. and Kelly, J. S., *Brain Res.*, **1975**, 86, 243.
287. Cummins, C. J., Glover, R. A. and Sellinger, O. Z., *Brain Res.*, **1982**, 239, 299.
288. Bauer, B. and Ehinger, B., *Brain Res.*, **1977**, 120, 447.
289. Iversen, L. L. and Johnston, G. A., *J. Neurochem.*, **1971**, 18, 1930.
290. Curtis, D. R., Hosli, E., Johnston, G. A. R. and Johnston, I. H., *Exp. Brain Res.*, **1968**, 5, 238.
291. Tsukada, Y., Nagata, Y., Hirano, S. and Matsutani, T., *J. Neurochem.*, **1963**, 10,
292. Roseth, S. and Fonnum, F., *Neurosci. Lett.*, **1995**, 183, 62.
293. Salceda, R., *Neurochem. Res.*, **1980**, 5,
294. Werman, R., *Comp. Biochem. Physiol.*, **1966**, 18, 745.
295. Agullo, L., Jimenez, B., Aragon, C. and Gimened, C., *Eur. J. Biochem.*, **1986**, 159, 611.
296. Komura, J., Tamai, I., Senmaru, M., Terasaki, T., Sai, Y. and Tsuji, A., *FEBS Lett.*, **1997**, 400, 131.
297. Tamai, I., Senmaru, M., Terasaki, T. and Tsuji, A., *Biochem. Pharmacol.*, **1995**, 50, 1783.
298. Hitzemann, R. J. and Loh, H. H., *J. Neurochem.*, **1978**, 30, 471.
299. Sanchez del Pino, M. M., Hawkins, R. A. and Peterson, D. R., *J. Biol. Chem.*, **1992**, 267, 25951.
300. Krnjevic, K., *Brit. Med. Bull.*, **1965**, 21, 10.
301. Seebach, D. and Matthews, J. L., *J. Chem. Soc. Chem. Comm.*, **1997**, 2015.
302. Wu, F. S., Gibbs, T. T. and Farb, D. H., *Eur. J. Pharm. Mol. Pharm.*, **1993**, 246, 239.
303. Akagi, H. and Miledi, R., *Neurosci. Lett.*, **1988**, 95, 262.



304. Akagi, H. and Miledi, R., *Science*, **1988**, 246, 270.
305. DeFeudis, F. V., Munoz, L. M., Moya, M. F., Latorre, A. and Fando, J. L., *Gen. Pharmac.*, **1977**, 8, 311.
306. DeFeudis, F. V., Munoz, L. M., Vidal, M. A., Corrochano, G. and Sanchez del Alamo, M., *Gen. Pharmac.*, **1978**, 9, 341.
307. Parker, I., Sumikawa, K. and Miledi, R., *Proc. R. Soc. Lond.*, **1988**, 233, 201.
308. Watkins, J. C., *Biochem. Soc. Symp.*, **1972**, 36, 33.
309. Connolly, G. P. and Duley, J. A., *TiPS*, **1999**, 20, 218.
310. Roberts, E., *Arch. Biochem. Biophys.*, **1954**, 48, 395.
311. Phil, A. and Fritzson, P., *J. Biol. Chem.*, **1955**, 213, 345.
312. Matthews, M. M. and Traut, T. W., *J. Biol. Chem.*, **1987**, 262, 7232.
313. Fonnum, F., *Biochem. J.*, **1965**, 96, 66.
314. McBride, W. J., Aprison, M. H. and Kusano, K., *J. Neurochem.*, **1976**, 26, 867.
315. Curtis, D. R. and Watkins, J. C., *J. Neurochem.*, **1960**, 6, 117.
316. Breckenridge, R. J., Nicholson, S. H., Nicol, A. J. and Suckling, C. J., *Biochem. Pharmacol.*, **1981**, 30, 3045.
317. Harris, R. C. and Dunnett, M., *Methods and compositions for increasing the anaerobic working capacity in tissue*, 909513, PAT 10-12-99 05965596, 1997, UK.
318. Nofre, L. and Ouar, S., *Heterocyclic sweeteners derived from N-carbamoyl-, N-thiocarbamoyl or N-amidino-glycine or beta-alanine*, 88430421, EPA 89-25 0321369, 1988, Universite Claude Bernard, France.
319. Agarwal, S. K. D. and Johary, P. C., *Sharkara*, **1974**, 13, 89.
320. Baim, M. and Koehler, D., *Beta-amino acid ester derivatives of alcoholic actives having extended duration of activity*, 88308801, EPA 89-14 0310299, 1988, The Procter and Gamble Company, USA.
321. Chernobrovkin, M. G., Ananeva, I. A., Shapovalova, E. N. and Shapingun, O. A., *Zavodskaya Laboratoriya, Diagnostika Materialov*, **2003**, 69, 7.
322. Lacharriere, D. and Breton, *Use of an agonist of a receptor associated to a chloride channel in the treatment of wrinkles*, 95402155, EPA 96-14 0704210, 1995, L'Oreal, France.

323. Hirao, T., Masuda, Y. and Takahashi, M., *Cosmetic for improving wrinkles*, 09220240, PAJ 02-01-99 11049628, 1997, Shiseido Co. Ltd., Japan.
324. Biergiesser, H., Gatermann, C., Carstensen, S., Janeke, G., Doering, T., Schreiner, V., Siefken, W. and Sauermann, G., *Cosmetic and dermatological compositions containing amino acids for the prevention of dry skin and the negative effects on skin homeostasis*, DE 10133197, 2003, Germany.
325. DeLacharriere, O., *Compositions and methods for treating wrinkles and/or fine lines of the skin*, 050959, PAT 11-02099, 1999, L'Oreal, France.
326. DeLacharriere, O. and Breton, L., *Use of an agonist of a receptor associated with a chloride channel in the treatment of wrinkles*, EP 704210, 1996, Europe.
327. Kamashita, T., Wada, M. and Nagata, T., *New beta-alanine derivative, its production and detergent composition containing the same compound*, 09163007, PAJ 01-01-99 11012240, 1997, Mitsui Chem Inc., Japan.
328. Moriyama, M., Tanabe, H., Hanazawa, H. and Kajihara, Y., *Aqueous liquid cleaning composition*, 528095, PAT 01-27-98 05712232, 1995, Kao Corporation, Japan.
329. Heinzman, S., Eis, M. and Armstrong, M., *Amino-functional compounds as builder/ dispersants in detergent compositions*, 144823, PAT 00-00-90 04959409, 1988, The Procter & Gamble Company (USA).
330. Sano, K. and Hattori, T., *Detergent composition*, 338520, PAT 06-25-96, 1995, Ajinomoto Co. Inc., Japan.
331. Zabotto, A. and Contamin, J., *Cosmetic cleaning composition*, 854817, PAT 00-00-88 04732692, 1986, L'Oreal, France.
332. Rubino, A., *Zirconium-aluminum-polyol buffered anti-perspirant complexes*, 431639, PAT 00-00-76 3981986, 1974, Armour Pharmaceutical Co., USA.
333. Elsnau, W., *Antiperspirant stick*, 632128, PAT 00-00-77 0409792, 1975, The Procter & Gamble Co., USA.
334. Jacobs, M. E., *Compositions containing tyrosine derivatives and aminocarboxylic acids and oxidizing agents for coloring hair or skin*, US 4390341, 1983, US.
335. Mahieu, C. and Papantoniou, C., *Cosmetic compositions for the treatment of the hair and skin contain polymer constituted essentially by repeating units of the beta-alanine type*, 981258, PAT 02-14-95 05389362, 1992, Societe Anonyme dite: L'Oreal, France.

336. Kiffel, W. and Tyson, T., *Hair reviver composition containing flim-forming amino acids*, 063952, PAT 00-00-89 04837012, 1987, S. C. Johnson & Son Inc., USA.
337. Grollier, J. and Fourcadier, C., *Cosmetic composition for delaying the apperance of an oily aspect of hair*, 747443, PAT 00-00-88 04735797, 1985, L'Oreal, France.
338. Rave, T., *Preparation of hydrophobic poylolefin fibers for use in papermaking*, 819435, PAT 00-00-79 04154647, 1977, Hercules Inc., USA.
339. Rave, T., *Glyoxal modified poly (beta-alanine) strengthening resins for use in paper*, 651374, PAT 00-00-78 04082730, 1976, Hercules Inc., USA.
340. Takamiya, S. and Kimura, T., *Process for preparing a substrate for a lithographic plate*, 91119284, EPB 95-26 0485968, 1991, Fuji Photo Film Co., Japan.
341. Kobayashsi, F., *Negative type image recording material.*, 949707, NDN 217-0363-8610-3, 1997, Fuji Photo Film Co. Ltd. (NDN 217-0363-8610-3), Japan.
342. Rihova, B., Germano, Y. and Kufudaki, O., *Composition for treating cancer*, 787209, PAT 06071888, 1997, Aliatros Medical,
343. Durette, P., Hagmann, w., Kopka, I., Maccoss, M., Mills, S., Mumford, R. and Magriotis, P., *Substituted beta-alanine derivatives as cell adhesion inhibitors*, 00071572, PCT 11-23-00 00071572, 2000, Merck & Co., Inc., USA.
344. Abood, N., Flynn, D., Laneman, S., Nosal, R. and Schretzman, L., *Intermediates for amidino phenyl pyrrolidine beta-alanine urea analogues*, 467417, PAT 08-19-97, 1995, G. D. Searle & Co., USA.
345. Asgharnejad, M. and Shiromani, P., *Compositions for inhibiting platelet aggreagation*, 145871, PAT 10-10-00 06129932, 1998, Merck & Co., USA.
346. Horwell, D., Pritchard, M. and Richardson, R., *Pro-drugs for CCK antagonists*, 661254, PAT 03-10-98, 1996, Morris Plains, USA.
347. Krooth, R. S., May, S. R. and Stern, H. J., *J.Theor. Biol.*, **1977**, 66, 595.
348. Tan, C., The design and synthesis of novel  $\beta$ -substituted  $\beta$ -amino acids as anti-epileptogenics, PhD, Queen's University, Kingston. 2000.
349. Barker, G. A. and Ellory, J. C., *Exp. Physiol.*, **1990**, 75, 3.
350. Buhendwa, M., The design and synthesis of uracil analogues for the treatment of epilepsy, MSc, Queen's University, Kingston. 2002.

351. Burckhalter, J. H. and Scarborough, H., *J. A. Pharm. Ass.*, **1955**, *44*, 545.
352. Wenzel, D., *J. A. Pharm. Ass.*, **1955**, *44*, 550.
353. Wenzel, D. and Koff, G., *J. A. Pharm. Ass.*, **1956**, *45*, 669.
354. Tyynela, J., Sohar, I., Sleat, D. E., Gin, R. M., Donnelly, R. J., Baumann, M., Haltia, M. and Lobel, P., *Embo J*, **2000**, *19*, 2786.
355. Vuana, B. M., Pieroni, O. I. and Cabaleiro, M. C., *J. Chem. Res.*, **2000**, *35*, 318.
356. Bhat, C. and Munson, R., The diethyl and dimethyl ethers of 2,4-pyrimidinediol and of 5-methyl-2,4-pyrimidinediol, In *Synthetic Procedures in Nucleic Acid Chemistry*, Interscience Publishers, New York, 1968, 83.
357. Harden, D., Mokrosz, M. and Strekowski, L., *J. Org. Chem.*, **1988**, *53*, 4137.
358. Uno, H., Terakawa, T. and Suzuki, H., *Synthesis*, **1989**, *1989*, 381.
359. Strekowski, L., Watson, R. and Faunce, M., *Synthesis*, **1987**, *1987*, 579.
360. Jones, R. G. and Gilman, H., *Org. React.*, **1951**, *6*, 339.
361. Gilman, H. and Jones, R. G., *J. Am. Chem. Soc.*, **1941**, *63*, 1441.
362. Parham, W. E., Jones, L. D. and Sayed, Y. A., *J. Org. Chem.*, **1975**, *40*, 2394.
363. Parham, W. E., Jones, L. D. and Sayed, Y. A., *J. Org. Chem.*, **1976**, *41*, 1184.
364. Parham, W. E. and Sayed, Y. A., *J. Org. Chem.*, **1974**, *39*, 2053.
365. Jakiela, D. J., Helquist, P. and Jones, L. D., *Org. Synth.*, **1990**, *7*, 326.
366. Ponton, J. and Helquist, P., *J. Org. Chem.*, **1981**, *46*, 118.
367. Dellaria, J. F., Brooks, D. W., Moore, J. L. and Sallin, K. J., *K. J., N-(Arylamidoalkyl)-N-hydroxyurea compounds having lipoxxygenase inhibitory activity*, US5514702, 1996, USA.
368. Rarey, M., Kramer, B. and Lengauer, T., *J. Comput.-Aided Mol. Design*, **1997**, *11*, 369.
369. Rarey, M., Kramer, B., Lengauer, T. and Klebe, G., *J. Mol. Biol.*, **1996**, *261*, 470.
370. Rarey, M., Wefing, S. and Lengauer, T., *J. Comput.-Aided Mol. Design*, **1996**, *10*, 41.
371. Kuntz, I. D., *Science*, **1992**, *257*, 1078.

372. Mizutani, M. Y., Tomioka, N. and Itai, A., *J. Mol. Biol.*, **1994**, *243*, 310.
373. Taufer, M., Crowley, M., Price, D., Chien, A. A. and Brooks, C. L., *Con. Comp.:Prac. Exp.*, **2004**, *17*, 1627.
374. Ghose, A. K. and Crippen, G. M., *J. Comp. Chem.*, **1985**, *6*, 350.
375. Teodoro, M. L., Phillips, G. N. and Kavraki, L., Molecular docking: A problem with thousands of degrees of freedom., IEEE International Conference on Robotics and Automation (ICRA), 2001, Seoul, Korea.
376. Apostolakis, J., Pluckthun, A. and Caflisch, A., *J. Comp. Chem.*, **1998**, *19*, 21.
377. Gillet, V. J., Newell, W., Mata, P., Myatt, G., Sike, S., Zsoldos, Z. and Johnson, A. P., *Protein: Struct. Funct. Genet.*, **1994**, *8*, 195.
378. Blaney, J. M. and Dixon, J. S., *Perspect. Drug Disc. Design*, **1993**, *1*, 301.
379. Klebe, G. and Mietzner, T., *J. Comput.-Aided Mol. Design*, **1994**, *8*, 583.
380. Bursulaya, B. D., Totrov, M., Abagyan, R. and Brooks, C. L., *J. Comput.-Aided Mol. Design*, **2003**, *17*, 755.
381. Böhm, H. J., *J. Comput.-Aided Mol. Design*, **1992**, *6*, 593.
382. Bohm, H. J., *J. Comput.-Aided Mol. Design*, **1994**, *8*, 243.
383. Sandak, B., Wolfson, H. J. and Nussinov, R., *Proteins*, **1998**, *32*, 159.
384. Luty, B. A., Wasserman, Z. R., Stouten, P. F. W., Hodge, C., N., Zacharias, M. and McCammon, J. A., *J. Comp. Chem.*, **1995**, *16*, 454.
385. RCSB, Research Collaboratory for Structural Bioinformatics, Protein Data Bank (PDB) files, [www.rcsb.org/pdb/welcome.do](http://www.rcsb.org/pdb/welcome.do)
386. NCBI, National Center for Biotechnology Information, Entrez Protein Sequence files, [www.ncbi.nlm.gov/entrez/query.fcgi?db=Protein](http://www.ncbi.nlm.gov/entrez/query.fcgi?db=Protein)
387. EMBL-EBI, European Molecular Biology Laboratory-European Bioinformatics Institute, ClustalW Alignment Program, [www.ebi.ac.uk/clustalw/](http://www.ebi.ac.uk/clustalw/)
388. Dobritzsch, D., Schneider, G., Schnackerz, K. D. and Lindqvist, Y., *EMBO*, **2001**, *20*, 650.
389. Dobritzsch, D., Ricagno, S., Schneider, G., Schnackerz, K. D. and Lindqvist, Y., *J. Biol. Chem.*, **2002**, *277*, 13155.

- 390. Yokota, H., Fernandez-Salguero, P., Furuya, H., Lin, K., McBride, O. W., Podschun, B., Schnackerz, K. D. and Gonzalez, F. J., *J. Biol. Chem.*, **1994**, 269, 23192.
- 391. Hamajima, N., Matsuda, K., Sakata, S., Tamaki, N., Sasaki, M. and Nonaka, M., *Gene*, **1996**, 180, 157.
- 392. Abendroth, J., Niefind, K. and Schomburg, D., *J. Biol. Chem.*, **2002**, 320,
- 393. Abendroth, J., Niefind, K., May, O., Siemann, M., Syltatk, C. and Schomburg, D., *Biochem.*, **2002**, 41, 8589.
- 394. Kim, G. J. and Kim, H. S., *Biochem. J.*, **1998**, 330, 295.
- 395. Lundgren, S., Gojkovic, Z., Piskur, J. and Dobritzsch, D., *J. Biol. Chem.*, **2003**, 278, 51851.
- 396. Bergin, A. M. and Connolly, M., *Neurol. Clin.*, **2002**, 20, 1163.
- 397. Merritt, H. H. and Putnam, T. J., *Arch. Neurol. Psychiat.*, **1938**, 39, 1003.
- 398. Dichter, M. A., *Adv. Neurol.*, **1998**, 76, 1998.
- 399. HyperChem for SGI, Version 7.5, HyperChem, 2003.
- 400. Moon, J. B. and Howe, W. J., *Proteins*, **1991**, 11, 314.
- 401. Leach, A. R. and Kuntz, I. D., *J. Comp. Chem*, **1990**, 13, 730.
- 402. Brown, M. L., Brown, G. B. and Brouillette, W. J., *J. Med. Chem.*, **1997**, 40, 602.